

City University of New York (CUNY)

## CUNY Academic Works

---

Dissertations, Theses, and Capstone Projects

CUNY Graduate Center

---

1972

### The Effect of Periodicity Instability on the Detection of Interaural Time-of-Arrival Difference

Roy F. Sullivan

*Graduate Center, City University of New York*

[How does access to this work benefit you? Let us know!](#)

More information about this work at: [https://academicworks.cuny.edu/gc\\_etds/2191](https://academicworks.cuny.edu/gc_etds/2191)

Discover additional works at: <https://academicworks.cuny.edu>

---

This work is made publicly available by the City University of New York (CUNY).

Contact: [AcademicWorks@cuny.edu](mailto:AcademicWorks@cuny.edu)

72-24,160

SULLIVAN, Roy F., 1938-

THE EFFECT OF PERIODICITY INSTABILITY ON THE  
DETECTION OF INTERAURAL TIME-OF-ARRIVAL  
DIFFERENCE.

The City University of New York, Ph.D., 1972  
Psychology, experimental

University Microfilms, A XEROX Company, Ann Arbor, Michigan

THE EFFECT OF PERIODICITY INSTABILITY  
ON THE DETECTION OF INTERAURAL  
TIME-OF-ARRIVAL DIFFERENCE

by

ROY F. SULLIVAN, M.A.

A dissertation submitted to the  
Graduate Faculty in Psychology in partial  
fulfillment of the requirements for the  
degree of Doctor of Philosophy,  
The City University of New York.

1972

This manuscript has been read and accepted for the  
Graduate Faculty in Psychology in satisfaction of  
the dissertation requirement for the degree of  
Doctor of Philosophy.

May 7, 1972  
date

[signature]

\_\_\_\_\_  
Chairman of Examining Committee

May 8, 1972  
date

[signature]

\_\_\_\_\_  
Executive Officer

Eric Heinemann

\_\_\_\_\_  
Louis Gerstman

\_\_\_\_\_  
Joseph Hall II

\_\_\_\_\_  
Supervisory Committee

The City University of New York

PLEASE NOTE:

Some pages may have  
indistinct print.

Filmed as received.

University Microfilms, A Xerox Education Company

## ACKNOWLEDGEMENTS

Sincere appreciation is expressed to Dr. Eric Heinemann for undertaking the supervision of this project and for his guidance and encouragement as thesis advisor.

Gratitude is also acknowledged to Dr. Louis Gerstman and Dr. Joseph Hall II for their extended tenures as members of the thesis committee.

In addition, deep thanks must be rendered the following individuals:

-to Dr. Ira A. Polisar, Director of the Department of Otorhinolaryngology and to Mr. William K. Klein, Director of The Long Island College Hospital, without whose support this research would not have been possible.

-to Susan L. Smith and John E. Buckley, good friends and loyal subjects - - who still hear pulse trains on disquieted nights!

-to Richard Goldman for his assistance in computer processing portions of the data.

-to Dr. Harry Levitt for his counsel on an analysis of variance procedure for comparing predicted and obtained fittings to empirical data.

-to Dr. Newman Guttman for support in his initial tenure on the thesis committee.

-to Sharain Gordon, a special debt of gratitude is owed for her steadfast determination to produce each draft type-script page, table of data and mathematical formula as if it was final copy.

-to my family and friends for their forbearance; especially to my sons, Glenn Peter and Evan Christopher, who grew despite the thesis.

This thesis is dedicated to  
the memory of a great man:

FRANCIS T. SULLIVAN.

## TABLE OF CONTENTS

	<u>PAGE</u>
ACKNOWLEDGMENTS . . . . .	iii
LIST OF TABLES . . . . .	vi
LIST OF FIGURES . . . . .	viii
 Chapter	
I. INTRODUCTION . . . . .	1
II. EXPERIMENT I: INSTRUMENTATION AND CALIBRATION .	16
III. EXPERIMENT I: METHODS AND PROCEDURES. . . . .	34
IV. EXPERIMENT I: RESULTS AND DISCUSSION. . . . .	49
V. MODEL. . . . .	80
VI. EXPERIMENT II: BACKGROUND . . . . .	111
VII. EXPERIMENT II: INSTRUMENTATION AND PROCEDURES .	125
VIII. EXPERIMENT II: RESULTS AND DISCUSSION . . . . .	145
IX. GENERAL APPLICATIONS OF THE MODEL. . . . .	195
X. SUMMARY. . . . .	221
REFERENCES. . . . .	224



## LIST OF TABLES

<u>Table</u>		<u>Page</u>
4.1	Parameters of the Least-Squares Lines of Best Fit to the $d'$ Psychometric Function Points: $J_e = 0$ . . . . .	54
4.2	Reciprocal Slopes and Intercepts for the Linear Least-Squares Best Fits and Weighted-Zero Fits to the $d'$ Psychometric Function Points: $J_e = 0$ . . . . .	56
4.3	Successive Degrees and Algebraic Signs of Polynomial-Fitted Percent Correct Psychometric Functions Beyond $P = .001$ : $J_e = 0$ . . . . .	64
4.4	$\beta_{obt}$ for Each Subject by Relative Sensation Level, . . . . .	77
7.1	100 Hz Low-Pass rms Noise Voltage Transformation to $J_e$ ( $\sigma$ ) in $\mu\text{sec}$ . . . . .	130
7.2	$\chi^2$ Against a Normal Distribution for $J_e = 160 \mu\text{sec}$ . Z-Score Sample Distribution (Fig. 7.7) . . . . .	142
7.3	Combinations of $J_e$ and Sensation Level Used for Each Subject in Experiment II. . . . .	144
8.1	Parameters of the Unweighted First-Order Least-Squares Fittings to the Experiment II Data Compared With Parameters Predicted by the Model . . . . .	156
8.2	Analysis of Variance for Unweighted First-Order Least-Squares Fittings to Experiment II Data Points. . . . .	158
8.3	Parameters of the Zero-Weighted First-Order Least-Squares Fittings to the Experiment II Data Compared with Parameters Predicted by the Model . . . . .	159
8.4	Model Parameter Estimates: $J_{iv}$ , $N_e$ and $E$ Derived from Experiment I and II $d'$ Data Fittings. . . . .	168
8.5	$\beta_{obt}$ for Subject SLS, by Sensation Level and $J_e$ , from Experiment II Data. . . . .	192
8.6	$\beta_{obt}$ for Subject RFS, by Sensation Level and $J_e$ , from Experiment II Data. . . . .	193

<u>Table</u>		<u>Page</u>
8.7	$\beta_{\text{obt}}$ for Subject JEB, by Sensation Level and $J_e$ , from Experiment II Data. . . . .	194
9.1	Predicted $\Delta T$ Values for Noise Burst Ongoing Disparity as $f(X_t)$ ; Data of Zerlin (1959). . .	201
9.2	Predicted $\Delta T$ Values for $\Delta\phi$ as $f(\text{Hz})$ ; Data of Zwisllocki and Feldman (1956); Klumpp and Eady (1956) . . . . .	206
9.3	Estimates of Internal Temporal Noise in the Literature . . . . .	215
9.4	Predicted $J_{iy}$ Values for 500 Hz $\Delta\phi$ Data of Zwisllocki and Feldman (1956) . . . . .	220

# LIST OF FIGURES

<u>FIGURE</u>		<u>PAGE</u>
1.1	A. $\Delta t$ Data of Wallach, Newman and Rosenzweig (1949) B. $\Delta t$ Data of Klumpp and Eady (1956) . . . . .	4
1.2	$\Delta T$ Data of Hall (1964) . . . . .	6
2.1	A. Audiology Research Laboratory B. RELOPS: Relay Logic Programming System C. Subject apparatus contained in soundproof booth. . .	18
2.2	Block diagram of the stimulus generation and control instrumentation employed in Experiments I and II . . . .	20
2.3	Oscilloscopic displays of electrical and acoustic pulse stimuli; filtered and unfiltered . . . . .	24
2.4	One hundred channel analog averager simulating a differential response to a two-channel unfiltered rectangular 100 $\mu$ sec. pulse input. . . . .	27
2.5	Autocorrelation functions for the 4.8 kHz low-pass filtered earphone acoustical output to an NBS 9A coupler. .	31
3.1	A. Experimental trial intervals B. Listen interval; AXA observation sub-intervals . . .	36
3.2	Graphically simulated relationships for the AXA paradigm pulse train inputs to AD and AS in Experiment I, $J_e = 0$ .  $d' \Delta t$ psychometric functions; $J_e = 0$	38
4.1	. . . . .Subject SLS . . . . .	51
4.2	. . . . .Subject RFS . . . . .	52
4.3	. . . . .Subject JEB . . . . .	53
	Percent Correct $\Delta t$ psychometric functions; $J_e = 0$ :	
4.4	. . . . .Subject SLS . . . . .	60
4.5	. . . . .Subject RFS . . . . .	61
4.6	. . . . .Subject JEB . . . . .	62

<u>FIGURE</u>		<u>PAGE</u>
4.7	$\Delta t$ Data of Wallach, et. al. (1949), for click pair stimuli, replotted in the form of Percent Correct psychometric functions. . . . .	67
4.8	$\Delta t$ Data of Hall (1964), for click pair stimuli, replotted to make dB SL the parameter of each Percent Correct psychometric function . . . . .	69
	HIT and FALSE ALARM $\Delta t$ psychometric functions; $J_e = 0$ :	
4.9	. . . . . Subject SLS. . . . .	74
4.10	. . . . . Subject RFS. . . . .	75
4.11	. . . . . Subject JEB. . . . .	76
5.1	Model for pulse train interaural time-of-arrival difference discrimination . . . . .	82
5.2	Theoretical distribution of $\Delta t$ neural effect ( $\Delta t_1$ ) at the Coincidence Detector. . . . .	91
5.3	Simulated $d'$ $\Delta t$ psychometric functions for an Ideal Observer using samples of 20 pulses per observation with various superimposed values of external jitter ( $J_e$ ) . . .	96
7.1	Graphically simulated relationships for the AXA paradigm pulse inputs to AD and AS in Experiment II; $J_e \neq 0$ . . . .	127
7.2	Distributions of $J_e$ in the AS channel photographed from oscilloscope displays of 100-channel analog averager output. . . . .	133
	Averager-Simulated response to $\Delta t$ when $J_e \neq 0$ :	
7.3	. . . . . $J_e = 20 \mu\text{sec. rms}$ . . . . .	135
7.4	. . . . . $J_e = 40 \mu\text{sec. rms}$ . . . . .	136
7.5	. . . . . $J_e = 80 \mu\text{sec. rms}$ . . . . .	137
7.6	. . . . . $J_e = 160 \mu\text{sec. rms}$ . . . . .	138
7.7	Representative digital computer-generated Z-score histogram of 400-interval sample $J_e$ distribution for 2.00 Volts rms input ( $J_e = 160 \mu\text{sec.}$ ), . . . . .	141

<u>FIGURE</u>		<u>PAGE</u>
	d' At psychometric functions; $J_e \neq 0$ :	
8.1	. . . . . SLS @ 60 dB SL. . . . .	147
8.2	. . . . . SLS @ 40 dB SL. . . . .	148
8.3	. . . . . SLS @ 10 dB SL. . . . .	149
8.4	. . . . . RFS @ 40 dB SL. . . . .	150
8.5	. . . . . RFS @ 20 dB SL. . . . .	151
8.6	. . . . . RFS @ 10 dB SL. . . . .	152
8.7	. . . . . JEB @ 60 dB SL. . . . .	153
8.8	. . . . . JEB @ 40 dB SL. . . . .	154
8.9	. . . . . JEB @ 10 dB SL. . . . .	155
	Predicted and Obtained effects of $J_e$ on $\Delta T$ :	
8.10	. . . . . Subject SLS. . . . .	164
8.11	. . . . . Subject RFS. . . . .	165
8.12	. . . . . Subject JEB. . . . .	166
	Percent Correct At psychometric functions, $J_e \neq 0$ :	
8.13	. . . . . SLS, 60 dB SL, . . . . .	172
8.14	. . . . . SLS, 40 dB SL. . . . .	173
8.15	. . . . . SLS, 10 dB SL. . . . .	174
8.16	. . . . . RFS, 40 dB SL. . . . .	175
8.17	. . . . . RFS, 20 dB SL. . . . .	176
8.18	. . . . . RFS, 10 dB SL. . . . .	177
8.19	. . . . . JEB, 60 dB SL. . . . .	178
8.20	. . . . . JEB, 40 dB SL. . . . .	179
8.21	. . . . . JEB, 10 dB SL. . . . .	180

FIGUREPAGE

HIT and FALSE ALARM  $\Delta t$  psychometric functions,  $J_e \neq 0$ :

8.22	. . . . . SLS 60 dB SL . . . . .	183
8.23	. . . . . SLS 40 dB SL . . . . .	184
8.24	. . . . . SLS 10 dB SL . . . . .	185
8.25	. . . . . RFS 40 dB SL . . . . .	186
8.26	. . . . . RFS 20 dB SL . . . . .	187
8.27	. . . . . RFS 10 dB SL . . . . .	188
8.28	. . . . . JEB 60 dB SL . . . . .	189
8.29	. . . . . JEB 40 dB SL . . . . .	190
8.30	. . . . . JEB 10 dB SL . . . . .	191
9.1	Ongoing $\Delta t$ JND's for 5 kHz low-pass filtered noise obtained by Zerlin (1959) with $\Delta T$ values predicted by the model . . . . .	200
9.2	Pure tone $\Delta \phi$ data of Klumpp and Eady (1956) and Zwislocki and Feldman (1956) with $\Delta T$ values pre- dicted by the model . . . . .	205
9.3	A. $\Delta T$ data of Guttman, et. al. (1960) with slopes predicted by the model . . . . . B. $\Delta T$ data of Yost, et. al. (1971) with slopes predicted by the model . . . . . C. $\Delta T$ data of Houtgast, et. al. (1968) with slopes predicted by the model . . . . .	208
9.4	Data of Nordmark (1970) on the effects of degree of randomness on the just noticeable differences in time for pulse train pitch and lateralization . . . . .	213
9.5	A. Data of Pollack (1971) on the effect of pulse amplitude on diotic jitter thresholds. . . . . B. Data of Zwislocki, et. al. (1956) on $\Delta \phi$ as a function of SL at 500 Hz . . . . .	218

## CHAPTER I

### INTRODUCTION

This investigation was carried out to determine the effect of a controlled periodicity instability on the Just Noticeable Difference (JND) in interaural time of arrival for pulse train stimuli. This JND shall be called  $\Delta T$ . The variable of physical interaural time-of-arrival difference shall be known as  $\Delta t$ . The temporal instability or external jitter will be referred to as  $J_e$ , calibrated in rms microseconds ( $\mu\text{sec.}$ ).

By observing the magnitude of  $J_e$  necessary to increase the  $\Delta T$ , one may derive an estimate of the internal instability or internal noise, which may place a lower limit on  $\Delta T$ . This hypothetical construct, internal noise, also reported in rms  $\mu\text{sec.}$ , is called  $J_{iy}$ . It is proposed here that the magnitude of  $J_{iy}$  systematically increases with decreasing intensity of stimulation.

The study is reported in two parts. The first presents  $\Delta T$  psychometric functions obtained at three Sensation Levels (SL's) using temporally stable pulse train stimuli. Part II reports the effects of  $J_e$  on these functions. A statistically based model is proposed to explain the results.

#### REVIEW OF THE RELEVANT LITERATURE:

One of the earliest formal studies of auditory localization was that of E. H. Weber in 1846 (Boring, 1942). The role of interaural

time-of-arrival difference as a primary localization cue was not fully recognized until the work of von Hornbostel and Wertheimer (1920). They sought to reduce the then prevailing "phase theory" of pure tone localization to a common "time theory" (Boring, 1942).

In order to investigate adequately the role of the isolated  $\Delta t$  cue, impulsive stimuli have always been preferred because of the lack of ambiguity in identifying the transient stimulus onset. The first published research on this topic, making effective use of electronic instrumentation capable of generating impulsive stimuli with inter- and intrachannel accuracy in the microsecond range, was by Wallach, Newman, and Rosenzweig (1949). Until the present only that study and two others using pulse or click stimuli have published  $\Delta T$  data in the form of psychometric functions. The first, as stated, was by Wallach et al. (1949). The others were by Klumpp and Eady (1956) and Hall (1964). Of all of these, only Hall reports the effects of SL on the  $\Delta T$  psychometric function.

The results of these studies (Wallach et al., 1949; Klumpp et al., 1956; Hall, 1964) are reproduced in Figs. 1.1 and 1.2. In each of these studies, the stimulus was a single pair of dichotic clicks. Klumpp et al. (1956) also presented subjects with a two-second burst of 15 pulses per second (pps), reporting an average  $\Delta T$  of 11  $\mu$ sec. for 13 subjects. Pulse trains have been used as  $\Delta t$  stimuli in a number of published psychophysical investigations



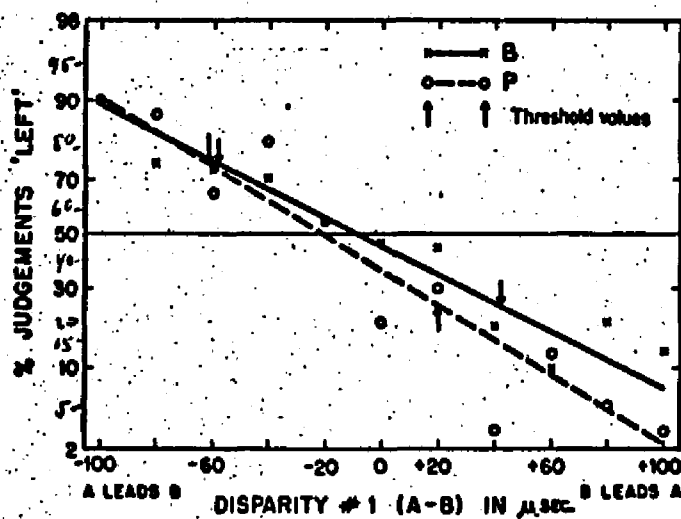
Figure 1.1a

$\Delta T$  data of Wallach, Newman and Rosenzweig (1949). Ability of two subjects to distinguish "right" from "left". Ordinate is percentage of reports "left". A single pair, each, of reference and test clicks were presented. The abscissa is  $\Delta t$ . Each point represents 40 observations.

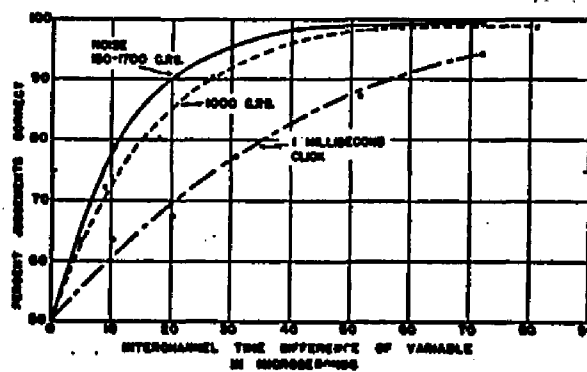
Figure 1.1b

$\Delta T$  data of Klumpp and Eady (1956). Percent Correct detection as a function of  $\Delta t$ . There were 10 listeners per function, 120 observations per point, per listener for click pairs; 9 listeners per function, 80 judgements per point, per listener for pure tones and noise.

EXPERIMENT	STIMULI	DISPARITY # 1	INTERVAL	DISPARITY # 2
I	AB	100, -80, -60, -40 -20, 0, +20, +40 +60, +80, +100	None	None



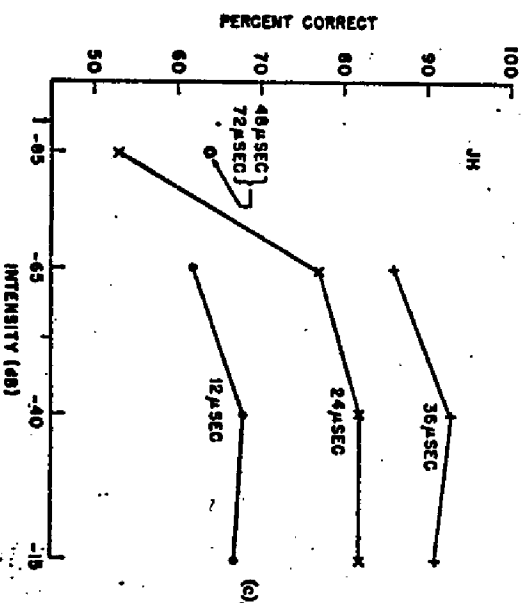
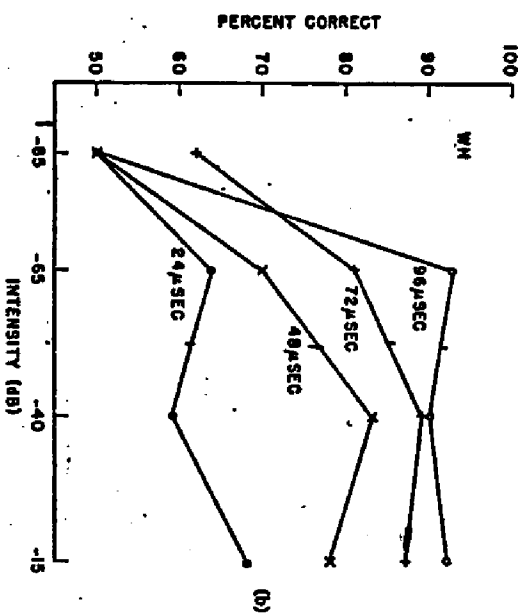
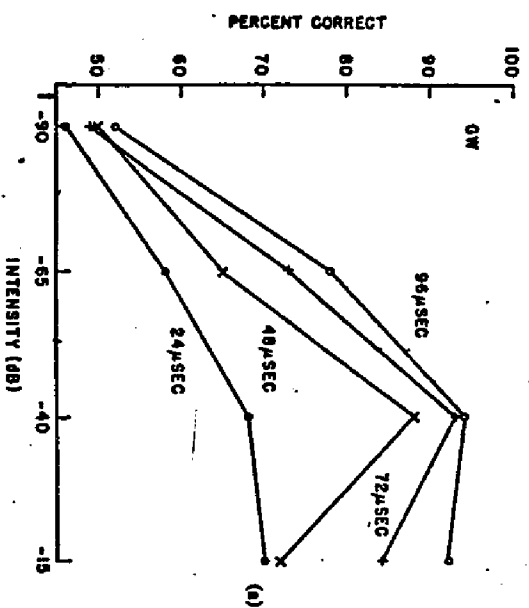
A



B

Figure 1.2

$\Delta T$  data of Hall (1964). Percent Correct detection as a function of overall intensity, three subjects. The parameter of each curve is  $\Delta t$ . Each point is based on a minimum of 120 judgements. Arrows indicate approximate dB values of monaural threshold for each subject.



(Bekesy, 1930; Christman et al., 1955; David et al., 1958, 1959; Guttman et al., 1960; Mickunas, 1963). In each of them, however, data are presented in the form of psychophysical functions with parameters more complex than the simple pulse train  $\Delta T$  psychometric function.

For example, Bekesy (1930; see also 1960) and Mickunas (1963) investigated perceived displacement of fused dichotic pulse train images as a function of  $\Delta t$ . Christman et al. (1955) and David et al. (1958, 1959) reported the magnitude of unilateral deciBel shift necessary to offset the subjective displacement effect of a given  $\Delta t$  as a function of pulse train SL. Guttman (1960) reported the effects of Sensation Level and pulse repetition frequency (prf) on the perceived fusion of two successive clicks in one ear with a single, interposed,  $\Delta t$  click presented to the contralateral ear (Fig. 9.3a).

Only Klumpp et al. (1956) used pulse train stimuli solely to obtain  $\Delta T$ . They reported  $\Delta T$  in psychometric function form using single click pairs, 1-kHz tones, and narrow band noise stimuli (Fig. 1.1b). Klumpp et al. (1956), however, cited only the average  $\Delta T$  value of 11  $\mu$ sec. for the single SL pulse train stimulus described above. There appears to be no information concerning the form of the psychometric function for the pulse train  $\Delta T$  and the effect of SL on it.

#### PULSE TRAIN $\Delta T$ ; MULTIPLE OBSERVATIONS:

A general review of the literature reveals typical estimates of the  $\Delta T$  for single click pair stimuli within the range of 20 to 40  $\mu\text{sec}$ . However, smaller values of  $\Delta T$  have been obtained for:

(a) pulse train stimuli, viz., 11  $\mu\text{sec}$ . (Klumpp et al., 1956) and 19  $\mu\text{sec}$ . (Bekesy, 1930); (b) pure tone bursts, viz., 11  $\mu\text{sec}$ . at 1 kHz (Klumpp et al., 1956; Zwisllocki et al., 1956); and (c) noise bursts, viz., 5.5  $\mu\text{sec}$ . for a burst of 5 kHz low pass filtered white noise of duration longer than 700 milliseconds (msec.) (Zerlin, 1959).

The pure tone and noise bursts may be operationally considered as multiply-presented stimuli. The former may be viewed as a succession of sinusoidal cycles, the latter as a train of amplitude peaks randomly spaced in time.

This improvement of  $\Delta T$  with multiple stimulus presentations is not inconsistent with statistical theory which states that the mean of a population is estimated with a precision that increases as the square root of the number of observations in the sample. Green and Swets (1966, Chapter 9) derive an integration model of detection theory which predicts that  $d'$  will increase as  $N^{\frac{1}{2}}$  where  $N$  is the number of observations. They demonstrate multiple observation data, including Swets et al. (1959), to support this model.

As variables which may directly affect  $\Delta T$ , neither variation in prf for a constant stimulus duration nor varied duration of stimulus

for a constant prf have been investigated. In this regard the findings of Guttman et al. (1960) are relevant. At three Sensation Levels, 10, 20, and 40 dB, permuted with four prf's, 8, 20, 50 and 125 pps, they determined "the minimum interval at which two monaural clicks can be resolved" in fusion with a single click delivered to the contralateral ear. Their JND's, ranging from 3 msec. through 6 msec., decrease at a slightly slower rate than predicted from an application of the  $N^{\frac{1}{2}}$  model (Fig. 9.3a). This approximation may be considered close when one notes that the observation interval duration, called  $X_c$  in the present study, was under control of the listener. Harmon et al. (1963) presented an electronic neural model specifically in terms of these (Guttman et al., 1960) data. In describing the effect of N on the model's output, Harmon et al. (1966) state:

"...as stimulus repetition rate was increased by a factor of 16, the minimum detectable interval between two input pulses diminished by a factor of two."

The concept of  $\Delta t$  detectability proportional to  $N^{-\frac{1}{2}}$  is modified in a model, outlined in Chapter V, derived from the results of the present study. In this model  $\Delta t$  detectability is proportional to  $N_e^{-\frac{1}{2}}$ . The construct  $N_e$  represents the average number of stimuli used by the subject in arriving at a decision on each trial. The ratio  $(N_e/N)^{\frac{1}{2}}$  is defined in the model as the construct E, the human

observer's efficiency relative to that of the Ideal Statistical Observer. Specific predictions of the present model are applied, in Chapter IX, to the pure tone interaural phase difference ( $\Delta\phi$ ) JND data of Zwisllocki et al. (1956) and Klumpp et al. (1956) as well as the noise burst ongoing interaural  $\Delta t$  JND data of Zerlin (1959). It may be shown that, in the general case,  $\Delta t$  is inversely proportional to  $E(N^{\frac{1}{2}})$ .

#### PULSE TRAIN $\Delta t$ : PSYCHOMETRIC FUNCTIONS AND SENSATION LEVEL:

Of those studies concerned with the  $\Delta t$  for click stimuli, only the investigations of Wallach et al. (1949), Klumpp et al. (1956), and Hall (1964) present data which may be cast in psychometric-function form. Furthermore, only Hall (1964) presents a family of psychometric functions whose parameter is SL. These data are reproduced, as published, in Figs. 1.1 and 1.2. The data of Wallach et al. (1949) and Hall (1964) are also graphically reconstructed in Chapter IV. The X/Y coordinates (Figs. 4.7 and 4.8) represent  $\Delta t$  in  $\mu\text{sec.}$  and Percent Correct, respectively.

The form of each function may be described as negatively accelerated, sloping upwards from the 50%-chance detectability level, for a  $\Delta t$  of 0, to asymptote. The replotted data of Hall (1964) (Fig. 4.8) demonstrate a decrease in declivity of each function and a concomitant increase in the  $\Delta t$  derived therefrom, with decreasing SL.



The effect of SL on the pulse train  $\Delta T$  may be indirectly ascertained in a number of related studies. For example, the trading relationship between interaural time difference and interaural intensity difference has been reported to depend upon overall intensity of the dichotic stimuli (David et al., 1958, 1959; Deatherage et al., 1959). As SL increases, the trading ratio, of  $\Delta t$  in  $\mu\text{sec.}$  to  $\Delta i$  in dB, decreases systematically. Deatherage et al. (1959), using low pass filtered click pairs, found low intensity (15 dB SL) values on the order of 120  $\mu\text{sec./dB}$ . At 40 dB higher (55 dB SL), the value had dropped to about 20  $\mu\text{sec./dB}$ . Trading ratios on the same order of magnitude were reported for pulse train stimuli by David et al. (1958, 1959). That is,  $\Delta t$  discrimination tends to become poorer at lower SL's.

Mickunas (1963) used electronically controlled pulse train stimuli, replicating Bekesy's 1930 "brass tube" measurements of auditory laterality as a function of interaural time-of-arrival difference. Mickunas (1963) had listeners match apparent position of an air puff in relation to the forehead with perceived position of the sound image produced by the pulse train. He found, as did Bekesy (1930), that apparent laterality of the image varies linearly with  $\Delta t$ . Incorporating into his study the additional variable of Sensation Level, Mickunas (1963) reported the slope of his perceived displacement function, obtained from a given listener, to be

independent of Sensation Level at either 30 dB or 60 dB SL.

However, considering the findings of Deatherage et al. (1959), David et al. (1958, 1959), Zwisllocki et al. (1956), and Zerlin (1959), it is clear that both Mickunas' (1963) SL's were at the asymptote of the function relating  $\Delta T$  to SL.

Two studies reporting the effect of Sensation Level on  $\Delta T$  for pure tone and noise stimuli are particularly relevant. Zwisllocki et al. (1956) reported a systematic decrease in the interaural  $\Delta\phi$  for pure tone stimuli as a function of increased SL, within limits (Fig. 9.4b). The dB asymptote for this improvement in  $\Delta\phi$  varies with frequency; viz., through 30 dB SL at 250 Hz, 50 dB SL at 500 Hz, and 70 dB SL at 1 kHz. For pure tones,  $\Delta\phi$  asymptote may be more a function of sound pressure level (spl) than SL. Zerlin (1959) reports a similar decrease in the ongoing interaural disparity,  $\Delta T$ , for an 800 msec. burst of noise, from 12.5  $\mu$ sec. at 23 dB spl through 5.5  $\mu$ sec. at 83 dB spl. Asymptote for each of these two studies cited immediately above, where overall intensity was a variable, appears to be reached within the range of 30 dB through 60 dB SL. This is also the SL range in which the minimum JND values for monotic  $\Delta f$  and  $\Delta I$  discrimination have been obtained (Harris, 1952, 1963).

It is postulated in this thesis that the systematic increase in size of the  $\Delta T$  with decreasing SL is attributable to an

increase in the magnitude of internal noise,  $J_{iy}$ , correlating with the intensitive sensitivity of those sensorineural channels serving the  $\Delta t$  stimuli.

#### INTERNAL NOISE:

The concept of internal noise has had a lengthy history in psychophysics. Green (1964) states that internal noise:

"[as a]...random perturbation of the sensory processes, was the main impetus toward the development of psychophysical methods. Internal noise is an inferred quantity, its presence deduced from its manifest effects....On an operational level, internal noise is equivalent to the observation that the same physical stimulus may elicit different responses. In a sense, then, internal noise is the limiting factor in a trial-by-trial prediction of the subject's response."

Concerning physiological internal noise, manifest as a temporal uncertainty in the auditory neural pathways, Pollack (1968b) presents a comprehensive review of the literature. He states:

"There is an indirect way of estimating the temporal jitter of the auditory system. If we impose an external jitter on top of the internal system jitter, and if we find no change in sensitivity until we impose an external jitter greater than a critical level, we might have a basis for estimating the lower bound of the internal jitter..."

However, he goes on to state that his data, in the form of psychophysical functions of JND percent diotic jitter, as a function of percent baseline jitter, do not support this theory. As the majority of his reported stimulus periods are brief enough to be considered within the range of spectral processing within the auditory system, as opposed to temporal processing, this approach to a quantification of internal noise should not have been discarded so easily.

Actually, this method for estimating internal noise, through superimposition of external noise on a  $\Delta t$  detection task, was considered by this author as early as 1965 (Grason-Stadler Corporation, personal correspondence). The initial idea was derived from a study of Bekesy (1933; see also 1960) in which he estimated the physiological decay time of a pure tone stimulus by decreasing the acoustical decay time until the change was no longer noted.

In his didactic article on psychoacoustics and detection theory, Green (1960) suggests that, for the signal-known-exactly observer,

"...one can show how a specific type of internal noise can simply be treated as adding noise at the input of the detection device. Thus one can evaluate the psychophysical function and it will be shifted to the right by some number of decibels due to the internal noise."

However, as did Pollack (1968b), Green (1960) rejects this assumption on the basis of psychophysical data presented.

In the same article Green proposes three steps toward the ultimate specification of internal noise:

"....If the concept is to have any importance it must be made specific. This implies that we have to (1) state exactly what this noise is, i.e., that we have to characterize it mathematically, (2) specify in what way it interacts with the detection or discrimination process, and (3) evaluate specifically what effect it will have on performance. Unless these steps can be carried out the ad hoc nature of the assumption vitiates its usefulness."

The two Experiments in this study have been designed with these steps in mind.

## CHAPTER II

## EXPERIMENT I: INSTRUMENTATION AND CALIBRATION

Fig. 2.1a is a photograph of the instrumentation employed in this investigation carried out in the Audiology Research Laboratory, Division of Audiology of the Department of Otolaryngology, The Long Island College Hospital, Brooklyn, New York. Fig. 2.1b presents RELOPS, a custom Relay Logic Programming System for observation trial control and response recording. Fig. 2.1c shows the subject apparatus contained in the IAC Model 400 sound-isolated test room. Typical interior noise levels during a run, measured on a calibrated General Radio 1551-B sound pressure level meter, were: 27 dB A; 44 dB B; 59 dB C. A block diagram of the instrumental array used in Experiments I and II is illustrated in Fig. 2.2.

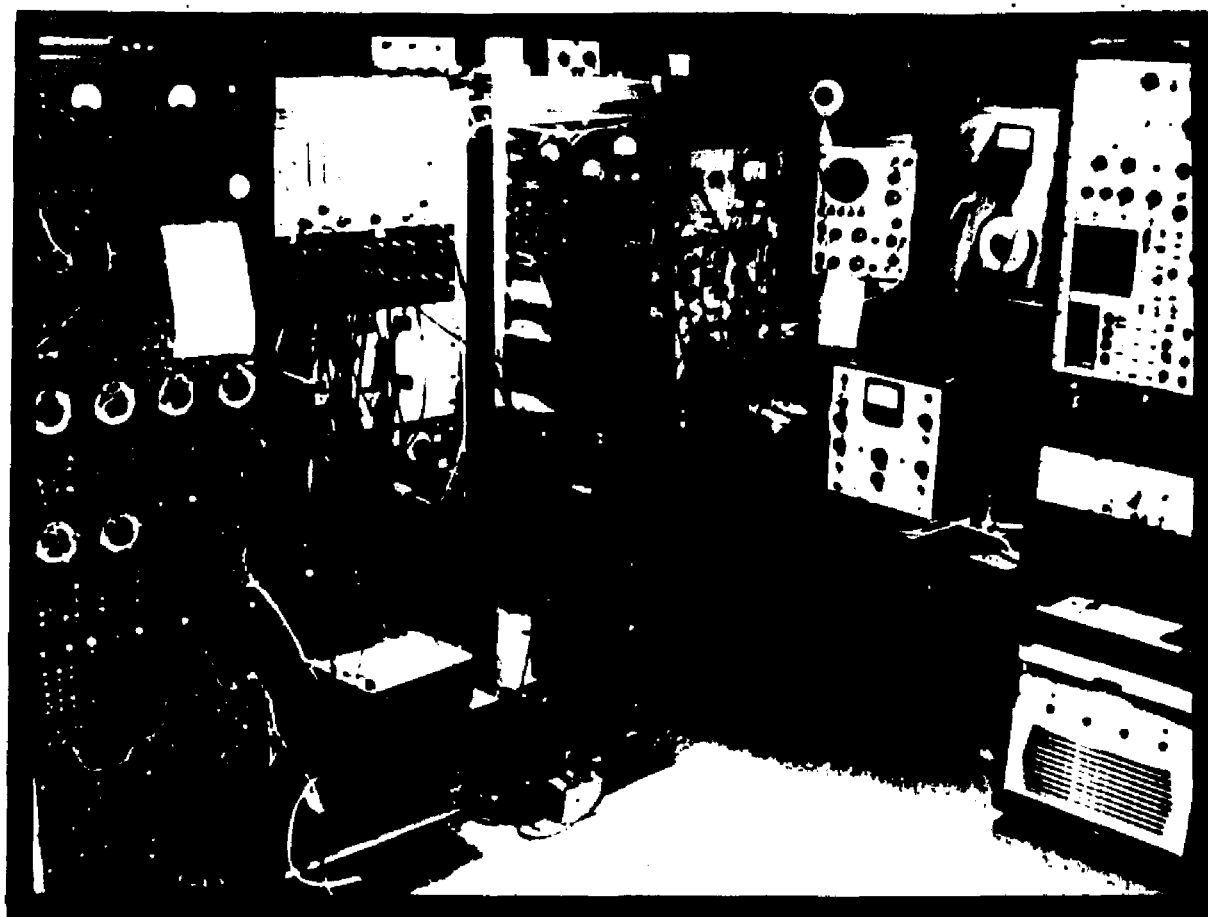
## RELOPS:

A Relay Logic Programming System, RELOPS, was used to control this experiment and provide a permanent record of the raw data. This system (Fig. 2.1b) was designed, wired, hand-constructed, and finished in entirety by the investigator, using only OEM components.

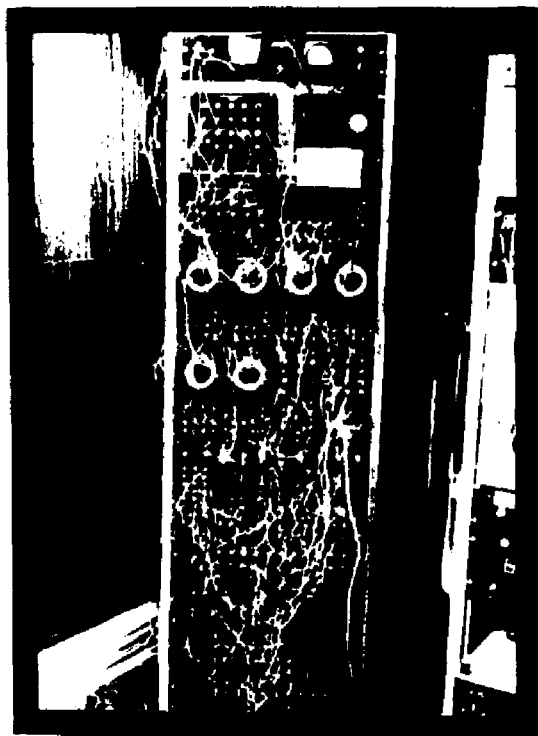
The a priori probability of signal occurrence,  $P(s)$ , is determined by 35 mm punched-film, mounted on a Gerbrands three-channel, sprocket-feed film advance. The tape programmer control for the system was built by the investigator. Six plug-in, 15-second range, electro-mechanical timers, controlled the subdivisions of each observation trial: REST, READY, LISTEN, RESPOND, REINFORCE. These intervals were visually delineated for the subject, with optional

Figure 2.1

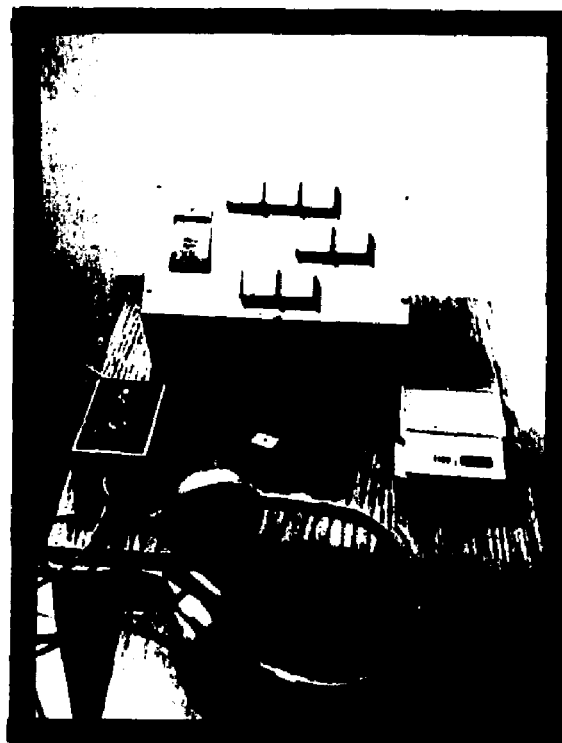
- A. Audiology Research Laboratory; Division of Audiology, Department of Otolaryngology, The Long Island College Hospital, Brooklyn, New York.
- B. RELOPS: Relay Logic Programming System for Audiological Research.
- C. Subject apparatus contained in soundproof test booth.



A



B



C

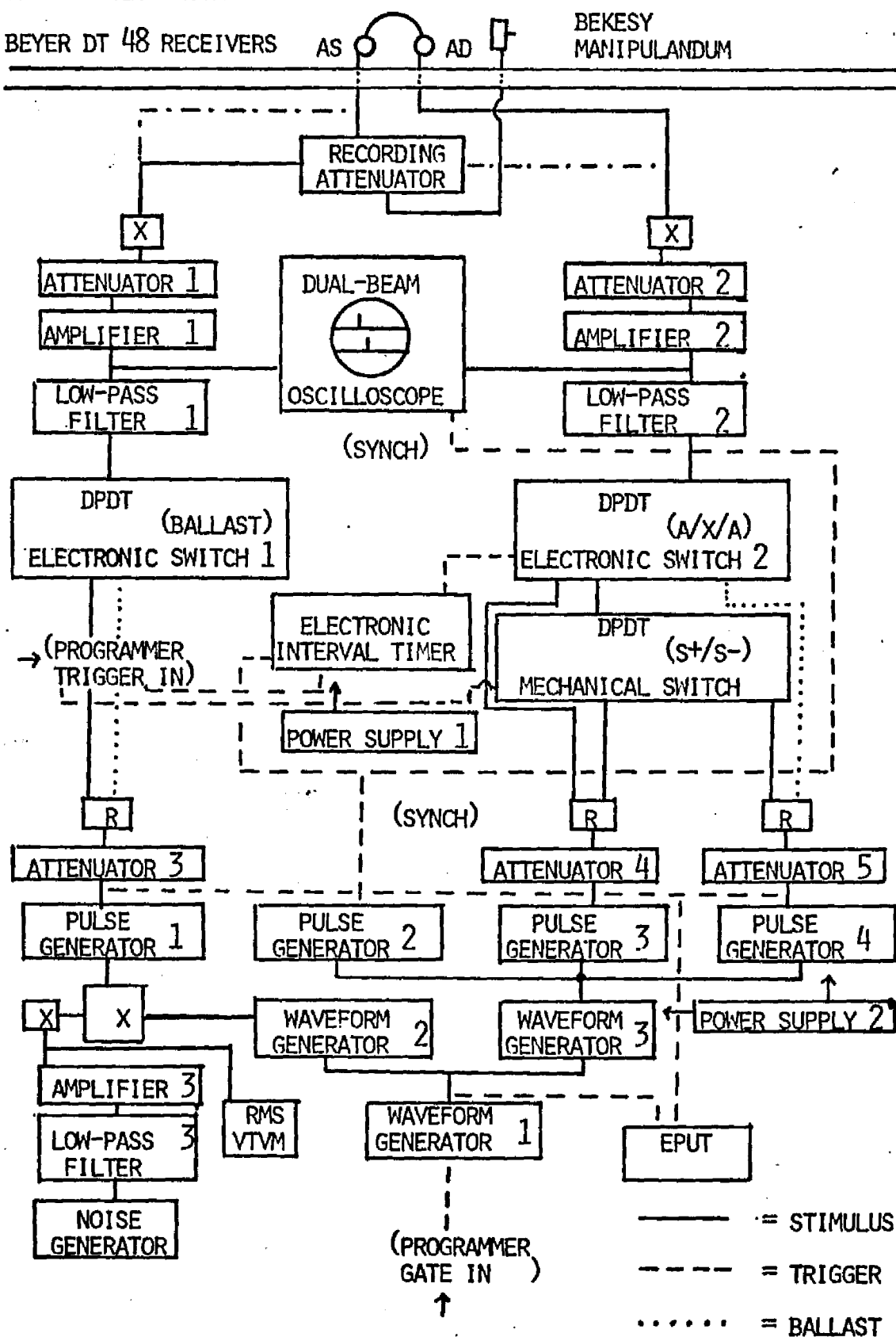


Figure 2.2

Block diagram of the stimulus generation and control instrumentation employed in Experiments I and II.

IAC 400 TEST ROOM

BEYER DT 48 RECEIVERS

AS  ADBEKESY  
MANIPULANDUM

immediate feedback, by means of a subject interface and subject station box (Fig. 2.1c).

2.2 The number of practice and data trials was sorted through five DPDT bistable relays and a 10x12 level stepping switch. Individual responses were automatically segregated into the decision theory categories of "Hit", "Miss", "False Alarm", and "Correct Rejection". Data were integrated and displayed on a bank of four, four-digit electro-mechanical counters. A permanent trial-by-trial record of the data was kept through a five-channel, three-digit printout counter in the format: N; N/P(S|s); N/P(N|s); N/P(S|n); N/P(N|n). Twenty-four volt positive DC logic was provided by a voltage-regulated power supply.

#### SYSTEM ARTICULATION AND CALIBRATION:

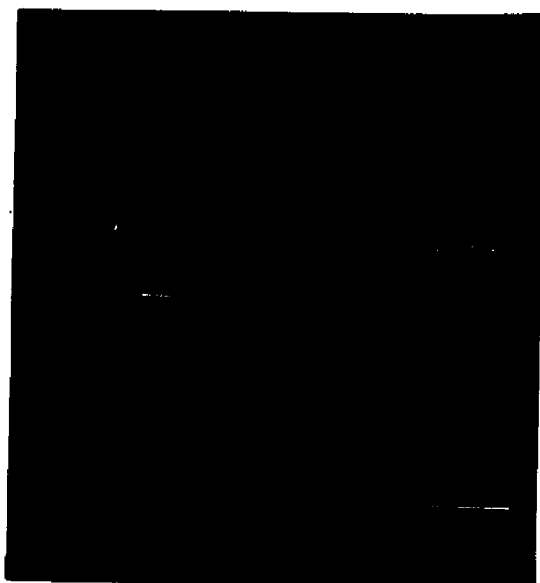
Durations of the component intervals of each trial (Figs. 3.1; 3.2) were controlled by the timers in RELOPS. Waveform Generator 1, a Tektronix Type 162, provided the basic 50-msec., 20-pps sawtooth ramp. This ramp was gated by a 4.00-second DC voltage, timed and triggered through DPDT relays in RELOPS. Aided by an idle option incorporated into these timers, all outputs were found replicable within a range of  $\pm 25$  msec. as observed on a Beckman Model 7350-A EPUT/Timer with oven-controlled crystal time base. This inaccuracy could result in a  $\pm 1$  pulse count in the A-reference segments (Fig. 3.1b) of the observation interval. The X segment of the observation interval was electronically timed by a Grason-Stadler Model 471 pulse-synchronized timer, so that exactly 20 pulses were gated on every trial.

Waveform Generators 2 and 3 were driven by Waveform Generator 1 at a 20 pps rate, with ramp durations of 10 and five msec., respectively. Pulse Generator 1, Tektronix Type 161, driven by Waveform Generator 2, provided a 100  $\mu$ sec. duration, electrically negative, rectangular pulse (Fig. 2.3a, lower trace). This ultimately served as the source of acoustic stimulus to the left ear (AS). Pulse Generators 2, 3, and 4 were driven by Waveform Generator 3, providing similar, matched, 100  $\mu$ sec. duration, electrical rectangular pulses. Pulse Generator 2 supplied triggering to the electronic interval timer, Tektronix 502 mod. dual-beam oscilloscope, and EPUT. Pulse Generator 3 provided all S+ stimuli to the right ear (AD) during the 1000 msec. X sub-interval of the LISTEN interval (Figs. 3.1; 3.2). Pulse Generator 4 provided all S- stimuli to AD during the 1.50 second A-reference and X-test sub-intervals of the AXA observation period. The pulse train period was strictly maintained at 50.00 msec., monitored by the EPUT. Calibration of the dichotic pulse pair simultaneity during the S- sub-intervals and the  $\Delta t$  lead to AD, was monitored to 10  $\mu$ sec. through the EPUT and to one  $\mu$ sec. accuracy with the oscilloscope.

Long-term accuracy of periodicity and  $\Delta t$  were also estimated by simulating repeated, alternate 1000 msec. bursts of S+ and S- to a 100 channel PAR Model TDH-9 Analog Average Response Computer. Averaging time and averager storage time constant were 10 minutes and 5.0 seconds, respectively. Averaged results indicate a high degree of stability. The unfiltered rectangular electrical signals, maintaining strict periodicity ( $J_e = 0$ ) with representative  $\Delta t$

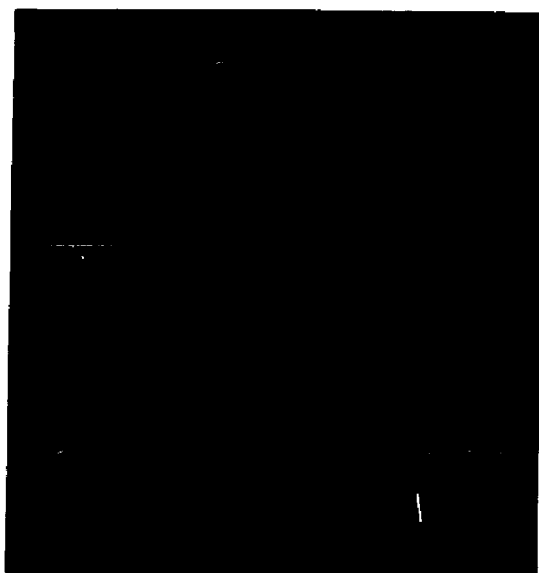
Figure 2.3

Oscilloscope displays of electrical and acoustical pulse stimuli, filtered and unfiltered. Time base is 100  $\mu$ sec. per horizontal division in A and B, 200  $\mu$ sec. per division in C.



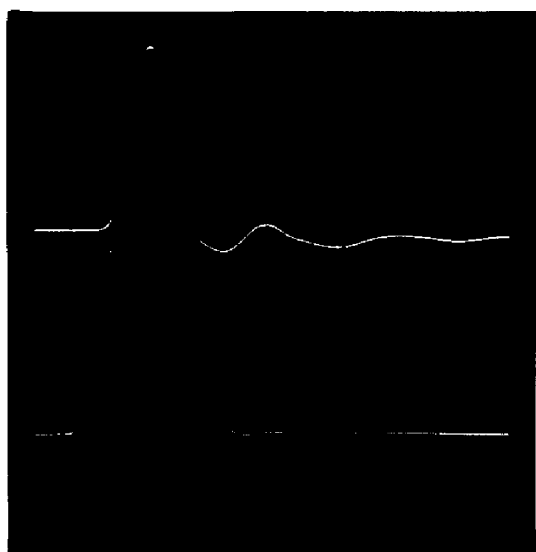
ELECTRICAL INPUT, 4.8 kHz LP FILTERED

ELECTRICAL INPUT, UNFILTERED 100 USEC.



ACOUSTICAL OUTPUT NBS 9A COUPLER

ELECTRICAL INPUT, 4.8 kHz LP FILTERED



AS ABOVE, SWEEP RATE 1/2

values, are depicted in Fig. 2.4. The total sweep duration is 1 msec., 10  $\mu$ sec. per bin.

Stability of the Tektronix signal generators was improved by substitution of 10-turn, wire-wound potentiometers for the single-turn carbon verniers provided by the manufacturer. The subsequently determined standard deviation, for 400 randomly sampled interpulse intervals (IPI's), was 3.29  $\mu$ sec. in the AS channel. This interval extended from a common 50 msec. trigger point, commencing run-down of all four pulse generators, to the appearance of the AS pulse. The AS channel (PG 1) was selected for IPI calibration as it had the longer duration trigger ramp, 10 msec., and therefore greater potential for instability. Interchannel instability was estimated to be significantly less than three  $\mu$ sec. by observation of both AD and AS pulse outputs on the one  $\mu$ sec./cm range of the dual-beam oscilloscope. Subsequent experimentation indicated (Chapter VIII) that interchannel instability less than 20  $\mu$ sec. had negligible effect on  $\Delta T$ .

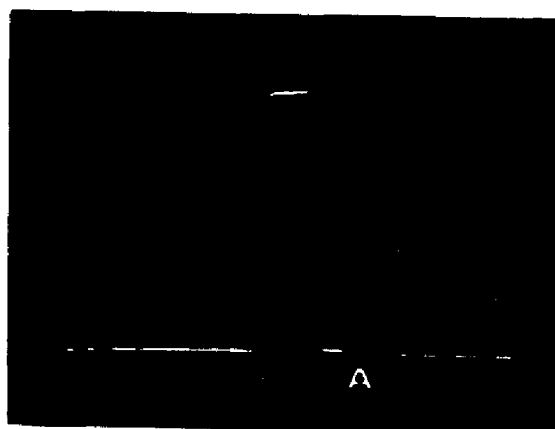
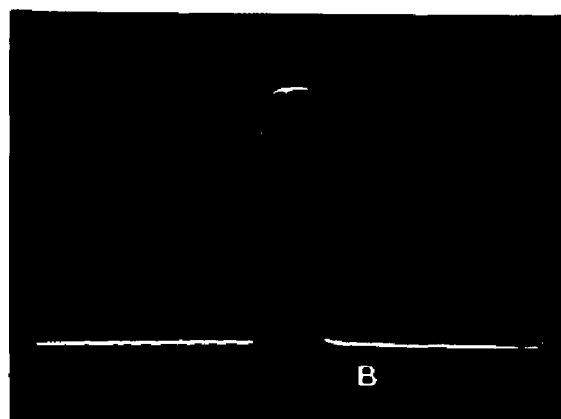
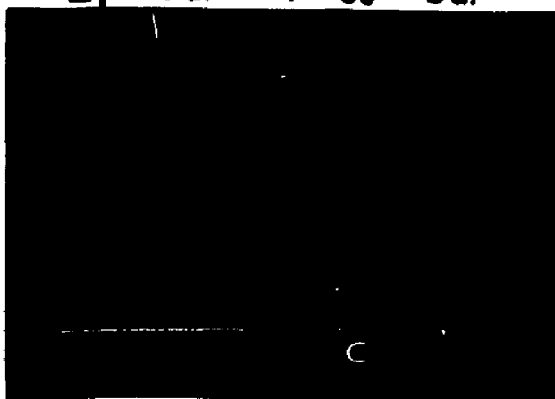
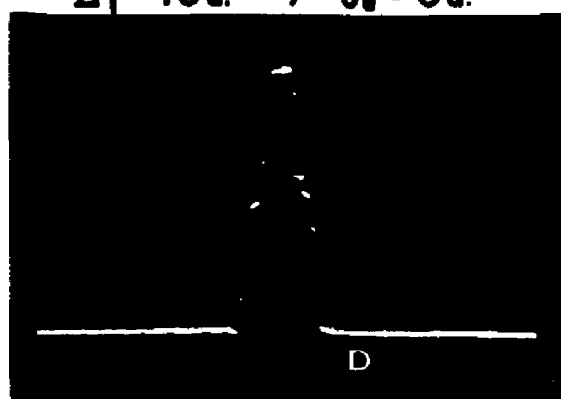
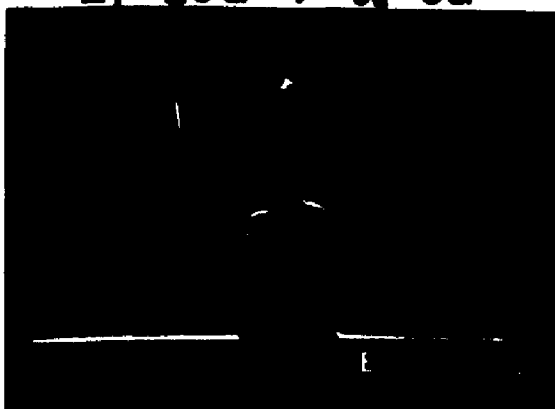
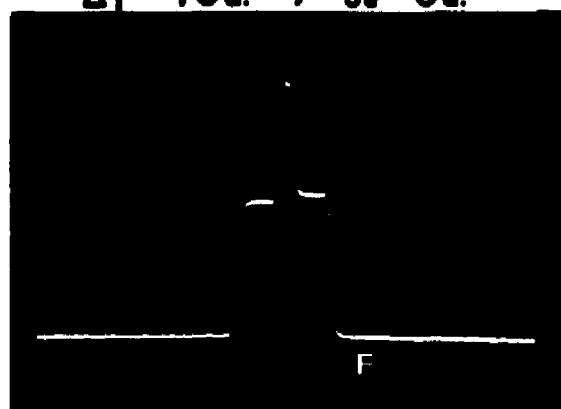
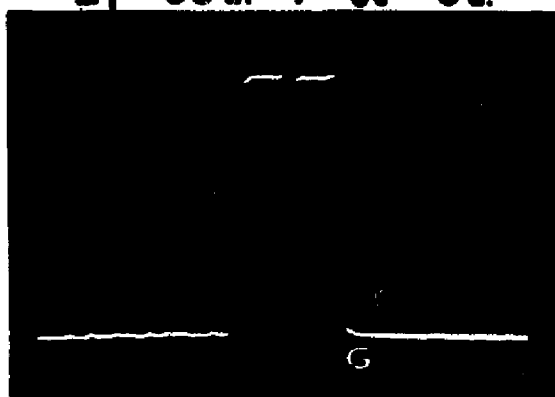
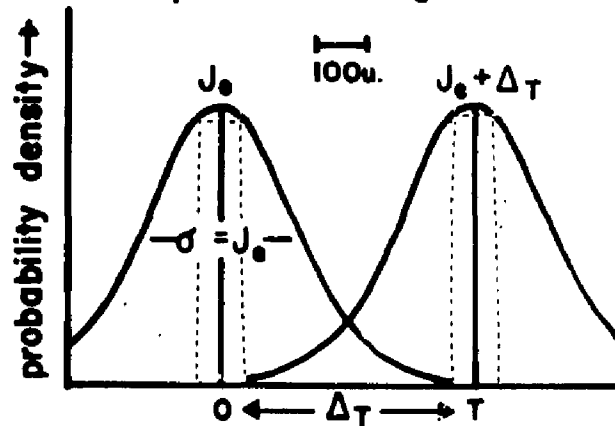
Two channels of a three-channel punched-film advance in RELOPS read the 200-trial loop of tape, punched according to a table of random numbers (Rand Corp., 1966), to represent  $P(s) = P(n) = 0.5$ . Six such tapes were fabricated. They could be started at any point on the loop. Consequently, some runs of 50 trials contained slightly more or less than 25 S+ trials, the balance being made up, on that run, by S- trials. Across four runs, totalling 200 data trials, S+ and S- parity generally prevailed.

A DPDT relay, under control of the tape programmer, switched to

Figure 2.4

One hundred channel analog averager simulating a differential response to a two-channel unfiltered rectangular 100  $\mu$ sec. pulse input. Leading edges of the alternating inputs are separated by the indicated values of  $\Delta t$  in  $\mu$ sec. Pulse height differentials in D, E, and F are artifacts of averager input amplitude imbalance. Pulse heights in G are compensated. Oscilloscope total sweep duration is 1 msec., 100  $\mu$ sec. per division.




 $\Delta_T = 0u. / J_0 = 0u.$ 

 $\Delta_T = 10u. / J_0 = 0u.$ 

 $\Delta_T = 20u. / J_0 = 0u.$ 

 $\Delta_T = 40u. / J_0 = 0u.$ 

 $\Delta_T = 60u. / J_0 = 0u.$ 

 $\Delta_T = 80u. / J_0 = 0u.$ 

 $\Delta_T = 100u. / J_0 = 0u.$ 


either S+ or S- during the REST interval of the trial. A fail-safe in RELOPS insured completion of the electro-mechanical switching prior to commencement of the LISTEN observation interval. The electronic interval timer was triggered from RELOPS after 1.5 seconds of the 4.0 second LISTEN interval had elapsed. On both S+ and S- trials, the electronic timer triggered DPDT electronic switch 2, Grason-Stadler Model 829-E. This switching was accomplished with a 10 msec. rise-decay time during the 50 msec. silent interval between pulses, bridging the 1.50 second A and 1000 msec. X sub-intervals (Fig. 3.2). Duration of the test sub-interval,  $X_t$ , was 1000 msec.,  $\pm 50 \mu\text{sec.}$  Exactly 20 pulses were passed in each X observation sub-interval.

Special care was taken to avoid interaction between pulses and electrical switching transients. It should be noted that electronic switching was inserted only in the AD channel. The switching paradigm is schematically illustrated in Fig. 3.2. Electrical switching artifacts could be observed in the AD channel on the dual-beam oscilloscope. However, the same transients were present on both S+ and S- trials. The switching artifact of the fully articulated system was attended, by a panel of impartial listeners, through the output transducers in the absence of the physical pulse stimuli. The switching transient could not be differentially detected in the presence or absence of the signal.

Electronic switch 1, Grason-Stadler 829-D, served only as reactive line ballast to match stimulus frequency content between the AS and AD channels. Passive variable LC filters 1 and 2, Allison Model

2-BR, were adjusted to limit the frequency content of electrical pulse stimuli from each channel below 4.8 kHz. The roll-off was 30 dB per octave beyond the half-power point. The effect of filtering on physical stimulus latency and rise time may be observed in Figs. 2.3a, upper trace, and 2.3b and 2.3c, lower trace.

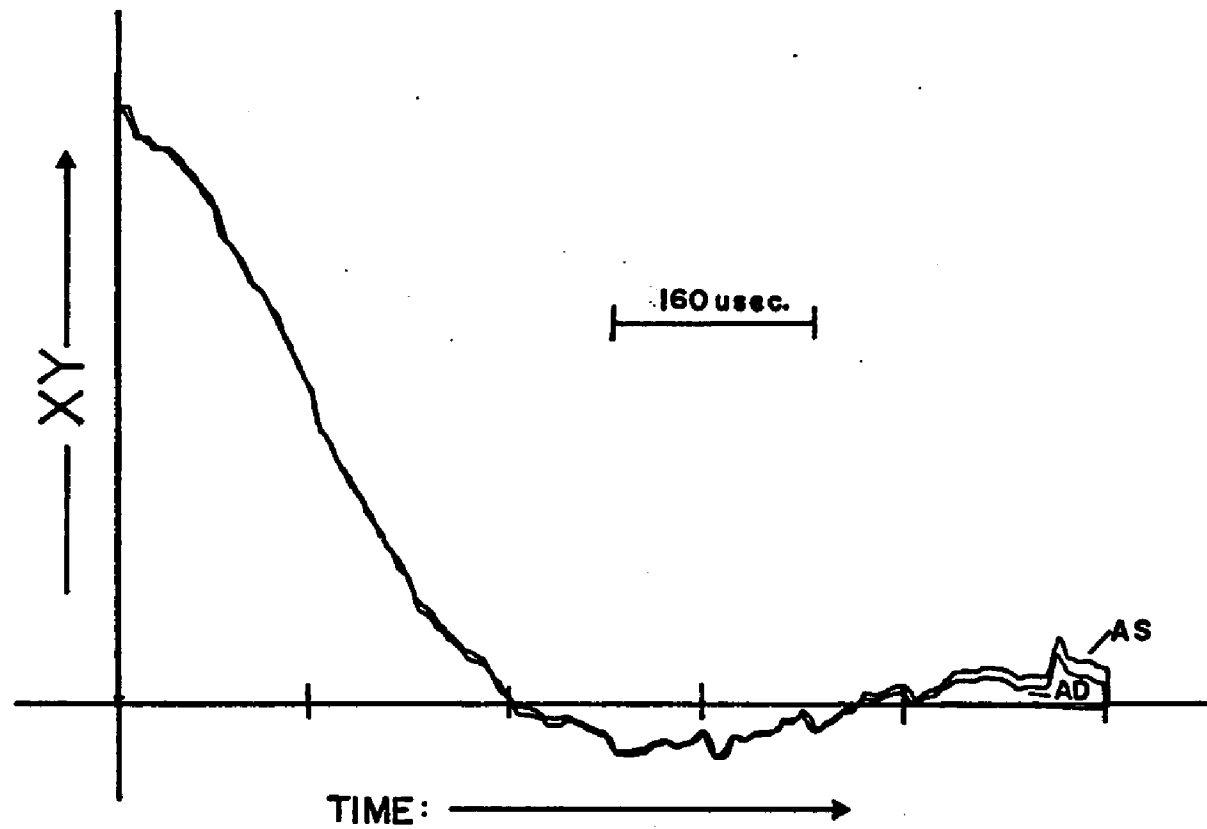
The exact degree of stimulus matching achieved between channels can be seen in Fig. 2.5. A PAR Model 101 Correlation Function Computer was used to generate overlapped autocorrelation functions of the acoustical outputs from the two earphones. The low-pass cutoff frequency was selected in order to provide a compromise between maximally punctiform acoustic output and minimally reduced overall amplitude. These measurements were made from the earphones, via condenser microphone in an artificial ear, to an oscilloscope display.

Filter outputs led to dual McIntosh 30 watt power amplifiers and 1 and 10 dB step, 110 dB total, Hewlett-Packard 350-BR Attenuators, respectively. Finer control of intensity was achieved, at a point in the instrumental array immediately following the pulse generators, by means of four banks of Langevin 600 ohm RAT 500 series precision attenuators, in steps of .1, 1, and 10 dB.

The output of either HP attenuator could be led through a .25 dB-step Grason-Stadler Model 3262-A recording attenuator operating at a 2 dB per second rate. Acoustical stimuli were ultimately delivered to the subject by means of headband-mounted Beyer Model DT-48 magnetic receivers with supra-aural cushions. Electrical voltage checks (B&K Model 2416 rms voltmeter) and time calibration

Figure 2.5

Autocorrelation functions for the 4.8 kHz. low - pass filtered earphone acoustical output to an NBS 9A coupler. AS and AD are superimposed as indicated.



checks (EPUT and CRO), together with necessary adjustments, were performed before and after each run. In addition, the system's electrical stimulus outputs were continuously monitored during the course of each run.

#### ACOUSTICAL CHARACTERISTICS:

Figs. 2.3b and 2.3c demonstrate the 4.8 kHz low-pass filtered electrical input and acoustical output of the earphones. Acoustical measurements were made with a B&K Model 4152 NBS Type 9-A coupler, B&K Model 4132 one-inch pressure field condenser microphone, B&K Model 2613 Cathode Follower, and B&K Model 2603 Microphone Amplifier. The response of the latter instrument was flat through the 2-40,000 Hz range. The output was photographed from the face of the dual-beam CRO with a Polaroid Model 110-A tripod-mounted camera with appropriate close-up lenses, using ASA 3000 speed film. The time base depicted is 100  $\mu$ sec. per horizontal division in Figs. 2.3a and 2.3b; 200  $\mu$ sec. per horizontal division in Fig. 2.3c.

In response to the unfiltered 100  $\mu$ sec. rectangular input pulse, having a nominally observed rise time of eight  $\mu$ sec. (Fig. 2.3a, lower trace), the earphone followed with an estimated rise time of 100  $\mu$ sec. through the calibration system. It should be noted that, while the output of the calibration amplifier is rated as linear from 2 Hz through 40 kHz, the calibration microphone frequency response falls off sharply above 8 kHz. This limits the maximum acoustical rise time measurable by this method to  $1/4f$  seconds. This is approximately equivalent to 31  $\mu$ sec. when the stimulus is

passed below 8 kHz. In response to the 4 kHz low-pass filtered input, with an estimated electrical rise time of 150  $\mu$ sec. (Figs. 2.3b and 2.3c, lower trace), the acoustical output, a compression pulse, followed with a measured rise time of approximately 170  $\mu$ sec. (Figs. 2.3b; 2.3c, upper trace).

For sound pressure level calibration, a variation of the peak equivalent calibration method described by Deatherage (1961) was used. A half sine wave was matched in form and amplitude to the oscilloscopically displayed acoustical compression pulse. Observation indicated a best match at 2 kHz. Peak equivalent spl responses of the earphone, to that sine wave frequency input, were measured at 128.5 dB AD and 128.2 dB AS. The input level was nominally referenced to 10 dB below maximum output of the power amplifiers. This interchannel dB balance was observed to obtain at lower spl levels, until the ambient acoustical noise floor in the laboratory began to interact with the reduced acoustical pulse pressure level. The subjects' pulse detectability thresholds, for an unlimited duration 20 pps train of the stimulus as described, ranged from 35 dB through 40 dB peak equivalent sound pressure level. Acoustical calibration checks were repeated regularly throughout the course of data collection.

## CHAPTER III

## EXPERIMENT I: METHODS AND PROCEDURES

3.1 The acoustical stimulus consisted of a train of dichotic, 4.8 kHz, low-pass filtered rectangular compression pulses presented at a prf of 20 pps. The observation interval was of the AXA type (Fig. 3.1; 3.2), lasting 4.00 seconds, where X consisted of either S- or S+. The initial and final 1500 msec. of each observation interval served as subjective midline reference. That is, A always represented the S- condition, where  $\Delta t = 0$ .

3.2 The median 1000 msec., of each 4.00 sec. observation interval, served as the critical observation sub-interval, X. During the X portion of the AXA paradigm, pulses were presented to both ears either simultaneously (S-), or with a time lead to AD (S+). In Experiment I, the pulse train period was maintained at a constant 50.00 msec. Stimuli were presented at three representative SL's to each of three subjects. A method of constant stimulus, YES/NO paradigm with P(s) of 0.5 was used. Subjects were to indicate, by pushbutton selection, whether or not a shift to the right of subjective midline was perceived in the pulse train image during the X observation sub-interval. Four runs, of ten orientation trials and 50 data trials per run, were given each subject for the various combinations of  $\Delta t$  and SL selected for investigation.

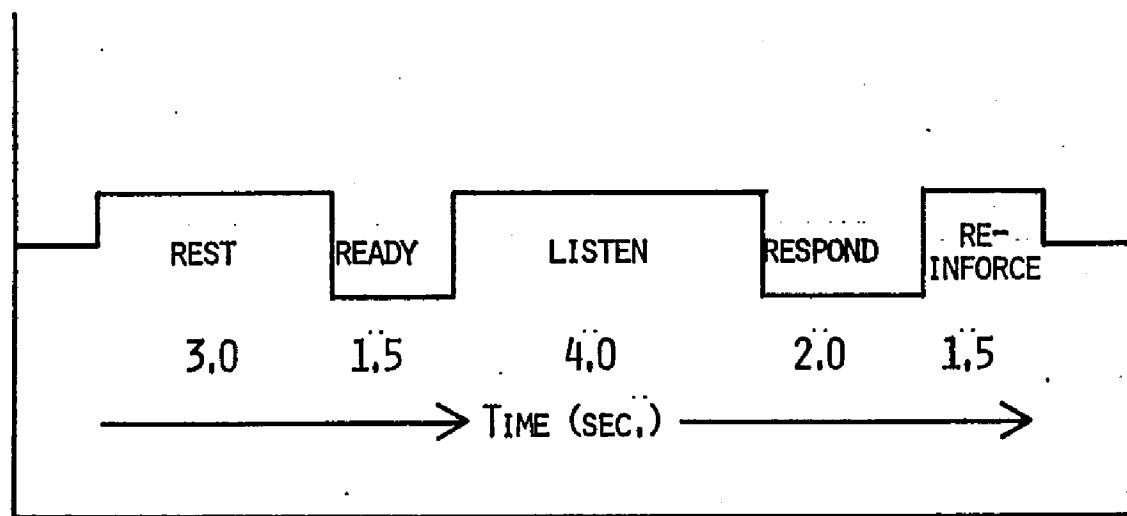
## SUBJECTS:

The one female (SLS) and two male (RFS, JEB) subjects were all 30 years of age at the outset of data collection. Both SLS and RFS

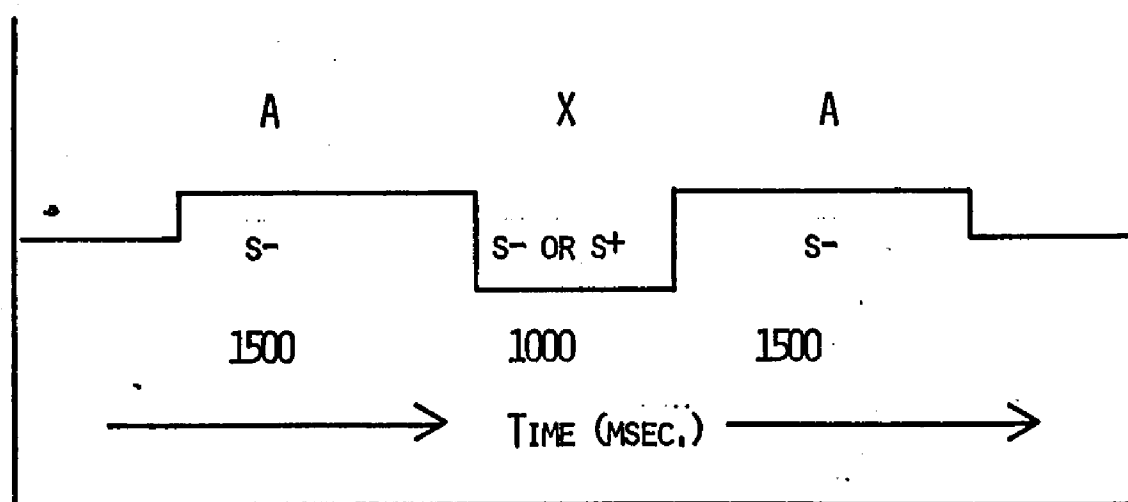


Figure 3.1

- A. Experimental trial intervals.
- B. LISTEN interval; AXA observation sub-intervals.



TRIAL PARADIGM



"LISTEN" INTERVAL

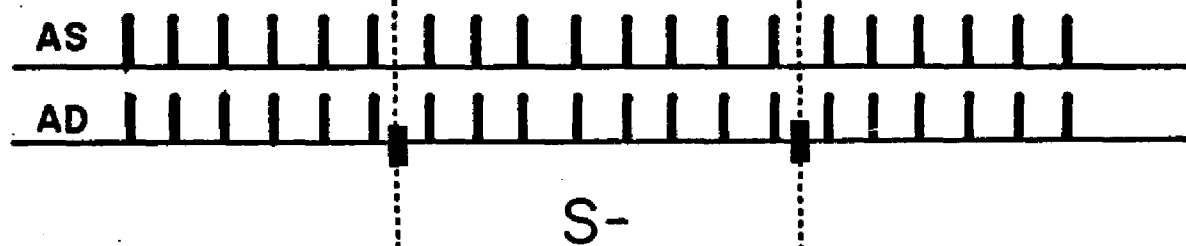
Figure 3.2

Graphically simulated relationships for the AXA paradigm pulse train inputs to AD and AS in Experiment I;  $J_e = 0$ ,

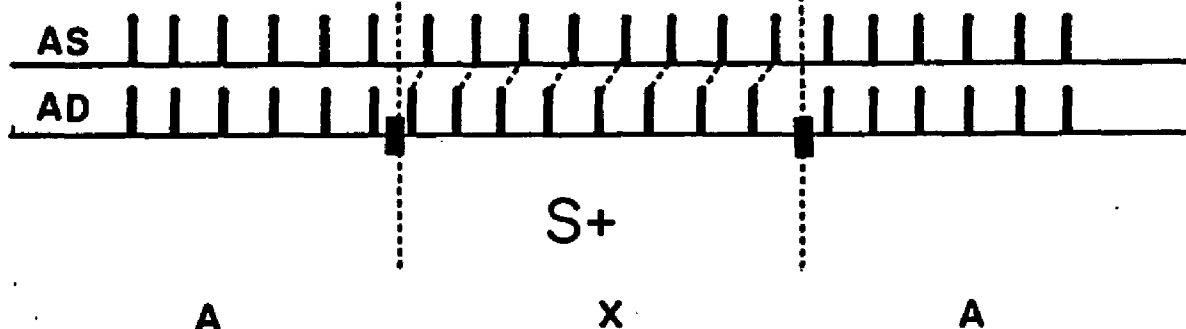
- A. S- condition, "blank" trial.
- B. S+ condition,  $\Delta t$  lead to AD.

# EXPERIMENT 1: $J_0 = 0$

a.



b.



A

X

A

TIME →

had extensive listening experience as participants in psychoacoustic experiments. JEB had no formal listening experience prior to this investigation. Each subject held a master's degree in audiology and volunteered his or her time to the study. All were employees in the Division of Audiology, Department of Otolaryngology, at The Long Island College Hospital, Brooklyn, New York.

Subjects were otoscopically examined and found to have bilaterally normal external auditory meati and tympanic membranes. The hearing of each subject met or exceeded a nominal screening level of 15 dB Hearing Level for pure tone sensitivity, within the frequency range 250 Hz through 4 kHz, according to the ISO 1964 audiometric standard (ISO, 1964). Two subjects (JEB and SLS) met the criteria throughout the entire audiometric frequency range at octave intervals from 125 Hz through 8 kHz. The third subject (RFS) demonstrated a traumatic type, punctiform, sensorineural notch, involving frequencies 6 kHz and above. His sensitivity was well within normal limits, however, through the previously stated screening frequency range. It should be noted that the pulse train stimulus was low-pass filtered at 4.8 kHz.

#### GENERAL PROCEDURES:

The following represents a description of steps taken and conditions which prevailed during the course of each listening session. Subjects were well practiced in these operations prior to undertaking actual data collection.

1. With the aid of a 100 dB recording attenuator, a pulse

detectability threshold was obtained in the right ear (AD).

Subjects were instructed to press the control switch when the 20 pps stimulus became audible, releasing it when it became in audible. This threshold was defined as the median point between positive and negative peaks of the continuous recording attenuator tracing averaged over a one-to-two-minute period. Pulse detectability thresholds ranged from approximately 35 dB to 40 dB peak equivalent spl for the three subjects. Typical tracing width was 5 dB. Once this level had been determined, it served a 0 dB Sensation Level. A similar threshold was always obtained from the left ear (AS) for reference purposes.

2. The pulse train spl was then raised in AD to the Sensation Level selected for investigation. For example, if the SL desired for study was 20 dB, and the subject presented a 40 dB spl peak equivalent threshold in AD, then the pulse train stimulus was presented to the right, or reference, ear at 60 dB peak equivalent spl.

3. With the appropriate SL pulse train presented to AD, the subject bracketed a median saggital plane lateralization of the pulse image by method of adjustment. This was accomplished by manipulating the intensity level of an identical, simultaneous pulse train in AS. This balance was made with the recording attenuator using a three-position control switch. Once subjective center had been achieved to the subject's satisfaction, it was tested for consistency by resetting the recording attenuator input and calling for another centering. If a  $\pm 2$  dB agreement was obtained, the amount of AS

attenuation remained fixed for the run. However, through the first 10 orientation trials of each run, subjects were permitted to add or subtract fixed levels of attenuation in steps of 0.25 dB in the AS channel. This correction was necessitated by the empirical observation of a drift in the subjectively centered pulse image, when it was gated in four-second, trial-by-trial intervals, through the early part of a run. This option was not available to subjects during the following 50 data trials.

4. On the basis of pilot data, three Sensation Levels were selected for each subject as being relatively representative of the spread of the family of  $\Delta T$  psychometric functions whose parameter is SL. In order to achieve the steepest psychometric function, tempered by a consideration for the subjects' tolerance thresholds, levels of 60 dB SL were necessary for subjects JEB and SLS, while a level of 40 dB SL sufficed for RFS.

Higher levels than 60 dB SL, approximately 100 dB peak equivalent spl, were judged uncomfortable by the first two subjects and resulted in no significant increase in slope of the psychometric function for the third subject. Sensation Levels of 5 dB resulted in too great a drifting of the subjectively centered pulse train image. This made results difficult to replicate in a reasonable number of trials.

As a consequence, the following Sensation Levels were selected for investigation:

Subject SLS: 60 dB SL; 40 dB SL; 10 dB SL.

Subject JEB: 60 dB SL; 40 dB SL; 10 dB SL.

Subject RFS: 40 dB SL; 20 dB SL; 10 dB SL.

These SL's, in decreasing order of intensity, shall be referred to as SL I, High; SL II, Medium; and SL III, Low.

5. It should be indicated at this juncture that, although Experiment I data are reported independently, they were obtained in the larger context of an experiment which incorporated conditions where pulse periodicity was intentionally perturbed (Experiment II).

6. Four runs, each consisting of 10 orientation and 50 data trials, were taken to represent the subject's response at each value of  $\Delta t$  for a given stimulus condition. The a priori probabilities were:  $P(s) = P(n) = 0.5$ . The total of 200 data trials per point was comprised of approximately 100 S+ and 100 S- presentations for every combination of  $\Delta t$ , SL, and  $J_e$ .

7. On a typical day, one subject may have completed as few as four runs or as many as 15. Each run consisted of 60 observations; 10 orientation and 50 data trials. Each trial took 12 seconds to complete. The entire run, exclusive of pre- and post-run calibration, took 12 minutes. Allowing for rest periods and calibration, the average run entailed about 30 minutes. Shorter sessions, with fewer runs, resulted in somewhat less average time per run. It was left to the subject's discretion to indicate when he or she felt ready to run or was too fatigued to continue. Data could not be



obtained on a regularly scheduled basis because of the variable clinic test schedule governing each of the three subjects.

8. With the exception of  $\Delta t$ , stimulus parameters remained constant during a listening session. For example, subject SLS might have devoted an entire afternoon to running an Experiment I condition; e.g.: 60 dB SL, with stable periodicity ( $J_e = 0$ ). The next session may have been run at a level of 40 dB SL with an intentionally perturbed stimulus periodicity ( $J_e \neq 0$ ); that is, Experiment II.

9. Using the YES/NO method,  $\Delta t$  remained constant for any given run but was generally varied in a quasi-random manner among the runs of the day. The only restriction applied to the ordering of  $\Delta t$  values for successive runs was that extreme leaps were to be avoided. A typical sequence of runs might be: 100  $\mu$ sec., 60  $\mu$ sec., 20  $\mu$ sec., 0  $\mu$ sec. (control), 40  $\mu$ sec., 80  $\mu$ sec., etc.

10. Intervals between  $\Delta t$  values were spaced to allow reasonable determination of the "grain" of the psychometric function. In the YES/NO procedure, the psychometric function is expected to rise, from the 50% chance performance level, in the absence of an S+ stimulus, to asymptote. For example, spacing may have been in 5  $\mu$ sec. or 10  $\mu$ sec. steps at SL I; 10  $\mu$ sec. and 20  $\mu$ sec. steps at SL II; and 20  $\mu$ sec. or 25  $\mu$ sec. at SL III. When percent correct scores, for a given function, exceeded 80%,  $\Delta t$  spacings were doubled. Functions were extended until scores for each of the four runs equalled or exceeded 90% correct for a given  $\Delta t$ .

# METHOD; ORIENTATION AND DATA TRIALS:

The following represent the specific methodological steps taken on each trial.

1. Durations of the intervals within each observation were comfortable for all subjects. The time pattern was the same for both orientation and data trials. Each observation was divided as shown in Fig. 3.1a; viz., REST, 3.0 sec.; READY, 1.5 sec.; LISTEN, 4.0 sec.; RESPOND, 2.0 sec.; REINFORCE, 1.5 sec. The trial paradigm recycled immediately from REINFORCE to REST. Figure 3.1b schematically illustrates the AXA sub-intervals contained within the LISTEN interval. The observation interval is referred to as an AXA paradigm, where A is the S- condition of 1500 msec. duration, containing 60 simultaneous pairs. The X portion of the observation interval, of duration  $X_t$ , 1000 msec., contains exactly 20 pulse pairs whose interaural time relationship will either be S- or S+. That is,  $\Delta t = 0$  or  $\Delta t \neq 0$ , respectively.

2. Figures 3.2a and 3.2b represent the S+ and S- conditions for Experiment I. Each vertical bar simulates a pulse. Actually, with a 20 pps repetition frequency and a 4-second LISTEN interval, each trial contained 80 pulses. A smaller number of pulses was used in the illustration to preserve clarity. The vertical alignments between pulses, in rows labelled AS and AD, indicate the temporal relationships of pulse presentations to each ear.

Figure 3.2b represents the S+ condition, where subjects were given a four-second burst of 20 pps clicks. During the median one-second

interval, the clicks delivered to AD were advanced by  $\Delta t$ , relative to AS. Slashes, in the AD channel representation, indicate the point of electronic switching. If the time lead was of requisite magnitude, it was perceived as a shift of the subjective intracranial pulse image from midline toward the lead ear (AD) and back to midline.

Figure 3.2a schematizes the "blank" trial, the S- control condition. Here, the stimulus consisted of a continuous four-second burst of diotic clicks. Electronic switching takes place in both the S- and S+ conditions. Pulse duration, relative pulse amplitude, prf, and period remained constant throughout Experiment I.

3. On each trial, the subject attended to the pulse train during the LISTEN interval. He reported by pushbutton, during the RESPOND interval, whether or not he noted any form of qualitative change during the median second of that four-second LISTEN interval. The change most typically noted was a shift in lateralization toward the lead ear, AD. However, subjective changes in pitch, quality, or loudness of the stimulus were also perceived by the subjects. Extra-temporal physical bases for these cues were effectively ruled out through procedures described in the preceding chapter.

4. The YES/NO version of the method of constant stimuli was employed throughout the study.

5. Each subject was provided with immediate CORRECT/WRONG visual reinforcement on the outcome of each trial. CORRECT was used to

avoid the directional connotation of "RIGHT".

6. The subjects were given 10 "free" trials at the outset of each run with the option to respond and receive immediate visual reinforcement or merely listen without reinforcement. During the run of 50 data trials, the subject may have missed some portion of the LISTEN interval because of a cough or momentary lapse of attention, etc. The subject was permitted to forego a response on that trial. The random programming tape advanced to the next trial state, with notation of this contingency inserted automatically into the data printout. Subjects were cautioned to avail themselves of this option sparingly. Examination of the records indicated its infrequent use.

7. The subject started each run by depressing the READY button on the subject box. The run ended automatically when 50 data trials had been completed.

8. Critical stimulus parameters were calibrated immediately before and after each run. These included pulse period, position of the AS reference pulse relative to Waveform Generator 1 ramp onset,  $\Delta t$ , pulse duration, and pulse amplitude. Stimulus output was monitored continuously on an oscilloscope during the course of each run at the final amplification input stage.

9. Data were tallied through a printout in RELOPS, trial by trial, in five 3-digit fields headed: (1) Cumulative Trial N, (2) Cumulative N "Hits", (3) Cumulative N "Misses", (4) Cumulative N "False

Alarms", (5) Cumulative N "Correct Rejections". Results of the first 10 orientation trials were printed separately from the data trials. Bypassed trials were noted by means of a repetition of the trial number with no change in response tallies.

#### FORMS OF THE DATA:

The collected data of both Experiments I and II were processed for graphic presentation as psychometric functions in three forms of display for each subject:

1.  $d'$ : Straight line fitted functions on X/Y coordinates of  $\Delta t$  and  $d'$ , respectively, with dB SL as parameter. According to the model developed in Chapter V, these functions should all radiate from the origin, with slope decreasing with Sensation Level. If the Y intercept is, in fact, 0, then performance may be simply characterized by a single number, i.e., the slope of each psychometric function. In order to compare results of the present study with  $\Delta t$  values obtained by others, reciprocal slope or slope<sup>-1</sup> of each  $d'$  psychometric function will be taken as the best estimate of  $\Delta T$ , the  $\Delta t$  JND.

2. Percent Correct: Functions were obtained of the quantity:

$$\% \text{ Correct} = P(S|s) P(s) + P(N|n) P(n), \quad (3.1)$$

which, for the symmetrical case where  $P(s) = P(n) = 0.5$ , becomes:

$$\% \text{ Correct} = P(S|s) + P(N|n) / 2. \quad (3.2)$$

These functions are presented with dB SL as parameter, having X/Y coordinates of  $\Delta t$  and Percent Correct, respectively. It is predicted that Percent Correct values will rise from 50%, at  $\Delta t = 0$ , to asymptote as the negatively accelerated upper half of the cumulative normal distribution.

3. HIT and FALSE ALARM rates: With SL as parameter, dual functions of  $P(S|s)$  and  $P(S|n)$ , as a function of  $\Delta t$ , are presented on the same X/Y coordinates. Given equal a priori stimulus probabilities, one may estimate the placement of the subject's criterion,  $\beta$ , in relation to the maximum Percent Correct, or Siegert's, Observer (Egan et al., 1962).

## CHAPTER IV

## EXPERIMENT I: RESULTS AND DISCUSSION

## d' DATA:

Figures 4.1, 4.2, and 4.3 show the  $d'$  psychometric functions for subjects SLS, RFS, and JEB, respectively. Each set of functions appears reasonably fitted by a straight line. The lines shown were fitted by the method of least squares using equal weighting on all points. This method shall be referred to as the method of best fit. Examination of the three sets of functions shows that they tend to originate at the origin of the X/Y coordinates. Finally, each subject demonstrates a decrease in slope with decrease in SL.

Each data point represents a tabled value of  $d'$  (Elliot, 1959) based on a mean  $P(S|s)$  and  $P(S|n)$  averaged across four runs of 50 trials each. With  $P(s) = 0.5$ , each point is based on 100 S+ and 100 S- trials.

Table 4.1 presents the parameters of each best-fit linear psychometric function by subject and by Sensation Level. Analysis of variance for the regressions yielded F-ratios which are shown with respective degrees of freedom and significance levels. Of the nine functions, eight exceed the .001 level as first-order fits and one (JEB, 60 dB SL) exceeds the .01 level. An analysis of variance was performed, comparing two approaches for fitting straight lines to the  $d'$  data. A natural, first-order least-squares fitting to the data was compared with a linear least-squares fitting where the line was weighted by a factor of 100 on the X/Y intercepts:  $d' = 0$ ,  $\Delta t = 0$ , in order to force the fitted line through the origin. This

## Figures 4.1 - 4.3

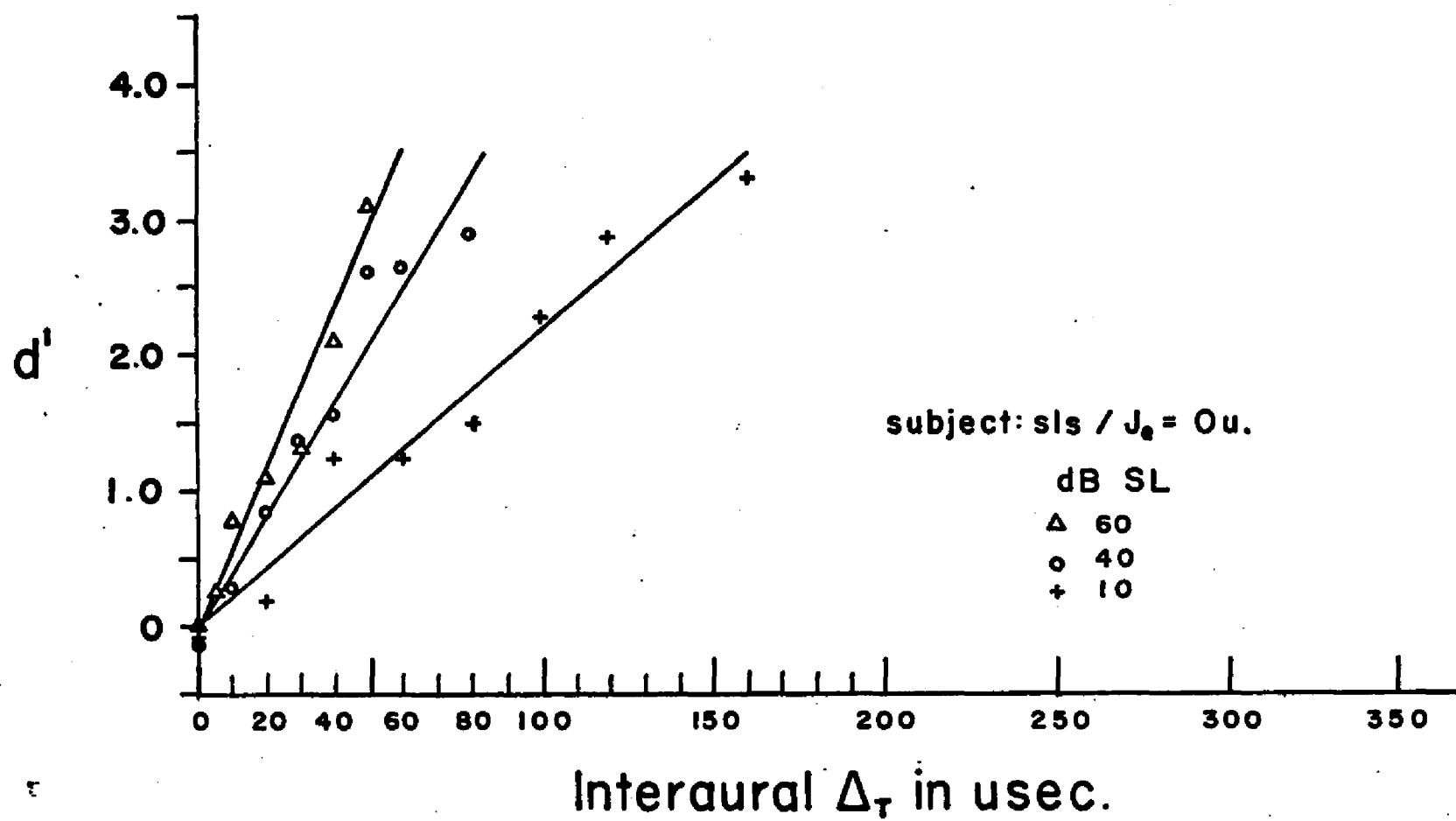
$d'$   $\Delta t$  psychometric functions,  $J_e = 0$ ; ordinate is  $d'$ , abscissa is  $\Delta t$  in  $\mu\text{sec}$ . Parameter of each function is Sensation Level. Lines represent least-squares best fits to the data.

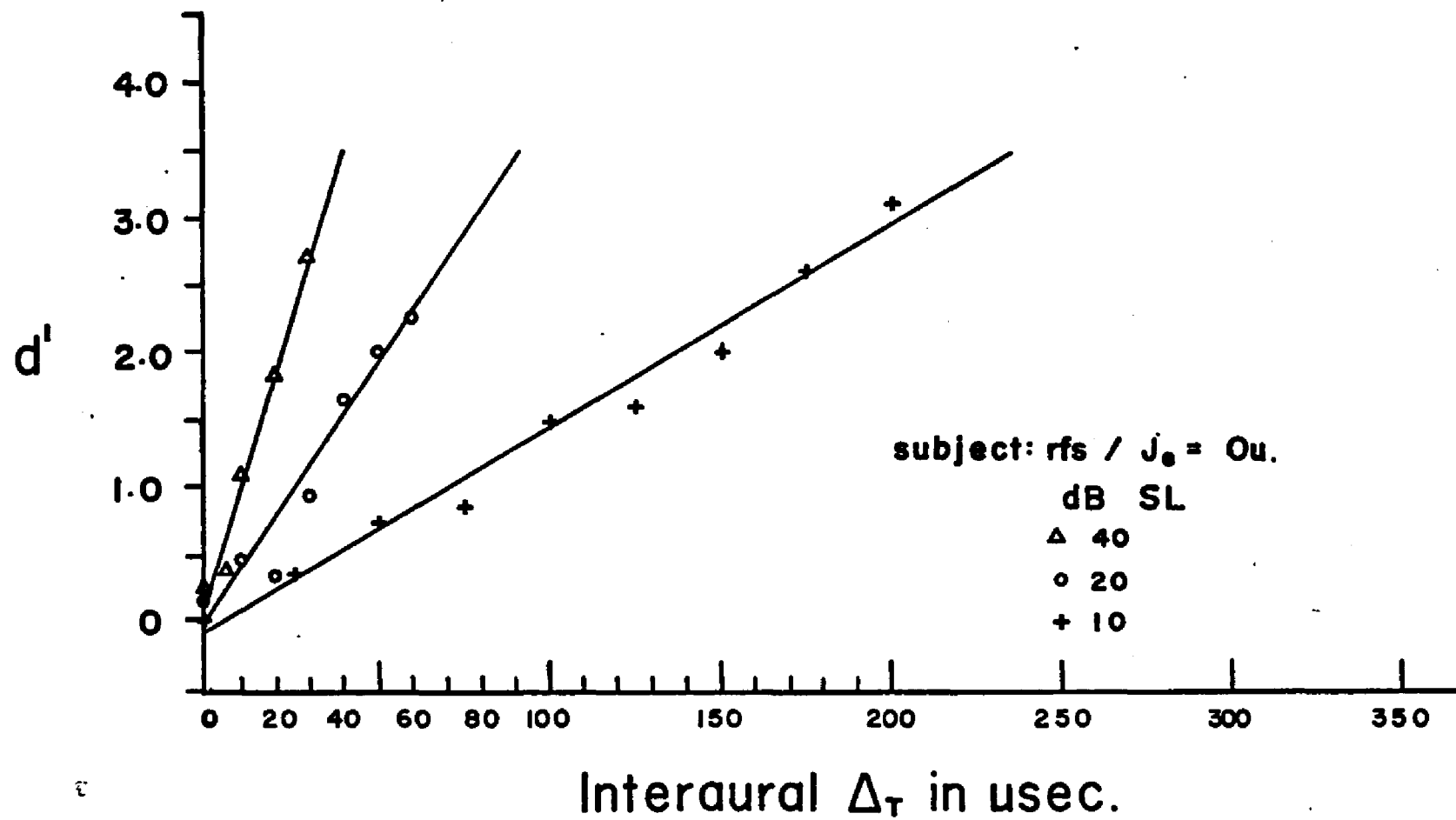
Fig. 4.1 Subject SLS

Fig. 4.2 Subject RFS

Fig. 4.3 Subject JEB







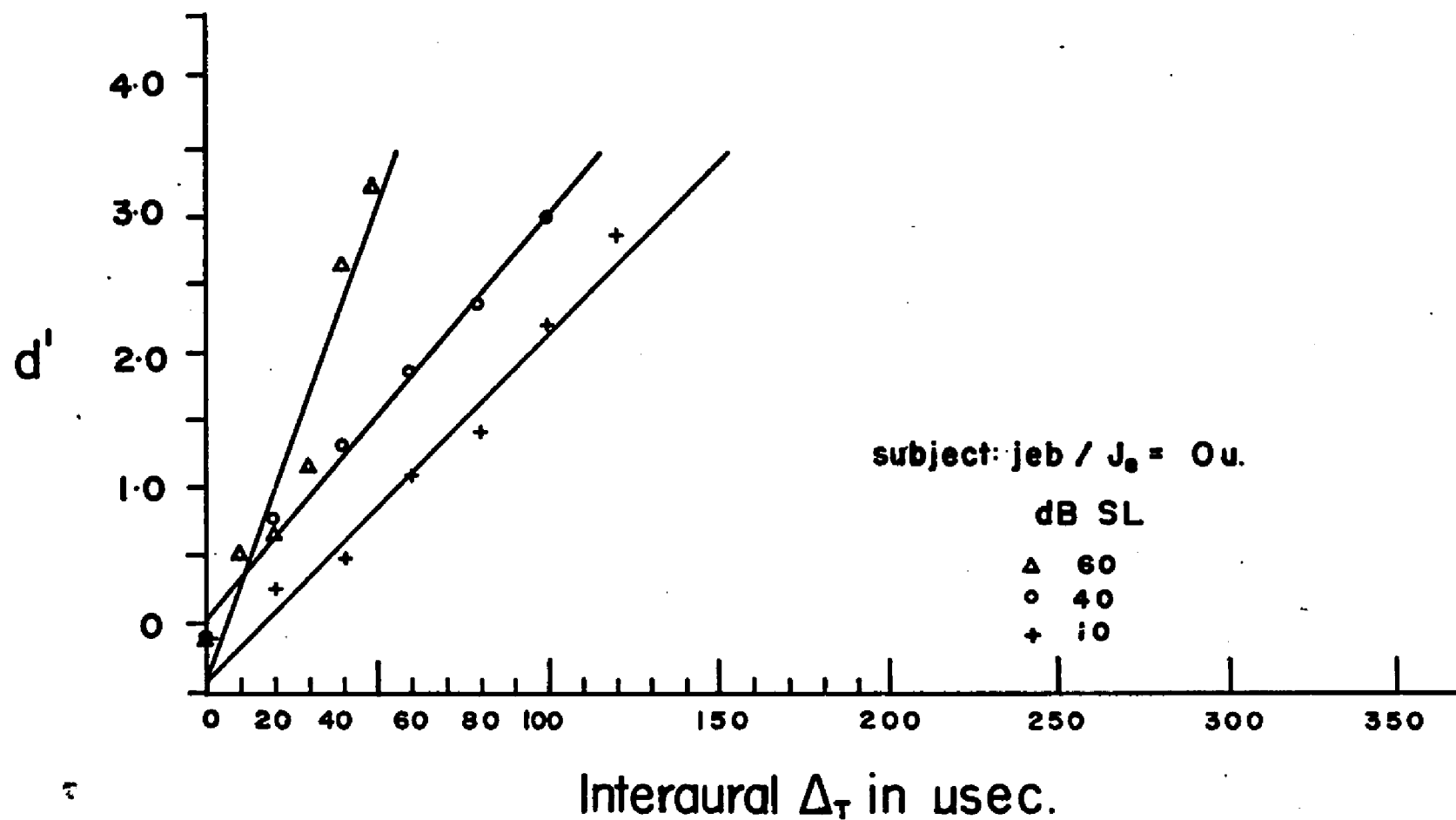


Table 4.1

Parameters of the Least-Squares Lines of Best Fit to the  $d'$  Psychometric Function Points:  $J_e = 0$ .

<u>Subject</u>	<u>Sensation Level</u>	<u>Slope in <math>d'/\mu\text{sec.}</math></u>	<u>Y Axis Intercept</u>	<u>Slope<sup>-1</sup> in <math>\mu\text{sec.}/d'</math></u>	<u>F - Ratio</u>	<u>d.f.</u>	<u>P.</u>
SLS	60 dB	.05621	-.02197	17.79	110.52	1/5	<.001
	40	.04129	+.00177	24.22	86.19	1/6	<.001
	10	.02196	-.02513	45.54	144.22	1/6	<.001
RFS	40 dB	.08444	+.15017	11.84	217.68	1/3	<.001
	20	.03842	-.03428	26.03	72.55	1/5	<.001
	10	.01489	-.06266	67.16	347.66	1/7	<.001
JEB	60 dB	.06794	-.36523	14.72	55.60	1/4	<.01
	40	.02970	+.05660	33.67	531.69	1/4	<.001
	10	.02544	-.38107	39.31	169.65	1/5	<.001

method of fitting a linear function to the data shall be referred to as a weighted-zero fit. None of the best-fit lines differs significantly from the weighted-zero functions. Results of the analysis and the reciprocal slopes of the best-fit and weighted-zero functions are reported in Table 4.2.

Examination of Figs. 4.1, 4.2, and 4.3 reveals a negligible Y-axis intercept correction for the best fitting lines to the data. As a consequence, reciprocal slope of each function ( $\text{slope}^{-1}$ ) conveniently constitutes the  $\Delta t$  value in  $\mu\text{sec.}$  corresponding to a  $d'$  of 1.00. As discussed in Chapter V, this  $\mu\text{sec.}$  value resulting in a  $d'$  of 1.00 may be interpreted both as the standard error of the mean of the assumed symmetrical  $f(x|s)$  and  $f(x|n)$  distributions, as well as  $\Delta T$ , the  $\Delta t$  JND. In a 2 AFC procedure, this also corresponds to a level of 75% correct.

Numbers in the first, best-fit column of Table 4.2 are the simple reciprocals of the slope of each function. The obtained Y-axis intercept values are located in the column immediately to the right. The next column, labelled Weighted Zero, contains reciprocal slopes of those line fits to the data which were constrained to traverse the origin. With the exception of subject JEB's functions at the 60 dB and 10 dB Sensation Levels, the effect of forcing the line to pass through the origin, when compared with the best fitting line to the data, is negligible.

Regardless of the procedure used in fitting straight lines to the data, all subjects demonstrate progressive decreases in slope from high through medium to low Sensation Levels. These empirical findings

Table 4.2

Reciprocal Slopes and Intercepts for the Linear Least-Squares Best Fits and Weighted-Zero Fits  
to the  $d'$  Psychometric Function Points:  $J_e = 0$ .

Subject	Sensation Level	Best Fit		Weighted-Zero		F*
		Slope <sup>-1</sup> in $\mu\text{sec.}/d'$	Y Axis Intercept	Slope <sup>-1</sup> in $\mu\text{sec.}/d'$	Y Axis Intercept	
SLS	60 dB	17.79	-.02	17.98	.00	1.20
	40	24.22	.00	24.21	.00	1.17
	10	45.54	-.03	46.02	.00	1.16
RFS	40 dB	11.84	+.15	10.96	.00	0.74
	20	26.03	-.03	26.53	.00	1.19
	10	67.16	-.06	69.16	.00	1.08
JEB	60 dB	14.72	-.37	17.21	-.01	0.88
	40	33.67	+.06	32.85	.00	1.11
	10	39.31	-.38	47.33	-.01	0.50

\*All F- Ratios N.S.;  $P > .05$ .

are in agreement with the intensity-related  $\Delta T$  shifts reported for click pair  $\Delta t$  stimuli (Hall, 1964), noise burst ongoing disparity (Zerlin, 1959), and pure tone phase difference (Zwislocki et al., 1956).

As the analysis of variance demonstrated no significant difference between least squares best fitting lines and weighted-zero lines fitted to the data, it was decided to base all graphic presentations of Experiments I and II  $d'$  data on the former, best fitting linear functions. Where the lines of best fit do transect the origin,  $\Delta T$ , nominally taken as the  $\mu\text{sec.}$   $\Delta t$  resulting in a  $d'$  of 1.00, may be estimated from slope<sup>-1</sup> of each function. It is assumed that any deviations of best-fitted functions from the origin are the result of extraneous variables. Consequently, where such a deviation from the origin exists, it is suggested that  $\Delta T$  be estimated from slope<sup>-1</sup> of the weighted-zero lines. To illustrate, the  $\Delta T$ 's of subjects SLS and RFS based on either best fit or weighted-zero fit lines to the data (Table 4.2) are virtually indistinguishable, within subject and SL, when the two methods are compared. The  $\Delta T$ 's of JEB, however, are better represented by slopes<sup>-1</sup> taken from the weighted-zero column.

Best  $\Delta T$  values were obtained at SL I, High, for all subjects. These were 18.0  $\mu\text{sec.}$  for subject SLS; 11.0  $\mu\text{sec.}$  for RFS; and 17.2  $\mu\text{sec.}$  for JEB. According to Woodworth (1938, page 523), these figures correspond to midline displacements in azimuth of one to two degrees for a sound source presented in a free field. Agreement is excellent with the only comparably reported  $\Delta T$  for pulse train

stimuli, viz., 11  $\mu$ sec. (Klumpp et al., 1956).

#### PERCENT CORRECT DATA:

Psychometric functions for pulse train  $\Delta T$  have yet to be reported. However, in order to compare  $\Delta T$  psychometric functions for click pair stimuli, appearing in the psychoacoustic literature, functions of Percent Correct are given using the data of this study previously described in terms of  $d'$ .

The values:

$$P(C) = [P(S|s) P(s) + P(N|n) P(n)], \quad (4.1)$$

which, for  $P(s) = P(n) = 0.5$ , is equivalent to:

$$P(c) = [P(S|s) + P(N|n)]/2, \quad (4.2)$$

were plotted on X/Y coordinates of  $\Delta t$  in microseconds and  $P(C)$  in percent, respectively. The  $P(C)$  psychometric functions are shown in Figs. 4.4, 4.5, and 4.6 for subjects SLS, RFS, and JEB, respectively. Functions rise from the origin of 50%, where  $\Delta t = 0$ , generally following a negatively accelerated course to asymptote. Reversals are evident, in some functions, in the 50-to-100- $\mu$ sec.  $\Delta t$  range. A decrease in slope with decreasing SL can be noted for each subject. The separation among functions appears greatest for subject RFS. The obtained form is in good agreement with those functions reported for click pair  $\Delta t$  detection by Wallach et al. (1949), Klumpp et al. (1956), and Hall (1964).



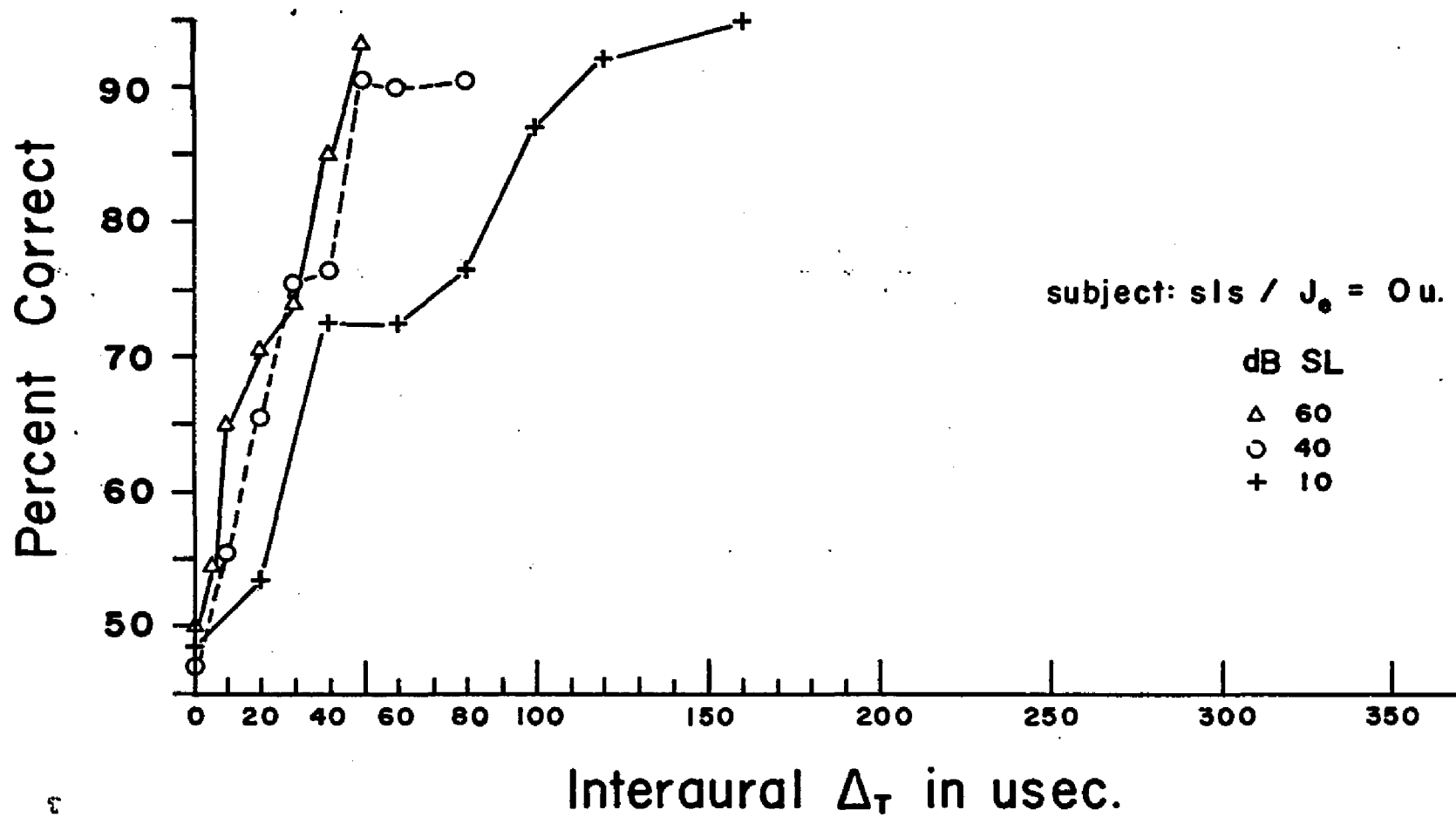
## Figures 4.4 - 4,6

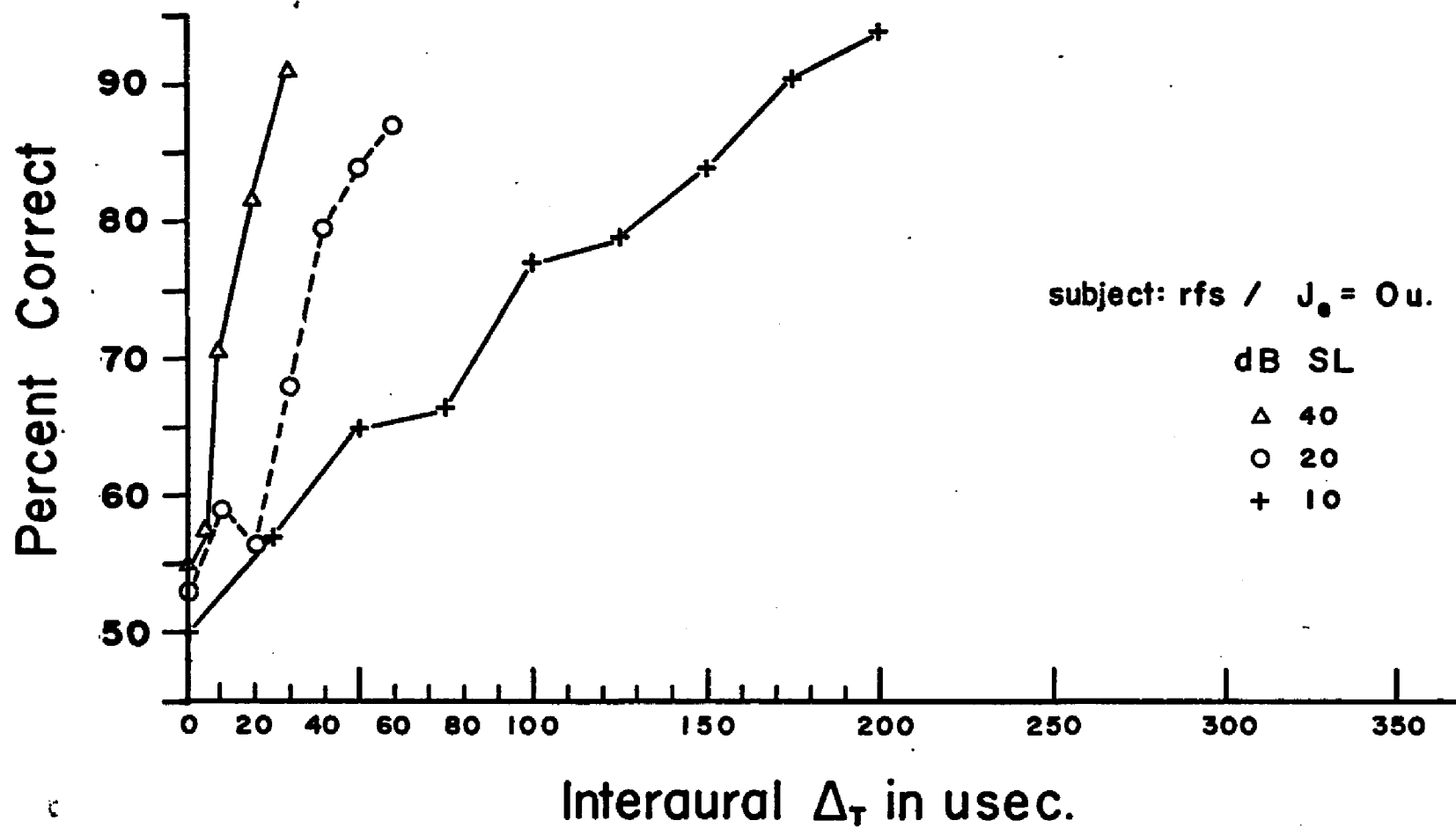
Percent Correct  $\Delta t$  psychometric functions;  $J = 0$ . X/Y  
coordinates are  $\Delta t$  in  $\mu\text{sec.}$  and  $[P(S|s) + P(N|n)]/2$ ,  
respectively.

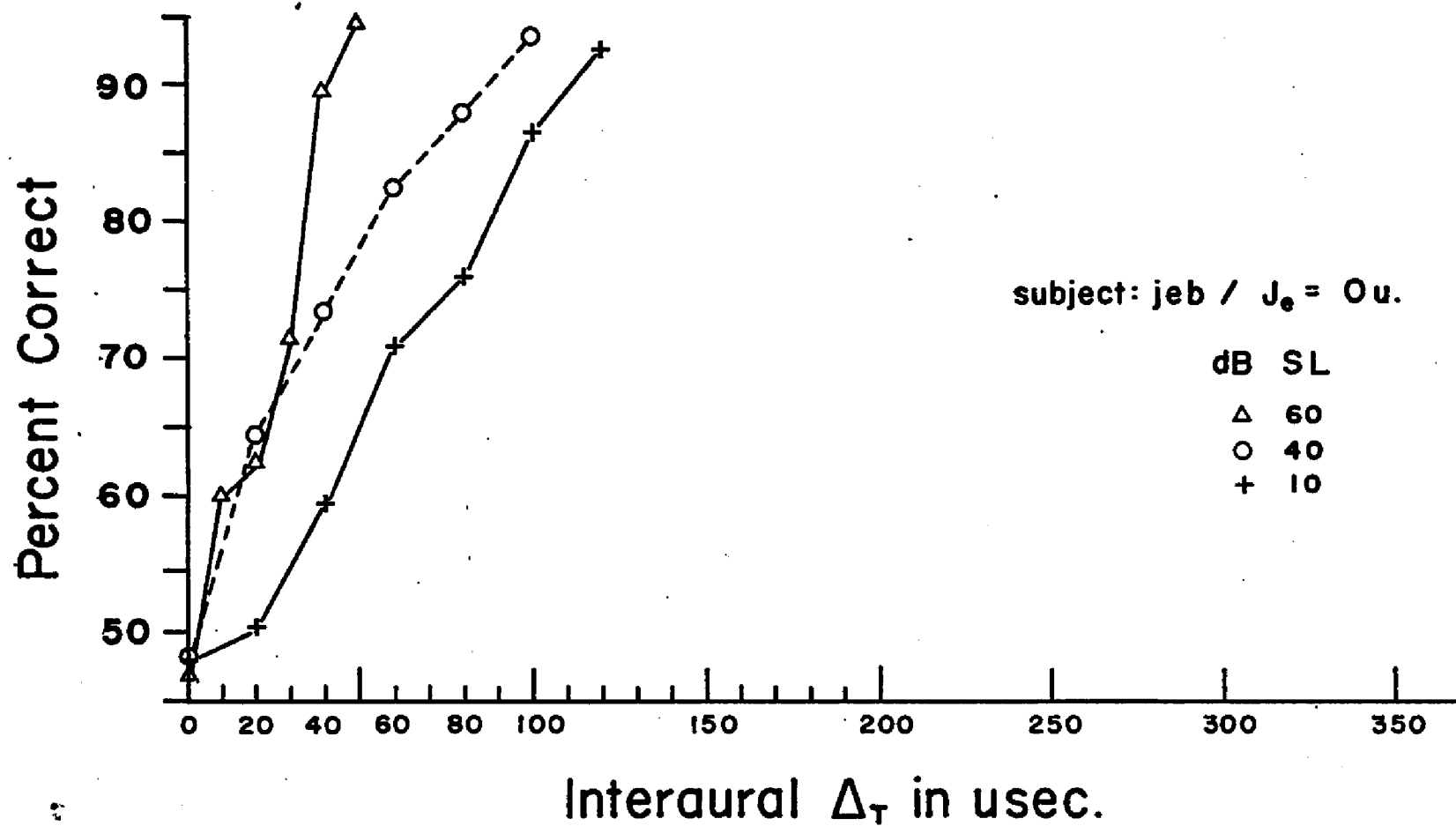
Fig. 4.4 Subject SLS

Fig. 4.5 Subject RFS

Fig. 4.6 Subject JEB







In order to study further the form of the  $P(C)$  psychometric functions, these data were subjected to a program of sequential polynomial regression fittings through the fourth order with the aid of an IBM 1800 TSX computer. Table 4.3 summarizes grossly the analysis of variance of successive order fittings to the data. As the polynomial analysis is based on relatively few points per function, a .001 value was selected as the critical probability. An asterisk indicates significance for the various orders of fitting. The algebraic sign of each particular order component is also given. The modal order of fitting appears between the second and third degree. There is a relatively consistent negative sign to components of the fitted functions greater than first-order. The RFS 40 dB function does not achieve significance as a first-order fit, as it is comprised of only five points with one and three degrees of freedom. These findings are consistent with the hypothesis that the obtained  $P(C)$  psychometric functions are essentially the upper half of a cumulative normal ogive.

Some attention was given to the irregularities or reversals in the  $P(C)$  functions noted within the 50- $\mu$ sec.-through-100- $\mu$ sec. range. An autocorrelation was performed on the physical acoustical stimuli through both earphones (Fig. 2.5), effectively ruling out any possible interaction between the initial pulse compression in one ear and its subsequent rarefaction in the contralateral channel. Intensive changes in the stimulus, as a function of  $\Delta t$ , were ruled out as well. While not critical to the model, it is interesting to note that these reversals appear in comparable functions reported by

Table 4.3

Successive Degrees And Algebraic Signs Of Polynomial Fitted Percent  
Correct Psychometric Functions Beyond  $P = .001$ :  $J_e = 0$ .

Subject	Sensation Level	1° d.f.	Polynomial Degree			
			1°	2°	3°	4°
SLS	60 dB	1/5	*+	*-	0	0
	40	1/6	*+	*-	0	0
	10	1/6	*+	*-	0	0
RFS	40 dB	1/3	0	0	0	0
	20	1/5	*+	0	0	0
	10	1/7	*+	*-	*-	0
JEB	60 dB	1/4	*+	0	0	0
	40	1/4	*+	*-	0	0
	10	1/5	*+	*+	*-	0

Summary

<u>Fit</u>	<u>Total</u>
N.S.	1
1°	1
2°	4
3°	3
4°	0

Legend

\*: ANOVA  $P < .001$   
 0: ANOVA N.S.  
 ±: Coefficient Sign

others, cited above.

4.6  
For example, the single function presented by Klumpp et al. (1956) (Fig. 1.1b) was obtained by averaging data across 13 listeners. As a consequence, individual differences may have been obscured. However, the obtained averaged point, at approximately 52  $\mu$ sec., falls below the fitted negatively accelerated function.

6  
Figure 4.7 is based on the data of Wallach et al. (1949), adapted from his original graph (Fig. 1.1a). Figure 4.7a shows the P(C) functions for each of two subjects, graphically reconstructed by averaging right and left judgments. Subjective bias corrections were incorporated, after the fact, by setting a  $\Delta t$  stimulus value of 0  $\mu$ sec. equivalent to a chance P(C) level of 50%. Reversals of the functions are apparent in the 50- $\mu$ sec.-through-100- $\mu$ sec. range for each of the two subjects. This becomes even more evident (Fig. 4.7b) when the data are averaged across both subjects.

Figure 4.8 presents the P(C)  $\Delta T$  psychometric functions for three subjects as obtained with a pulse pair stimulus paradigm by Hall (1964). These functions have been graphically reconstructed from his original data (Fig. 1.2) so that the parameter of each curve becomes SL, corresponding with the present P(C) data. A tendency toward reversals in the specified  $\Delta t$  range can be noted in a number of the functions obtained from Hall's three subjects.

It is suggested that these reversals may be the result of low-pass-filtering the stimulus in the present study below 4.8 kHz. While the click stimuli were unfiltered in the studies cited above, the output transducers used tend to roll-off in the same frequency

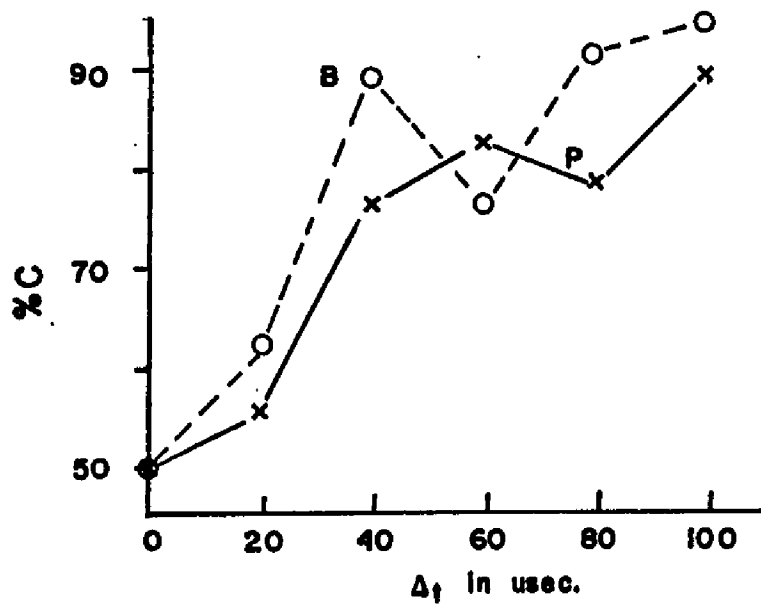
Figure 4.7

Δt data of Wallach, et. al. (1949) for click pair stimuli; replotted in the form of Percent Correct psychometric functions.

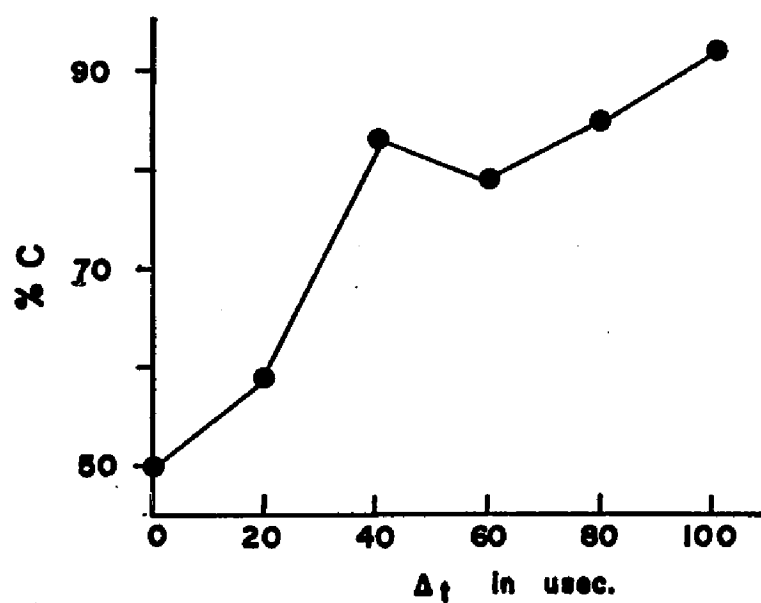
A. Data replotted with right and left judgements averaged and bias correction inserted by setting the 0 μsec. stimulus results equivalent to 50% detection, two subjects.

B. As in A, averaged over two subjects.





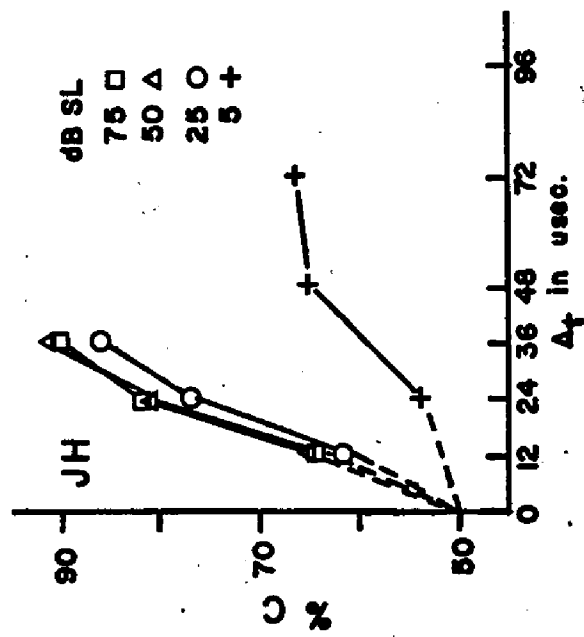
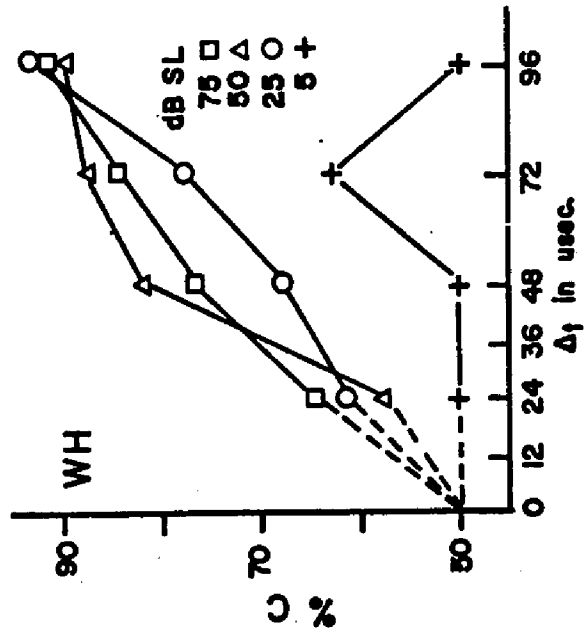
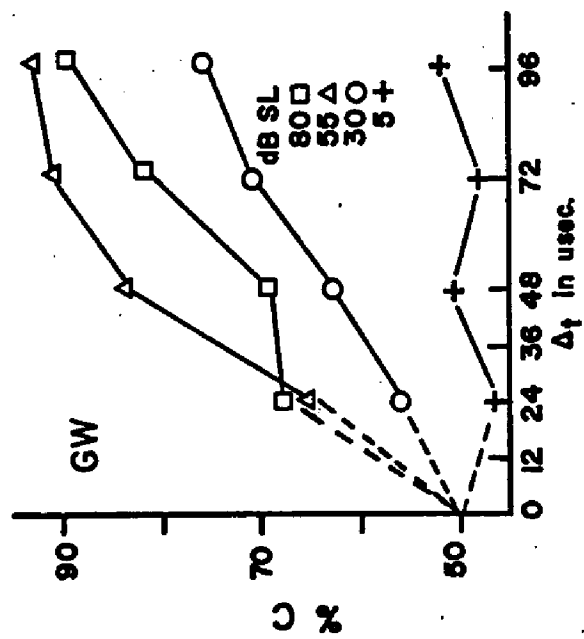
a.



b.

Figure 4.8

$\Delta t$  data of Hall (1964) replotted to make dB SL the parameter of each Percent Correct psychometric function. Stimuli are click pairs for each of three subjects.



range. Specifically, 50 to 100  $\mu$ sec. may correspond to the latency necessary for the lead ear pulse travelling wave to traverse the low-pass filter cutoff frequency area on the basilar membrane. When the lag ear cochlea receives its first click stimulus, the earliest centrally available neural information would be based on unequal amplitude ratios of basilar membrane displacement. A latency, on the order of magnitude in question, was presented in a basilar membrane model of Flanagan (1962) for a 4.5 kHz component of a rarefaction transient.

Another possible explanation may be found in the pattern of basilar membrane displacement for high frequency energy in compression pulses (Flanagan, 1962, pp. 970, 991). Specifically, preceding each major depression of the basilar membrane, there is a minor elevation of the membrane, which may interact with the major elevation. The graphically determined separation between these two upward movements of the basilar membrane, in Flanagan's (1962) model is comparable to the 50-through-100- $\mu$ sec. range of reversals in the P(C) functions of the present study.

#### HIT AND FALSE ALARM DATA:

In the present study, with symmetrical payoff matrices and an a priori P(s) of 0.5, it is postulated that subjects will perform as Maximum Percent Correct or Siebert's observers (Egan, 1962, p. 2b). The Ideal Observer (IO), operating under the strategy of maximizing P(C), or minimizing error, places his optimal decision criterion

4.3  $(\beta_{opt})$  along the likelihood ratio decision axis midway between means of the  $f(x|n)$  and  $f(x|s)$  distributions. The former has a mean of  $\Delta t = 0$ ; the latter has a mean of  $\Delta t > 0$  (Fig. 5.2). In the symmetrical case, the critical value of likelihood ratio  $(\beta_{opt})$  is equivalent to the ratio of a priori probabilities:

$$\beta_{opt} = P(n) / P(s) = .5/.5 = 1.00. \quad (4.3)$$

As  $\Delta t$  increases, the Ideal Observer maintains a criterial position midway between the means of the signal and noise distributions. If the mean value of an observation falls above the critical value of likelihood ratio, he votes YES; if below  $\beta_{opt}$ , he votes NO. Assuming normality and homogeneity of variance of both the  $f(x|n)$  and  $f(x|s)$  distributions, the Percent Correct psychometric function should grow as the negatively accelerated upper half of the cumulative normal distribution. Criteria held by human observers can be estimated a posteriori from the slope of the empirical ROC curves at a given data point. This corresponds to the critical value of likelihood ratio used by the subject in producing that point (Green et al., 1966, pp. 88 et seq.).

The HIT and FALSE ALARM data, obtained by YES/NO method, may be taken as estimates of  $P(S|s)$  and  $P(S|n)$  of the a posteriori probability distributions. Assuming two symmetrical normal distributions, one may then calculate the ratio  $f(x|s) / f(x|n)$  in terms of the respective heights of the ordinates corresponding to those probabilities. The decision criterion held by the human subject  $(\beta_{obt})$  may then be compared with the ideal decision criterion  $(\beta_{opt})$  of

1.00 for the present experimental conditions.

Figures 4.9, 4.10, and 4.11 present the mean values of  $P(S|s)$  and  $P(S|n)$  for each subject. The upper functions are  $P(S|s)$ , the lower are  $P(S|n)$ . Like symbols are used for each Sensation Level, with functions alternately presented as solid or dashed lines for the sake of clarity. Each point is the average of four HIT or FALSE ALARM ratios. One ratio was obtained from each run. Thus, based on 200 trials, half of which are S+, each point represents 100 trials under the conditions  $P(s)$  or  $P(n)$ . Data are truncated at upper limits corresponding to a  $d'$  of less than 3.5, as reported above for the  $d'$  and  $P(C)$ . Examining these functions, a complementary HIT/FALSE ALARM relationship, characteristic of Siebert's observer, can be noted.

Table 4.4 presents the values of  $\beta_{obt}$  for each subject at each of the three Sensation Levels. The average  $\beta_{obt}$  for subject SLS' three curves is 1.37. Her High, Medium, and Low SL mean  $\beta_{obt}$  values are 1.19, 1.57, and 1.34, respectively. Subject RFS averages a  $\beta_{obt}$  of 1.02 for the three curves, with individually determined mean  $\beta_{obt}$ 's of 1.00, 0.95, and 1.11, in order of descending Sensation Level. Subject JEB's mean  $\beta_{obt}$  was 0.98. High, Medium, and Low SL mean  $\beta_{obt}$ 's were 0.97, 0.92, and 1.04, for the third subject, in that order. These findings agree with Green et al. (1966, p. 91):

"The decision conditions which employ moderate probabilities and moderate decision values lead to actual criteria quite similar to the optimal ones."

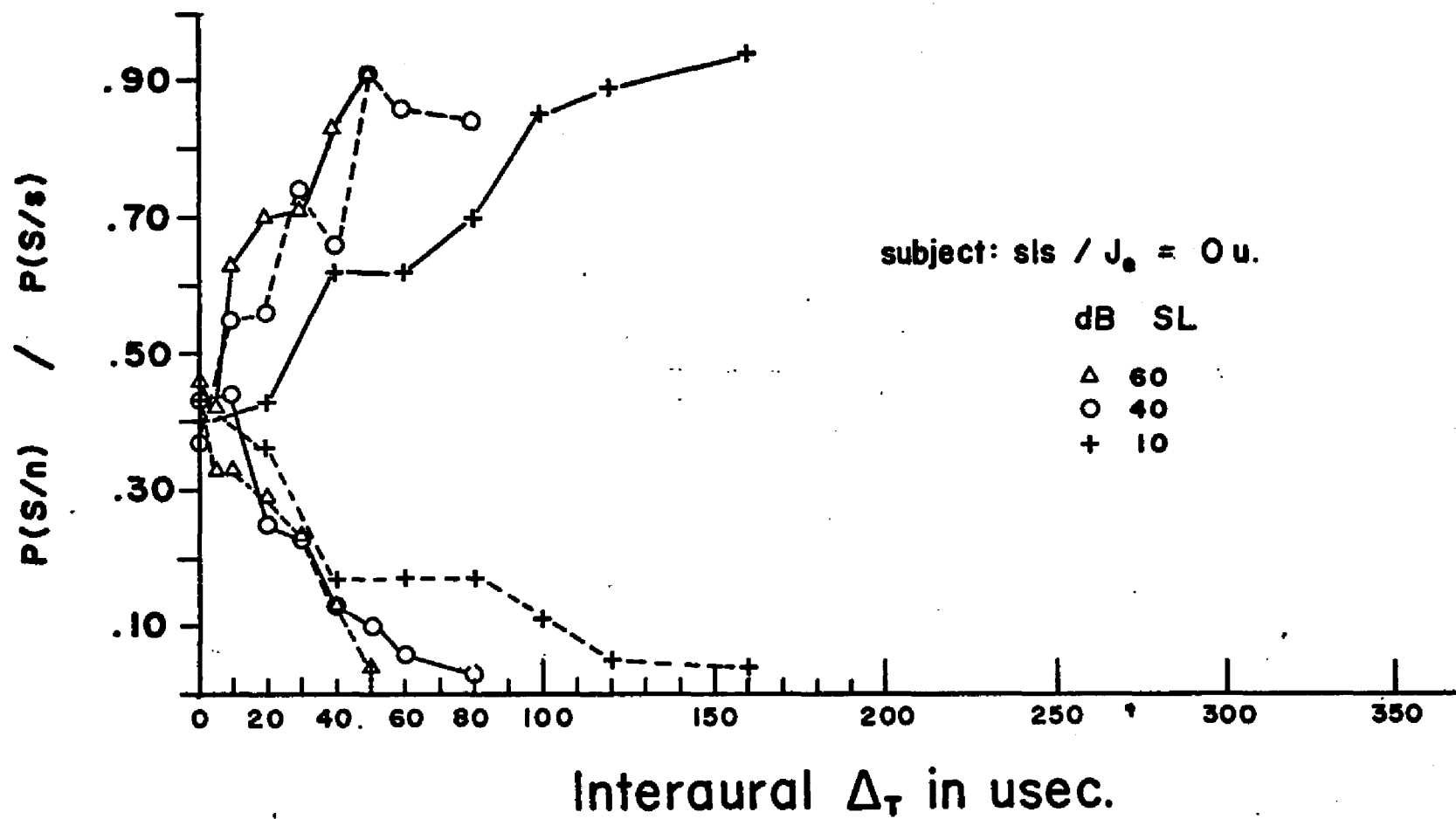
## Figures 4.9 - 4.11

HIT and FALSE ALARM  $\Delta t$  psychometric functions;  $J_e = 0$ . Lower functions represent  $P(S|n)$ , upper functions represent  $P(S|s)$ .

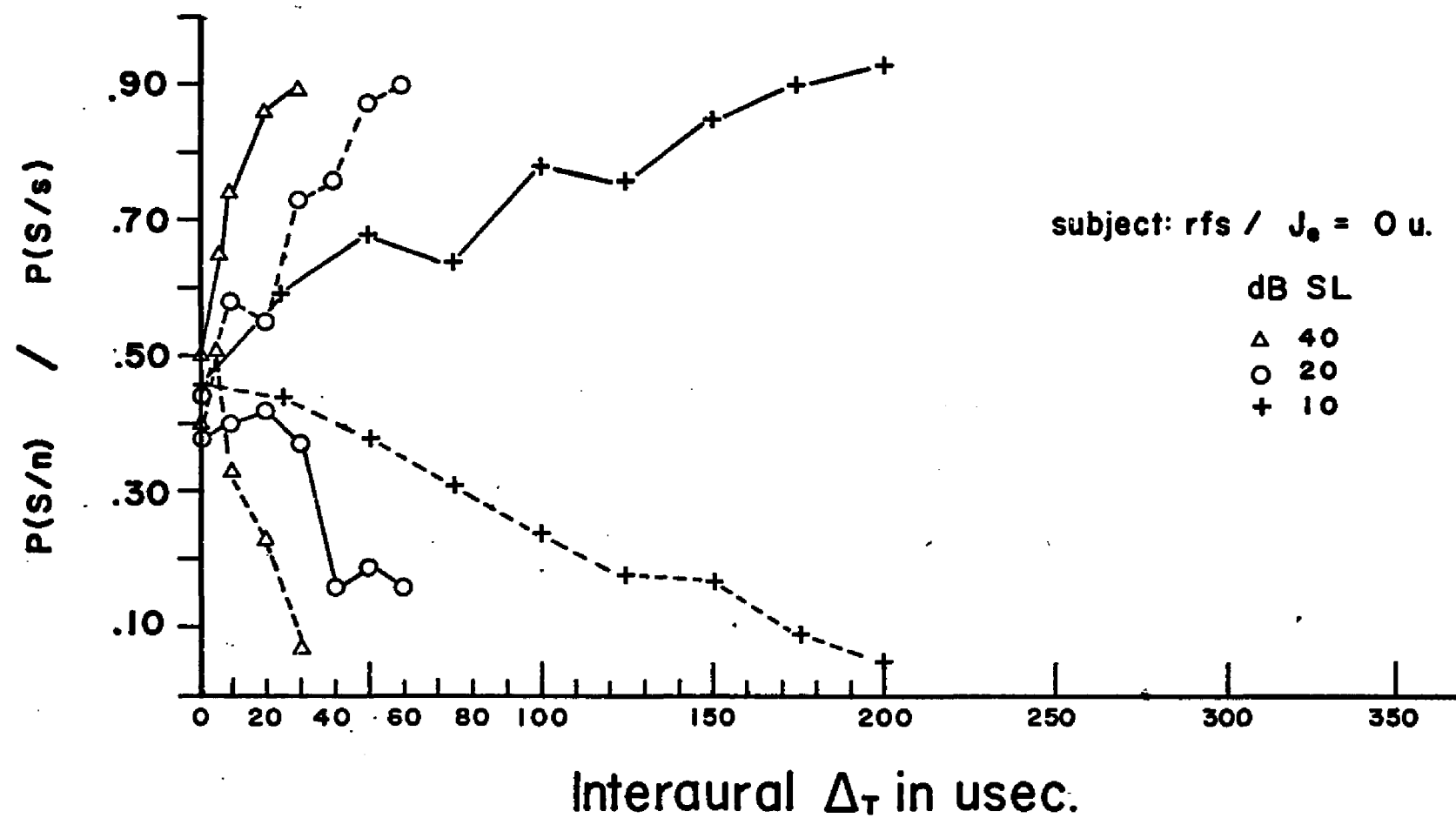
Fig. 4.9 Subject SLS

Fig. 4.10 Subject RFS

Fig. 4.11 Subject JEB







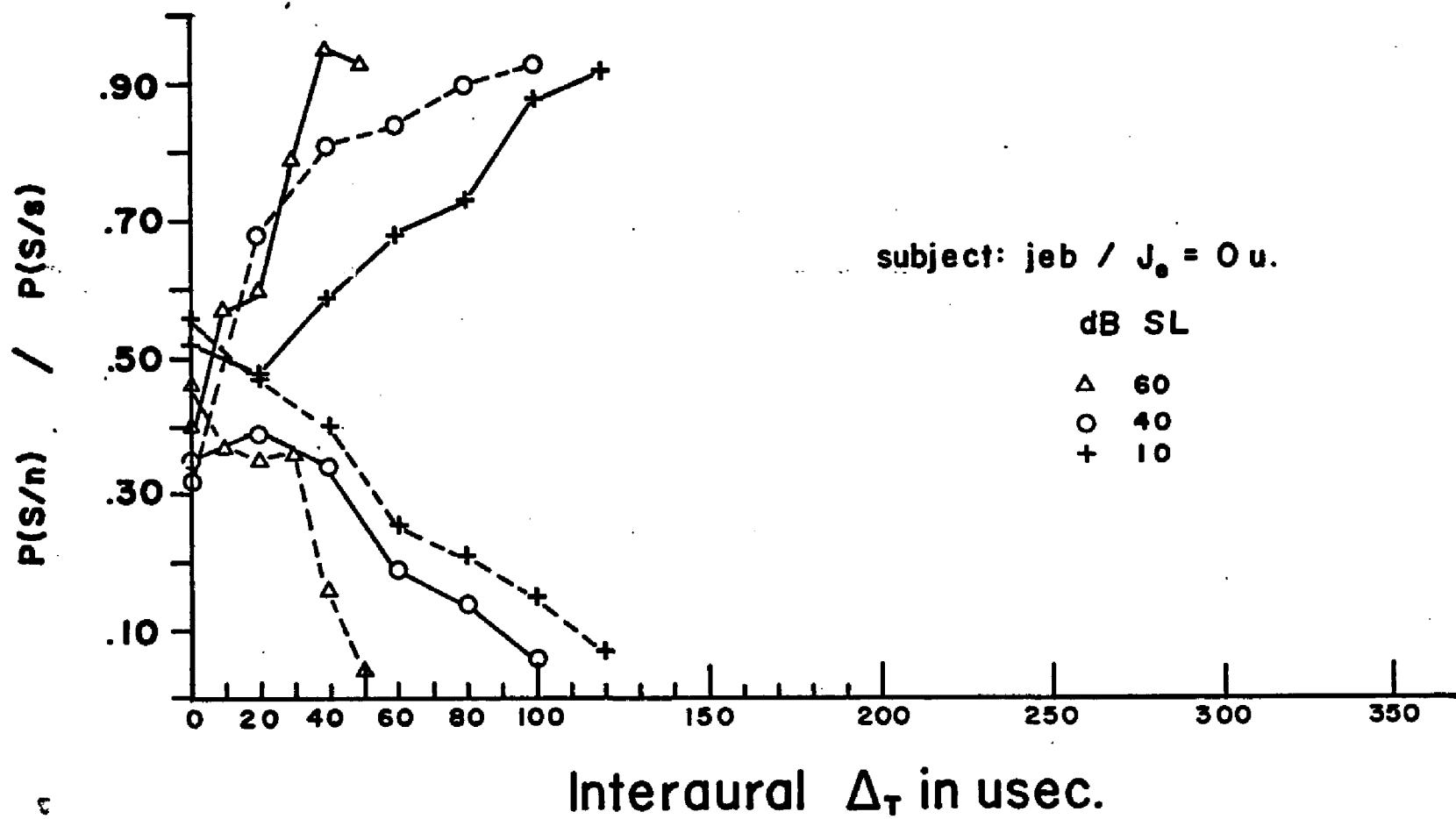


Table 4.4

 $\beta_{\text{obt}}$  For Each Subject By Relative Sensation Level.

		<u>SLS</u>	<u>RFS</u>	<u>JEB</u>
HIGH	$\bar{\beta}$	1.19	1.00	0.97
	Range	1.00 - 1.88	0.73 - 1.40	0.43 - 1.55
	$\beta$ @ 0 $\mu\text{sec.}$	1.00	1.03	0.97
	$\beta$ @ Max. $\mu\text{sec.}$	1.88	1.40	1.55
	N Points	7	5	6
MEDIUM	$\bar{\beta}$	1.57	0.95	0.92
	Range	0.92 - 3.59	0.72 - 1.22	0.79 - 1.20
	$\beta$ @ 0 $\mu\text{sec.}$	0.96	1.04	0.97
	$\beta$ @ Max. $\mu\text{sec.}$	3.59	0.72	1.20
	N Points	8	7	6
LOW	$\bar{\beta}$	1.34	1.11	1.04
	Range	0.99 - 1.80	0.91 - 1.67	0.87 - 1.15
	$\beta$ @ 0 $\mu\text{sec.}$	0.99	1.00	1.01
	$\beta$ @ Max. $\mu\text{sec.}$	1.29	1.28	1.12
	N Points	8	9	7
	$\bar{\bar{\beta}}$	1.37	1.02	0.98

4.1.1 It is noteworthy that, in the absence of S+, i.e., where  $\Delta t = 0$ , the mean value of  $\beta_{obt}$  for the three subjects across nine psychometric functions is 1.00, ranging from 0.96 through 1.04. There appears to be a trend toward higher values of  $\beta_{obt}$  with larger  $\Delta t$ . This latter finding is most consistently demonstrated, for all three Sensation Levels, by subject SLS.

#### CONCLUSIONS:

The data described above demonstrate the following:

1. As the  $d'$  psychometric function, obtained by YES/NO method, are well fitted by straight lines passing through the origin, the assumption of an underlying distribution of errors, which approximates the normal, appears justified.
2. The obtained decision criterion for each subject,  $\beta_{obt}$ , obtained from a posteriori response probabilities, approximates closely the optimal criterion,  $\beta_{opt}$ , based on a priori stimulus probabilities, costs, and values.
3. For each of the three subjects, within intensity limits explored, slopes of the psychometric functions for pulse train  $\Delta t$  detection decrease with Sensation Level.

These findings provide the basis for a model of  $\Delta t$  detection where the human subject's  $\Delta T$  performance is limited by a normally distributed temporal instability or internal noise ( $J_{iy}$ ). This instability affects adversely the comparison of  $\Delta t$  stimuli neural simulacra ( $\Delta t_1$ ) at a postulated central Coincidence Detector (CD).

u.<sup>11</sup>  
It is further offered that  $\Delta T$  increases with decreasing Sensation Level because of an increased inherent level of internal noise in those afferent neural pathways, having lower dB thresholds, which precede the Coincidence Detector. The model, presented in the following chapter, is designed to provide a framework for a meaningful estimate of the time-equivalent values of this SL-dependent internal noise ( $J_{iy}$ ).

79

## CHAPTER V

## MODEL

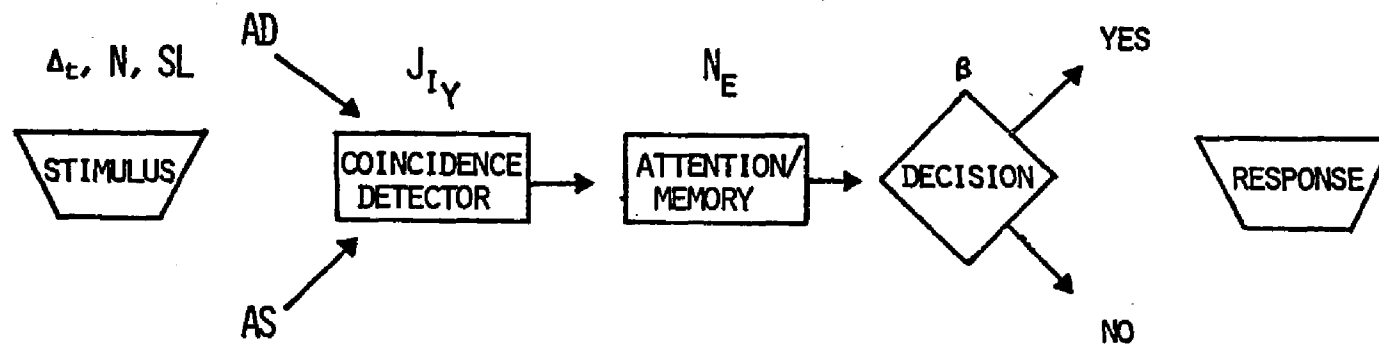
At the outset, it is assumed that pulse train  $\Delta t$  detection is less-than perfect in the Real Observer (RO) because of deficiencies in three areas (Fig. 5.1):

1. Coincidence Detector (CD) -- It is assumed that  $\Delta t$  is, at best, imperfectly represented to a central CD. The cause of this misrepresentation is postulated as a temporal variability in the distribution of neural simulacra ( $\Delta t_1$ ) of the  $\Delta t$  stimulus. This variance may be external ( $J_e^2$ ), internal ( $J_{iy}^2$ ) or both ( $J^2$ ).

2. Attention-Memory Efficiency -- Given  $N$  pulse pairs in a  $\Delta t$  pulse train stimulus, the Real Observer (RO) may fail to use all the information contained in an observation. This failure may be due to faulty attention, where the subject is not vigilant for all  $N$  pulse pairs in the observation sample. The deficiency may also be one of memory, arising from the inability of the RO to fully integrate the  $\Delta t$  information contained in the stimulus burst,  $N$  across time ( $X_t$ ). As a consequence, his ability to reduce the combined internal and external variance, by  $N$ , is impaired. This reduction in the total variance ( $J^2$ ), obtained by using multiple stimulus observations, is analogous to that achieved by converting a distribution of single values to a sampling distribution of values taken  $N$  at a time. The original standard deviation is then reduced proportionally to  $N^{-\frac{1}{2}}$ .

Figure 5.1

Model for pulse train interaural time-of-arrival difference  
discrimination.



BEHAVIORAL MODEL FOR PULSE TRAIN INTERAURAL TIME-OF-ARRIVAL DIFFERENCE DISCRIMINATION.



3. Decision -- Because of inadequate use of a priori stimulus probabilities or costs and values in the decision payoff matrix, the RO may be unable to develop and hold a consistent decision criterion. Based on the relatively stable obtained likelihood ratio data of Experiment I and the available literature (Green et. al., 1966) it was decided that this construct merely be noted as a potential source of error in  $\Delta t$  detection, given experimental conditions other than the present.

#### VARIABLES AND CONSTRUCTS:

The variables and constructs of the model are identified below prior to discussion. The numbers in parentheses following each definition represent the value(s) used in Experiments I and II.

#### CONTROLLED VARIABLES

AXA	The experimental paradigm, described in Chapter III, for the YES/NO psychophysical method.
$X_t$	Duration of the critical stimulus observation interval, X ( $X_t = 1.00$ sec.).
N	The number of dichotic pulse pairs presented during the X interval ( $N = 20$ ).
prf	Pulse repetition frequency (prf = 20 pps).
1/prf	Pulse train period ( $1/\text{prf} = 50$ msec.).
IPI	Interpulse interval in msec.

$P(s)$	A priori probability of an s+ stimulus occurring during X [ $P(s) = 0.5$ ].
$P(n)$	A priori probability of an s- or blank trial [ $P(n) = 0.5$ ].
$\beta_{opt}$	The optimal critical likelihood ratio or decision cutoff criterion ( $\beta_{opt} = 1.00$ ).

## INDEPENDENT VARIABLES

$\Delta t$	The physical interaural time-of-arrival difference in $\mu\text{sec.}$ between the two pulse stimuli of each dichotic pair in a train of sample size N. Also, when not specified otherwise, it represents $\bar{\Delta t}$ , the mean of the distribution of $\Delta t$ 's ( $\Delta t$ always indicates lead time to AD, in $\mu\text{sec.}$ ).
$J_e$	External noise - i.e., standard deviation of the distribution of externally imposed random periodicity perturbations of $\Delta t$ . (Experiment I, $J_e = 0$ ; Experiment II, $J_e = 20, 40, 80, 160 \mu\text{sec rms}$ ).
$\sigma_{\bar{\Delta t}}$	Standard error of the mean of the physical distribution of $\Delta t$ for sample size N:

$$\sigma_{\bar{\Delta t}} = J_e / N^{1/2} \quad (5.1)$$

$SL_y$  The deciBel Sensation Level,  $y$ , above the normally hearing subjects' unilateral (AD) pulse detectability thresholds. (High, Medium, Low; 60, 40, and 10 dB for subjects SLS and JEB; 40, 20, and 10 dB for RFS).

#### DEPENDENT VARIABLES

$\Delta T$  The  $\Delta t$  JND in  $\mu\text{sec}$ . obtained in an external stimulus background of temporal "quiet"; i.e.  $J_e = 0$ .

$\Delta T_J$  The  $\Delta t$  JND in  $\mu\text{sec}$ . obtained when the pulse train  $\Delta t$  is intentionally jittered; i.e.  $J_e \neq 0$ .

$\beta_{\text{obt}}$  The decision cutoff criterion actually employed by the subject. It is empirically estimated from the ratio of ordinate heights of the a posteriori  $P(S|s)$  and  $P(S|n)$  distributions for each data point.

#### CONSTRUCTS

$\Delta t_i$  Neural representation of the interaural time-of-arrival difference ( $\Delta t$ ) at the CD.

$J_{iy}$  Internal noise--i.e. standard deviation of the distribution of  $\Delta t_i$  for a stimulus presented at  $SL_y$ , as represented to the central CD when  $J_e = 0$ .

$J$  Total Noise - i.e., standard deviation of the  $\Delta t_i$  distribution as represented the CD when  $J_e \neq 0$ :

$$J = (J_e^2 + J_{iy}^2)^{1/2} \quad (5.2)$$

$N_e$  The average number of pulse pairs used by the observer in arriving at a  $\Delta t$  detection decision. In the Ideal Observer (IO),  $N_e = N$ . In the RO,  $N_e < N$ .

$E$  Efficiency Factor - efficiency of  $\Delta t$  detection for the RO relative to that for the IO when both CD's are subjected to the same total noise,  $J$ :

$$E = \Delta T_{J \text{ ideal}} / \Delta T_J \quad (5.3)$$

EXTERNAL NOISE;  $J_e$ :

The external component ( $J_e$ ) of the total noise ( $J$ ) affecting input to the CD, is a random disturbance in assigned relative interaural synchrony between pulse pairs of the physical stimulus train. That is, because of imperfect synchronization between pulse inputs delivered to each transducer, any individual pulse pair,  $\Delta t_k$ , may deviate from the assigned mean interaural time-of-arrival difference,  $\Delta t$ .

Treating the occurrence of  $\Delta t_k$  as if from a set of  $n$  discrete events, and postulating a Gaussian distribution for these random physical perturbations of relative interaural synchrony, the variance of this distribution of external noise, or jitter, is defined as:

$$J_e^2 = \left[ \sum_{k=1}^n (\Delta t_k - \bar{\Delta t})^2 \right] / n \quad (5.4)$$

5.6 An estimate of the standard deviation of the external jitter distribution,  $J_e$ , is based on  $n$  samples. In the present study, as described in Chapter VII,  $n$  is 400. Note that the  $J_e$  distribution is a difference distribution of errors between channels about a mean difference of  $\Delta t$ . To illustrate further; holding  $\Delta t$  constant,  $J_e$  may be considered the consequence of two independent variabilities of IPI about the mean pulse period,  $1/\text{prf}$ , one within each pulse train stimulus channel.

If the AD stimulus IPI variability ( $\sigma^2_{\text{IPI}_R}$ ) is independent of that in AS ( $\sigma^2_{\text{IPI}_L}$ ), then the centrally resulting value of  $J_e$  will be equal to the square root of the sums of the variances of IPI in each ear:

$$J_e = (\sigma^2_{\text{IPI}_R} + \sigma^2_{\text{IPI}_L})^{1/2} \quad (5.5)$$

Given equivalent, independent, values of  $\sigma^2_{\text{IPI}}$  in both input channels:

$$J_e = \sigma_{\text{IPI}}(2)^{1/2} \quad (5.6)$$

In order to simulate this stimulus condition (Eq. 5.6), it is only necessary to perturb the pulse period in one of the two channels with twice the variance attributable to either channel, individually. Maintaining a relatively invariant pulse period in the other channel:

$$J_e = (2\sigma^2_{\text{IPI}_L} + 0)^{1/2} \quad (5.7)$$

This technique is used in the present Experiment II. The pulse trains in both channels are synchronized to a mean IPI of 50 msec. The synchrony is held invariant in AD while  $J_e$  is super-

imposed on the periodicity of the AS pulse train. This simplifies the  $J_e$  calibration procedure as described in Chapter VII.

#### INTERNAL NOISE; $J_{iy}$ :

It is assumed that, independent of  $J_e$ , an equivalent misrepresentation of the stimulus period arises in each of the AD and AS neural input channels to the central CD. Various physiological bases for variation in stimulus-driven interspike interval (ISI) have been presented in the literature (Gray, 1966; Calvin and Stevens, 1967; Poussart, 1969). This internally-generated temporal variability ( $J_{iy}$ ) in the CD difference distribution is assumed to be approximated by the Gaussian form and independent of external jitter ( $J_e$ ).

The findings of Experiment I show an increase in  $\Delta T$  with decreasing Sensation Level. It is assumed, in the model, that  $\Delta T$  is proportional to  $J_{iy}$  which, in turn, increases with decreasing SL, below asymptote. Kiang (1965) provides some physiological evidence for the validity of this assumption. He reports (1965, p. 103) higher levels of spontaneous activity in those primary auditory afferent neurons having lower thresholds.

Internal noise is one of the factors potentially precluding perfect  $\Delta t$  detection.  $J_{iy}$  is defined as the variability in  $\Delta t_1$ , or dichotic pulse train neural representation, affecting the CD difference distribution, when the stimulus is presented at Sensation Level  $y$ . As with  $J_e$ , a zero correlation of ISI variability ( $\sigma_{ISI}$ ) between channels is postulated. Then:

$$J_{iy} = (\sigma_{ISI_R}^2 + \sigma_{ISI_L}^2)^{1/2} \quad (5.8)$$

## TOTAL NOISE, J:

The total imperfection in  $\Delta t_1$ , the  $\Delta t$  stimulus representation to the CD, is referred to as J. This total jitter is the sum of four independent variances, two external and two internal, viz.:

$$J = (\sigma^2_{IPI_R} + \sigma^2_{IPI_L} + \sigma^2_{ISI_R} + \sigma^2_{ISI_L})^{\frac{1}{2}} \quad (5.9)$$

The first two variances may be simulated by a single variance in physical monotonic IPI, i.e.,  $J_e^2$ . The last two variances may be also be set equal to a single figure representing the internally-contributed, SL-dependent variance, viz.  $J_{iy}^2$ . Therefore, the total noise variance at the CD,  $J^2$ , is the sum of the internal and external noise variances at  $SL_y$ :

$$J^2 = J_e^2 + J_{iy}^2 \quad (5.10)$$

The present Experiment II is an undertaking to provide meaningful empirical estimates of  $J_{iy}$  for representative Sensation Levels.

## THE IDEAL OBSERVER:

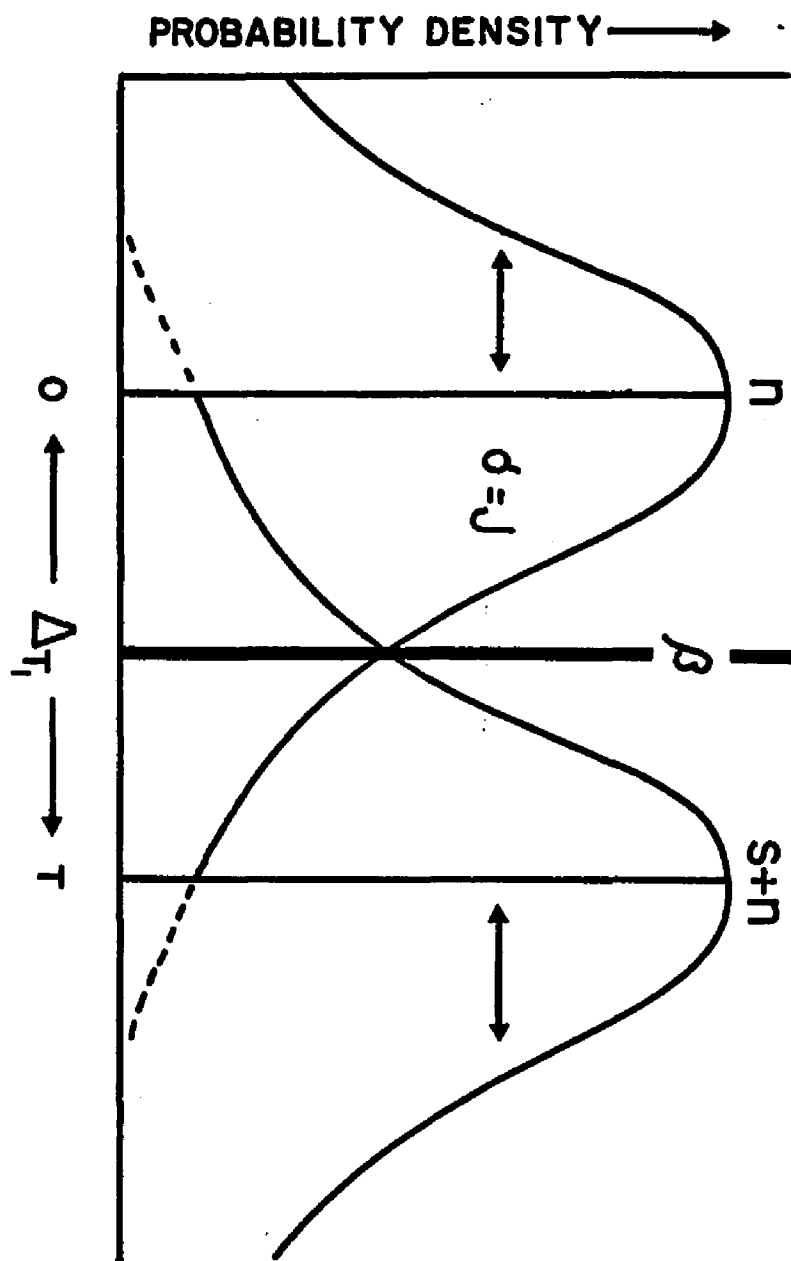
The IO, free of internal noise ( $J_{iy} = 0$ ), is presented with an N-size sample pulse train of imperfect periodicity ( $J_e \neq 0$ ). Possessing the attributes of perfect vigilance, faultless memory, and statistically optimum decision-making abilities, the IO is limited in  $\Delta t$  detection by the magnitude of  $J_e$  and by the number of pulse pairs (N) available as a basis for each decision.

The detection task is postulated as illustrated in Fig. 5.2. Let the X-axis be a monotonic transformation of  $\Delta t$  as represented to

Figure 5.2

Theoretical distributions of  $\Delta t$  neural effect ( $\Delta t_1$ ) at the  
Coincidence Detector.





the CD, viz;  $\Delta t_1$ .

The Y-axis is probability density. The mean of the  $f(x|n)$  distribution is zero. The mean of the  $f(x|s)$  distribution is  $\bar{\Delta t}$ . Assuming homogeneity of variance, the standard deviation of both distributions is J, as defined in Eqs. 5.9 and 5.10. With the introduction of  $\Delta t > 0$ , AD stimulus leading, the  $f(x|n)$  distribution is shifted to the right, becoming  $f(x|s)$ . The IO must then decide whether the stimulus sample in question arose from the  $f(x|s)$  or  $f(x|n)$  distributions.

Given an internal stimulus representation free of both internal and external noise ( $J = 0$ ), the IO would detect the condition  $\Delta t \neq 0$  upon presentation of a single pulse pair. However, as J increases, the detection task becomes statistical in nature. Placement of the response criterion  $\beta$ , becomes a necessary and critical consideration. It is understood that, for the assigned  $\Delta t$  detection task, the IO functions as a Maximum Percent Correct, or Seigert's Observer (Egan, et. al., 1962, p. 2b). Given the equal a priori probabilities of this study, the optimum likelihood ratio,  $\beta_{opt}$ , is calculated to a value of 1.00. In order to match this criterion, the IO must shift his placement of  $\beta$  along the decision axis with  $\Delta t_1$ , maintaining it midway between means of the  $f(x|n)$  and  $f(x|s)$  distributions.

If  $J \neq 0$ , the performance-limiting effect of increased variability may be reduced through multiple observations of the  $\Delta t$  stimulus ( $N > 1$ ) prior to a decision. Analogous to the statistical determination of a difference between two sample means, the mean

difference,  $\bar{\Delta t}$ , is divided by the standard error of the mean difference,  $\sigma_{\bar{\Delta t}}$ . The standard error is inversely proportional to  $N^{\frac{1}{2}}$ .

$$\sigma_{\bar{\Delta t}} = J/(N^{\frac{1}{2}}) \quad (5.11)$$

Substituting for J from Eq. 5.10:

$$\sigma_{\bar{\Delta t}} = [(J_e^2 + J_{iy}^2)/N]^{\frac{1}{2}} \quad (5.12)$$

By definition, the IO uses all pulse pairs presented in the stimulus train for a decision. The average number of pulse pairs,  $N_e$ , upon which any observer bases his decision, is equal to N for the IO. So, Eq. 5.12 may be restated as:

$$\sigma_{\bar{\Delta t}} = [(J_e^2 + J_{iy}^2)/N_e]^{\frac{1}{2}} \quad (5.13)$$

In the YES/NO psychophysical procedure as applied to  $\Delta t$  detection, given equal a priori stimulus probabilities, it is assumed that the IO functions in the following manner. During an observation interval, the IO is given a sample of size N from either the  $f(x|s)$  or  $f(x|n)$  distributions. If this  $\Delta t$  stimulus sample is noted to the right of the critical likelihood ratio,  $\beta$ , (Fig. 5.2) the IO votes "YES". If the sample is identified to the left of  $\beta$ , the IO votes "NO". The difference between means of the two distributions is  $\Delta t_1$ , the neural representation of  $\Delta t$  to the CD. As  $\Delta t$  is systematically varied, the observer produces, in effect, a distribution of Z-scores:

$$Z = \bar{\Delta t}/\sigma_{\bar{\Delta t}} \quad (5.14)$$

As both  $Z$  and  $d'$ , the index of detectability, are normally distributed, given a value for  $\bar{\Delta t}$ , with an available estimate of  $\sigma_{\bar{\Delta t}}$ , one may predict performance:

$$d'_{\text{pred}} = \bar{\Delta t} / \sigma_{\bar{\Delta t}} \quad (5.15)$$

Substituting for  $\sigma_{\bar{\Delta t}}$  with Eq. 5.13,

$$d'_{\text{pred}} = \bar{\Delta t} / [(J_e^2 + J_{iy}^2) / N_e]^{1/2} \quad (5.16)$$

$$d'_{\text{pred}} = \bar{\Delta t} (N_e^{1/2}) / (J_e^2 + J_{iy}^2)^{1/2} \quad (5.17)$$

From Eq. 5.10:

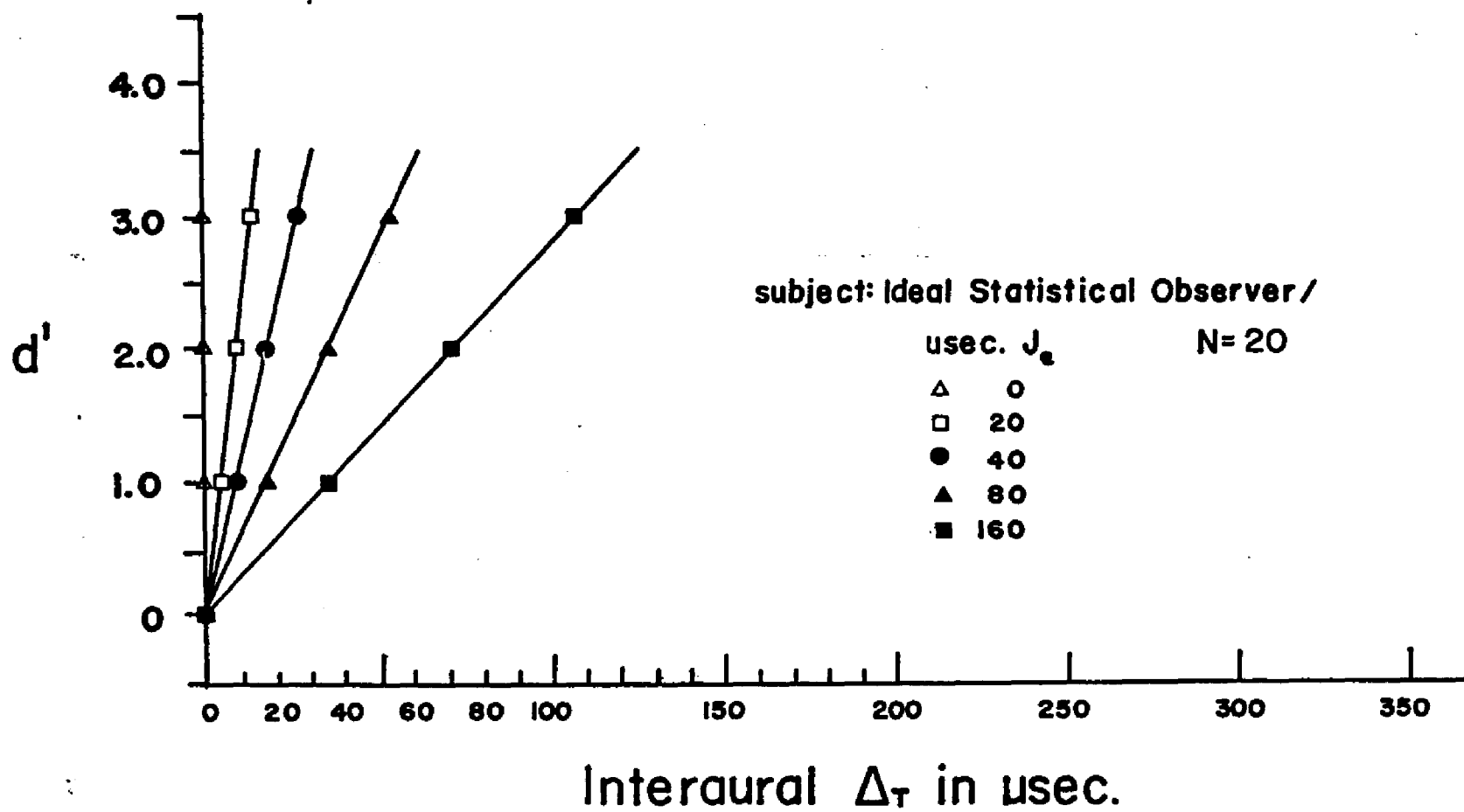
$$d'_{\text{pred}} = \bar{\Delta t} (N_e^{1/2}) / J \quad (5.18)$$

Therefore, if we specify  $J_e$  and  $N$ , with internal noise remaining at zero in the IO, we may generate a set of Ideal Observer cumulative  $d'$  distributions or  $d'$  psychometric functions for  $\Delta t$  detection. Assuming a Gaussian distribution for total noise,  $J$ , use of the  $d'$  statistic transforms the cumulative ogival functions into linear functions. Substituting 20 pulse pairs per observation for  $N_e$  and  $J_e$  values of 0, 20, 40, 80, and 160  $\mu\text{sec. rms}$ , respectively, the predicted IO  $d'$  psychometric functions are illustrated in Fig. 5.3. Note that the predicted slope is infinite where  $J_e$  is equal to zero. As soon as  $\Delta t > 0$ ,  $d'$  approaches infinity.

An accepted estimate of the JND is a  $d'$  index of 1.00. This corresponds to a 75% Correct detection level in a 2 AFC psychophysical procedure. Following from this, the  $\mu\text{sec. value}$  of  $\Delta T_J$ , the  $\Delta t$  JND where  $J_e \neq 0$ , is reached when  $\Delta t$ , the mean of the  $f(x|s)$  distribu-

Figure 5.3

Simulated  $d'$  vs  $\Delta t$  psychometric functions for an Ideal Observer using samples of 20 pulses per observation with various superimposed values of external jitter ( $J_e$ ). The parameter of each function is  $J_e$ .



is equal to  $\sigma_{\Delta t}$ , its standard error:

$$\Delta T_J = \sigma_{\Delta t} \quad (5.19)$$

Finally, substituting in Eq. 5.13, we have the basis for the  $\Delta T$  model:

$$\Delta T_J = [(J_e^2 + J_{iy}^2)/N_e]^{1/2} \quad (5.20)$$

In general,

$$\Delta T_J = (J^2/N_e)^{1/2} \quad (5.21)$$

In the IO,  $J_{iy}$  is equal to 0 and  $N_e$  is equal to  $N$ . Then, the only SL-dependent term disappears from Eq. 5.20:

$$\Delta T_{J \text{ ideal}} = (J_e^2/N)^{1/2} \quad (5.22)$$

The efficiency factor,  $E$ , is defined as the ratio of ideal to obtained  $\Delta t$  JND's:

$$E = \Delta T_{J \text{ ideal}} / \Delta T_J \quad (5.23)$$

As the IO performs optimally,  $N_e$  being equal to  $N$ ,  $E$  is always 1.00. It is demonstrated below, under discussion of the Real Observer, that, alternatively:

$$E = (N_e/N)^{1/2} \quad (5.24)$$

When  $J \neq 0$ , the  $\Delta t$  detection decision of the IO is based upon the ratio of ordinate heights of the  $f(x|n)$  and  $f(x|s)$  distribu-

tions, at the point along the likelihood ratio decision axis where the ideal criterion,  $\beta_{opt}$ , is located. The IO's placement of  $\beta_{opt}$  is assumed optimally based on all available information, including a priori stimulus probabilities and values in the payoff matrix. It is further given that the IO maximizes Percent Correct detection on each trial.

In the ideal case the optimum  $\beta$ ,  $\beta_{opt}$ , equals the obtained  $\beta_{obt}$ , and both are equal to a value of 1.00 when  $P(s) = P(n) = 0.5$ . In general:

$$\beta_{obt} = f(x|s) / f(x|n) \quad (5.25)$$

and

$$\beta_{opt} = [V_n \cdot N + V_n \cdot S) P(n)] / [(V_s \cdot S + V_s \cdot N) P(s)] \quad (5.26)$$

When costs and values are equivalent for all conditions, the optimum criterion is based on the ratio of a priori stimulus probabilities (Green & Swets, 1966):

$$\beta_{opt} = P(n) / P(s) \quad (5.27)$$

Green, et. al. (1966) report the ability of human observers to match and maintain ideal decision criteria near a value of unity. Inspection of the Experiment I data (Table 4.4) reveals that the subjects were, in fact, capable of performing as Maximum Percent Correct Observers, optimizing and maintaining their critical values



of likelihood ratio so that  $\beta_{\text{obt}}$  closely approximates the  $\beta_{\text{opt}}$  of 1.00.

#### THE REAL OBSERVER, RO:

The  $\Delta t$  detection task has been defined, for the Ideal Observer, IO, in terms of the model. It is assumed that performance of the Real Observer, RO, is governed by the same variables, constructs and processes, viz:

$$\Delta T_J = (J^2/N_e)^{1/2} \quad (5.21)$$

or, more specifically:

$$\Delta T_J = [(J_e^2 + J_{iy}^2) / N_e]^{1/2} \quad (5.20)$$

For the RO, the conditions  $J_{iy} > 0$  and  $N_e < N$  prevail by definition. Given the latter inequality, according to Eq. 5.24,  $E < 1.00$ , as well. As a consequence, in order to predict  $\Delta T_J$  for the RO, it is necessary to know  $J_e$  and to have estimates of  $J_{iy}$  and either  $N_e$  or  $E$ , given  $N$ . In Experiment I,  $J_e$  is 0. Therefore, from Eq. 5.20,  $\Delta T_J$  is defined in this specific instance as  $\Delta T$ :

$$\Delta T = (J_{iy}^2/N_e)^{1/2} \quad (5.28)$$

This is comparable to Eq. 5.22 for the IO.

Based on the findings of Experiment I, empirical estimates of  $\Delta T$  and  $\Delta T_J$  for the RO will be based simply on reciprocal slopes (slopes<sup>-1</sup>) of the least-squares first degree best fits to the empirical d' data. Assuming  $\beta_{\text{obt}} = \beta_{\text{opt}} = 1.00$ , and disregarding any deviation

of the Y-intercept from zero, the slope<sup>-1</sup> of each function represents  $\Delta T$  or  $\Delta T_J$  -- the  $\Delta t$  value corresponding to a  $d'$  of 1.00.

By introducing the RO to the experimental condition  $J_e \neq 0$ , his performance may be compared with that of the IO subjected to the same  $J_e$ . Correcting for the difference between  $\Delta T$  (where  $J_e = 0$ ) and  $\Delta T_J$  (where  $J_e \neq 0$ ), obtained at the same  $SL_y$ , the model permits isolated empirical estimations of both  $J_{iy}$  and  $N_e$ .

If  $J_{iy}$  is known, the rearranging of terms in Eq. 5.20 leads to an estimate of  $N_e$ , the average number of pulse pairs used by the RO in arriving at a decision on the outcome of each trial:

$$N_e = (J_e^2 + J_{iy}^2) / \Delta T_J \quad (5.29)$$

In order to isolate  $N_e$ : we square Eq. 5.20:

$$\Delta T_J^2 = (J_e^2 + J_{iy}^2) / N_e \quad (5.30)$$

This leads to:

$$\Delta T_J^2 = (J_e^2 / N_e) + (J_{iy}^2 / N_e) \quad (5.31)$$

Squaring Eq. 5.28, we have:

$$\Delta T^2 = J_{iy}^2 / N_e \quad (5.32)$$

So that:

$$\Delta T_J^2 = (J_e^2 / N_e) + \Delta T^2 \quad (5.33)$$

Rearranging terms,

$$(J_e^2/N_e) = (\Delta T_J^2 - \Delta T^2) \quad (5.34)$$

Finally, we have:

$$N_e = J_e^2 / (\Delta T_J^2 - \Delta T^2) \quad (5.35)$$

That is,  $N_e$  is equal to the quotient of the external noise variance divided by the difference between the squared  $\Delta T$  JND's obtained in that value of  $J_e$  and, at the same  $SL_y$ , under the external noise-free condition.

If we apply Eq. 5.35 to the Ideal Observer case,  $\Delta T_{ideal} \rightarrow 0$  (Fig. 5.3). Squaring Eq. 5.21,

$$\Delta T_{J_{ideal}}^2 = J_e^2 / N \quad (5.36)$$

Restating Eq. 5.35:

$$N_{e_{ideal}} = J_e^2 / (\Delta T_{J_{ideal}}^2 - \Delta T_{ideal}^2) \quad (5.37)$$

Substituting,

$$N_{e_{ideal}} = J_e^2 / [J_e^2 / N - 0] \quad (5.38)$$

Alternatively,

$$N_{e_{ideal}} = J_e^2 / (J_e^2 / N) \quad (5.39)$$

or

$$N_{e_{ideal}} = J_e^2 (N) / J_e^2 \quad (5.40)$$

Therefore,  $N_{e_{ideal}}$  is equal to  $N$ , for the IO and,

$$N_{e_{ideal}}/N = 1.00 \quad (5.41)$$

Having determined the value of  $N_e$ , it may be substituted in Eq. 5.28 in order to derive an empirical estimate of  $J_{iy}$  at any SL where only  $\Delta T$  has been obtained. Rearranging Eq. 5.28,

$$J_{iy} = (\Delta T) N_e^{1/2} \quad (5.42)$$

A test of the model arises in the experimental determination of an empirical value for  $N_e$  which is independent of SL, other factors constant. According to the model  $J_{iy}$ , must increase in order to compensate the increase in size of  $\Delta T$  with decreasing SL.

The efficiency factor  $E$  has been defined as the ratio:

$$E = \Delta T_{J_{ideal}} / \Delta T_J \quad (5.23)$$

where:  $J$  consists of only  $J_e$  for the IO;  $J$  is equal to  $(J_e^2 + J_{iy}^2)^{1/2}$  for the RO; and  $J_{IO}$  is equal to  $J_{RO}$ . That is,  $E$  is the ratio of  $\Delta T_J$ 's for Ideal and Real Observers where both are subjected to the same value of  $J$ .

Reiterating Eq. 5.22:

$$\Delta T_{J_{ideal}} = (J_e^2/N)^{1/2} \quad (5.22)$$

As  $J_e$ , by definition, equals  $J$  for the IO, and as

$$\Delta T_J = (J^2/N_e)^{1/2} \quad (5.21)$$

then,

$$\Delta T_{J_{\text{ideal}}} / \Delta T_J = (J^2/N)^{1/2} / (J^2/N_e)^{1/2} \quad (5.43)$$

$$" = [(J^2/N) (N_e/J^2)]^{1/2} \quad (5.44)$$

$$" = (N_e/N)^{1/2} \quad (5.45)$$

Thus,

$$E = (N_e/N)^{1/2} \quad (5.24)$$

Another test of the model arises in the empirical proof that  $N_e$  is a constant proportion,  $E^2$ , of  $N$ . For example, transposing and squaring Eq. 5.24:

$$N_e = E^2 N \quad (5.46)$$

Substituting the above in Eq. 5.21:

$$\Delta T_J = J/E(N^{1/2}) \quad (5.47)$$

and in Eq. 5.32,

$$\Delta T = J_{iy}/E (N^{1/2}) \quad (5.48)$$

It is assumed, for the model, that the concept of  $E$  obtains only for  $N < 1$  kHz, the upper limits for  $\Delta\phi$  perception according to Klumpp et. al. (1956) and Zwislöcki, et. al. (1956). A 1.00 second maximum integration time for  $N$  is also assumed. Therefore, the model is deemed potentially applicable only to those  $\Delta t$  stimulus

conditions with frequencies lower than 1 kHz and critical durations,  $X_t$ , of 1.00 second or less.

It is conceivable that an interaction exists between the RO and type of  $\Delta t$  stimulus. For example, because of the difference in degree of definition of the ongoing  $\Delta t$  cue, one might assume a lower value of  $E$  with a pure tone stimulus presented in a burst of  $N$  cycles, than with a pulse train stimulus consisting of  $N$  pulse pairs. A noise burst, with its transient, high amplitude peaks, might be more comparable to the latter.

$J_{iy}$  is assumed to be the standard deviation of both the  $f(x|n)$  and  $f(x|s)$  distributions when  $\Delta t$  stimuli free of  $J_e$  are presented at  $SL_y$ . It may be stated in a number of ways, viz.; as in Eq. 5.48, transposed:

$$J_{iy} = \Delta T [E(N^{\frac{1}{2}})] \quad (5.49)$$

Alternatively, as in Eq. 5.42:

$$J_{iy} = (\Delta T) N_e^{\frac{1}{2}} \quad (5.42)$$

Or, empirically, substituting Eq. 5.35 for  $N_e$  in the above:

$$J_{iy} = (\Delta T) [J_e^2 / (\Delta T_J^2 - \Delta T^2)]^{\frac{1}{2}} \quad (5.50)$$

The critical value of likelihood ratio used by the RO ( $\beta_{obt}$ ) may be calculated from the data. As described by Green, et. al. (1966, p. 91),  $\beta_{obt}$  may be obtained by converting the a posteriori values of  $P(S|s)$  and  $P(S|n)$  to equivalent ordinate heights of a

normal distribution. Then,

$$\beta_{\text{obt}} = f(x|s)/f(f|n) \quad (5.25)$$

Based on the results of Experiment I, given  $P(s) = P(n) = 0.5$  in Experiment II, it is assumed that the RO's will continue to approximate closely the ideal criterion,  $\beta_{\text{opt}} = 1.00$ .

THE PSYCHOPHYSICAL FUNCTION;  $\Delta T_J / J_e$ :

In order to describe the psychophysical relationship between  $\Delta T_J$  and  $J_e$ , one must first consider the internal noise-free Ideal Observer case, where:

$$\Delta T_{J_{\text{ideal}}} = (J_e^2 / N)^{1/2} \quad (5.22)$$

This simplifies to:

$$\Delta T_{J_{\text{ideal}}} = J_e / N^{1/2} \quad (5.51)$$

To calculate the desired ratio, we divide both sides of Eq. 5.51 by  $J_e$ :

$$\Delta T_{J_{\text{ideal}}} / J_e = 1 / N^{1/2} \quad (5.52)$$

$$\Delta T_{J_{\text{ideal}}} / J_e = N^{-1/2} \quad (5.53)$$

In the IO, the value of  $\Delta T_J$  is a constant proportion,  $N^{-1/2}$ , of  $J_e$ . The resulting psychophysical function is linear, intersecting the Y-axis at  $J_e = 0$ , with a slope of  $N^{-1/2}$ . Given the conditions of  $N = 20$  and the  $J_e$  values resulting in the IO psychometric functions illustrated

in Figs. 5.3, it may be shown that the resulting  $\Delta T_{J_{\text{ideal}}}/J_e$  function rises linearly with a slope of  $(20)^{-1/2}$  or .224.

An equivalent display may be plotted for the Real Observer. However, with the introduction of a non-zero value for  $J_{iy}$  in Eq. (5.20):

$$\Delta T_J = [(J_e^2 + J_{iy}^2)/N_e]^{1/2} \quad (5.20)$$

the psychometric function,  $\Delta T_J/J_e$ , is no longer linear, but hyperbolic, asymptotically dependent upon  $J_e$  at a given  $SL_y$ . In fact, it may be shown that, for a constant value of  $N_e$ , or its equivalent,  $E^2N$ , (Eq. 5.46) all such psychophysical functions obtained from the RO will tend toward the same asymptotic slope which is  $N_e^{-1/2}$ . As  $J_e^{2 \rightarrow \infty}$  in Eq. 5.20,

$$\Delta T_J \approx (J_e^2/N_e)^{1/2} \quad (5.54)$$

Therefore;

$$\Delta T_J/J_e \approx (1/N_e)^{1/2} \quad (5.55)$$

$$\Delta T_J/J_e \approx N_e^{-1/2} \quad (5.56)$$

In general, for the RO;

$$\Delta T_J/J_e \approx 1/E(N_e^{1/2}) \quad (5.57)$$

A "NEURAL" WEBER FRACTION,  $N_e^{-1/2}$ :

While developed independently, the foregoing treatment of



$N_e^{-1/2}$  is similar to the derivation of a "neural" Weber constant by Stewart (1963). He discusses neural pulse noise in a theoretical treatise on the role of neural noise in discrimination and recognition in a noise-free external environment. Stewart (1963) defines a "neural" Weber fraction as:

$$\sigma/m \propto 1/\sqrt{k} \quad (5.58)$$

$k$  is defined as the average rate per second of time-limited pulses;  $m$  is the "neural measure for the stimulus"; and  $\sigma$  is the "corresponding measure of uncertainty due to noise...The measure of neural discrimination". He states further, "It is implied that animal discrimination improves with stimulus intensity because the neural Weber fraction decreases as  $1/\sqrt{k}$ ".

#### THE MODEL, PROOF BY VALIDATION OF ITS CONSTRUCTS:

The present study, comprised of Experiments I and II, has been devised in order to test the values and validity of the constructs of the model. The following variables and constructs will be arrived at and examined critically, through an integration of the outcomes of Experiment I and II, in Chapter VIII, and IX:

$\Delta T$	Obtained in Experiment I, this $\Delta t$ JND has been shown to increase with decreasing SL below asymptote. Furthermore, as predicted, it may be adequately represented by the reciprocal slope of the $d'$ psychometric function, best-
------------	---

fitted by method of line of least-squares to the empirical data points.

$\beta_{\text{obt}}$ :

It has been preliminary demonstrated in Experiment I that each of the three subjects is able to approximate  $\beta_{\text{opt}}$  (Table 4.4) with such a degree of accuracy as to obviate the necessity for attributing any significant basic performance deficiency to this construct. In essence, the RO's appear to function as Maximum Percent Observers, given the conditions of this experiment.

$\Delta T_J$ :

To be determined in Experiment II through the fitting of  $d'$  psychometric functions by linear least-squares method of best fit at the three SL's previously selected for Experiment I. Values of  $J_e$ , large enough to affect discrimination performance at each SL, will be superimposed on the stimulus. If the model is supported, all functions will be naturally fitted by straight lines, radiating from the origin and decreasing in slope with increasing  $J_e$ . The  $\Delta t$  JND, corresponding to a  $d'$  1.00 is given by:

$$\Delta T_J = [(J_e^2 + J_{iy}^2) / N_e]^{1/2} \quad (5.20)$$

In general,

$$d'_{\text{pred}} = \bar{\Delta t}(N_e^{1/2}) / (J_e^2 + J_{iy}^2)^{1/2} \quad (5.17)$$

A statistical comparison will be made between the RO's performance and that predicted by the model for the IO operating with the empirically determined values of  $J_{iy}$  and  $N_e$ . The only empirical data used in predicting all  $\Delta T_J$  functions will be the three values of  $\Delta T$ , one obtained for each Sensation Level in Experiment I, and a single value of  $\Delta T_J$  secured in the condition  $J_e = 160 \mu\text{sec.}$  at the High Sensation Level in Experiment II. All remaining  $\Delta T_J$  functions should be accurately predicted by the model.

$N_e$ : The average number of pulse pairs per decision used by the RO will be empirically determined by application of Eq. 5.35 to the Experiment I and II data:

$$N_e = J_e / (\Delta T_J^2 - \Delta T^2) \quad (5.35)$$

Nominally,  $J_e$  will be adjusted to the maximum value of  $160 \mu\text{sec.}$  with  $\Delta T_J$  and  $\Delta T$  determined at the High Sensation Level. If, as predicted,  $N_e$  is a constant proportion of  $N$  for each subject, viz.,  $E^2$ , then  $J_{iy}$  may be accurately estimated for each  $SL_y$ .

$J_{iy}$ :

The Sensation Level-dependent internal noise,  $J_{iy}$ , will be empirically estimated as follows:

$$J_{iy} = (\Delta T) N_e^{\frac{1}{2}} \quad (5.42)$$

If the model is correct,  $J_{iy}$  must increase in order to compensate for  $\Delta T$  increasing with decreasing SL below asymptote.

 $N_e^{-\frac{1}{2}}$ 

The asymptotic slopes of the  $\Delta T_J/J_e$  psychophysical functions empirically derived from Experiment II should correspond to  $N_e^{-\frac{1}{2}}$  for each subject, regardless of SL.

Finally, in Chapter IX, the model will be applied, a posteriori, to existing  $\Delta T$  data reported in the literature in order to test the following features:

1. The proportionality of  $\Delta T$  to  $N^{-\frac{1}{2}}$ , when stimulus duration is held constant.
2. The proportionality of  $\Delta T$  to  $X_t^{-\frac{1}{2}}$ , when stimulus frequency is held constant.
3. The generality and range of  $J_{iy}$  for predicting other  $\Delta T$  results.
4. The independence of E from frequency up to 1 kHz.
5. The generality of E for predicting other  $\Delta T$  results.

## CHAPTER VI

## EXPERIMENT II: BACKGROUND

Experiment II was carried out with two goals. The first is a systematic exploration into the effects of pulse train periodicity jitter ( $J_e$ ) on  $\Delta T$ . The second is to estimate internal noise levels ( $J_{iy}$ ) affecting the  $\Delta t$  detection task at each SL. These  $J_{iy}$  levels are empirically determined through the model described in Chapter V.

The validity of this approach to internal noise is examined in a number of ways. For example, the experimentally derived  $J_{iy}$  values are used as fitting constants in the model to predict  $\Delta T$  performance for each subject in varying backgrounds of  $J_e$ . These results are reported in Chapter VIII.

In Chapter IX, the  $J_{iy}$  estimates, derived from the present study, are used to predict results of previously reported investigations of  $\Delta T$  with stimuli other than a 20-pps train of dichotic pulses. These studies include Klumpp et al. (1956) and Zwislocki et al. (1956) on  $\Delta\phi$  detection with dichotic tone burst stimuli, as well as Zerlin (1959) on  $\Delta t$  ongoing disparity detection with dichotic noise bursts. The magnitude of empirical  $J_{iy}$  values is also compared with internal temporal noise estimates derived by other investigators.

## APPROACH TO THE PROBLEM:

The approach of this study to estimating internal noise -- by increasing external noise until an effect on discrimination performance is noted -- was suggested by the work of Bekesy (1933) on physiological decay time for auditory stimuli. Green (1960) examined

the feasibility of estimating internal noise, assuming its additivity with external noise at the input stage. Based on the results of a tone-in-noise detection experiment, Green (1960, p. 1202) concludes negatively:

"But, of course, such an assumption can immediately be rejected since no shift in the psychophysical function can account for the data displayed in the figure."

6.2  
1  
Pollack (1968b), in one of his earlier articles on discrimination of absolute and relative pulse periodicity jitter, suggested an approach similar to that of Green (1960) for estimating "internal system jitter". Specifically, Pollack advocated increasing the value of external jitter until a change in observer discrimination performance had been effected. However, as in the case of Green (1960), Pollack's data did not support a consistent conclusion. He states (1968b, p. 314):

"Are we to conclude that the temporal precision of the auditory system plays no limiting role in the determination of auditory jitter thresholds? While this conclusion may seem to be reasonable on the basis of the available evidence, it is neither realistic nor attractive."

#### EXTERNAL TEMPORAL NOISE AND AUDITION:

The imposition of  $J_e$  upon a pulse train  $\Delta t$  detection task was developed independently by this investigator (Grason-Stadler Corporation, personal correspondence, 1965) as a means of estimating internal temporal noise. A formal topic proposal for the present study was filed with the City University of New York in November,

1967. A review of the psychoacoustic literature reveals only four other investigators or investigative teams reporting research on  $J_e$ , beginning in 1965 and continuing through the time of preparation of this chapter.

6.3 The earliest published report is by A. Rosenberg (1966). He was concerned with the effects of periodicity perturbation on the differential detection of diotically presented heteropolar and homopolar pulse patterns. Seven pulse periods ranged from 5 through 15 msec. He subjected trains of unfiltered 50-msec.-duration rectangular pulses to 12 rms values of  $J_e$  ranging from approximately 375  $\mu$ sec. to 4,125  $\mu$ sec. Jitter was produced by modulating the duration of a constant slope ramp function, with either a 20-kHz low-pass random noise or a 10-kHz sine wave, in a Schmitt trigger circuit. This resulted in a random time shift of the pulse trigger point without altering the average period.

Rosenberg's findings pose some difficulty for systematic interpretation in light of the present study. For example, his psychometric functions, of number of "different" judgements as a function of  $J_e$ , were non-monotonic. In addition, there was no limit placed on the number of stimulus observations permitted each subject prior to a decision.

Minimum values of  $J_e$  affecting discrimination ranged from 1,000 to 1,500  $\mu$ sec., with some dependence on pulse polarity paradigm. The  $J_e$  JND tended to be independent of pulse period within the range explored. However, as stimulus sample size was unlimited, at the subject's discretion, this latter result is not at odds with the

model. Rosenberg (1966, p. 927) indicates that for interpulse intervals larger than 15 msec. the pulse train polarity patterns were nondiscriminable without  $J_e$ .

Subsequent published references on pulse train jitter, with the exception of Nordmark (1970), are but peripherally relevant to the present study. Consequently, only brief mention will be given them.

6.4  
The  $J_e$  research of Cardozo, Ritsma, Domburg, and Neelen (1966), published in a Dutch-language reference of limited circulation, is cited by Pollack (1968b). Jitter was generated in a manner similar to that used by Rosenberg (1965). According to Pollack, they examined jitter discrimination thresholds for two interpulse intervals, 3 and 10 msec., filtering at different center frequencies over a wide range of durations. Pollack (1968b) -- correcting for his jitter calibration in semirange of a uniform distribution, while Cardozo et al. (1966) recorded jitter in standard deviation units of a normal distribution -- reports good agreement between the two studies.

Cardozo and Ritsma (1968) report briefly on each of five different experiments concerned with the perception of imperfect periodicity. Their Experiment II is a study on the effect of Gaussian jitter on pitch matching for differentially filtered 100- and 333-pps trains. Individual differences among four subjects were considerable (Cardozo et al., 1968, p. 161). A relative jitter of 5% marked the lower limit of influence on pitch matching for the 100-pps train, while less than 1% relative jitter affects discrimination with the 333-pps repetition rate. Amplifying the findings of his 1968 study, Cardozo (1970, p. 341) notes that subjects heard no



pulse train periodicity pitch, and were unable to perform pitch matching with acceptable accuracy, when the jitter exceeded 10 to 20%.

In the third experiment of five, Cardozo et al. (1968) report the effect of burst duration on the relative JND for jitter, at the two prf's mentioned above. They note (1968, p. 161) that:

"...the shorter the duration, D, the more difficulty one has in perceiving jitter. In fact, the just noticeable jitter rises slightly more steeply than inversely proportional to the duration D. With long durations, the just noticeable jitter gradually levels off. The transition is somewhere in the region of 0.1 second."

65  
It should be noted that the basic statistical principles of the present model may be construed to apply to  $J_e$  detection per se. In the model, where D is equivalent to  $X_t$ , the function, described in the paragraph above, would rise less steeply than inversely proportional to D, viz., as  $D^{-1/2}$ . This is based on the assumption that D varies proportionally with the number of pulses, N, while the observer functions in a statistical decision-making manner. The model's prediction is supported by the findings of Pollack (1968f) for low-frequency pulse rates. Both the 3- and 10-msec. periods of Cardozo et al. (1968) broach the 2-through-8-msec. range that Pollack (1969b, p. 1023) defines for intermediate pulse frequencies.

Cardozo and Neelen (1968), in another unseen, Dutch-language, reference cited by Pollack (1970), demonstrated differential effects of "harmonic and anharmonic filtering" on jitter detection.

Cardozo (1970) presents the results of two experiments on the

psychophysical interaction of random amplitude masking and Gaussian jitter in diotic pulse trains. Periods ranged from 2.5 to 20 msec. In his first study Cardozo (1970) demonstrates that a 10-to-20% relative jitter renders inaudible a pulse train, in a masked background, previously heard whenunjittered.

His second study, on two subjects, demonstrates a linear relationship, beyond the extended flat toe of each psychophysical function, between log relative jitter and a uniquely referenced signal-to-noise ratio. The average slope of his functions, across two subjects and four repetition rates, is -0.78. That is, the relative  $J_e$  JND increases as S/N ratio decreases. Cardozo (1970), through some questionable assumptions on the nature of the transfer function of amplitude noise to time jitter, proceeds to estimate internal temporal noise levels based on his data. These findings are discussed in the next section of this chapter.

The first publications of Pollack, on pulse train periodicity perturbation, appeared in 1968. His jitter-generating system, producing a uniform, rather than Gaussian, distribution of  $J_e$ , was digital in microstructure. Both pulse stimuli and  $J_e$  were generated by a PDP-8 computer. The same device was also programmed to present the pulse trains in a 2- or 4-AFC paradigm, varying parameters according to an appropriate adaptive psychophysical procedure.

Pollack's studies are far too complex for individual summary in this thesis. A listing of his topics for detailed investigation includes the following:

1. The absolute and relative JND's for pulse train jitter of various rates and durations (1968b, 1969a).
2. The effects of masking noise and pulse amplitude level on jitter detection (1969b).
3. The effects of jitter on diotic temporal gap detection (1968a, 1969c).
4. The effect of jitter on detection of dichotic gaps and pulse polarity shifts (1968f).
5. The effect of jitter on diotic interpulse interval discrimination (1968c, 1968d, 1968e).
6. The JND for jitter, as a function of uniform or random walk distribution of interval perturbations (1969d).
7. The effect of high, low, and band pass filtering on  $J_e$  detection (1971a).
8. The relative rôles of time jitter and amplitude jitter in  $J_e$  detection and the vector addition nature of their interaction (1971b).

Pollack's results are complex functions of pulse repetition frequency, pulse polarity paradigm, nature of the jitter distribution, number of pulses per observation, number of observations per decision, amplitude level, and frequency band limits of both pulse signal and background masking noise. It is not possible to summarize his findings in any consistent manner.

In general, however, minimum  $J_e$  JND's are on the order of 0.1% of the pulse period for long duration, high repetition rate, pulse trains with significant energy present in the most audible frequency range of 1 kHz to 2 kHz. Throughout his series of investigations Pollack continues to hold his original position favoring a spectral, rather than temporal, basis for the exquisitely fine  $J_e$  JND's (1968b, p. 308):

"The temporal precision of the auditory system, in contrast to its precision of spectral analysis, appears to be insufficient to account for minimal jitter thresholds."

Assaying Pollack's findings, it is this author's opinion that conclusive evidence remains to be adduced against a rôle for temporal processing in  $J_e$  detection, especially in the lower pulse frequency range; i.e., less than 100 pps. One may construe a successful application of the present model to the Experiment II  $J_e$  data as evidence of a temporal basis for low frequency pulse rate  $J_e$  processing in the auditory system.

Perhaps the finding of Pollack which is most relevant to the present study is his own conclusion supporting a statistical model for  $J_e$  detection (1968e, p. 968):

"Acute auditory-jitter thresholds--less than 1  $\mu$ sec. --are obtained at high pulse frequencies. Since individual units of the auditory nerve demonstrate a variability of the order of 1 msec., such precise jitter thresholds are probably due to a preneural, spectral analysis of the signal, rather than to a strictly temporal analysis upon the neural 'message'. A related finding is the greater effect on jitter thresholds of the number of interpulse intervals at high pulse frequencies. At low pulse

frequencies, [period > 8 msec.] jitter thresholds are nearly inversely proportional to the square root of the number of interpulse intervals (IPI's) as might be expected from a statistical detector. At higher pulse frequencies, thresholds change at even a faster rate than a statistical detector as a function of the number of IPI's. The results weakly suggest that operations beyond statistical averaging might be effective for the discrimination of jitter at high pulse frequencies."

Nordmark (1970), providing neither experimental detail nor supplementary reference, presents (Fig. 9.1) the results of two studies comparing the effects of jitter on the  $\Delta T$  for dichotic pulse trains and pitch discrimination for monotonic pulse trains, both of unstated frequency.

Personal correspondence (Nordmark, 1971) reveals that these data were obtained in an unpublished 1962 study. Concerning the design for his jitter generator, Nordmark (1971) says:

"...the randomness was achieved by adding noise to a triangular wave that triggered a pulse generator. I then had to estimate the sigma by sampling the time intervals (100) and compute it at a later time."

Nordmark (1970) fits the same linear 2.5 slope to the data, describing the relationship between jitter standard deviation and JND for both pitch and lateralization. The present model would predict such a linear relationship once the external noise effectively "swamped" the internal noise floor. However, the lack of information on pulse repetition frequencies used by Nordmark (1970) precludes further comment. His findings, "which were based on altogether too few trials" (Nordmark, 1971), will be presented,

relative to the present study, in Chapter IX.

#### ESTIMATES OF INTERNAL TEMPORAL NOISE:

Pollack (1968b) reviews the literature on physiological measurements of single-unit neural temporal instability. Among the most relevant findings cited is the work of Kiang (1965). In his 1965 monograph Kiang graphically demonstrates first-order auditory-unit standard deviations for pulse train stimuli between 500 and 1,000  $\mu$ sec. Pollack (1968b) points up the incongruity between single-unit variability, on this order of magnitude, and his minimum-jitter JND's in the one-to-two- $\mu$ sec. range.

Ephaptic transmission may limit a strict  $N^{\frac{1}{2}}$  reduction in standard deviation of the sample mean temporal input to a central Auditory Coincidence Detector from parallel nerve fibers responding to a click stimulus. However, one may anticipate some reduction, as postulated in the model, over that of a single unit responding to the same stimulus. It is not inconceivable that the combined parallel and serial inputs from the auditory neural pathways may be responsible for jitter JND's two orders of magnitude below the standard deviation of a single unit.

A small number of psychophysical estimates of internal temporal noise, derived by various means, have appeared in the literature. The earliest published estimate of internal noise was given by Durlach (1963) as a fitting constant to his Equalization-Cancellation model for interaural JND's. He sets the single-channel rms error at 105  $\mu$ sec. The combined two-channel error, viz.,  $105 \times (2)^{\frac{1}{2}}$ , is

reported as 150  $\mu$ sec. The latter figure is analogous to  $J_{iy}$  in the present model but is independent of Sensation Level. Durlach (1966) uses this internal noise value in his E-C model to predict the pure tone  $\Delta T$  results of Klumpp et al. (1956) and Zwisllocki et al. (1956). He achieves reasonable accuracy for frequencies below 1 kHz.

The complexities of E-C model rule out any realistic comparison with the present model. Schenkel (1967, p. 23), proposing an "Accumulation Theory" of binaural masked thresholds, described Durlach's (1963) model in the following terms:

"The inhomogeneity of the EC model and the considerable mathematical operations that are necessary to compute the masked thresholds make it rather complex and do not satisfy the desire of [sic] a simple model to describe all binaural-masked thresholds."

Houtgast and Plomp (1968) arrive at 110  $\mu$ sec. as an empirically determined estimate of the standard deviation of the central "stimulation pattern" for binaural inputs. They investigated the  $\Delta t$  JND for a gated octave band of white noise centered about 500 Hz, both in quiet and in a background of uncorrelated but similarly filtered, continuous dichotic noise, incorporating a constant 400- $\mu$ sec. delay. This last feature resulted in a veridical separation of the two noise band images. Noise burst duration was a key variable in their study. They achieve an 80- $\mu$ sec. internal noise figure for a single channel, based on a minimum obtained  $\Delta T$  of 9  $\mu$ sec. with a 300-msec. burst of 500-Hz octave band noise (Fig. 9.3c).

Concerning derivation of this estimate, Houtgast et al. (1968, p. 811) state:

"The stimulus, being an octave band of noise around 500 Hz, contains 150 'periods' in 300 msec. and, consequently, the lateral position for the stimulus duration should be considered to be built up by averaging 150 information units. The statistical inaccuracy in each of them,  $\underline{s}/2$ , is then equal to  $9\sqrt{150} = 100$  [sic]  $\mu\text{sec}$ . So  $\underline{s}$  is about 80  $\mu\text{sec}$ ."

This estimate of "statistical inaccuracy" appears to be independent of Sensation Level. The derivation of  $(\underline{s}/2)$  may be compared with that for  $J_{iy}$  in the present model, viz.:

$$J_{iy} = (\Delta T) N e^{-\frac{1}{2}}. \quad (5.42)$$

Paraphrasing Houtgast et al., above, we have:

$$\underline{s}/2 = (\Delta T) N^{-\frac{1}{2}}, \quad (6.1)$$

where N is the number of "periods" in the noise burst. It should be pointed out that in the above quotation  $9\sqrt{150}$  would correctly equal 110, not the published figure of 100.

Another approach to estimating rms internal time noise is found in the work of Cardozo (1970), cited above. He reports the effects of white noise masking on rms jitter detectability thresholds using pulse trains with periods of 2, 5, 5, 10, and 20 msec. He incorporates a number of questionable assumptions on the transfer function relating amplitude noise to time noise. Then he proceeds to mathematically demonstrate that the temporal jitter, resulting from direct mixing of a pulse train with rms random amplitude noise, must be proportional to that amplitude, provided that the peak signal-to-



rms-noise ratio is significantly greater than unity. Pollack (1971) subsequently suggests a vector interaction between amplitude jitter and time jitter in pulse trains.

Cardozo (1970) arrives at multiple estimates of internal noise, varying as a function of pulse repetition frequency but independent of SL. Specifically, his prf-dependent internal noise estimates are: 800  $\mu$ sec. at 50 pps, 80  $\mu$ sec. at 100 pps, 25  $\mu$ sec. at 200 pps, and 15  $\mu$ sec. at 40 pps. This approach is logically inconsistent with the model proposed in Chapter V.

In a published discussion of Cardozo's (1970) research, Smoorenburg (1970, p. 348) briefly cites his own  $\Delta f$  JND experiment with pulse trains:

613  
 "...by jittering the pulses externally and measuring the increase of just-noticeable difference it is possible to obtain an estimate of the internal jitter. And, in accordance with the preceding, I found that the internal jitter depends on the repetition frequency rather than on the filter frequency (70  $\mu$ sec. for 200 Hz and 35  $\mu$ sec. for 400 Hz). I did not find a significant contribution from peripheral internal jitter of, for example, the detection mechanism; a jitter which is expected to be related to the place of detection at the basilar membrane or to the filter frequency. However, electrophysiological data suggests that the peripheral jitter cannot be of minor importance because it is certainly not a magnitude smaller than the estimates of 70  $\mu$ sec. and 35  $\mu$ sec. which I obtained for the whole process."

None of the reports cited above ascribes an SL-dependence to internal noise. The last two studies (Cardozo, 1970; Smoorenburg, 1970) imply a direct dependence of internal noise on pulse repetition frequency. The present model assumes that  $J_{iy}$  is dependent

upon SL and independent of pulse repetition frequency at a given SL. All the above-reported estimates will be compared with those derived from Experiment II in Chapter IX.

6/14

## CHAPTER VII

## EXPERIMENT II: INSTRUMENTATION AND PROCEDURES

7. With the addition of components necessary for  $J_e$  generation and control, the basic equipment for Experiment II is essentially that used in Experiment I, as described in Chapter II. The system articulation, outlined below, is referred to the block diagram (Fig. 2.2) in Chapter II. The psychophysical method for Experiment II is the same as in Experiment I, described in Chapter III, with the exceptions noted below. The Experiment II stimulus paradigms are illustrated in Fig. 7.1. These may be compared with the Experiment I paradigms shown in Chapter III, Fig. 3.2. Although Experiments I and II are treated separately in this thesis, data collection was randomly interspersed for both studies.

## SYSTEM ARTICULATION:

On those Experiment II runs where  $J_e \neq 0$ , the jitter generation-and-control circuitry was activated. These components are illustrated in the lower left-hand corner of Fig. 2.2. The 20-kHz low-pass output of a Grason-Stadler 455B random noise generator was further frequency-limited below 100 Hz through an Allison 2BR filter. This effectively ruled out the possibility of supernumerary pulses being triggered during the  $J_e \neq 0$  observation trials.

The filter output was then amplified through a B&K Model 2112 audio spectrometer functioning as an extremely low-noise, wide-band amplifier (2 Hz - 40 kHz). Noise voltage levels were monitored at the amplifier output with a B&K 2416 rms VTVM. Through a dual

Figure 7.1

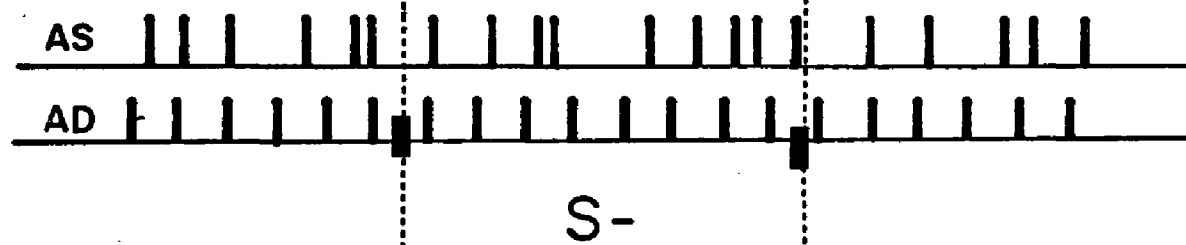
Graphically simulated relationships for the AXA paradigm  
pulse inputs to AD and AS in Experiment II;  $J_e \neq 0$ .

A. S- condition; "blank" trial.

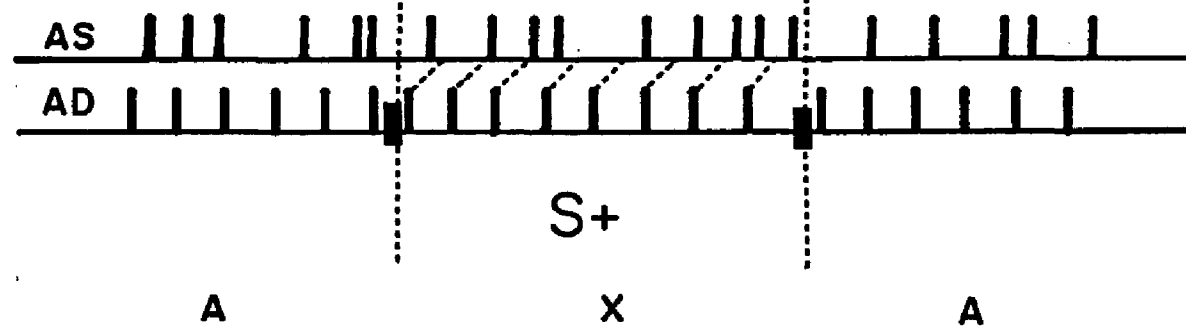
B. S+ condition;  $\Delta t$  lead to AD.

EXPERIMENT II:  $J_0 \neq 0$

a.



b.



TIME →

transformer circuit, the amplifier output was then floated, stepped-up in voltage, and mixed with the 10 msec. duration sawtooth ramp of Waveform Generator (WG) 2. The WG 2 ramp function was triggered by WG 1 at the basic 50 msec. stimulus period. In turn, it triggered pulses for the AS or  $J_e$  channel.

The result of this articulation was a continuous low frequency random noise modulation of the DC-biased WG 2 ramp. This shifted the AS channel IPI about a mean of 50 msec., randomly in time, proportional to the noise input voltage. A strict 20 pps repetition rate was maintained through the highest level of  $J_e$ ;  $J_{e_{max.}} = 160 \mu\text{sec. rms.}$  The AD interpulse interval and pulse repetition frequency remained constant throughout the experiment.

#### $J_e$ CALIBRATION:

In addition to the Experiment I calibration procedures previously outlined, the following operations were used to transfer rms modulating noise voltages to equivalent  $J_e$  values in  $\mu\text{sec.}$ . The degree of normal approximation was established for the distribution of AS channel IPI perturbations. All components are listed as labelled in Fig. 2.2.

The EPUT, in an A-B timing mode, triggered "on" at the start of each WG 1 ramp. WG 1 dictated the 50 msec. base period to both the AS  $J_e$  channel (WG 2) and the AD  $\Delta t$  channel (WG 3). Ramp durations for WG's 2 and 3 were 10 msec. and 5 msec., respectively. The EPUT was triggered "off" at onset of the PG 1 output. PG 1 was calibrated to trigger near mid-ramp, 4.00 msec. from the simultaneous start of the WG 1 50 msec. ramp and WG 2 10 msec. ramp. This A-B interval was read every 6 seconds to the nearest 10  $\mu\text{sec.}$ . This last value was the

smallest measurement unit in time available on the Beckman 7350 A EPUT. Trial-by-trial readouts were hand-recorded in four blocks of 100 IPI's each. Modulating noise input voltages were randomized among blocks in 6 dB steps from .0625 volts rms, through 2.00 volts rms. Noise measurements were made as described above.

In order to estimate the system noise floor, 4 blocks of 100 IPI's were collected with an equivalent pure resistance substituting for the noise generator. The obtained instrumentation artifact of  $J_e$  was calculated at 3.3  $\mu$ sec. In Experiment I, where  $J_e = 0$ , these additional components were disconnected, resulting in an oscilloscopically-observed improvement in stability over the above variability (Fig. 2.4). Application of the above measurement procedure to the Experiment I instrumental noise floor resulted in no deviations noted outside the 10  $\mu$ sec. minimum unit of the EPUT; i.e. range  $\leq \pm 5 \mu$ sec..

Random deviations in the 50 msec. base period of WG 1 were estimated on the same order of magnitude as those intrinsic to the  $J_e$  channel, and therefore of no significance to the experiment. This entailed a potential error in period on the order of  $10^{-4}$  percent, common to both channels.

Table 7.1 summarizes the block data analysis on sample  $J_e$  values used in Experiment II, as well as the  $J_e$  system noise floor. Lesser modulating noise voltages than 0.25 volts, ( $J_e = 20 \mu$ sec.) were determined, by preliminary investigation, to have no observable effects on slopes of the steepest  $\Delta T$  psychometric functions. Voltages significantly greater than 2.00 volts (160  $\mu$ sec.) resulted in the triggering of supernumerary pulses.

Table 7.1

100Hz low-pass rms noise voltage transformation to  $J_e$  ( $\sigma$ ) in  $\mu\text{sec}$ . Each block contains 100 intervals from the basic PRF trigger point to the  $J_e$  channel pulse sampled every 6 seconds.  $\chi^2$  values are computed against the normal distribution over thirteen  $1/2 \sigma$  intervals within the range  $\pm 3.25 \sigma$ , d.f. = 12.

PARAMETER		BLOCK 1	BLOCK 2	BLOCK 3	BLOCK 4	BLOCK 1-4
0 — — — — —	$\bar{X}$	4000.10	4000.10	4002.00	3999.60	4000.45
	$\sigma^2$	6.99	8.99	16.00	7.84	10.80
	$\sigma$	2.64	3.00	4.00	2.80	3.29
	sk	.43	.27	1.50	- 1.39	0.86
	k	11.26	8.09	.25	9.10	5.85
0.25 volts rms	$\bar{X}$	3997.90	3998.10	3999.00	4001.10	3999.03
	$\sigma^2$	470.59	319.39	509.00	439.79	436.30
	$\sigma$	21.69	17.87	22.56	20.97	20.89
	sk	.39	- .35	- 0.12	- 0.00	0.02
	k	- 0.23	0.26	0.41	- 0.19	0.05
	$\chi^2$	27.79	13.63	18.69	8.87	15.20
	P	<.01	NS	NS	NS	NS
0.50 volts rms	$\bar{X}$	4001.40	3996.20	4000.10	4004.90	4000.65
	$\sigma^2$	1764.04	1619.56	1450.99	1274.99	1537.08
	$\sigma$	42.00	40.24	38.09	35.71	39.21
	sk	- .20	.16	.58	- .21	0.06
	k	- .55	- .68	.83	.33	- 0.14
	$\chi^2$	16.34	12.90	31.80	9.55	30.20
	P	NS	NS	<.01	NS	<.01
1.00 volts rms	$\bar{X}$	4002.70	4003.50	4003.00	4001.40	4002.65
	$\sigma^2$	5449.71	8646.75	6705.00	6698.04	6875.48
	$\sigma$	73.82	92.99	81.88	81.84	82.92
	sk	- .16	- .19	.10	.23	- 0.15
	k	- .10	- .11	- .49	.13	- 0.07
	$\chi^2$	6.45	11.32	5.29	12.52	14.57
	P	NS	NS	NS	NS	NS
2.00 volts rms	$\bar{X}$	4016.60	4003.70	4001.30	4000.60	4005.55
	$\sigma^2$	30702.44	26145.31	22981.31	23703.64	25925.20
	$\sigma$	175.22	161.70	151.60	153.96	161.01
	sk	.12	.15	- .12	- .12	0.00
	k	- .50	- .28	.33	.68	0.02
	$\chi^2$	7.66	8.92	13.48	21.67	5.05
	P	NS	NS	NS	P<.05	NS



Block means cluster closely about the median interval of 4000.00  $\mu\text{sec.}$ . Variance, standard deviation, skewness, and kurtosis are presented for individual blocks of 100 IPI's and for the total of 400 intervals at each level of  $J_e$ . These parameters were calculated from the hand-recorded samples with the aid of a general descriptive statistical computer program. From the data in Table 7.1, it is evident that the transformation of rms voltage to rms time is linear, even for IPI samples as small in number as 100.

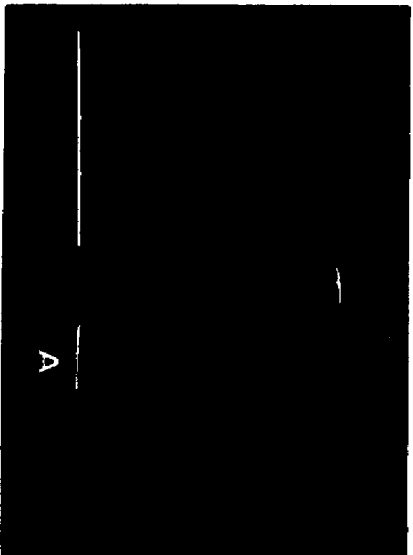
Two additional analyses of  $J_e$  IPI samples were carried out. The first described symmetry of the  $J_e$  distribution as a function of  $\Delta t$ . The second assessed the IPI distributions' approximation to a Gaussian form. Figure 7.2 illustrates the AS channel IPI distributions as a function of  $J_e$ . A 10 minute train of unfiltered 100  $\mu\text{sec.}$  pulses was delivered in the AS channel to a 100 channel PAR model TDH-9 analog averager. Each baseline represents 1.00 msec. total time, 100  $\mu\text{sec.}$  per division, 10  $\mu\text{sec.}$  per bin. The averager time constant remained at 5.0 seconds. Symmetry about the mean of each distribution is demonstrated for the four values of  $J_e$  used in Experiment II.

The above procedure was then modified by using the AD channel pulse output to shift the averager sweep trigger point by  $\Delta t$  at a rate of once per second. The joint interaction of  $J_e$  and  $\Delta t$  can be seen in Figs. 7.3 through 7.6. It may be observed that shifts in  $\Delta t$  have no influence on relative symmetry of the  $J_e$  distributions.

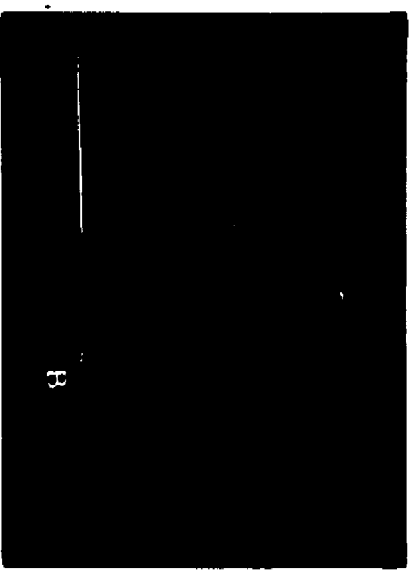
Finally, the original IPI sample calibration data were subjected to a computer-run Chi Square test against the normal distribution. Table 7.1, mentioned above, contains the Chi Square values and associated probabilities for each of the  $J_e$  levels used in Experiment II. The IPI data were arrayed in  $1/2 \sigma$  steps with a  $\pm 3.25 \sigma$  limit. Table

Figure 7,2

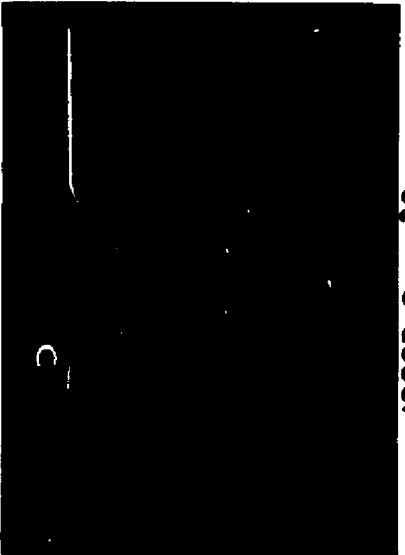
Distributions of  $J_e$  in the AS channel photographed from oscilloscope displays of 100-channel analog averager output. Distributions include area beneath 100  $\mu$ sec. duration rectangular pulse; prf = 20 pps.



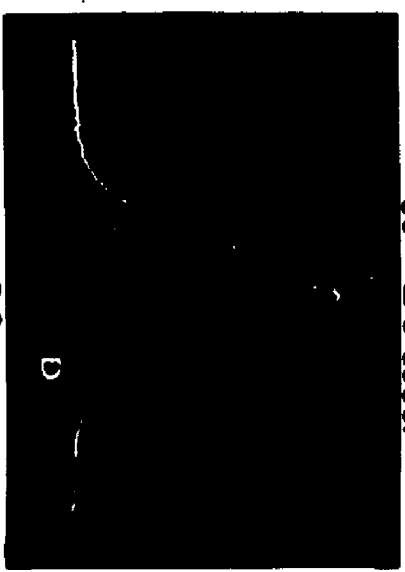
$J_e = 0 \text{ usec.}$



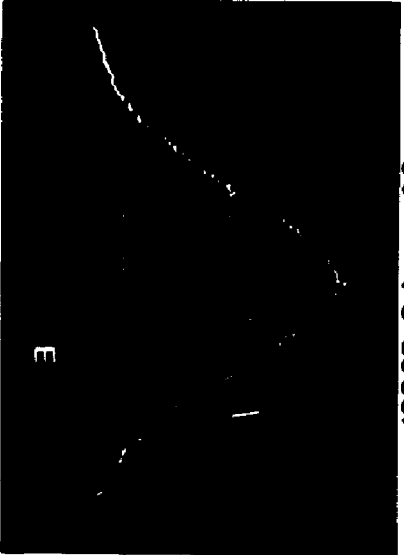
$J_e = 20 \text{ usec.}$



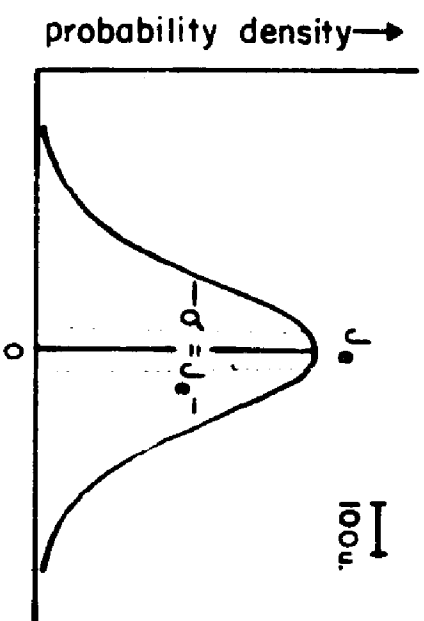
$J_e = 40 \text{ usec.}$



$J_e = 80 \text{ usec.}$



$J_e = 160 \text{ usec.}$



## Figures 7.3 - 7.6

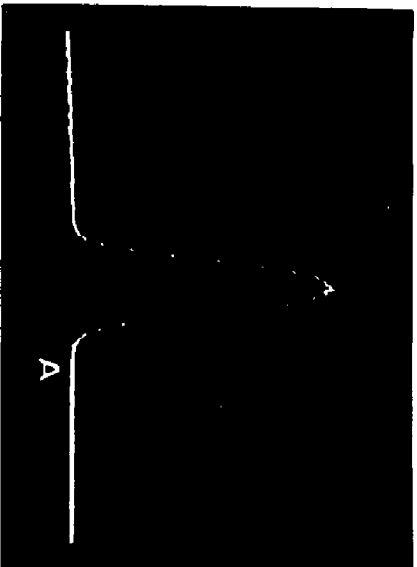
Averager-simulated responses to  $\Delta t$  where  $J_e \neq 0$ . Parameter of each figure is  $J_e$  a  $f(\Delta t)$ . The 100-channel analog averager output is displayed on an oscilloscope, 100  $\mu\text{sec.}/\text{division}$ .

Fig. 7.3  $J_e = 20 \mu\text{sec. rms.}$

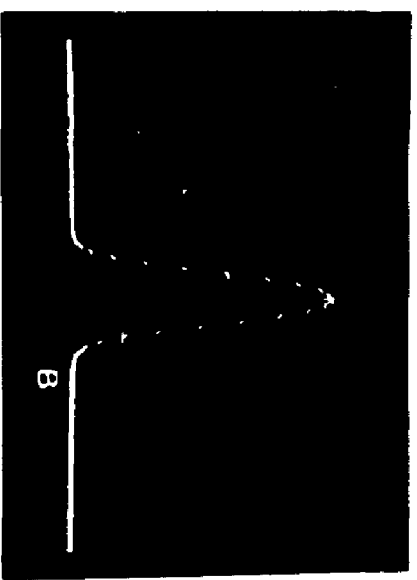
Fig. 7.4  $J_e = 40 \mu\text{sec. rms.}$

Fig. 7.5  $J_e = 80 \mu\text{sec. rms.}$

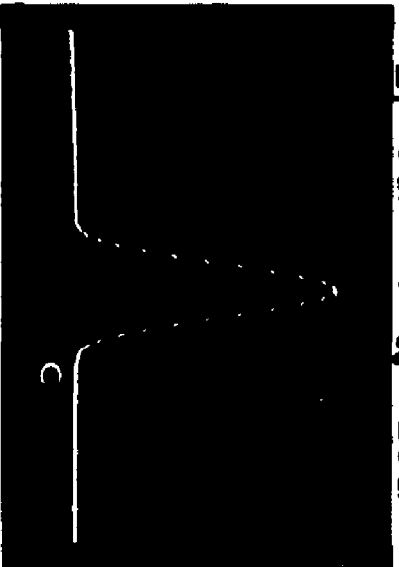
Fig. 7.6  $J_e = 160 \mu\text{sec. rms.}$



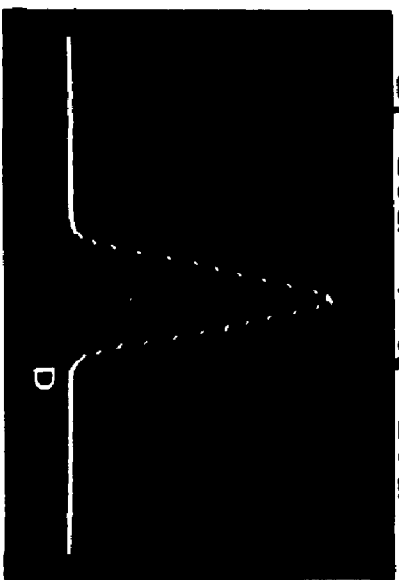
$\Delta T = 0u.$  /  $J_0 = 20u.$



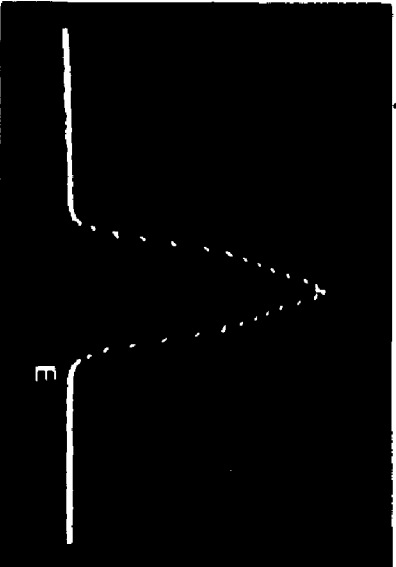
$\Delta T = 20u.$  /  $J_0 = 20u.$



$\Delta T = 40u.$  /  $J_0 = 20u.$



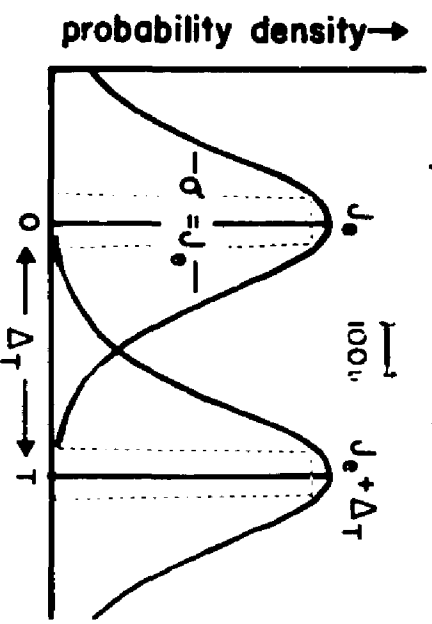
$\Delta T = 60u.$  /  $J_0 = 20u.$

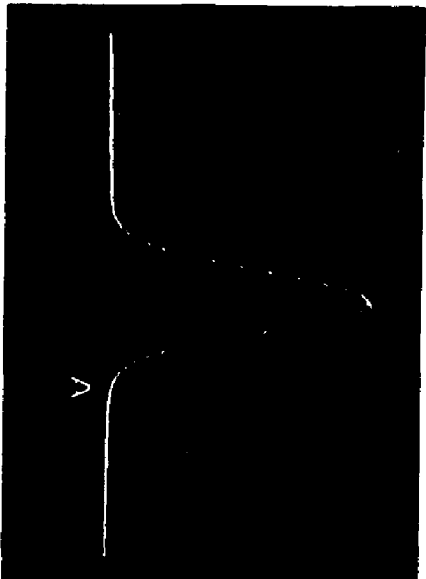


$\Delta T = 80u.$  /  $J_0 = 20u.$

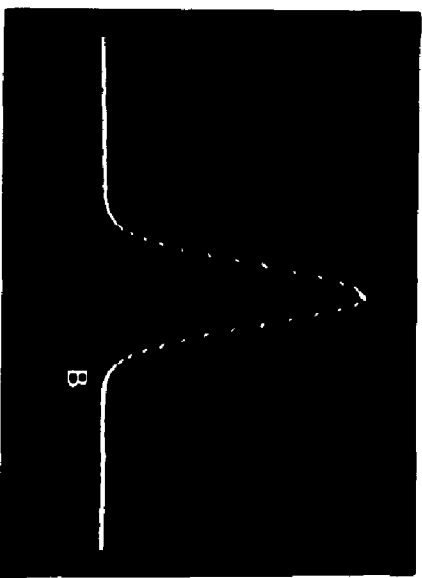


$\Delta T = 100u.$  /  $J_0 = 20u.$

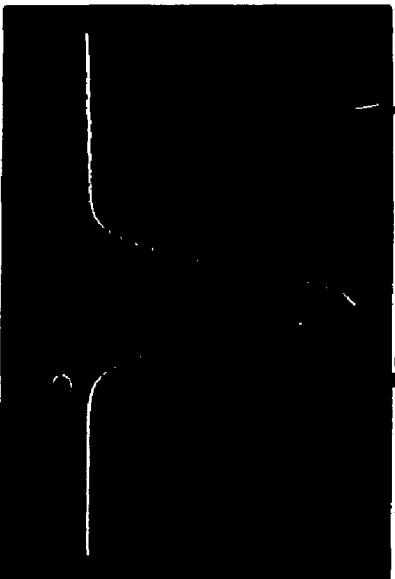




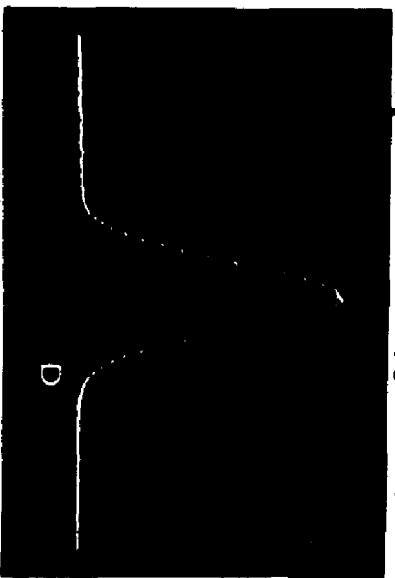
$\Delta T = 0u.$  /  $j_0 = 40u.$



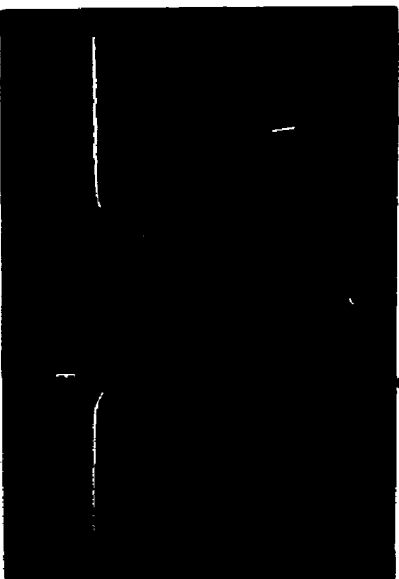
$\Delta T = 20u.$  /  $j_0 = 40u.$



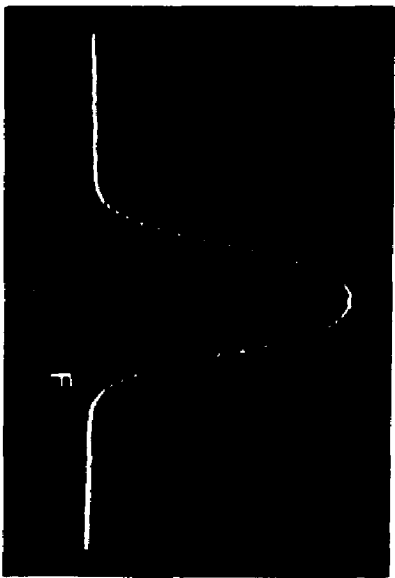
$\Delta T = 40u.$  /  $j_0 = 40u.$



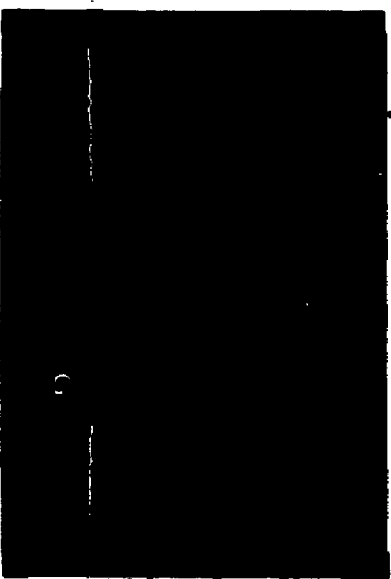
$\Delta T = 60u.$  /  $j_0 = 40u.$



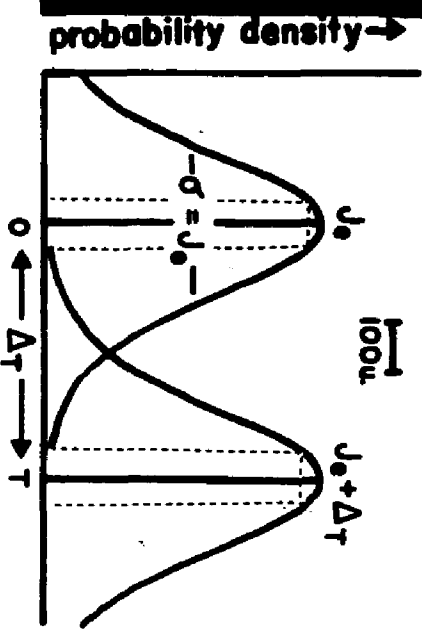
$\Delta T = 80u.$  /  $j_0 = 40u.$

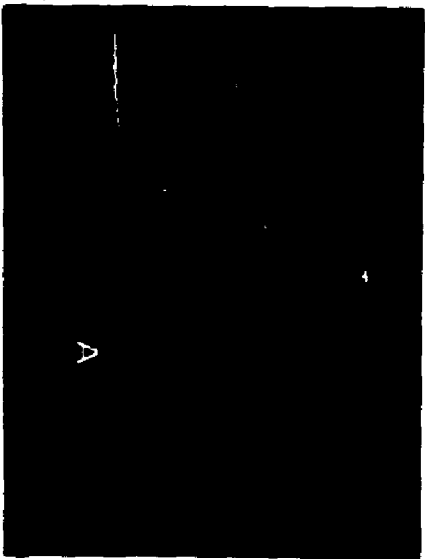


$\Delta T = 100u.$  /  $j_0 = 40u.$

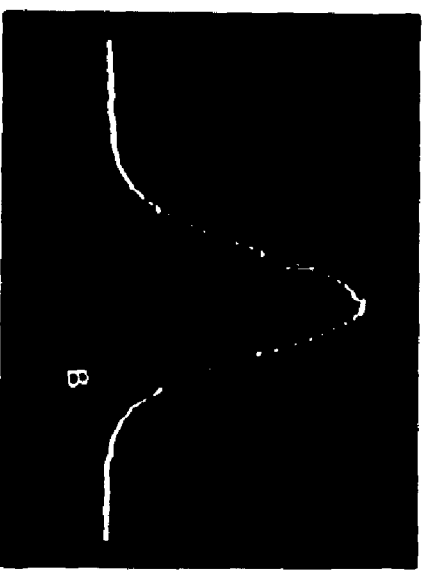


$\Delta T = 140u.$  /  $j_0 = 40u.$

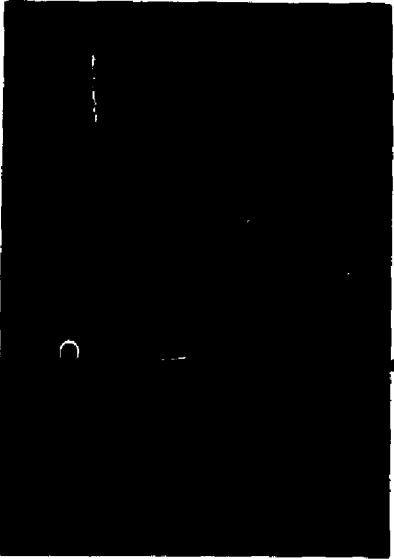




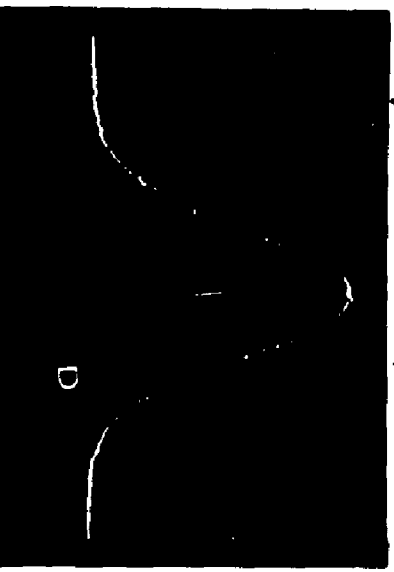
$\Delta T = 0 \text{ u.} \quad / \quad J_0 = 80 \text{ u.}$



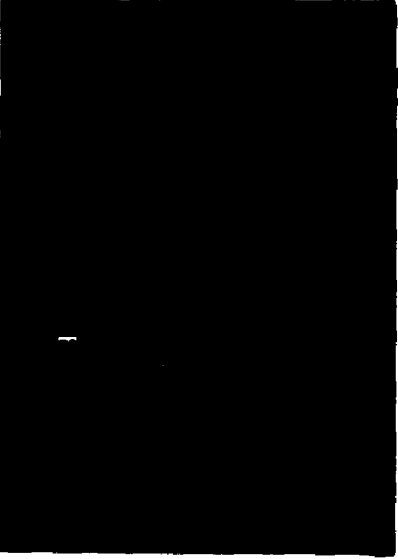
$\Delta T = 40 \text{ u.} \quad / \quad J_0 = 80 \text{ u.}$



$\Delta T = 80 \text{ u.} \quad / \quad J_0 = 80 \text{ u.}$



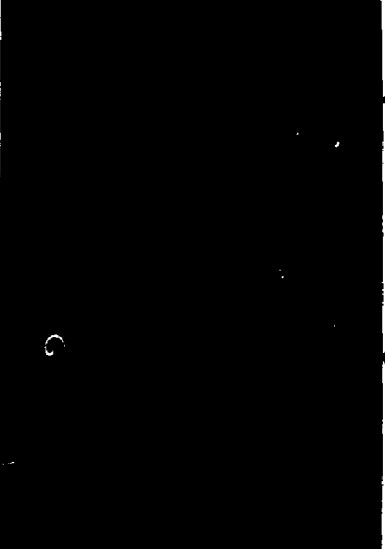
$\Delta T = 120 \text{ u.} \quad / \quad J_0 = 80 \text{ u.}$



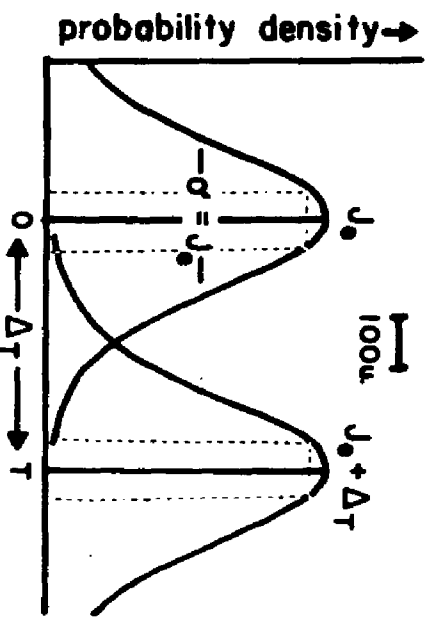
$\Delta T = 160 \text{ u.} \quad / \quad J_0 = 80 \text{ u.}$

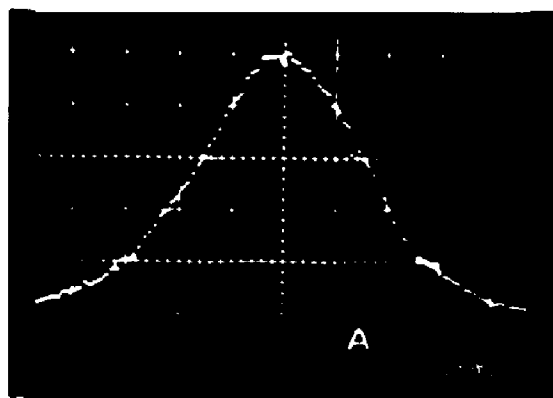
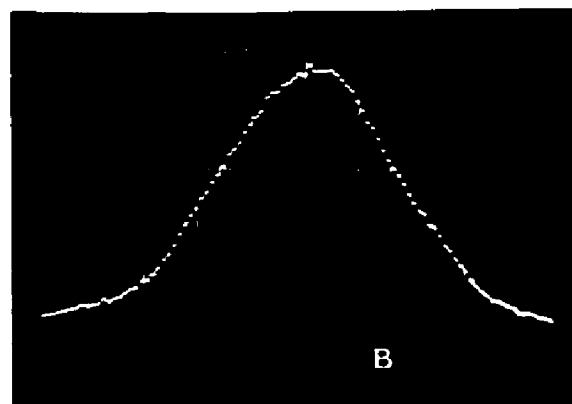
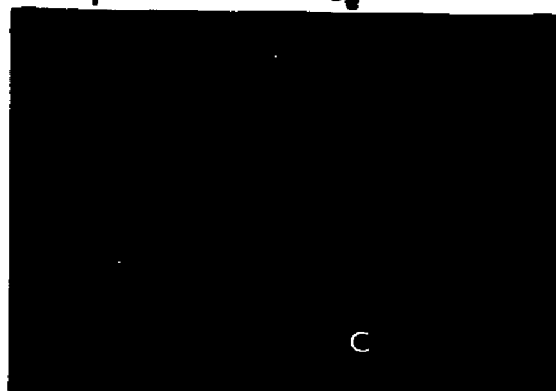
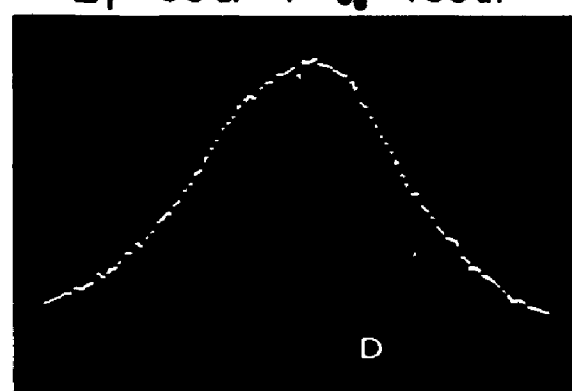
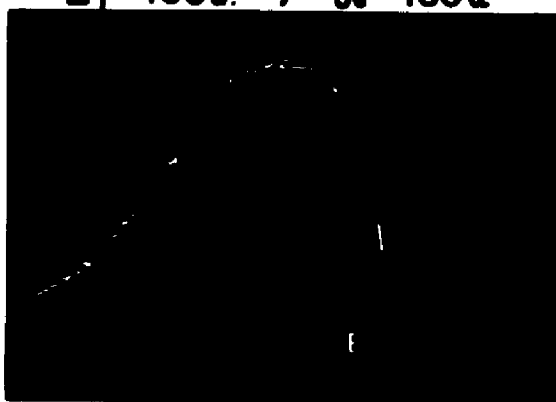
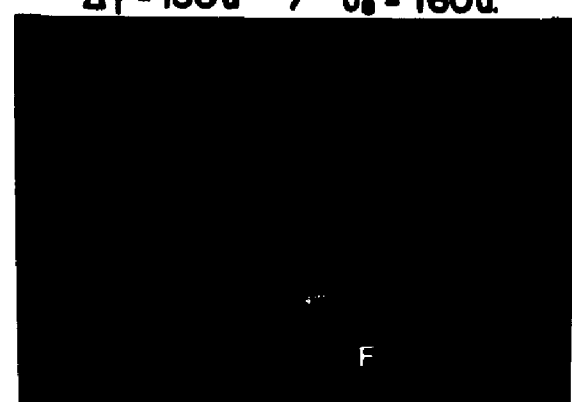
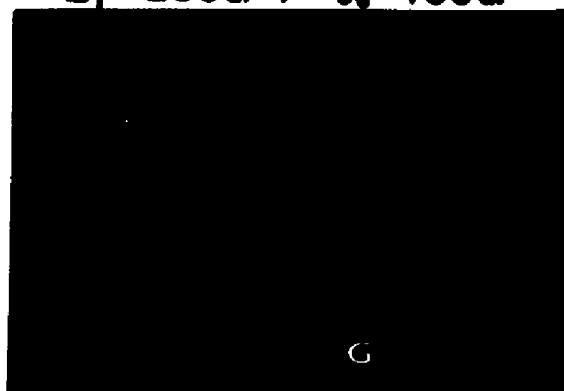
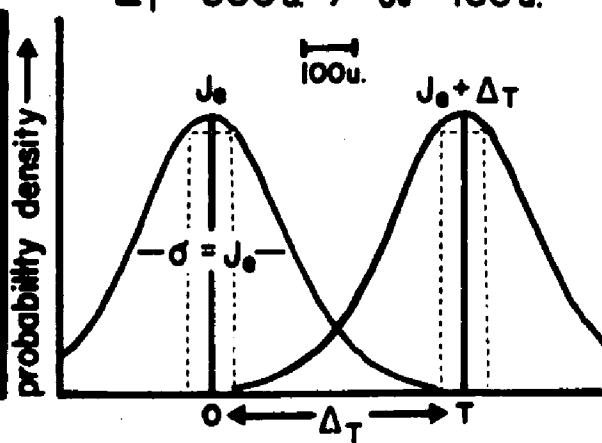


$\Delta T = 200 \text{ u.} \quad / \quad J_0 = 80 \text{ u.}$



$\Delta T = 240 \text{ u.} \quad / \quad J_0 = 80 \text{ u.}$




 $\Delta_T = 0u \quad / \quad J_0 = 160u.$ 

 $\Delta_T = 50u \quad / \quad J_0 = 160u.$ 

 $\Delta_T = 100u \quad / \quad J_0 = 160u.$ 

 $\Delta_T = 150u \quad / \quad J_0 = 160u.$ 

 $\Delta_T = 200u \quad / \quad J_0 = 160u.$ 

 $\Delta_T = 300u \quad / \quad J_0 = 160u.$ 

 $\Delta_T = 400u \quad / \quad J_0 = 160u.$ 




7.2 is a sample printout of the computer-run Chi Square test. Figure 7.7 is a representative sample from a series of computer-generated IPI histograms. Both Table 7.2 and Fig. 7.7 represent 400 IPI's with 2.00 volts rms input (160  $\mu$ sec.). All  $J_e$  distribution samples are good approximations to the normal.

#### METHODS AND PROCEDURES:

Psychophysical methods and operational procedures used in Experiment II are essentially those described in Chapter II for Experiment I. Runs were carried out in sequences of related  $\Delta t$  values under a single combination of SL and  $J_e$ . For example, a typical Experiment II session might consist of five  $\Delta t$  values run at the 10 dB SL with  $J_e = 80 \mu$ sec.. A minimum of one orientation run was given at the start of each session and upon change in the prevailing conditions of SL and  $J_e$ . Calibration checks of  $\Delta t$ , IPI and  $J_e$  were made before, after, and where possible, during each run.

Subjects SLS, RFS, and JEB, participated in both experiments. Each was well-practiced and run to asymptote of performance at all combinations of SL and  $J_e$  prior to formal data collection.

As in Experiment I, subjects centered the intracranial pulse image, at the appropriate SL, with  $J_e = 0$ . They were instructed to attend to the stimulus during the LISTEN interval, noting whether or not the image shifted to the right of midline during the X sub-interval of the AXA observation interval. The Experiment II s+ and s- paradigms are schematized in Fig. 7.1. However, when the  $J_e$  and SL combinations resulted in a perceptibly fluctuating midline image, subjects were requested to judge whether or not the image shifted to the right, on the average, more during the X sub-interval than during the immediately surrounding

Figure 7.7

Representative digital computer-generated Z-score histogram of 400-interval sample  $J_e$  distribution for 2.00 Volts rms input ( $J_e = 160 \mu\text{sec}$ ). Analysis interval is  $0.5 \sigma$ ; range:  $\pm 3.25 \sigma$ ;  $= 161.01 \mu\text{sec}$ .

FREQUENCY	0	2	3	12	21	50	70	87	65	45	26	13	5	1	0
87								0000							
84								0..0							
81								0..0							
78								0..0							
75								0..0							
72								0..0							
69								00000..0							
66								0.. ..0							
63								0.. ..00000							
60								0.. .. ..0							
57								0.. .. ..0							
54								0.. .. ..0							
51								0.. .. ..0							
48								00000.. .. ..0							
45								0.. .. ..00000							
42								0.. .. ..0							
39								0.. .. ..0							
36								0.. .. ..0							
33								0.. .. ..0							
30								0.. .. ..0							
27								0.. .. ..0							
24								0.. .. ..00000							
21								00000.. .. ..0							
18								0.. .. ..0							
15								0.. .. ..0							
12								00000.. .. ..00000							
9								0.. .. ..0							
6								0.. .. ..0							
3								00000.. .. ..00000							
Z-SCORE TABULATION OF J(E)															
LEVEL 7: 2.00 VOLTS rms															
GROUPS 1 - 4; N = 400															
MEAN 4005.55 usec.															
S.D. 161.01 usec.															
EACH INCREMENT IN HEIGHT EQUALS 3 POINTS															
-3.2-3.2-2.7-2.2-1.7-1.2-0.7-0.2 0.2 0.7 1.2 1.7 2.2 2.7															
-2.8-2.3-1.8-1.3-0.8-0.3 0.1 0.6 1.1 1.6 2.1 2.6 3.2 3.2															
-2.9-2.4-1.9-1.4-0.9-0.4 0.0 0.5 1.0 1.5 2.0 2.5 3.0															

Table 7.2

$\chi^2$  Against a Normal Distribution for  $J_e = 160 \mu\text{sec}$ . Z-Score Sample Distribution (Fig. 7.7).

N	MEAN	VARIANCE	STANDARD DEVIATION	M3	M4	SKEWNESS	KURTOSIS
400	100.5550	259.2520	16.1013	2.9495	203272.1088	0.0007	0.0244
TABULATION PARAMETERS-							
	LOWER BOUND	UPPER BOUND	NO. OF INTERVALS	INTERVAL SIZE			
	-3.25	3.25	13	0.50			
UPPER CUMULATIVE PERCENT IN							
INTERVAL	Z	PERCENTAGE	INTERVAL	OBSERVED	EXPECTED	(O-E)	(O-E) <sup>2</sup>
AT LOWER BOUND 0.0005769							
1	-2.75	0.0029798	0.0024028	2.	0.9611	1.0388	1.0792
2	-2.25	0.0122245	0.0092446	3.	3.6978	-0.6978	0.4870
3	-1.75	0.0400592	0.0278346	12.	11.1338	0.8661	0.7501
4	-1.25	0.1056498	0.0655906	21.	26.2362	-5.2362	27.4182
5	-0.75	0.2266274	0.1209776	50.	48.3910	1.6089	2.5887
6	-0.25	0.4012937	0.1746663	70.	69.8665	0.1334	0.0178
7	0.25	0.5987063	0.1974125	87.	78.9650	8.0349	64.5605
8	0.75	0.7733726	0.1746663	65.	69.8665	-4.8665	23.6830
9	1.25	0.8943502	0.1209776	45.	48.3910	-3.3910	11.4991
10	1.75	0.9599408	0.0655906	26.	26.2362	-0.2362	0.0558
11	2.25	0.9877755	0.0278346	13.	11.1338	1.8661	3.4824
12	2.75	0.9970202	0.0092446	5.	3.6978	1.3021	1.6955
13	3.25	0.9994230	0.0024028	1.	0.9611	0.0388	0.0015
LOW	-3.25	-	-	0.	0.2308	-0.2308	0.0532
HIGH	3.25	-	-	0.	0.2308	-0.2308	0.0532
SUMS				400.	400.0000	N. S.	
CHI-SQUARE-				5.0516, WITH 12 DEGREES OF FREEDOM.			

A sub-intervals.

This task was mastered by the subjects with a high relative consistency. Examination of the raw data point distributions, among the sets of four runs of 50 trials, revealed a typical range of  $\pm 0.5 d'$  units for each  $\Delta t$  value. Scatter among runs, at a single  $\Delta t$  value tended to be greater at lower SL's and with larger values of  $J_e$ .

Data are presented in Chapter VIIII. Each run consisted of 10 orientation and 50 data trials. Each data point consisted on four such runs by YES/NO method,  $P(s) = 0.5$ , in an AXA paradigm. Table 7.3 represents the Sensation Levels and  $J_e$  values for each of the three subjects participating in Experiment II.

Table 7.3

Combinations of  $J_e$  and Sensation Level used for Each Subject in Experiment II.

Relative Sensation Level	Subject SLS		Subject JEB		Subject RFS	
	SL	$J_e$	SL	$J_e$	SL	$J_e$
HIGH	60 dB	20 $\mu$ sec.	40 dB	20 $\mu$ sec.	60 dB	--
		40		40		40 $\mu$ sec.
		80		80		80
		160		160		160
MEDIUM	40 dB	40 $\mu$ sec.	20 dB	40 $\mu$ sec.	40 dB	40 $\mu$ sec.
		80		80		80
		160		160		160
LOW	10 dB	80 $\mu$ sec.	10 dB	80 $\mu$ sec.	10 dB	80 $\mu$ sec.
		160		160		160

## CHAPTER VIII

## EXPERIMENT II: RESULTS AND DISCUSSION

## d' DATA:

Figures 8.1 through 8.9 illustrate the d' data of Experiment II from each of the three subjects. Conditions of  $J_e$  and Sensation Level are as described in Table 7.3. Each point is based on 200 trials in four runs of 50, with  $P(s) = P(n) = 0.5$ . As in Experiment I, data were truncated below  $d' = 3.5$ . This cut-off corresponds to a Percent Correct score of approximately 95%. The nine graphic displays are arranged, in sequence, by subject and SL, within subjects.

The most steeply sloping solid line functions in each figure were derived from data of Experiment I, representing the condition  $J_e = 0$ . Each solid line, in Figs. 8.1 through 8.9, is the least-squares best-fit to the sets of data points. Obtained fitting parameters for each Experiment II function, including slope<sup>-1</sup> and Y-axis intercept, are given in Table 8.1. The fitting parameters for the  $J_e = 0$  condition of Experiment I are found in Table 4.2.

Reciprocal slope is used as a descriptive parameter for all d' psychometric functions in this study. This is consistent with the predictions of the model, that all d' psychometric functions will be linear, each radiating from the X/Y coordinates:  $0 \mu\text{sec}/0 d'$ . If this assumption is borne out, then slope<sup>-1</sup> coincides with the  $\mu\text{sec.}$  value of  $\Delta t$  leading to a d' of 1.00, a generally accepted estimate of the JND.

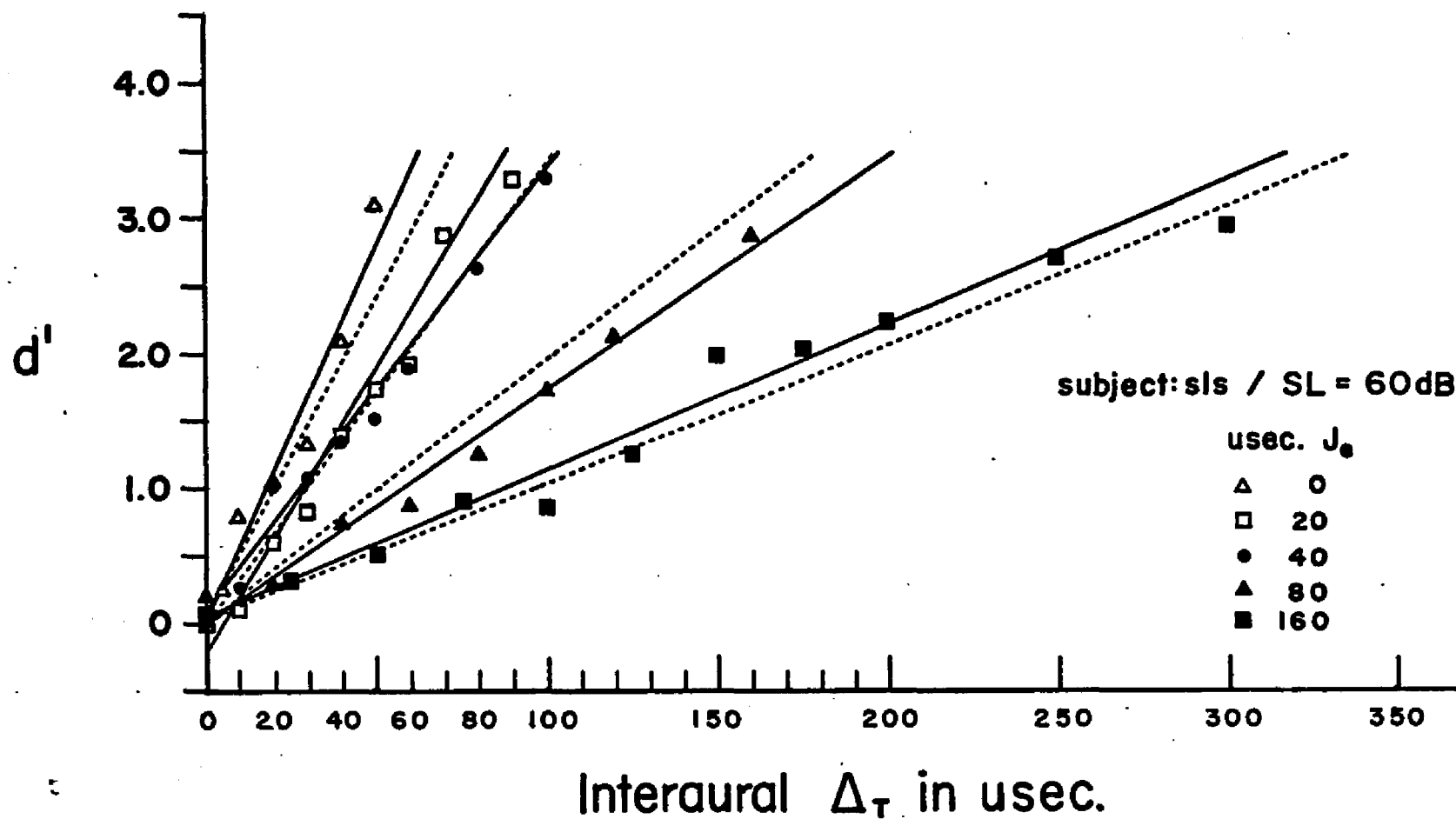
Adequacy of a linear fit to these d' data was tested by means of an analysis of variance incorporated into an IBM polynomial regression

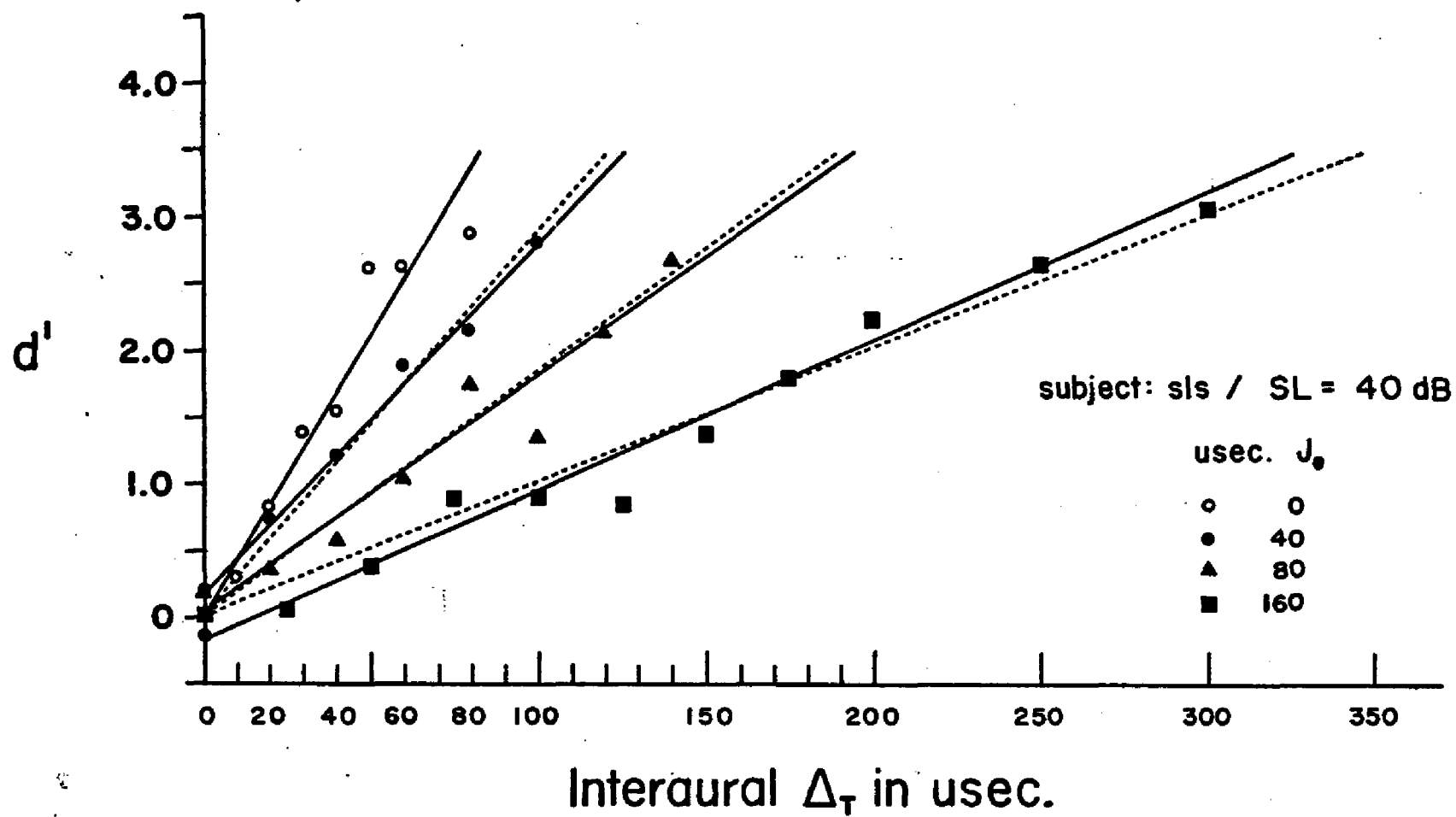
## Figures 8.1 - 8.9

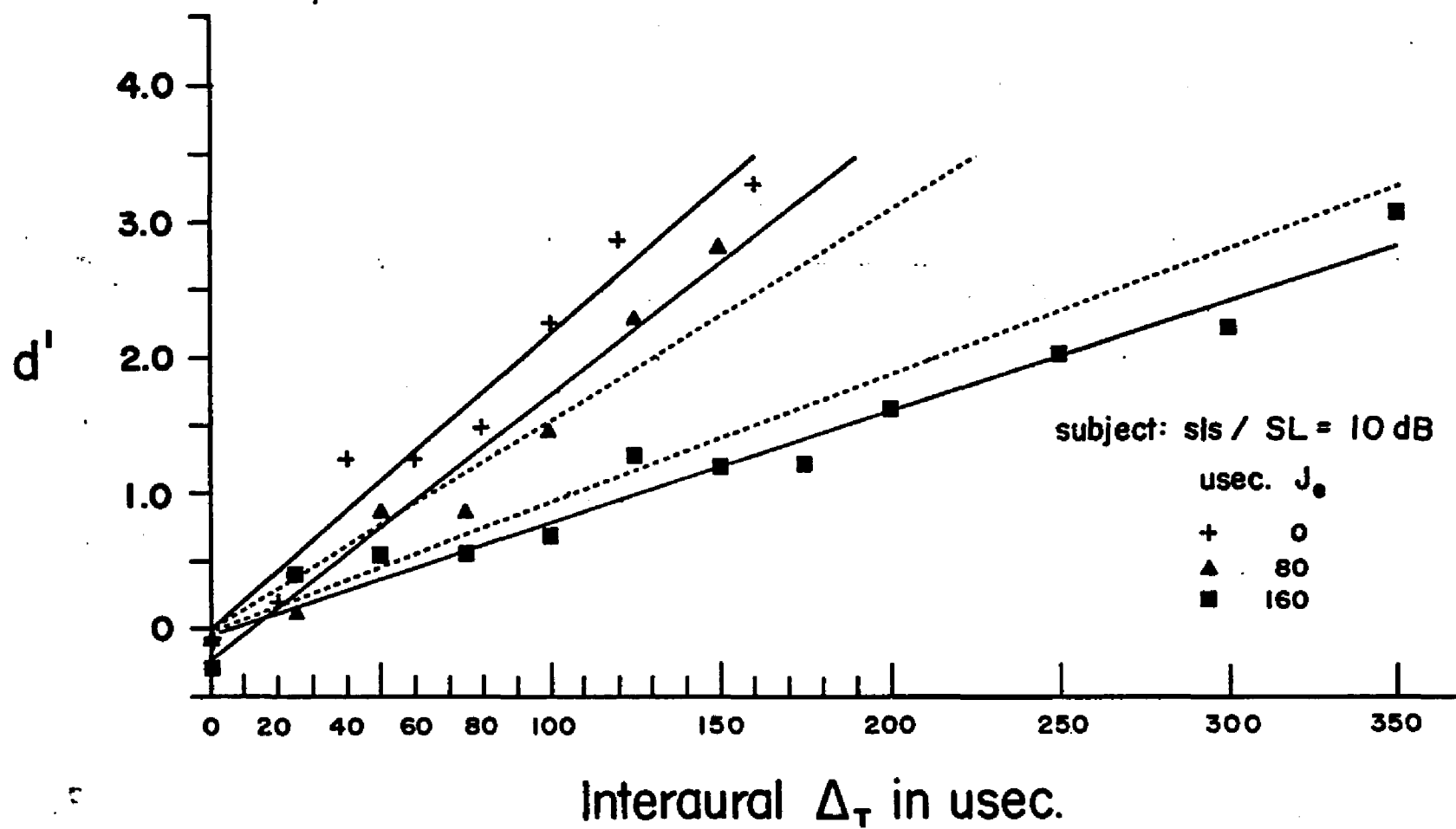
$d'$  At psychometric functions;  $J_e \neq 0$ . Solid lines are least-squares best-fittings to the data points. Dashed lines are fittings predicted by the model. Each point represents 200 trials. Experiment I data ( $J_e = 0$ ) are included as the steepest functions in each figure:

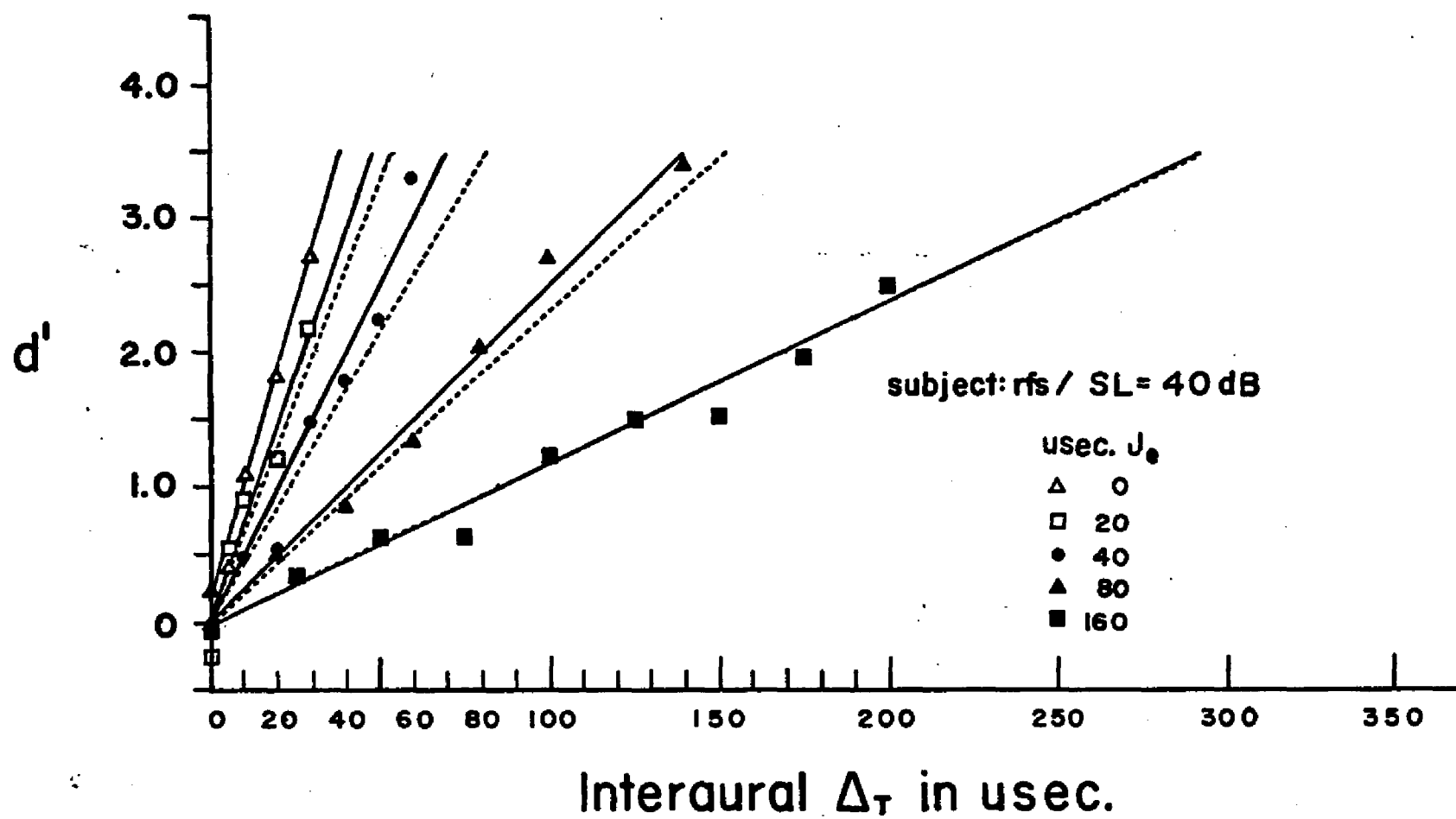
<u>FIGURE</u>	<u>SUBJECT</u>	<u>SENSATION LEVEL</u>
8.1	SLS	60 dB
8.2		40
8.3		10
8.4	RFS	40 dB
8.5		20
8.6		10
8.7	JEB	60 dB
8.8		40
8.9		10

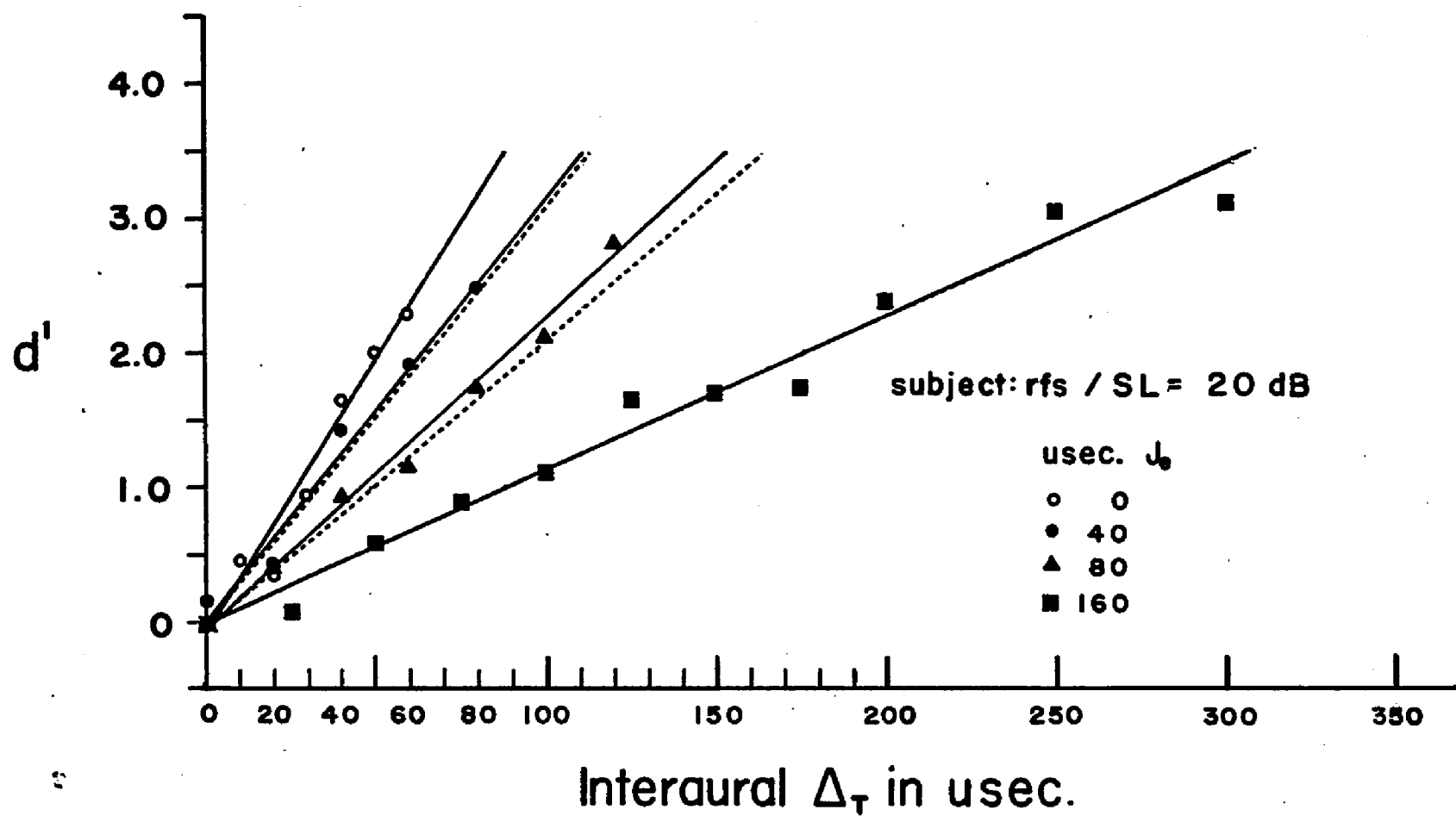


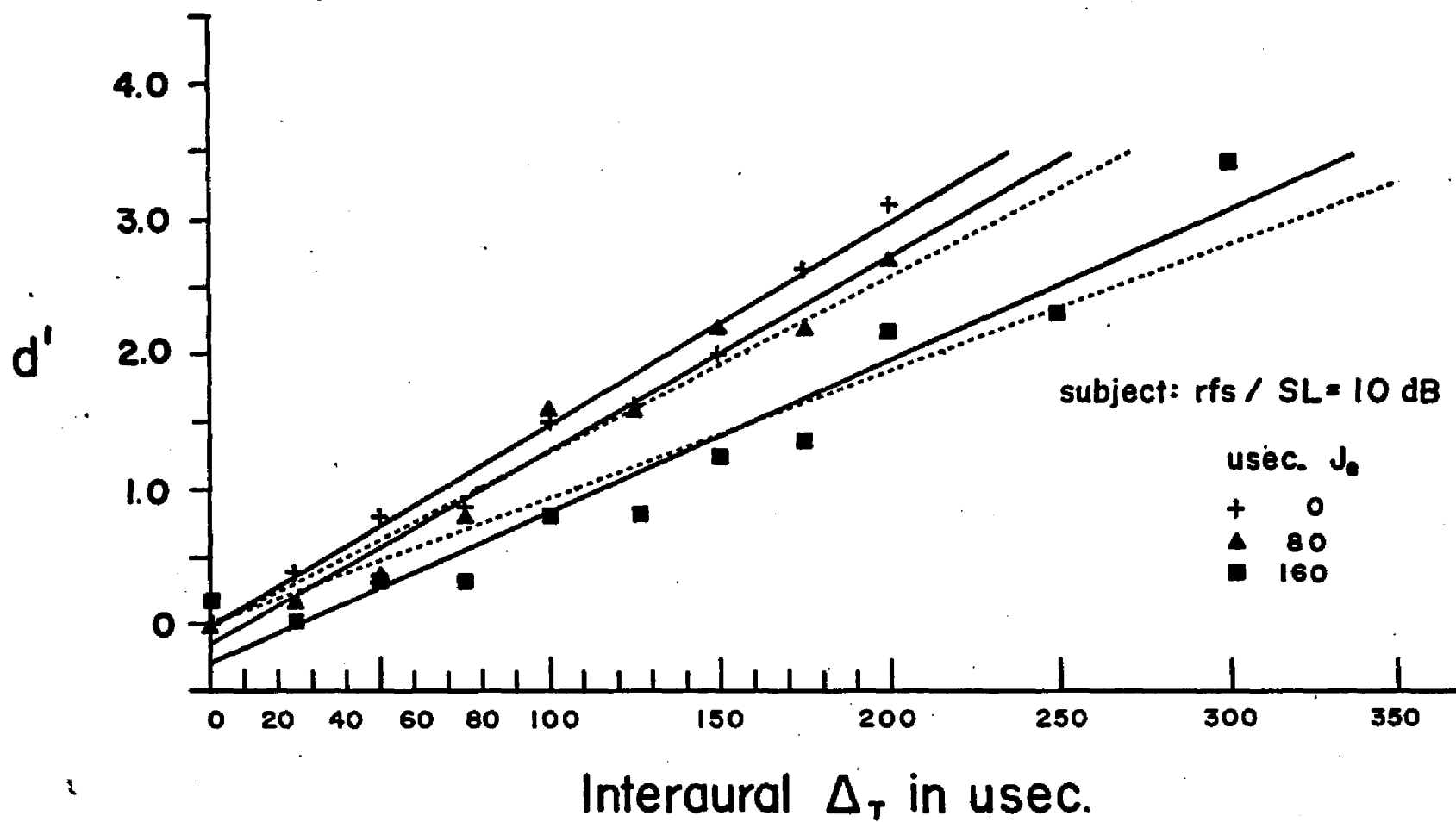


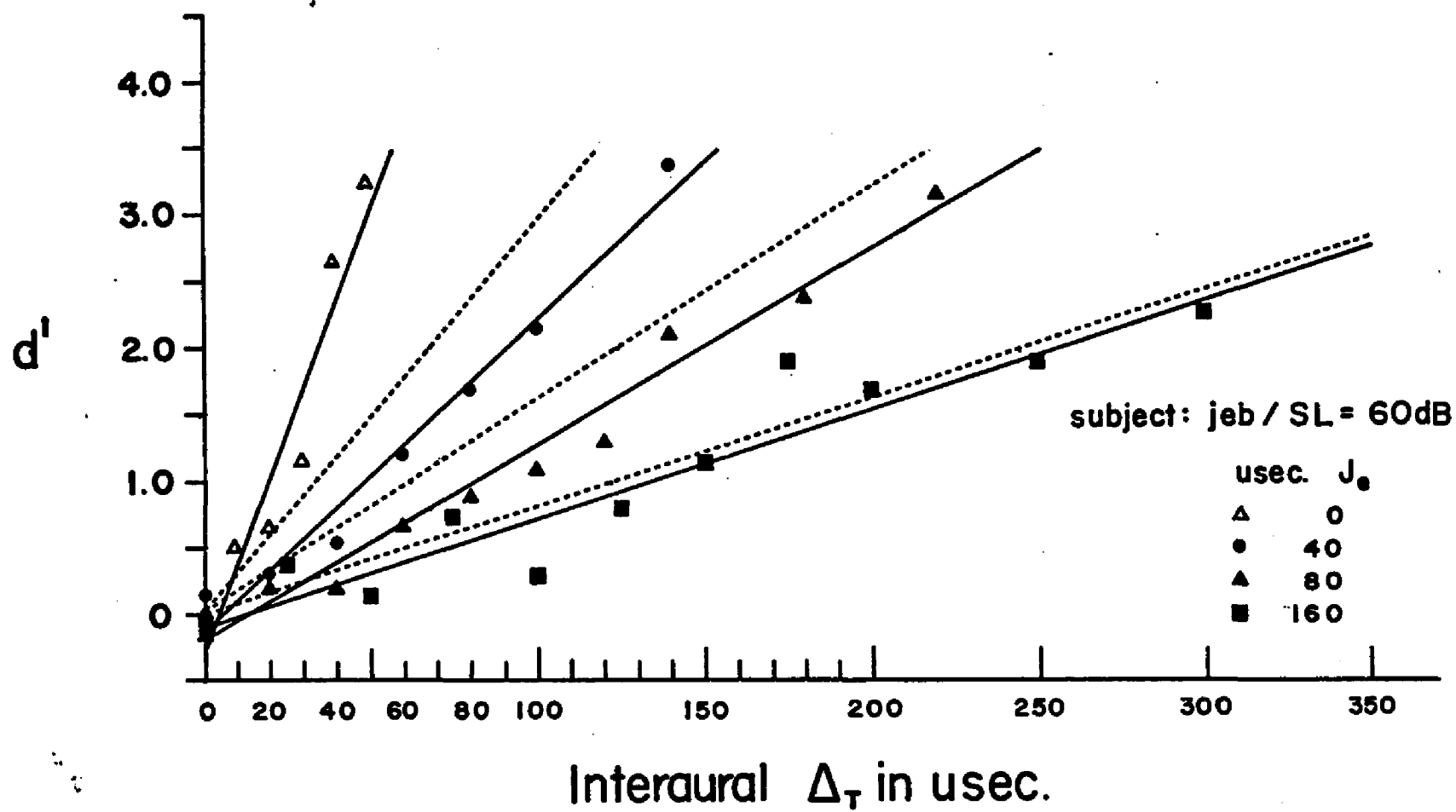


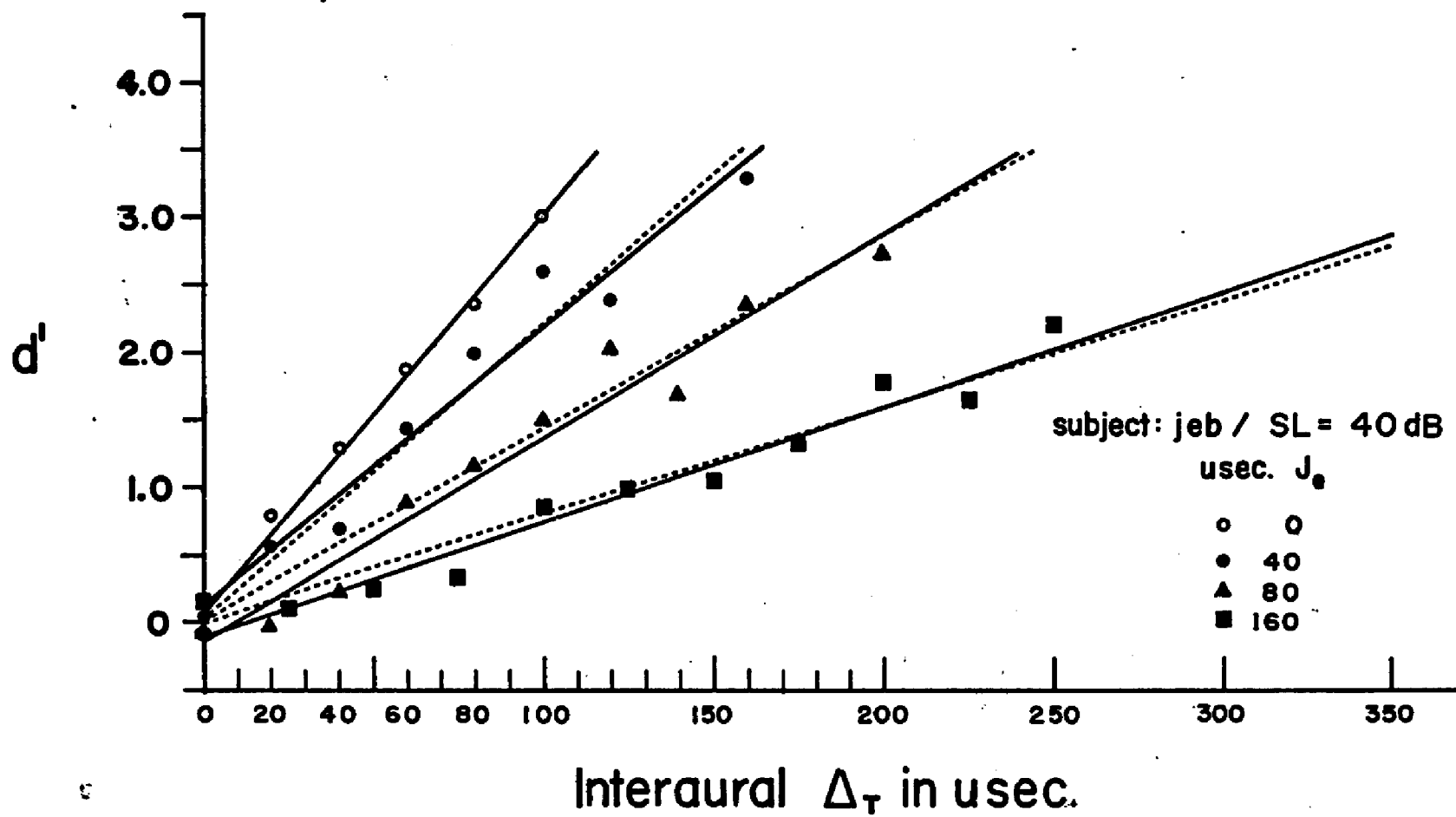














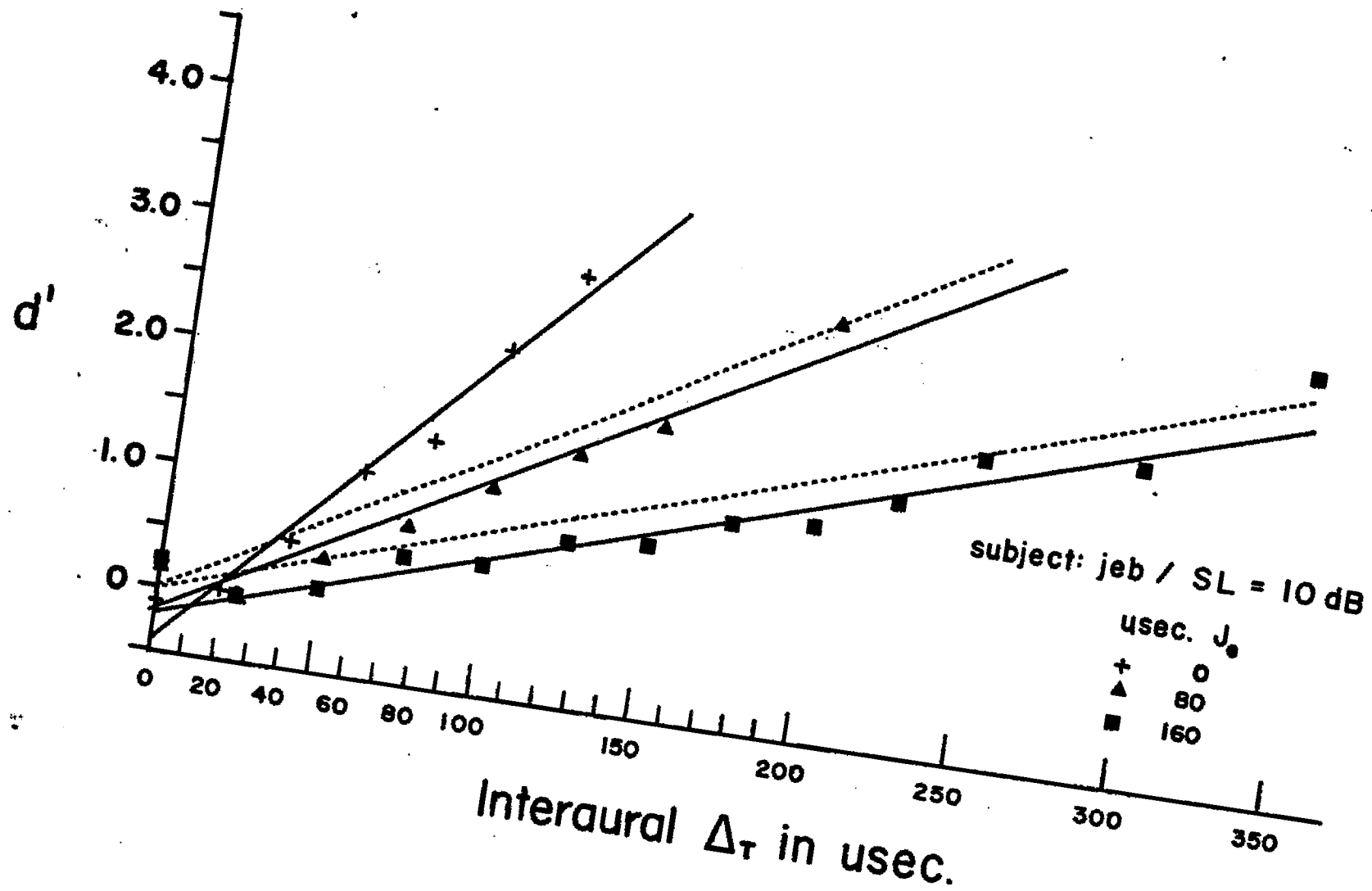


Table 8.1

Parameters of the Unweighted First-Order Least-Squares Fittings to  
the Experiment II Data Compared With Parameters Predicted by the Model.

<u>Subject SLS</u>							
<u>Sensation Level</u>	<u>J<sub>e</sub> in <math>\mu</math>sec.</u>	<u>Slope in <math>\mu</math>sec./d'</u>	<u>Fitted Y-Axis Intercept</u>	<u>Predicted Slope in <math>\mu</math>sec./d'</u>	<u>F-Ratio</u>	<u>d.f.</u>	<u>P.</u>
60dB	20	25.49	-.21	21.43	10.02	9/7	<.01
	40	31.94	+.11	29.78	1.04	9/7	NS
	80	57.80	.00	50.97	2.93	8/6	NS
	160	97.18	+.08	97.18	1.10	10/9	NS
40	40	38.70	+.21	34.02	1.85	6/4	NS
	80	57.44	+.04	53.56	0.84	8/6	NS
	160	93.02	-.13	98.56	1.01	11/9	NS
10	80	51.36	-.28	66.00	1.58	7/5	NS
	160	120.77	-.03	105.84	2.33	12/10	NS
<u>Subject RFS</u>							
40dB	20	14.02	-.01	15.83	0.86	5/3	NS
	40	20.20	-.04	24.12	1.49	7/5	NS
	80	39.62	-.05	43.67	1.93	7/5	NS
	160	84.89	-.05	84.89	0.97	8/7	NS
20	40	32.89	+.06	33.46	0.85	5/3	NS
	80	43.96	-.07	49.44	2.11	7/5	NS
	160	89.05	-.01	88.00	0.84	11/9	NS
10	80	70.13	-.15	79.23	1.11	9/7	NS
	160	90.83	-.28	107.59	1.16	11/9	NS
<u>Subject JEB</u>							
60dB	40	42.05	-.15	33.59	8.23	7/5	<.05
	80	68.21	-.21	62.15	4.43	10/8	<.05
	160	121.65	-.08	121.65	0.99	10/9	NS
40	40	48.22	+.12	45.22	0.83	8/6	NS
	80	65.92	-.15	69.13	0.99	10/8	NS
	160	118.34	-.09	125.36	0.91	11/9	NS
10	80	71.84	-.20	72.05	1.76	8/6	NS
	160	128.87	-.16	127.00	1.66	13/11	NS

program. Obtained F-ratios and associated probabilities of significance are shown in Table 8.2. A first-order fitting appears appropriate for each of the 26 Experiment II functions. A similar result was reported in Chapter IV for the nine Experiment I functions. Examination of the Y-axis intercepts for all nine  $d'$  figures suggests that, as predicted by the model, the fitted lines pass through the origin.

In order to derive single-figure estimates of  $\Delta T$ , unaffected by the minimal Y-intercept deviations noted in Table 8.1, the Experiment II data were re-fitted by first degree functions weighted by a factor of 100 on the 0/0 coordinates, to cross the origin. This weighted-zero procedure (Table 8.3) effectively corrects for all Y-intercept chance departures from the origin.

With regard to the empirically-estimated constructs of the model:  $J_{iy}$ ,  $N_e$ , and  $E$ , the effect of constraining the fitted lines to pass through the origin is minimal. However, as this is the course predicted by the model for the psychometric functions, slopes  $^{-1}$  on the weighted-zero functions are offered as more consistent single-figure estimates of  $\Delta T$ . These are used subsequently in construction of the predicted and obtained  $\Delta T_j/J_e$  psychophysical functions (Figs. 8.10-8.12).

By way of review, predicted slopes  $^{-1}$  are estimated as follows:

$$\Delta T_J = [(J_e^2 + J_{iy}^2)/N_e^{\frac{1}{2}}] \quad (5.20)$$

Predicted individual data points are estimated by:

$$d'_{\text{pred}} = \Delta t(N_e^{\frac{1}{2}})/(J_e^2 + J_{iy}^2)^{\frac{1}{2}} \quad (5.17)$$

Table 8.2

Analysis of Variance for Unweighted First-Order Least-Squares Fittings to Experiment II Data Points.

<u>Subject SLS</u>					<u>Subject RFS</u>					<u>Subject JEB</u>				
dB SL	$J_e$	d.f.	F- Ratio	P.	dB SL	$J_e$	d.f.	F- Ratio	P.	dB SL	$J_e$	d.f.	F- Ratio	P.
60dB	20 $\mu$ sec.	1/7	318.79	<.001	40dB	20 $\mu$ sec.	1/3	45.53	<.01	60dB	40 $\mu$ sec.	1/5	171.46	<.001
	40	1/7	440.87	<.001		40	1/5	78.25	<.001		80	1/8	271.52	<.001
	80	1/6	315.51	<.001		80	1/5	505.00	<.001		160	1/9	74.74	<.001
	160	1/9	281.36	<.001		160	1/7	228.65	<.001					
40dB	40 $\mu$ sec.	1/4	625.24	<.001	20dB	40 $\mu$ sec.	1/3	132.90	<.01	40dB	40 $\mu$ sec.	1/6	140.66	<.001
	80	1/6	79.36	<.001		80	1/5	459.34	<.001		80	1/8	187.02	<.001
	160	1/9	339.74	<.001		160	1/9	300.42	<.001		160	1/9	190.60	<.001
10dB	80 $\mu$ sec.	1/5	118.29	<.001	10dB	80 $\mu$ sec.	1/7	217.25	<.001	10dB	80 $\mu$ sec.	1/6	158.12	<.001
	160	1/10	233.34	<.001		160	1/9	137.09	<.001		160	1/11	216.94	<.001

Table 8.3

Parameters of the Zero-Weighted First-Order Least-Squares Fitting  
to the Experiment II Data Compared with Parameters Predicted by  
the Model.

Sensation Level	<u>Subject SLS</u>						
	<u>Best-Fitted</u>			<u>Predicted</u>			P
	$J_e$ in $\mu\text{sec.}$	Slope in $\mu\text{sec./d'}$	Y-Axis Intercept	Slope in $\mu\text{sec./d'}$	F- Ratio	d.f.	
60 dB	20	27.93	-.01	21.33	8.01	9/8	<.01
	40	30.39	.00	29.17	1.12	9/8	NS
	80	57.74	.00	49.34	5.05	8/7	<.05
	160	93.63	.00	93.65	1.00	10/10	NS
40	40	34.94	.00	33.77	1.28	6/5	NS
	80	56.09	.00	51.94	1.13	8/7	NS
	160	99.11	.00	95.05	1.07	11/10	NS
10	80	59.00	-.01	65.03	1.14	7/6	NS
	160	123.15	.00	102.79	3.30	12/11	<.05
<u>Subject RFS</u>							
40 dB	20	14.15	.00	15.39	1.00	5/4	NS
	40	20.52	.00	24.24	1.83	7/6	NS
	80	40.37	.00	44.62	2.98	7/6	NS
	160	87.18	.00	87.20	1.00	8/8	NS
20	40	31.81	.00	34.22	1.32	5/4	NS
	80	45.43	.00	50.74	3.13	7/6	NS
	160	89.29	.00	90.49	0.93	11/10	NS
10	80	75.47	.00	81.57	1.24	9/8	NS
	160	104.06	-.01	110.76	1.00	11/10	NS
<u>Subject JEB</u>							
60 dB	40	44.90	-.01	36.08	4.79	7/6	<.05
	80	75.53	-.01	65.73	2.14	10/9	NS
	160	128.04	.00	128.04	1.00	10/10	NS
40	40	45.79	.00	45.66	0.88	8/7	NS
	80	71.02	.00	71.44	0.90	10/9	NS
	160	125.63	.00	131.07	0.99	11/10	NS
10	80	80.19	-.01	79.15	0.91	8/7	NS
	160	141.04	-.01	135.42	1.03	13/12	NS

$J_e$  is the amount of external jitter in rms  $\mu\text{sec.}$   $J_{iy}$  represents the empirically-based estimate of internal noise affecting the subject's  $\Delta T$  performance at a given  $SL_y$ .  $\Delta T_J$  and  $\Delta T$  are given to represent the  $\Delta t$  JND at  $SL_y$  where  $J_e \neq J_e = 0$ , respectively. In Experiment I,  $J_e = 0$ , therefore:

$$\Delta T = (J_{iy}^2 / N_e)^{\frac{1}{2}} \quad (5.28)$$

Transposing the above, one arrives at  $J_{iy}$ , the internal noise estimate for  $SL_y$ :

$$J_{iy} = (\Delta T) N_e^{\frac{1}{2}} \quad (5.42)$$

$N_e$  is the empirical estimate of the average number of pulse pairs used by the subject in arriving at a YES/NO decision on the outcome of each trial:

$$N_e = J_e^2 / (\Delta T_J^2 - \Delta T^2). \quad (5.35)$$

As data scatter appeared smaller at higher  $SL$ 's, with  $J_e$  (Eq. 5.35) representing the maximum jitter used in Experiment II (160 sec.),  $\Delta T_J$  is the JND for each subject at the same High  $SL$ , where  $J_e = 0$ ; i.e., as in Experiment I. Numerical estimates of all the above constructs, derived from both least squares best-fitted and weighted-zero fitted lines to the data, are given in Table 8.4.

Dashed lines, in Figs. 8.1 through 8.9 are those predicted by the model for each of the 26 functions obtained in Experiment II. Parameters of the predicted and obtained best fits are presented in

Table 8.1. The F-ratios and associated probability levels are derived from an analysis of variance performed to compare the first order least-squares best fits to the obtained points with the functional forms predicted by the model.

Out of 26 possible pair comparisons of obtained and predicted linear fittings to the functions, across three subjects, only two differ beyond the five percent level of significance and one pair differs beyond the one percent level. The last function, subject SLS, 60 dB,  $J_e = 20 \mu\text{sec.}$ , is clearly asymmetrical relative to the orientation of other obtained functions in the High SL series. Two functions of subject JEB, 60 dB SL:  $J_e = 40 \mu\text{sec.}$  and  $80 \mu\text{sec.}$ , differed at the five percent level. His predicted functions were steeper than the obtained.

It should be noted that the only empirical data used in predicting each subject's functions were a single value of  $\Delta T_J$ , obtained in Experiment II with  $J_e = 160 \mu\text{sec.}$  at the High SL, and one value of  $\Delta T$  for each of the three SL's obtained in Experiment I at the same SL. As a consequence, in the analyses of variance of best fit obtained vs. predicted fit, one degree of freedom (slope) is lost for three of the 26  $\Delta T_J$  functions predicted, with no degrees of freedom lost for the remaining 23.

A similar analysis was performed on the weighted-zero lines fitted to the same data points. Reciprocal slopes of these linear obtained and predicted functions, are presented in Table 8.3. Analysis of variance of the weighted-zero obtained vs. predicted line fittings to the data, revealed only four differences beyond the

five percent level. One difference is at the one percent level (SLS, 10 dB/  $\mu$ sec.) and three at the five percent level (SLS: 60 dB/80  $\mu$ sec; 10 dB/160  $\mu$ sec; JEB 60 dB/40  $\mu$ sec). In these analyses, an additional degree-of-freedom is gained because the fitted lines are constrained to pass through the origin. It is noteworthy that, independent of procedures for fitting lines to the data, no statistically significant difference appears for any subject at the medium Sensation Level.

#### PSYCHOPHYSICAL FUNCTIONS; $\Delta T_J/J_e$ :

Using weighted-zero  $d'$  slopes<sup>-1</sup> as estimates of  $\Delta T$ , Figs. 8.10 through 8.12 illustrate a comparison of obtained  $\Delta T_J$ 's with those predicted by the model, as  $f(J_e)$ . Numerical values are given in Table 8.3. Each solid point is a  $\Delta T_J$ , based on from 1000 to 2600 individual trials. The actual number of trials per point depends upon declivity of the psychometric function and, consequently, the number of  $\Delta t$  values sampled in constructing each function. Experiments I and II, combined, entailed approximately 108,000 trials across the three subjects.

The dashed lines, in Figs. 8.10 - 8.12, are constrained to cross the predicted points (Table 8.3), at each value of  $J_e \neq 0$ . According to the model, all such predicted psychophysical functions of  $\Delta T_J/J_e$  originate at the empirical value of  $\Delta T$ ; and rise to the same asymptotic slope:  $N_e^{-1/2}$ . Subjects RFS and JEB appear to provide closest approximations to the functional forms predicted through the model.



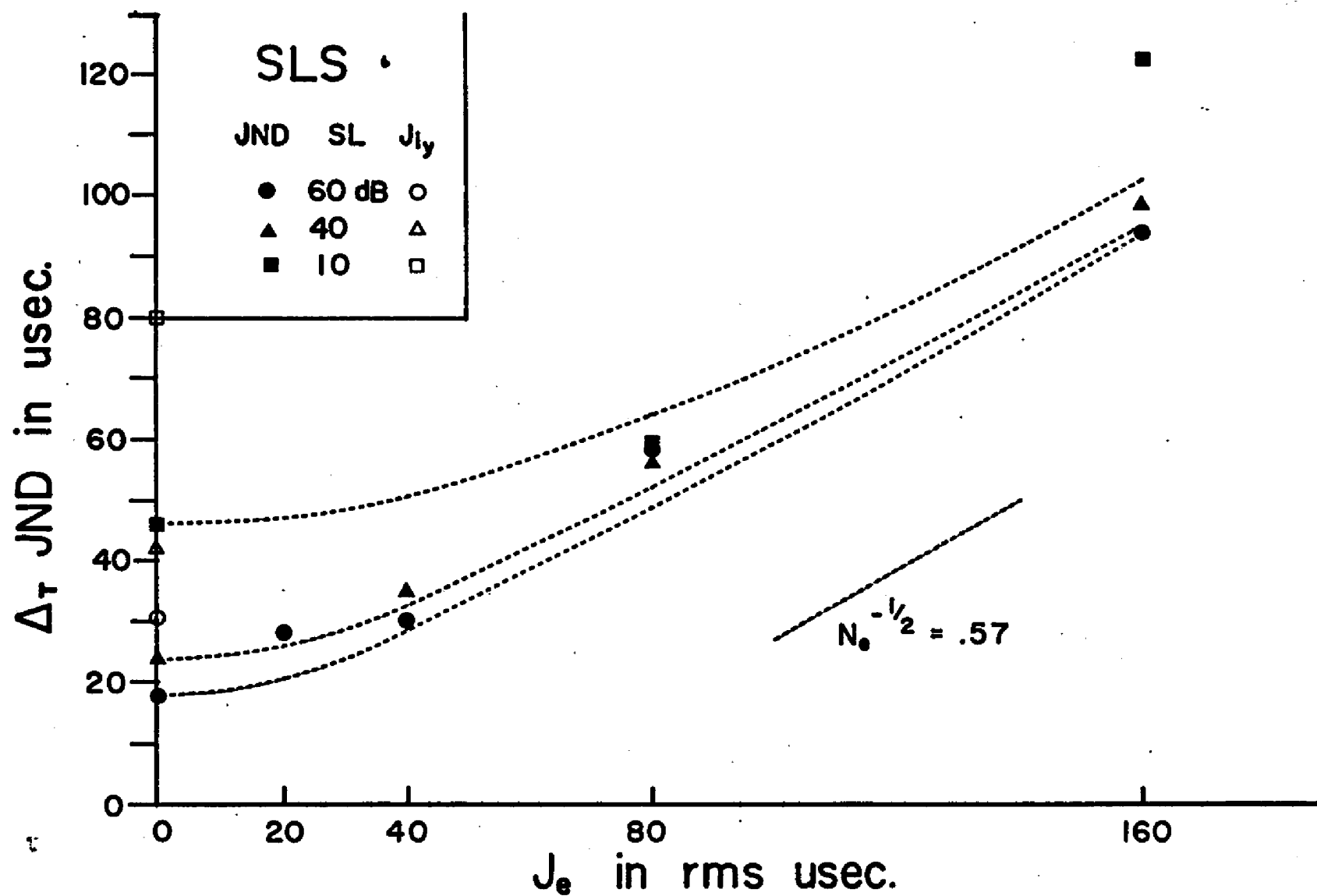
## Figures 8.10 - 8.12

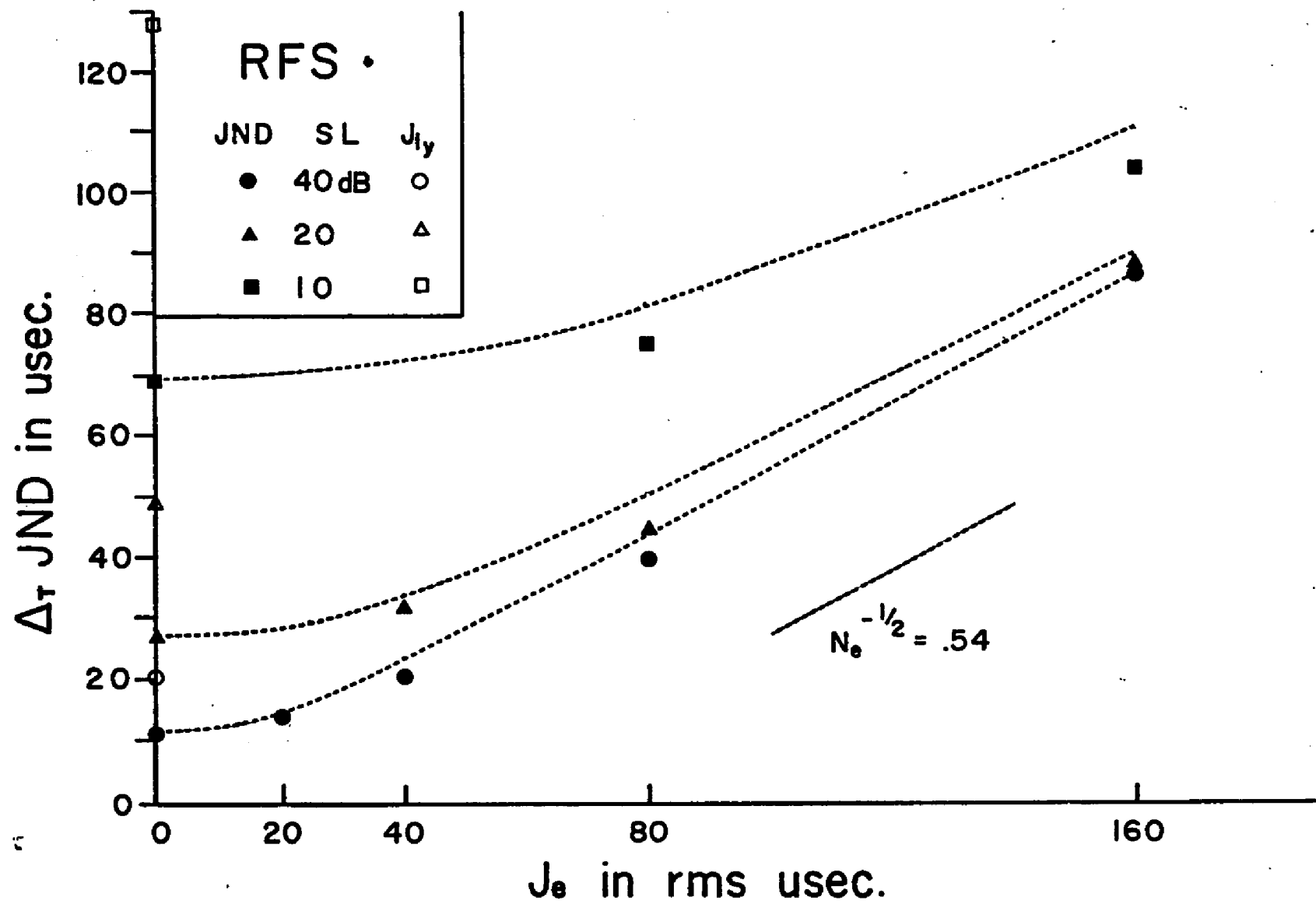
Predicted and obtained effects of  $J_e$  on  $\Delta T$ . Open symbols are empirical estimates of  $J_{iy}$ .  $N_e^{-1/2}$  is the predicted asymptotic slope of each function, per subject. Solid points represent from 1000 to 2600 trials.

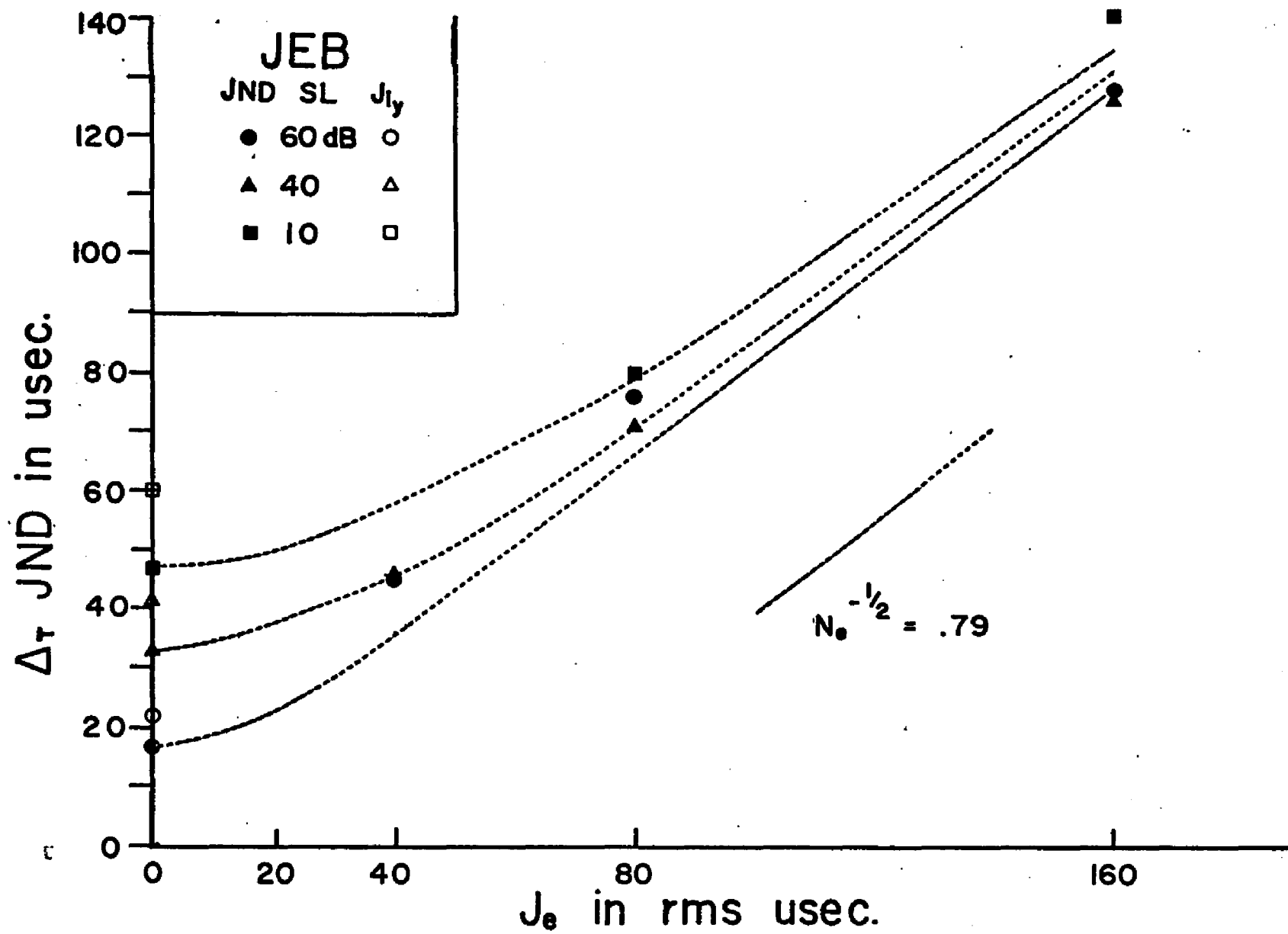
Fig. 8.10 Subject SLS

Fig. 8.11 Subject RFS

Fig. 8.12 Subject JEB







Assertions of the model concerning the geometric additivity of internal ( $J_{iy}$ ) and external ( $J_e$ ) noise, and the growth of internal noise with decreasing SL, tend to be supported by the data. The interaction of  $J_{iy}$  and  $J_e$ , affecting  $\Delta T_J$ , may be observed graphically (Figs. 8.10 - 8.12). As  $J_e$  grows large with respect to  $J_{iy}$ , shown in open symbols, it is obvious that the asymptotic slopes of the predicted  $\Delta T_J/J_e$  psychophysical functions approach a constant limiting value for each subject, independent of Sensation Level. In effect, the external,  $J_e$ , ultimately "swamps" the internal noise,  $J_{iy}$ , totally dominating the  $\Delta T$  discrimination performance of the Subject.

8.6  
6  
Treating  $\Delta T_J/J_e$  as a "neural" Weber fraction (Stewart, 1963), it is shown in Chapter V that the limiting slope of these psychophysical functions is equal to the value:  $N_e^{-1/2}$ . It can be determined, by inspection (Figs. 8.10 - 8.12) that the predicted and obtained limiting psychophysical function slopes are in good agreement within each subject.

Table 8.4 presents the  $N_e^{-1/2}$  estimates derived from both least squares best fit and weighted-zero fitted lines to the  $d'$  data. Values of  $N_e^{-1/2}$  appear largely independent of fitting method, as well. The mean value of  $N_e^{-1/2}$ , averaged across subjects, is .61. Individual  $N_e^{-1/2}$  values, based on the weighted-zero slopes<sup>-1</sup>, range from .54 and .57, for subjects SLS and RFS, respectively, to .78 for JEB.

#### MODEL CONSTRUCTS, $J_{iy}$ :

Internal noise estimates,  $J_{iy}$ , are given for each subject by Sensation Level in Table 8.4. Little difference appears as a

Table 8.4

Model Parameter Estimates:  $J_{iy}$ ,  $N_e$  and  $E$  Derived from  
Experiment I and II  $d'$  Data Fittings.

$$J_{iy} = (\Delta T) N_e^{\frac{1}{2}}$$

SUBJECT

<u>Sensation Level</u>	<u>SLS</u>	<u>RFS</u>	<u>JEB</u>	<u><math>\bar{X}</math></u>
HIGH (60,40,60 dB SL)	29.8 $\mu$ sec. *(31.3 $\mu$ sec.)	22.4 $\mu$ sec. (20.3 $\mu$ sec.)	19.5 $\mu$ sec. (21.7 $\mu$ sec.)	23.9 $\mu$ sec. (24.4 $\mu$ sec.)
MEDIUM (40,20,40 dB SL)	40.6 (42.1)	49.2 (49.1)	44.6 (41.4)	44.8 (44.2)
LOW (10,10,10 dB SL)	76.3 (80.1)	127.0 (127.9)	52.1 (59.7)	85.1 (89.2)

$$N_e = J_e^2 / (\Delta T_J^2 - \Delta T^2)$$

$N_e$	2.80 (3.03)	3.62 (3.42)	1.76 (1.59)	2.73 (2.68)
$N_e^{\frac{1}{2}}$	1.67 (1.74)	1.90 (1.84)	1.32 (1.26)	1.65 (1.64)
$N_e^{-\frac{1}{2}}$	.60 (.57)	.53 (.54)	.76 (.79)	.61 (.61)

$$E = (N_e/N)^{\frac{1}{2}}$$

$E$	.37 (.39)	.43 (.41)	.30 (.28)	.37 (.37)
-----	--------------	--------------	--------------	--------------

\*(Values derived from weighted-zero functions)

consequence of fitting procedures selected. Individual  $J_{iy}$  estimates, derived from weighted-zero fittings, are displayed as open symbols intercepting  $J_e = 0$  (Figs. 8.10 - 8.12). For noise-free Ideal Observers,  $J_{iy}$  is 0 at all SL's.

Upper Sensation Level internal noise values (Table 8.4) are in close agreement among subjects. In fact, the total range of empirically-derived  $J_{iy}$  estimates is only 10  $\mu$ sec. at both the High and Medium SL's. The range of internal noise values is considerably greater at the low, 10 dB, SL.

#### MODEL CONSTRUCTS, $N_e$ :

Estimates of  $N_e$  are also given in Table 8.4. This construct represents the average number of pulses, out of the 20 pairs available, used by the subject in arriving at his trial-by-trial YES/NO  $\Delta T$  decision. The Ideal Observer would use all 20, therefore;

$$N_{e_{ideal}} = N = 20.$$

Subject RFS appears most efficient, among the three, using an average of 3.6 pulses, as estimated from the best-fit  $d'$  data. Subject JEB is least efficient, with  $N_e = 1.8$ . For SLS,  $N_e = 2.8$ . The estimate of  $N_e$ , averaged across three subjects, is 2.7. This average value is the same for either best-fit or weighted-zero fittings to the psychometric function data.

#### MODEL CONSTRUCTS, $E$ :

In Table 8.4,  $E$  is the model's efficiency construct. This may be construed as the ratio of improvement in  $\Delta T$  obtained by the human subject, versus the Ideal Observer, both given  $N$  sample

observations to arrive at each trial-by-trial pulse train  $\Delta t$  detection decision. In the model,  $E$  is defined as:

$$E = (N_e/N)^{\frac{1}{2}} \quad (5.24)$$

Given a background of  $J_e$ , the Ideal Observer, having no internal noise, presents an  $E$  of 1.00. Values of  $E$  empirically derived from the unweighted fittings to the data of Experiments I and II range from .43 for subject RFS to .30 for JEB. Subject SLS presented an  $E$  of .37. The mean value, across three subjects, is .37, regardless of procedure used to fit the data.

#### PERCENT CORRECT DATA:

In order to maintain consistency with the form used in reporting Experiment I results, Experiment II data are also plotted in Percent Correct/ $\Delta t$  form in Figs. 8.13 through 8.21. Points represent 200 trials each,  $P(s) = 0.5$ . The  $P(C)$  functions are similar in form to those obtained in Experiment I (Figs. 4.4 - 4.6). The general form of each curve is that of a negatively accelerated function, rising from  $P(C) = .50$  at  $\Delta t = 0$  through asymptote, truncated at  $P(C) = .95$ . This is consistent with predictions of the model that the  $P(C)$  curve represents the upper half a cumulative normal ogive, in the case of symmetrical a priori probabilities.

Inspection of the functions reveals the presence of reversals in the range from  $\Delta t = 50 \mu\text{sec.}$  through  $100 \mu\text{sec.}$ . This finding was previously noted in Chapter IV for the  $P(C)$  functions obtained in Experiment I, where  $J_e = 0$ .

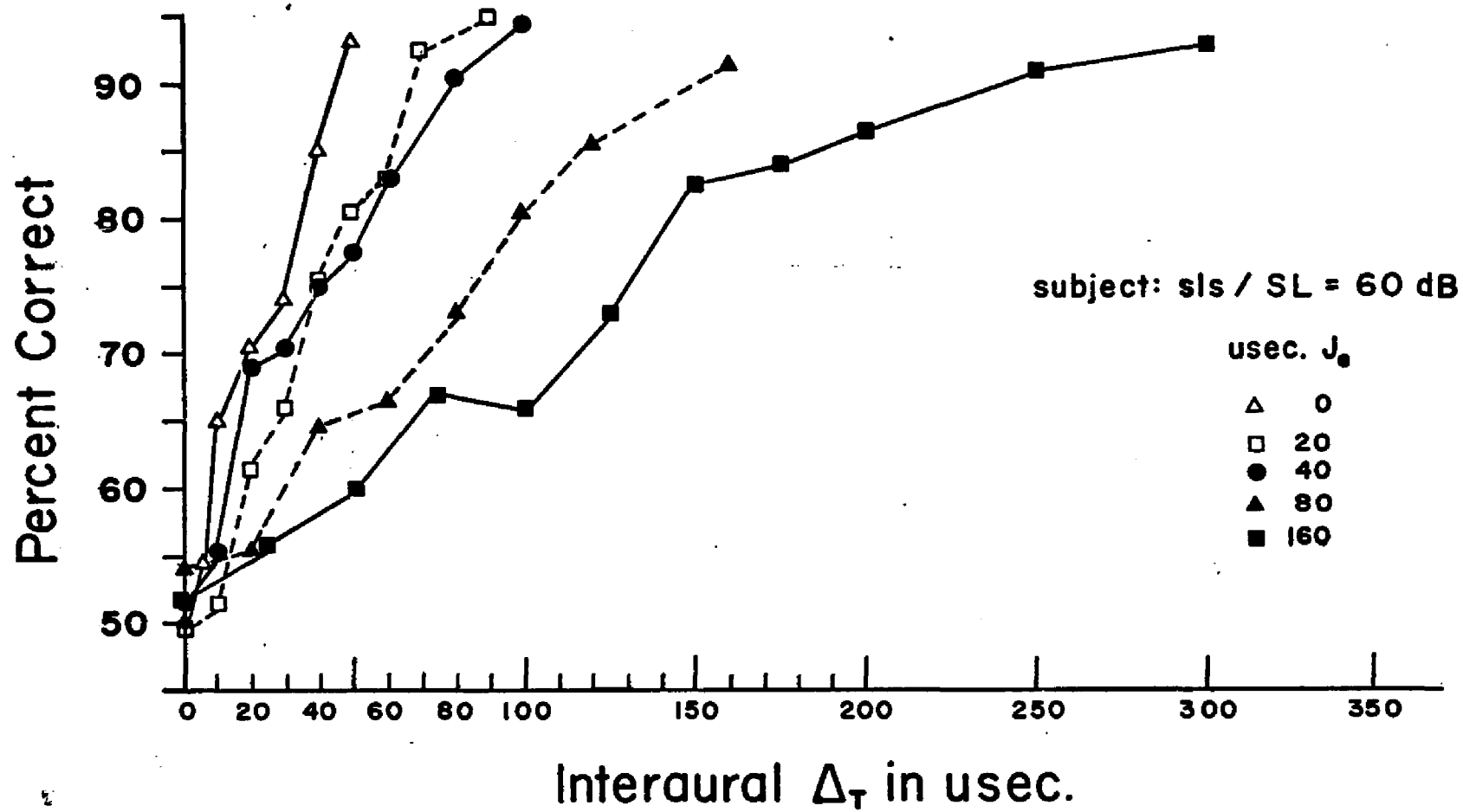


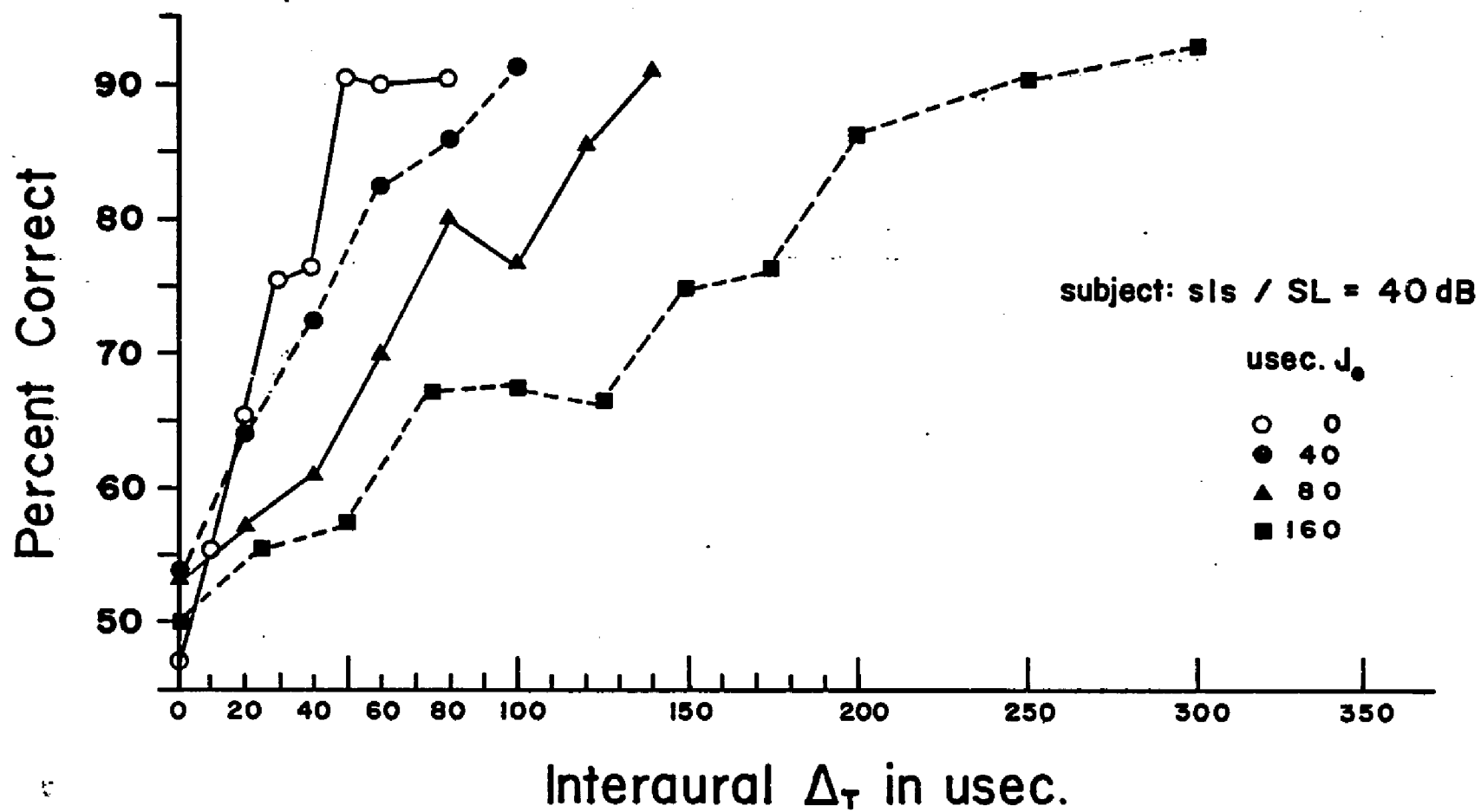
## Figures 8.13 - 8.21

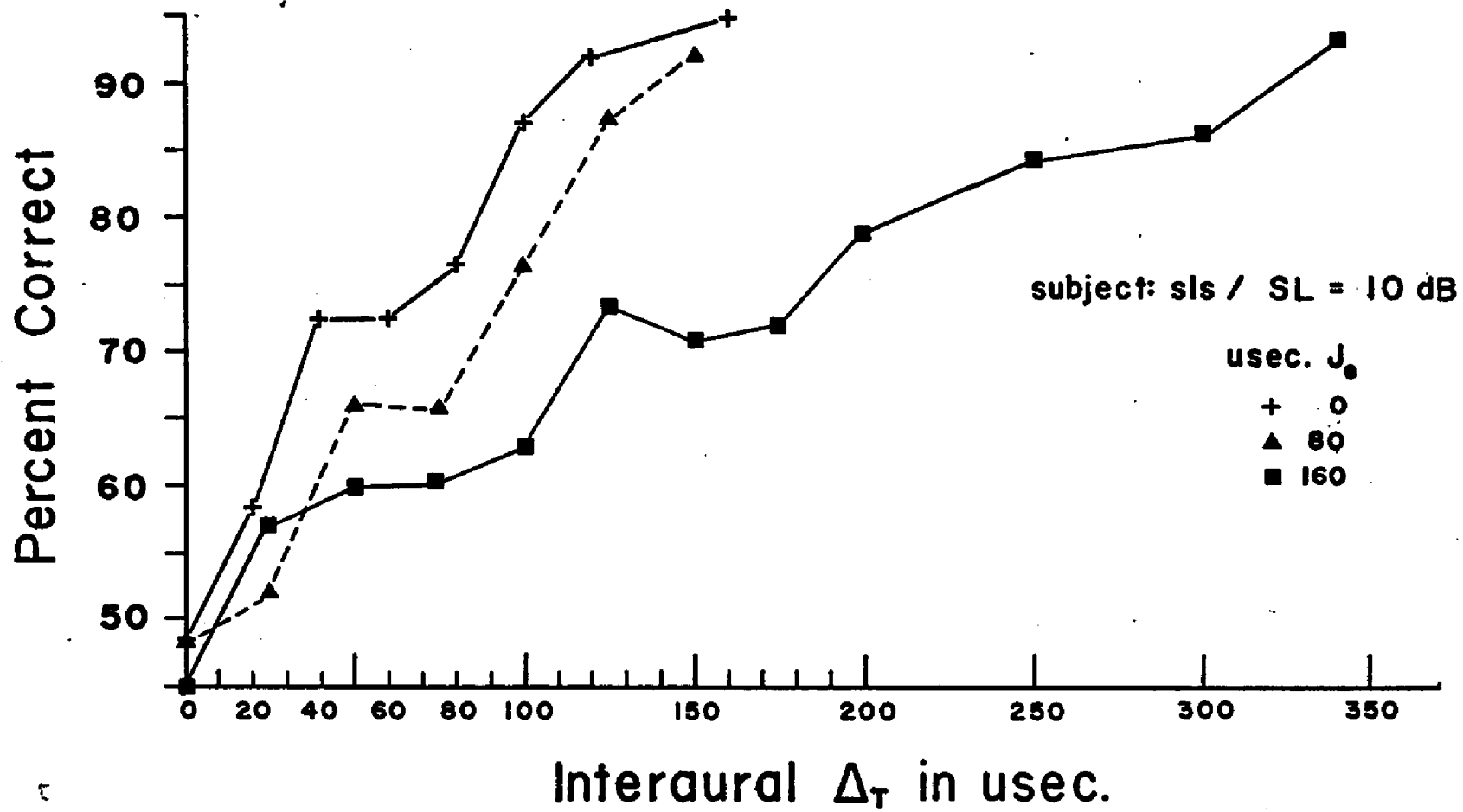
Percent Correct  $\Delta t$  psychometric functions;  $J_e \neq 0$ . X/Y coordinates are  $\Delta t$  in  $\mu\text{sec.}$  and  $[P(S|s) + P(N|n)]/2$  respectively.

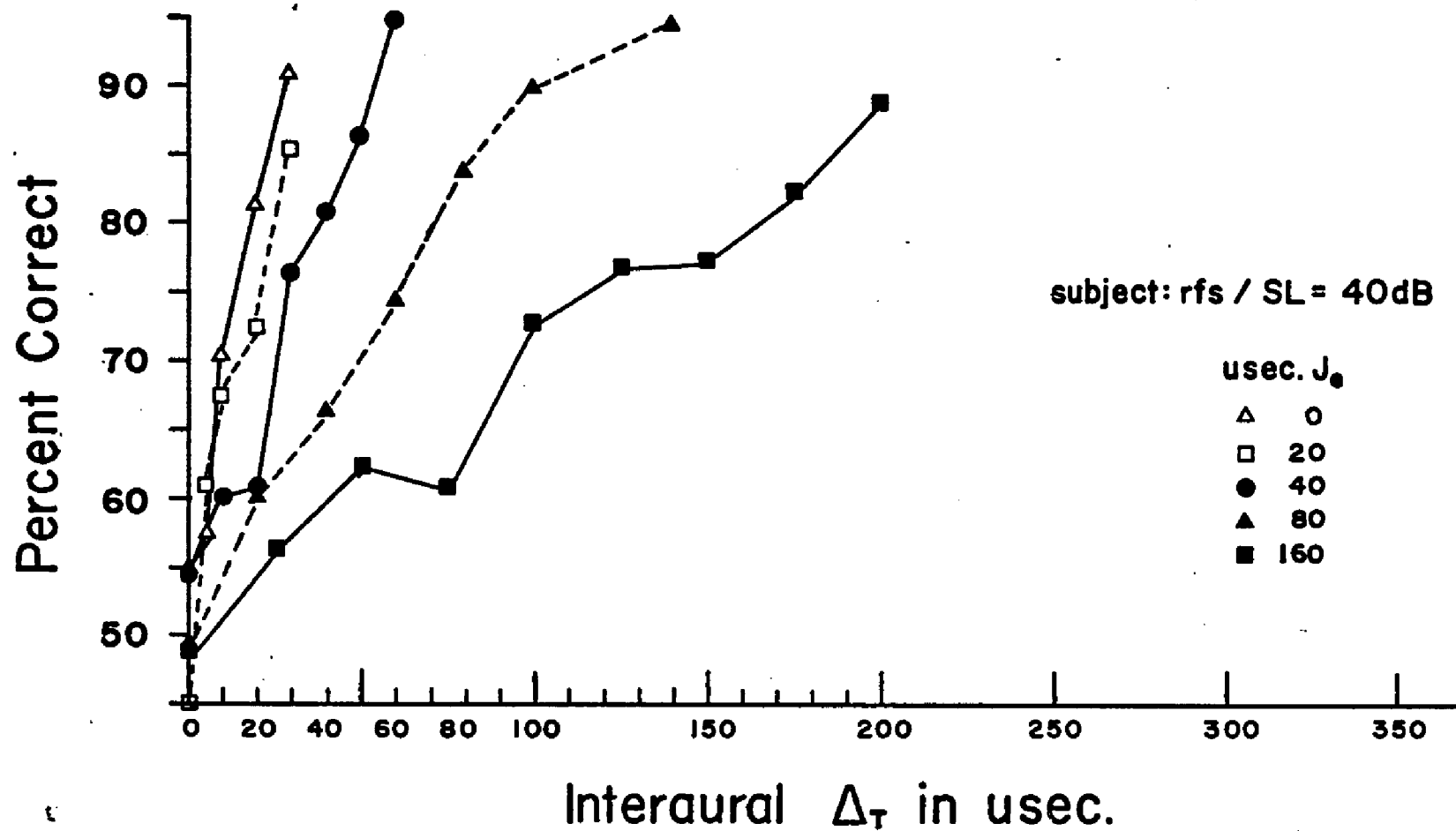
Experiment I data ( $J_e = 0$ ) included as the steepest functions in each figure:

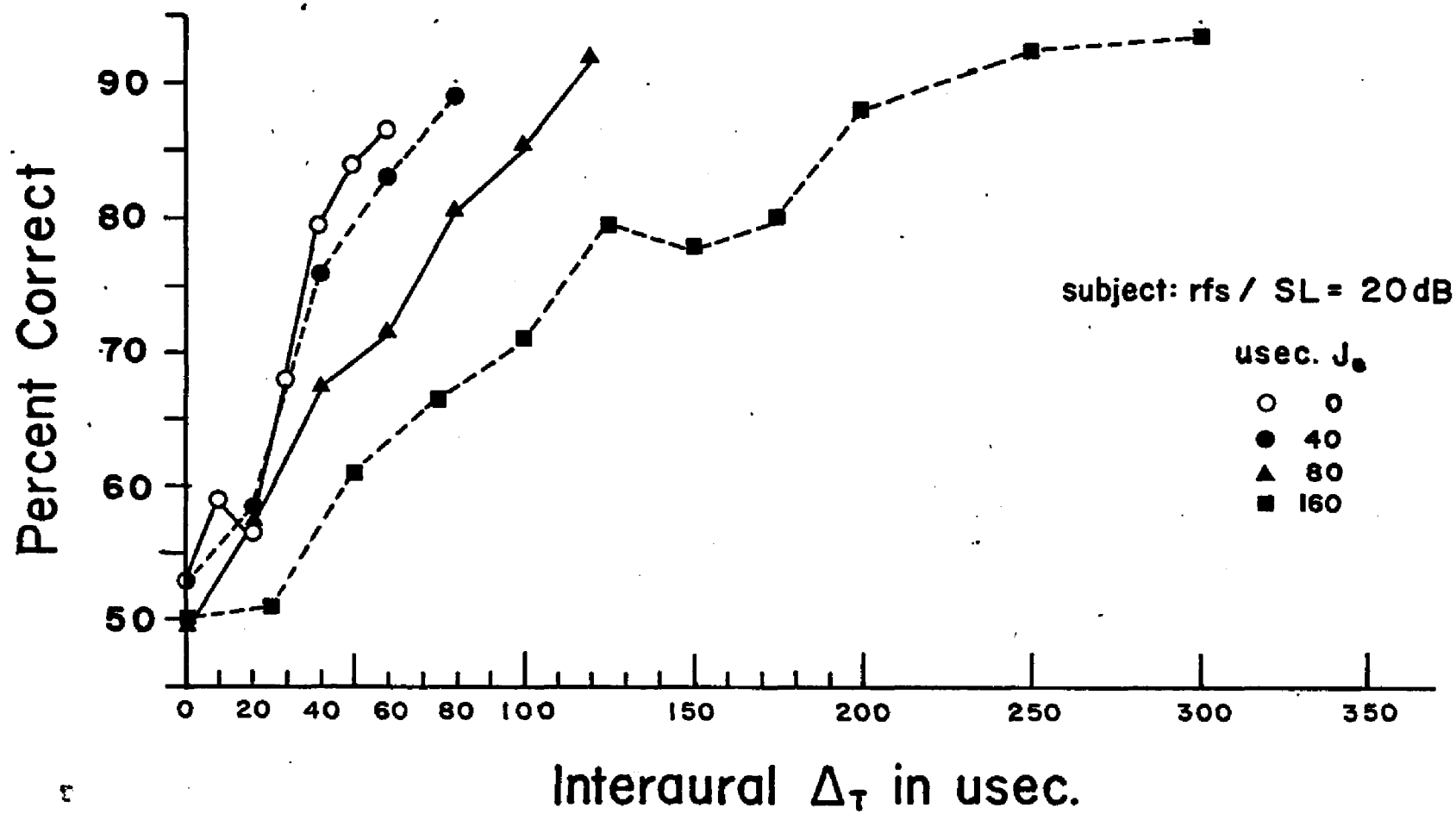
<u>FIGURE</u>	<u>SUBJECT</u>	<u>SENSATION LEVEL</u>
8.13	SLS	60 dB
8.14		40
8.15		10
8.16	RFS	40 dB
8.17		20
8.18		10
8.19	JEB	60 dB
8.20		40
8.21		10

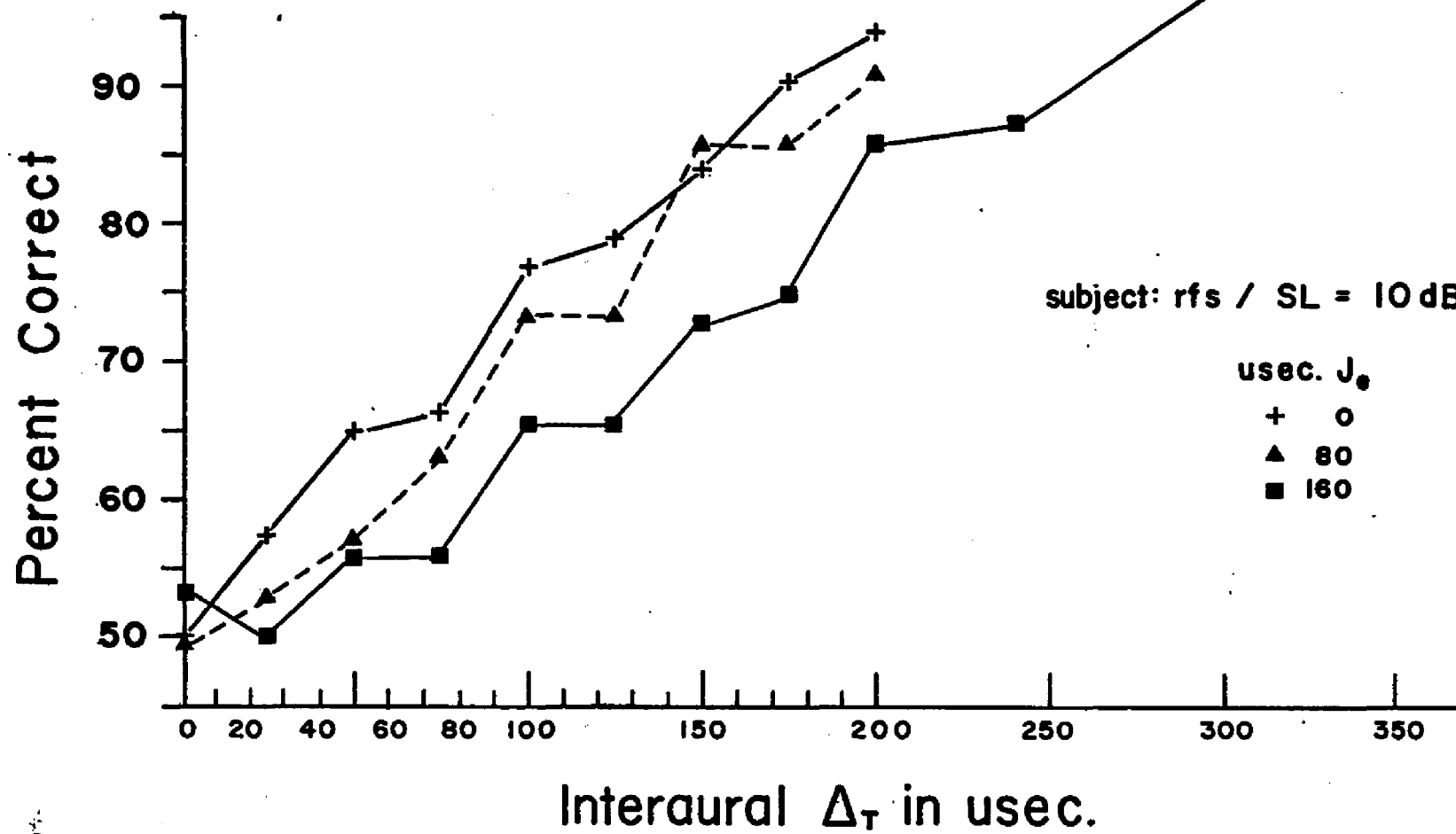


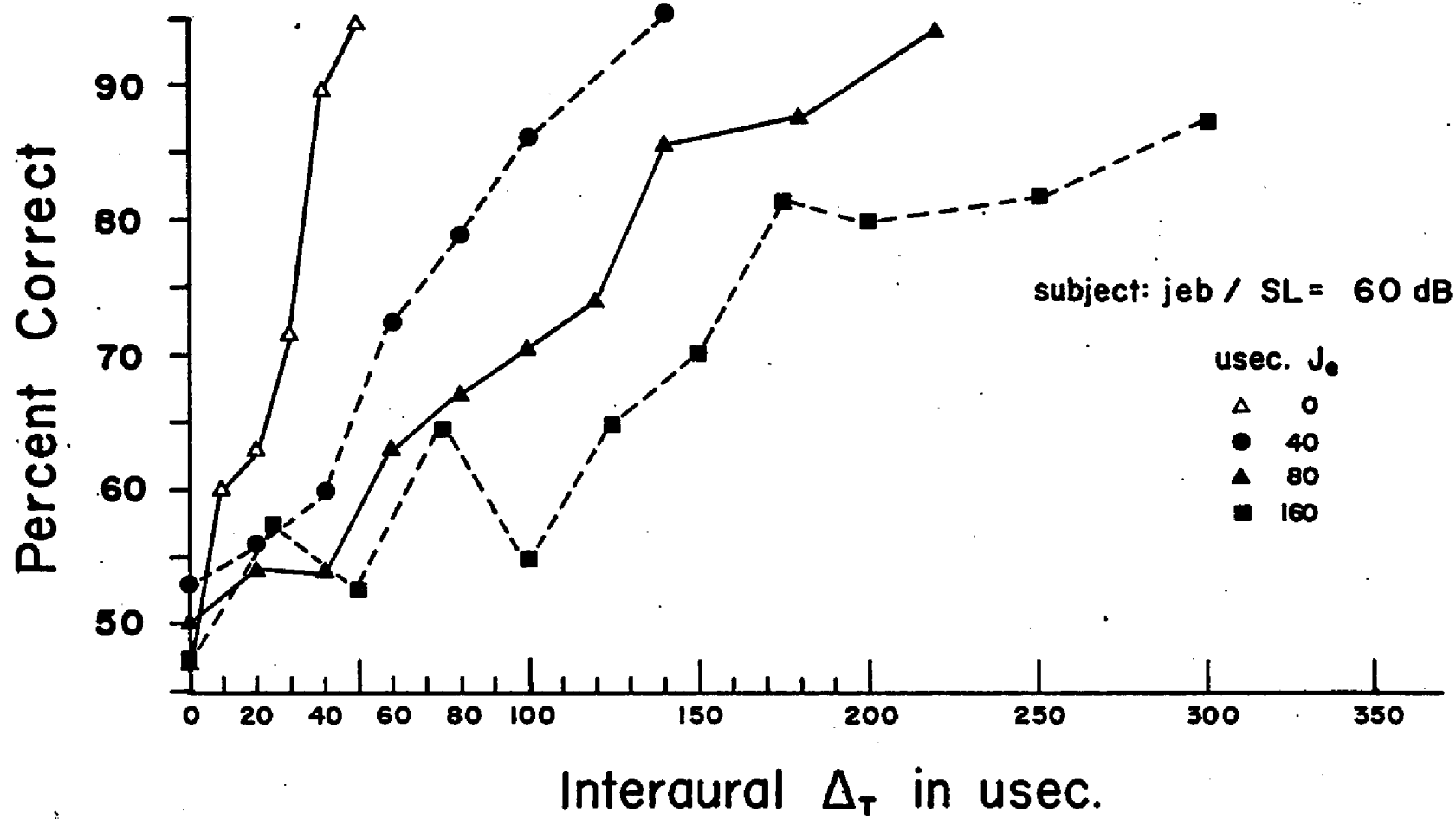




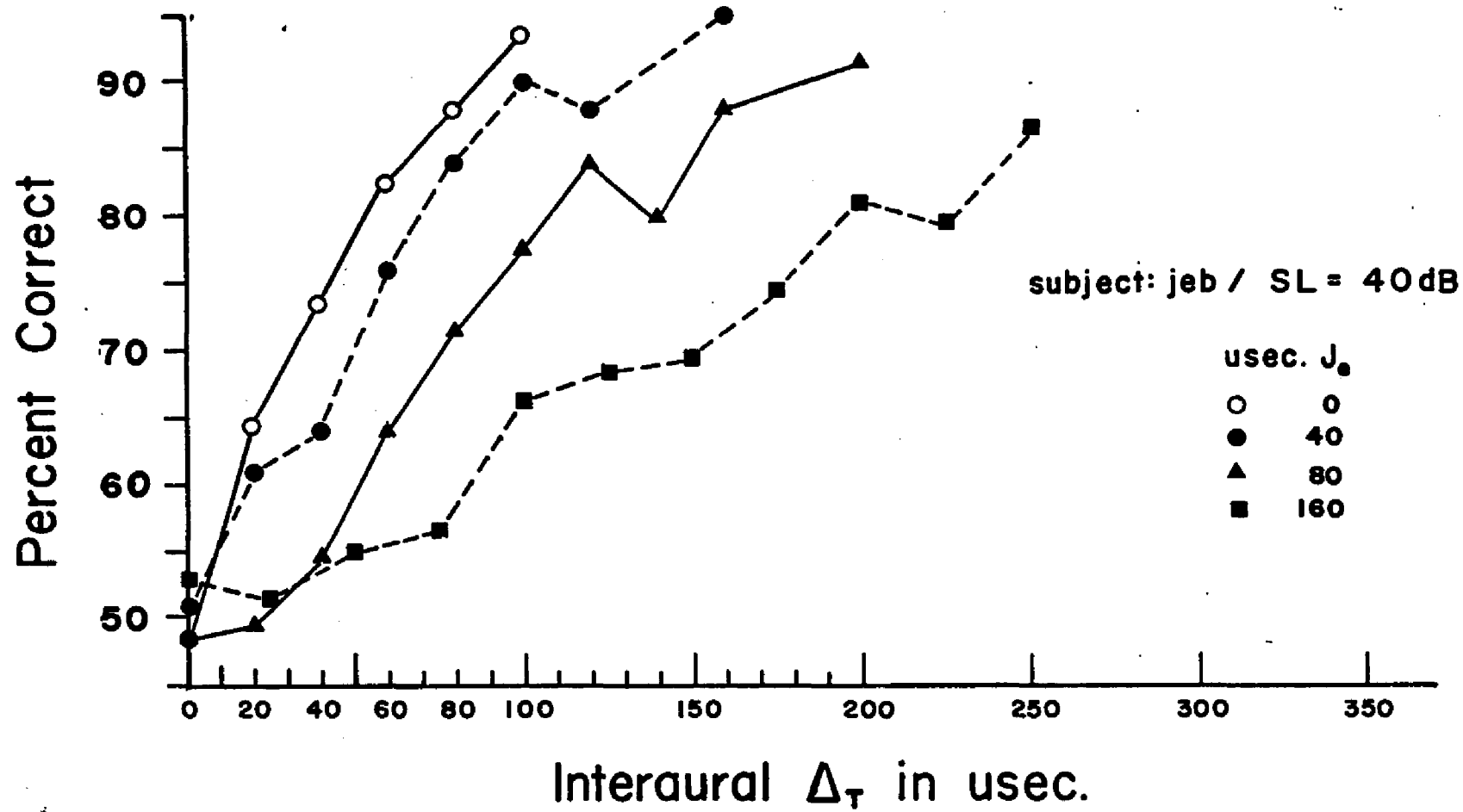


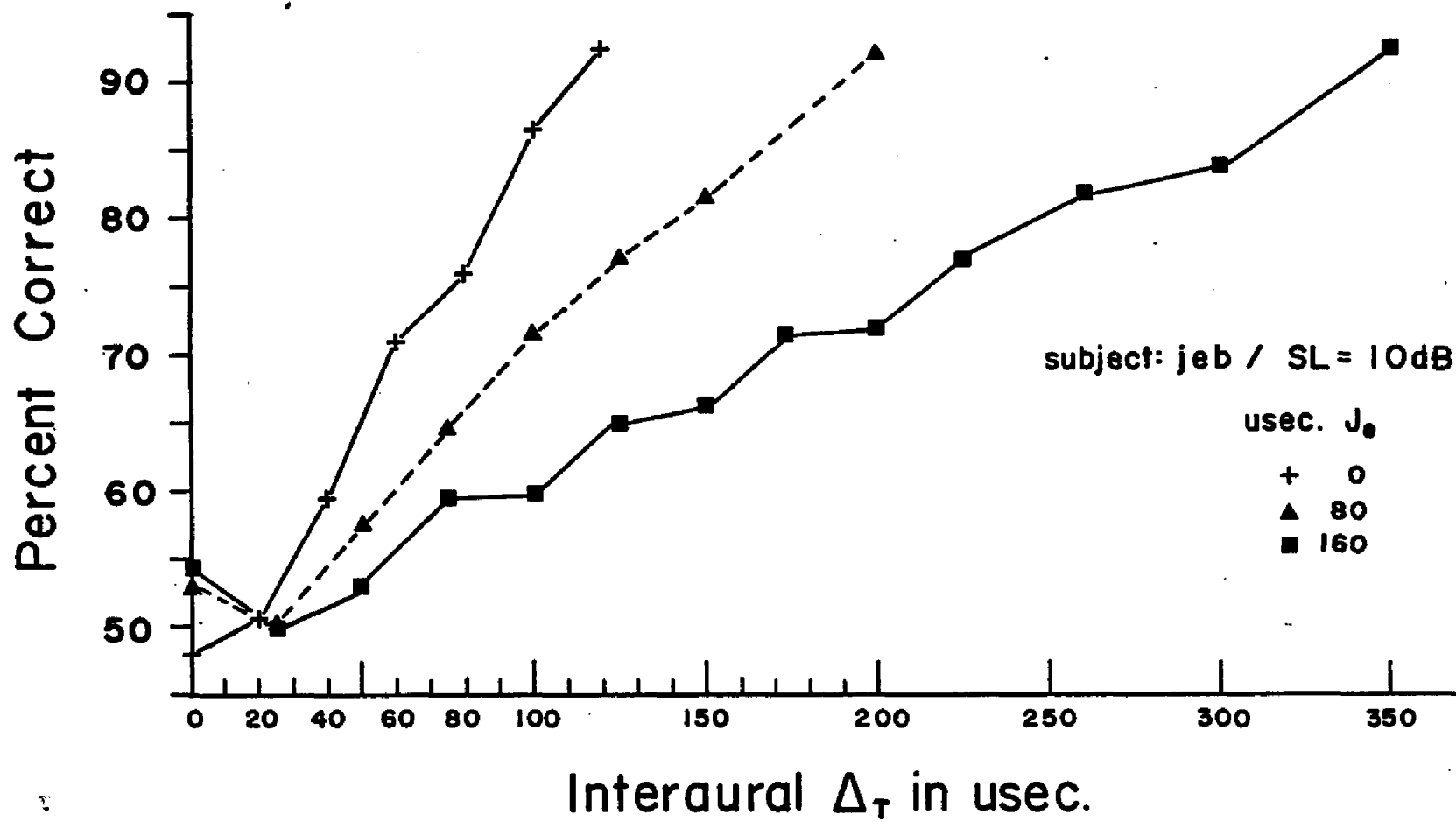












## HIT AND FALSE ALARM DATA:

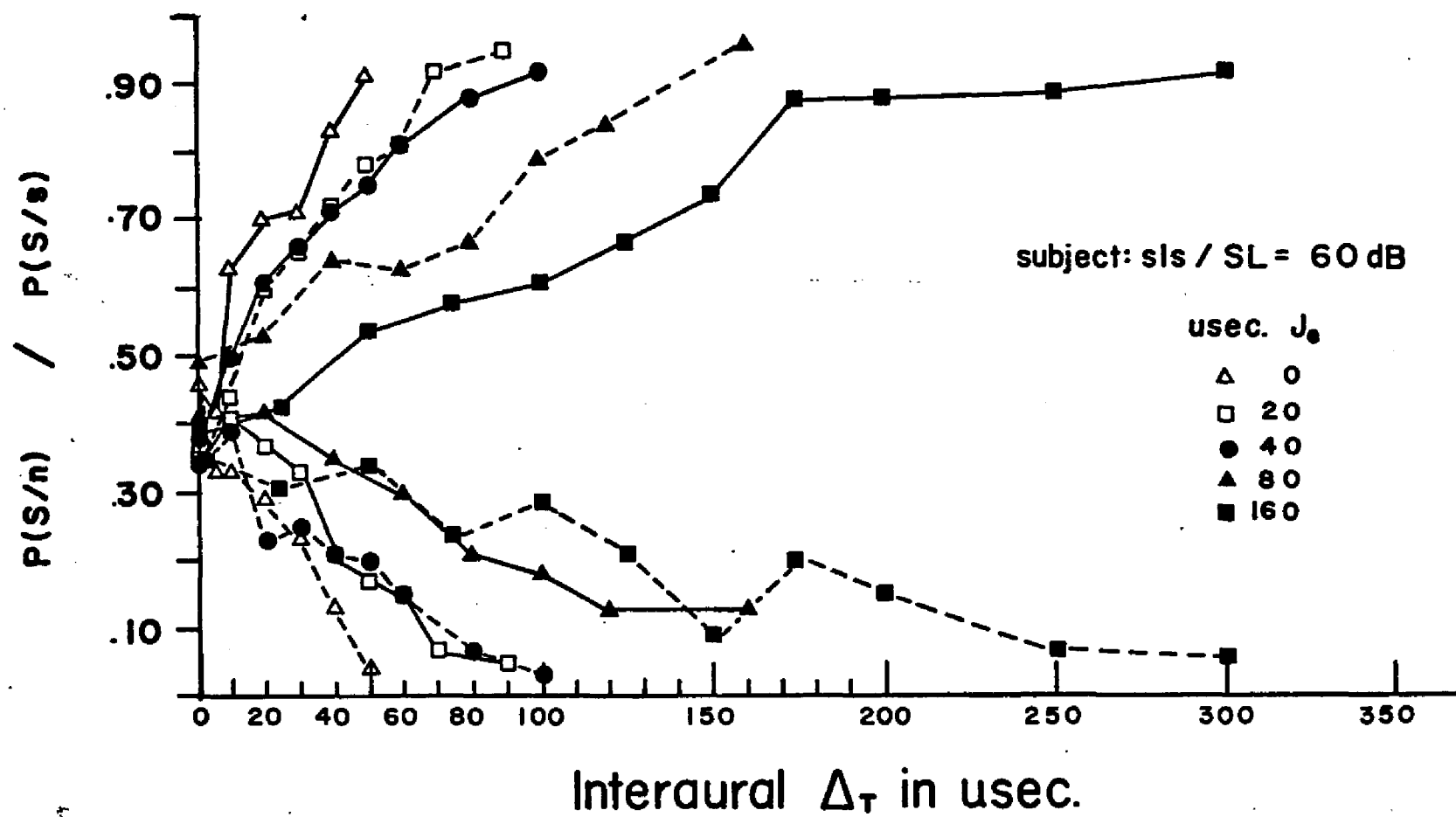
Consistent with the method of reporting of Experiment I results, the data of Experiment II are presented as HIT AND FALSE ALARM ratios (Figs. 8.22 - 8.30). These functions represent the average values of  $P(S|s)$  and  $P(S|n)$  obtained by subject and Sensation Level. Data points represent 100 trials each. The upward, negatively accelerated curves are fitted to data points obtained in response to S+ trials. The downward, positively accelerated functions represent S- trial results. The solid and dashed curves are alternated for the sake of clarity. Relative symmetry of these functions can be noted about .50 on the Y-axis.

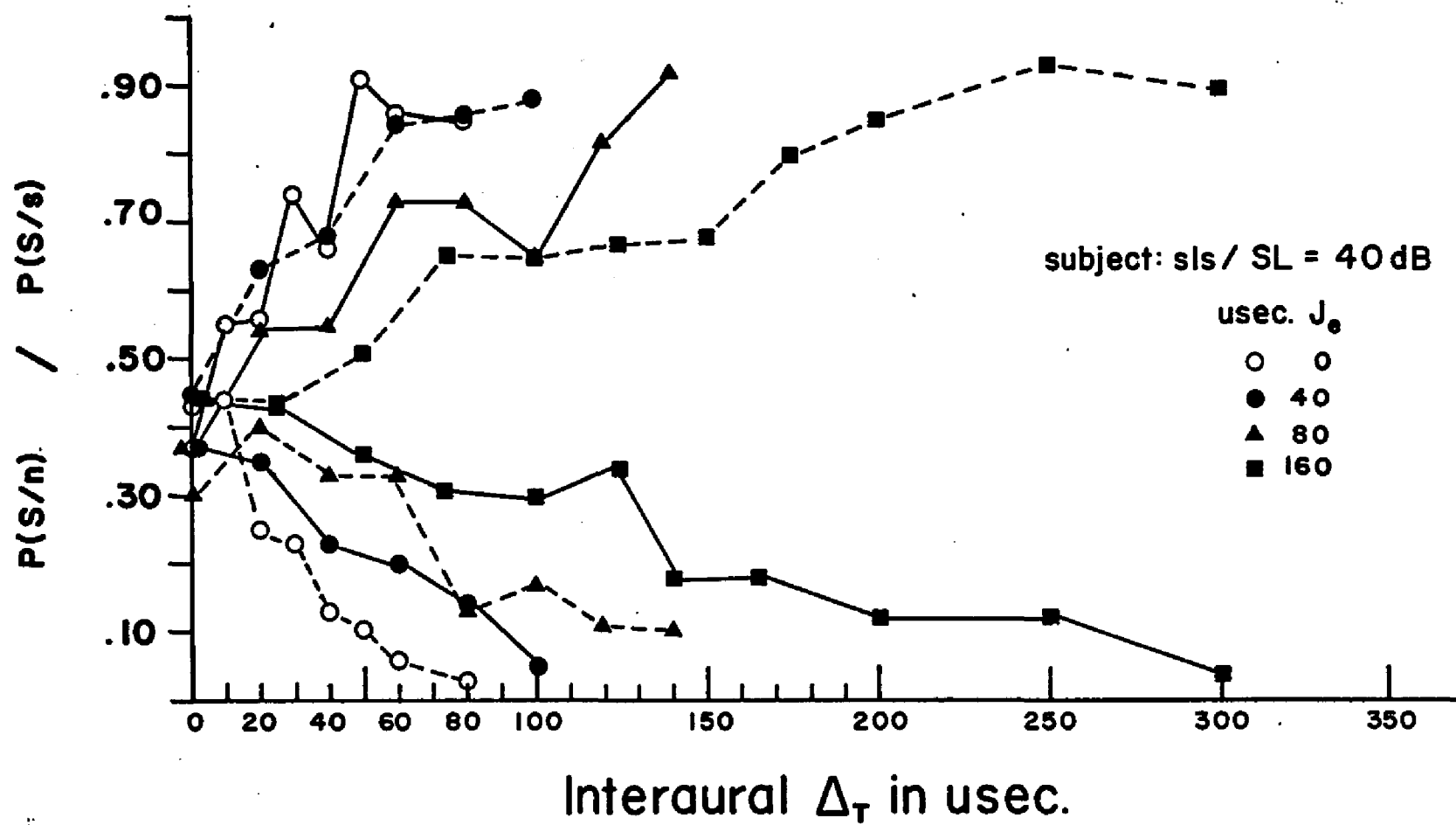
Values of  $\beta_{obt}$ , the obtained decision criterion, or critical values of likelihood ratio used by the subjects (Tables 8.5 - 8.7) were based on the  $P(S|s)$  and  $P(S|n)$  data (Green, et al, 1966). As the ratio  $P(n)/P(s) = 1.00$  for both experiments, the resulting optimum or Hea decision theory criterion,  $\beta_{opt}$ , is 1.00. Criteria trends noted for the subjects in Experiment I remain constant in Experiment II. Subjects RFS and JEB closely approximate the  $\beta_{opt}$  of 1.00.  $\beta_{obt}$ 's are .93 and .97, respectively. Subject SLS yields a  $\beta_{obt}$  of 1.16. The values of  $\beta_{obt}$ , averaged across both experiments by subject, are: .95 for RFS; .97 for JEB; and 1.21 for SLS. Subject SLS appears consistently more conservative in her decision-making than the other two subjects in the study.

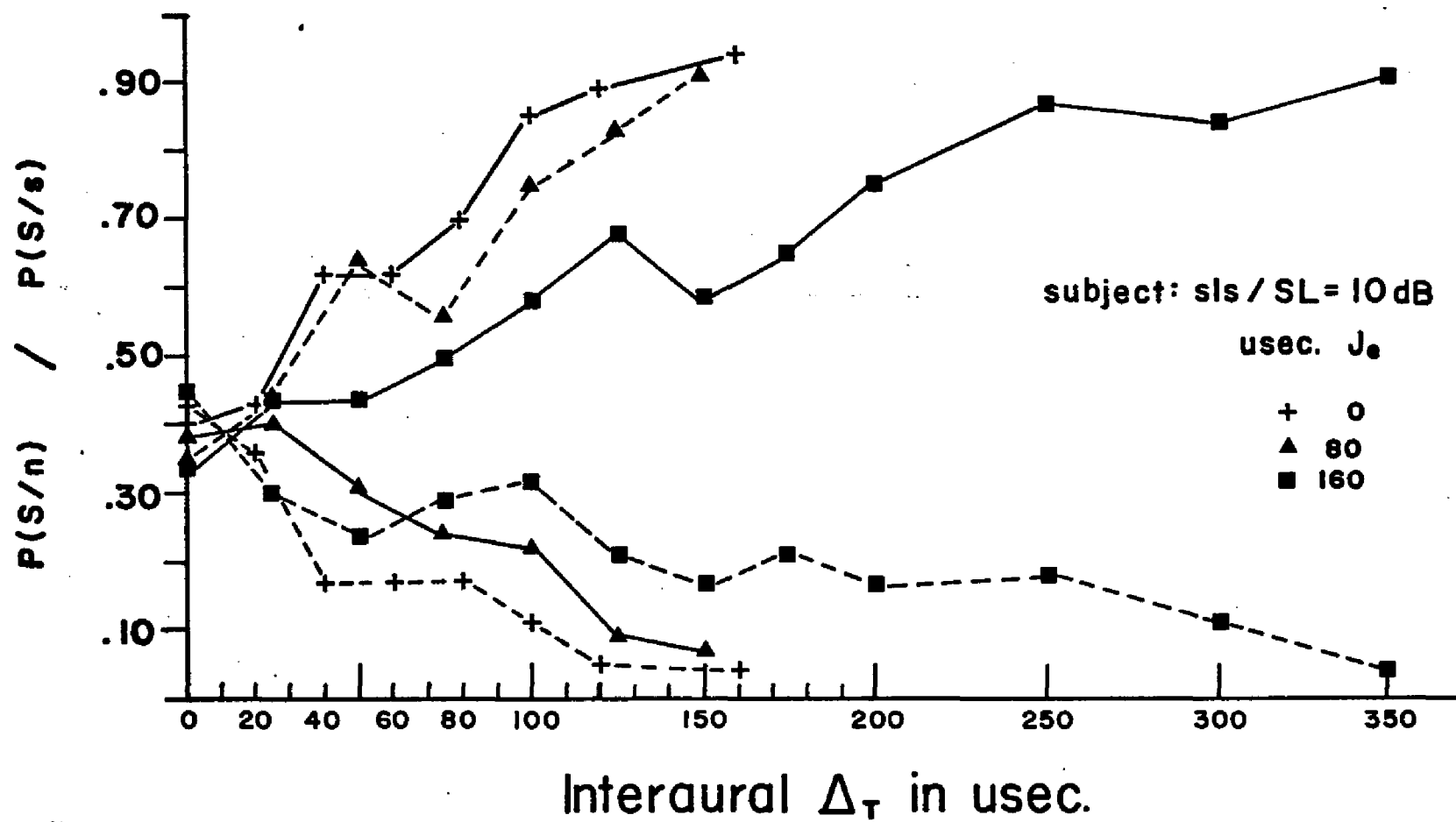
## Figures 8.22 - 8.30

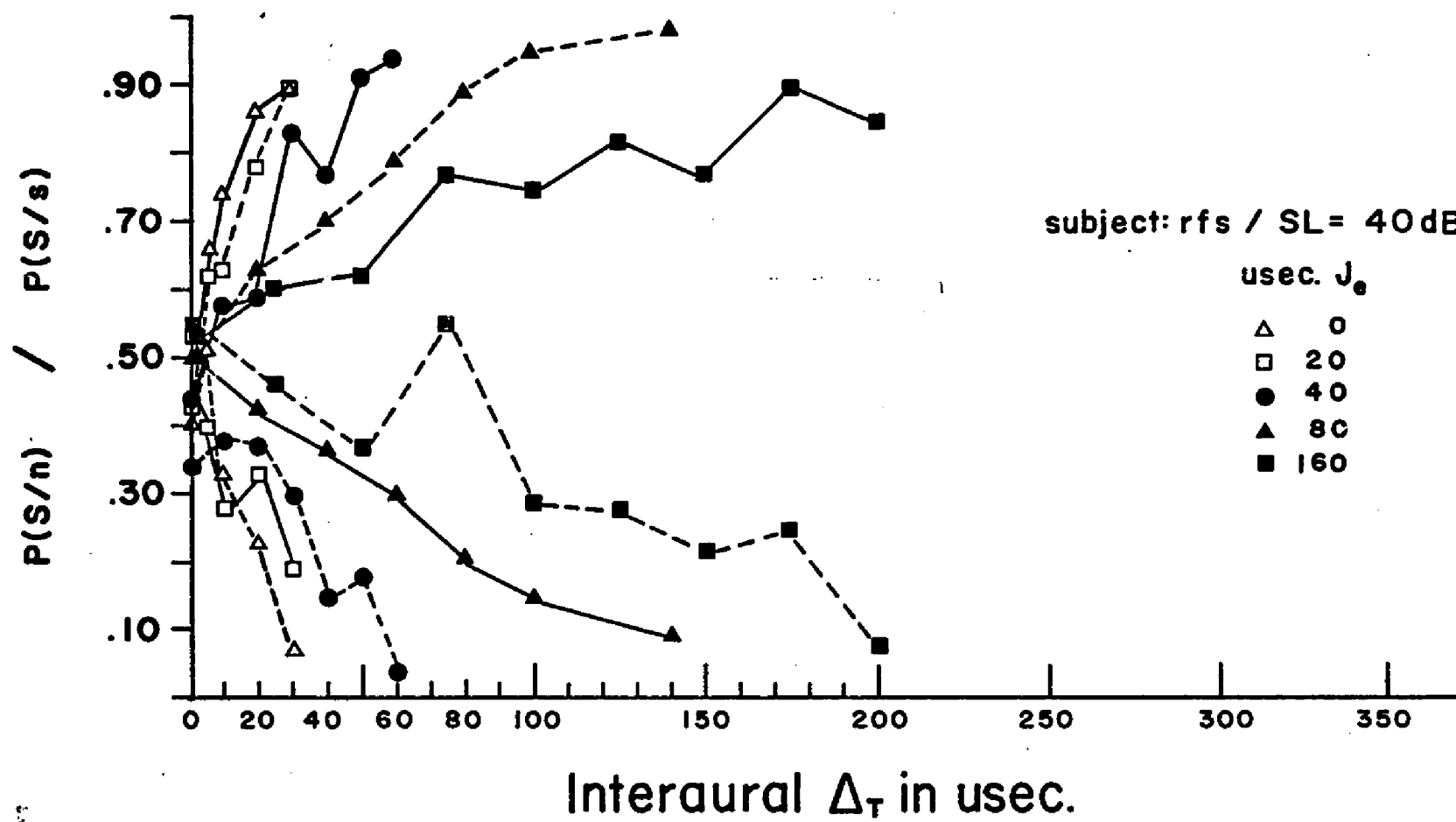
HIT and FALSE ALARM  $\Delta t$  psychometric functions;  $J_e \neq 0$ . Lower functions are  $P(S|n)$ ; upper functions are  $P(S|s)$ . Experiment I data ( $J_e = 0$ ) are included as the steepest functions in each figure.

<u>FIGURE</u>	<u>SUBJECT</u>	<u>SENSATION LEVEL</u>
8.22	SLS	60 dB
8.23		40
8.24		10
8.25	RFS	40 dB
8.26		20
8.27		10
8.28	JEB	60 dB
8.29		40
8.30		10

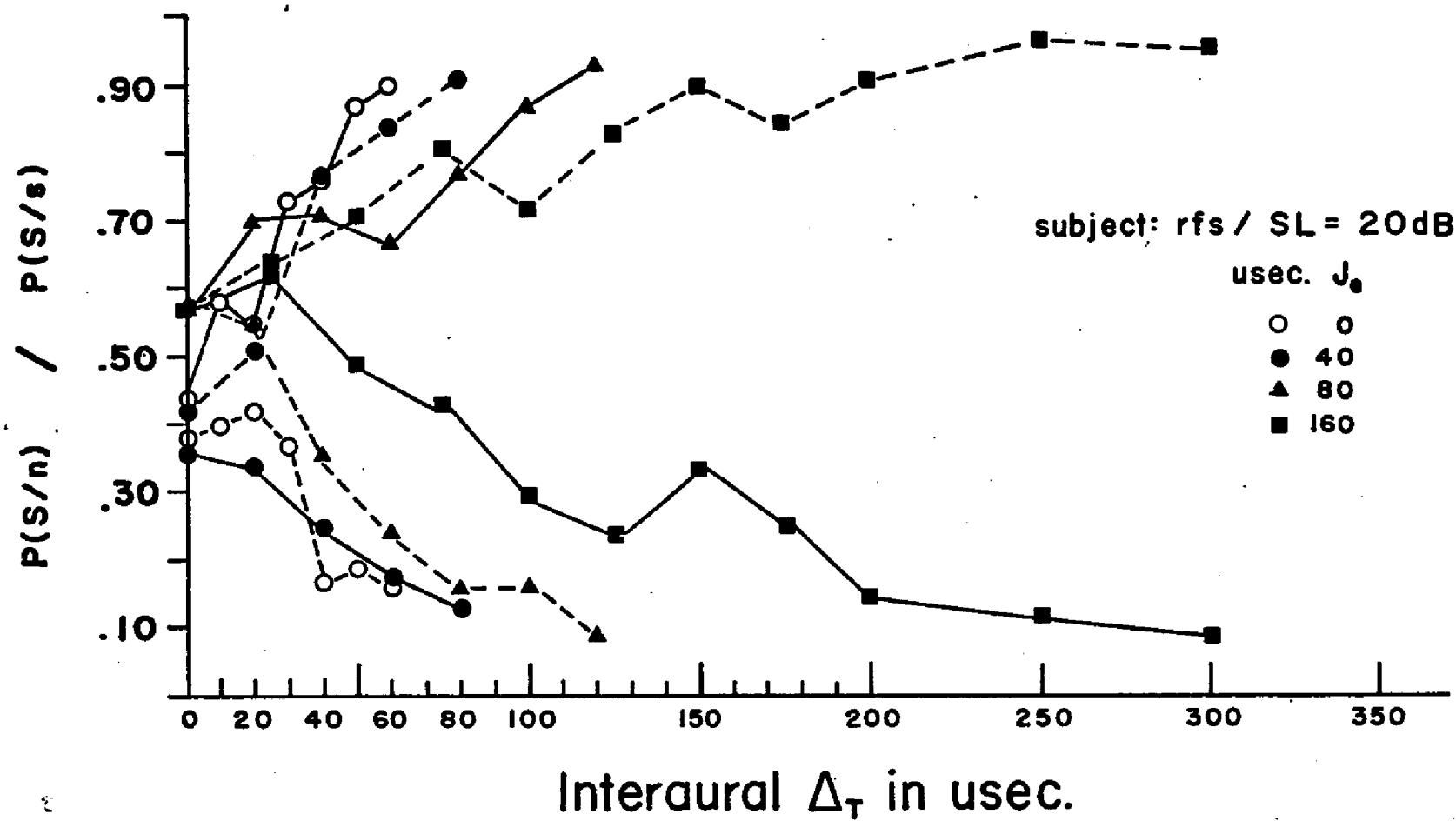


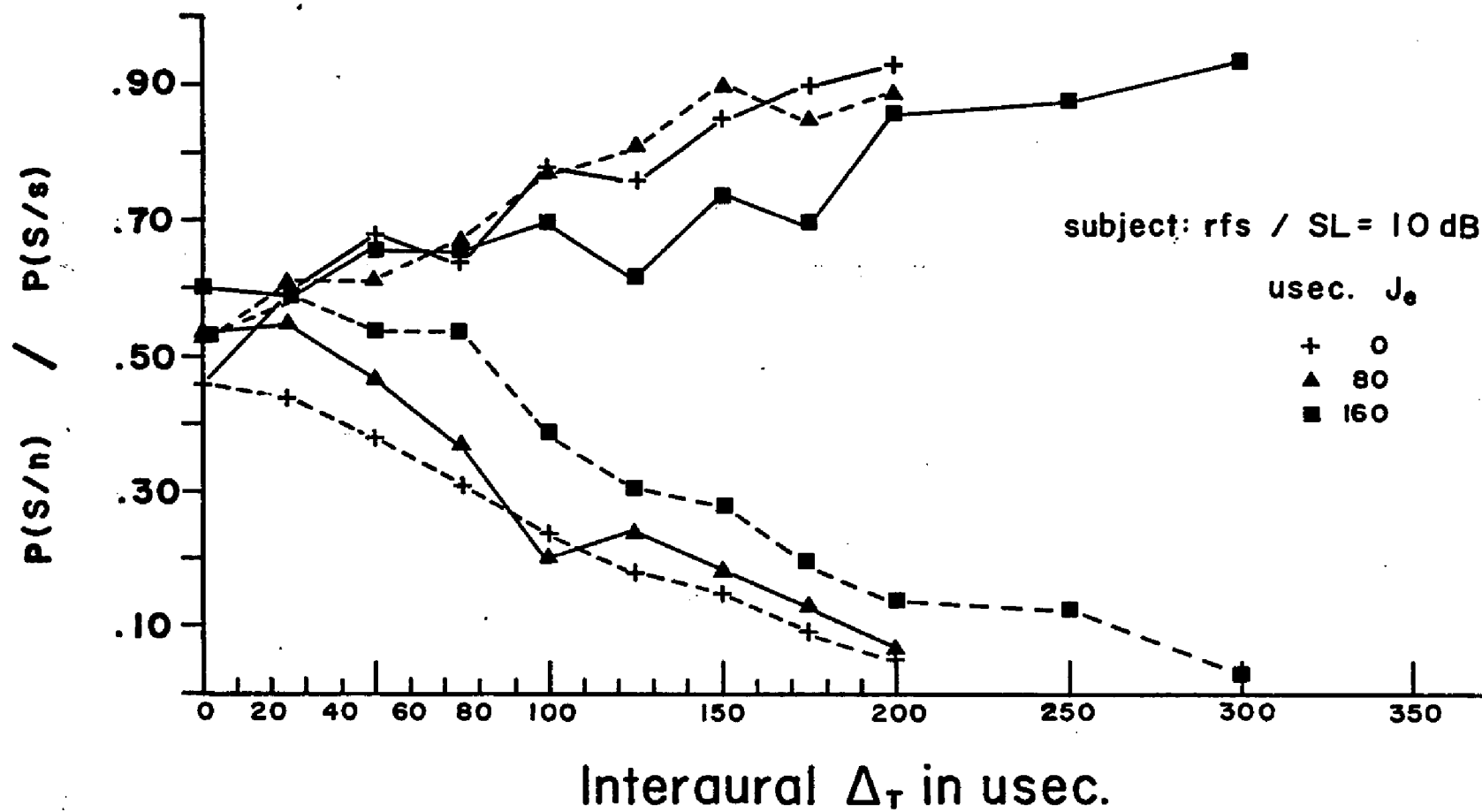


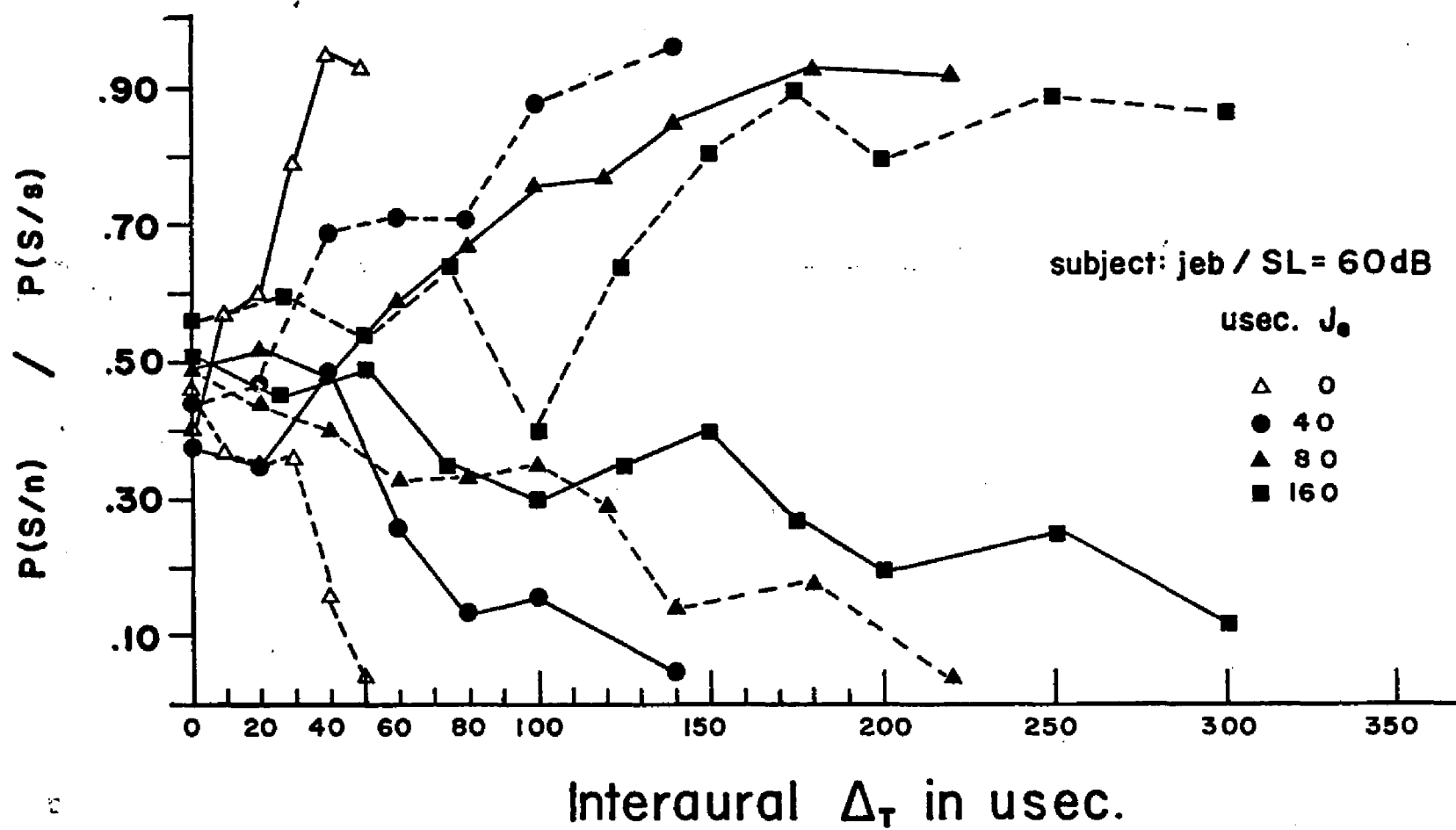


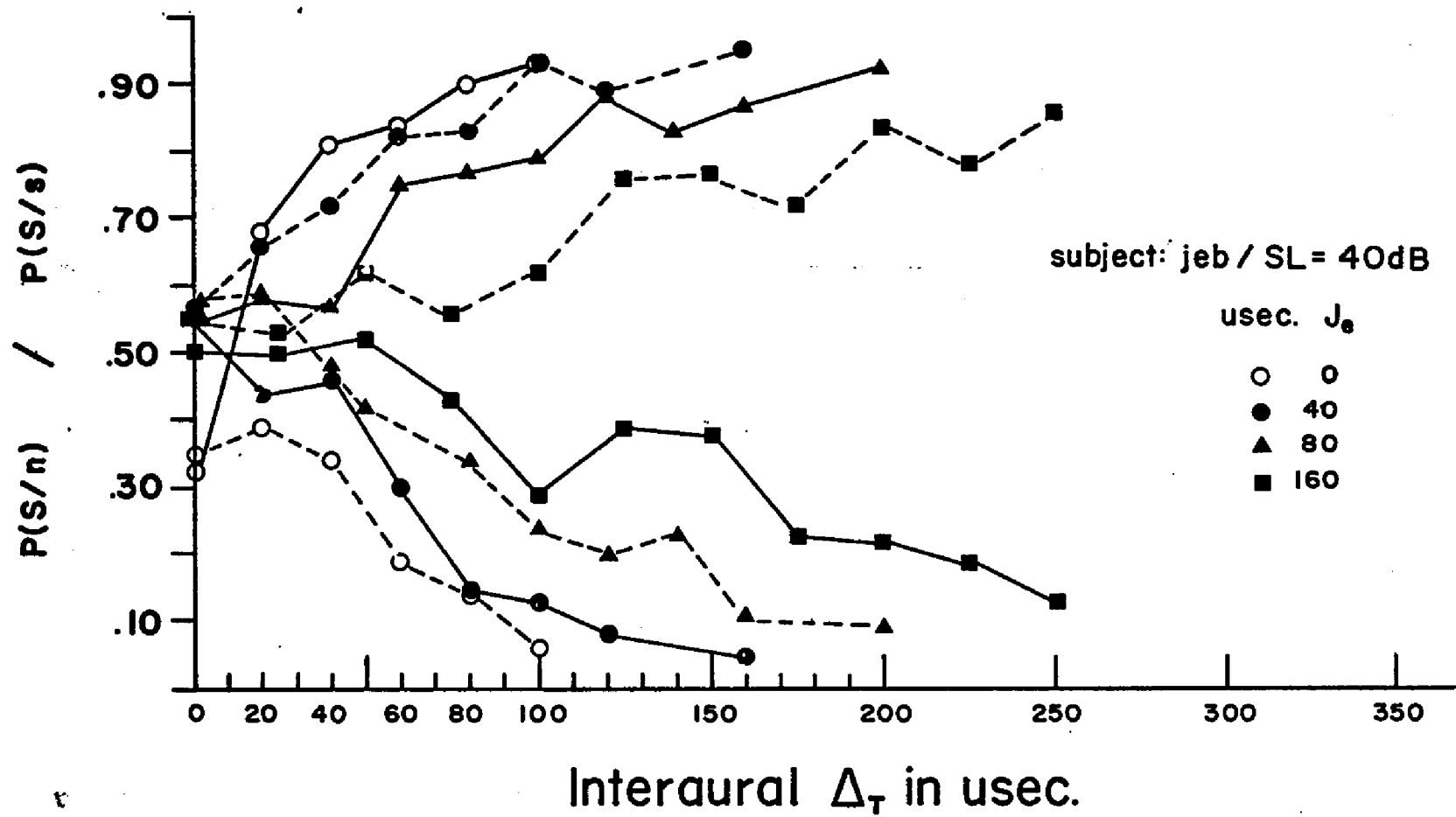












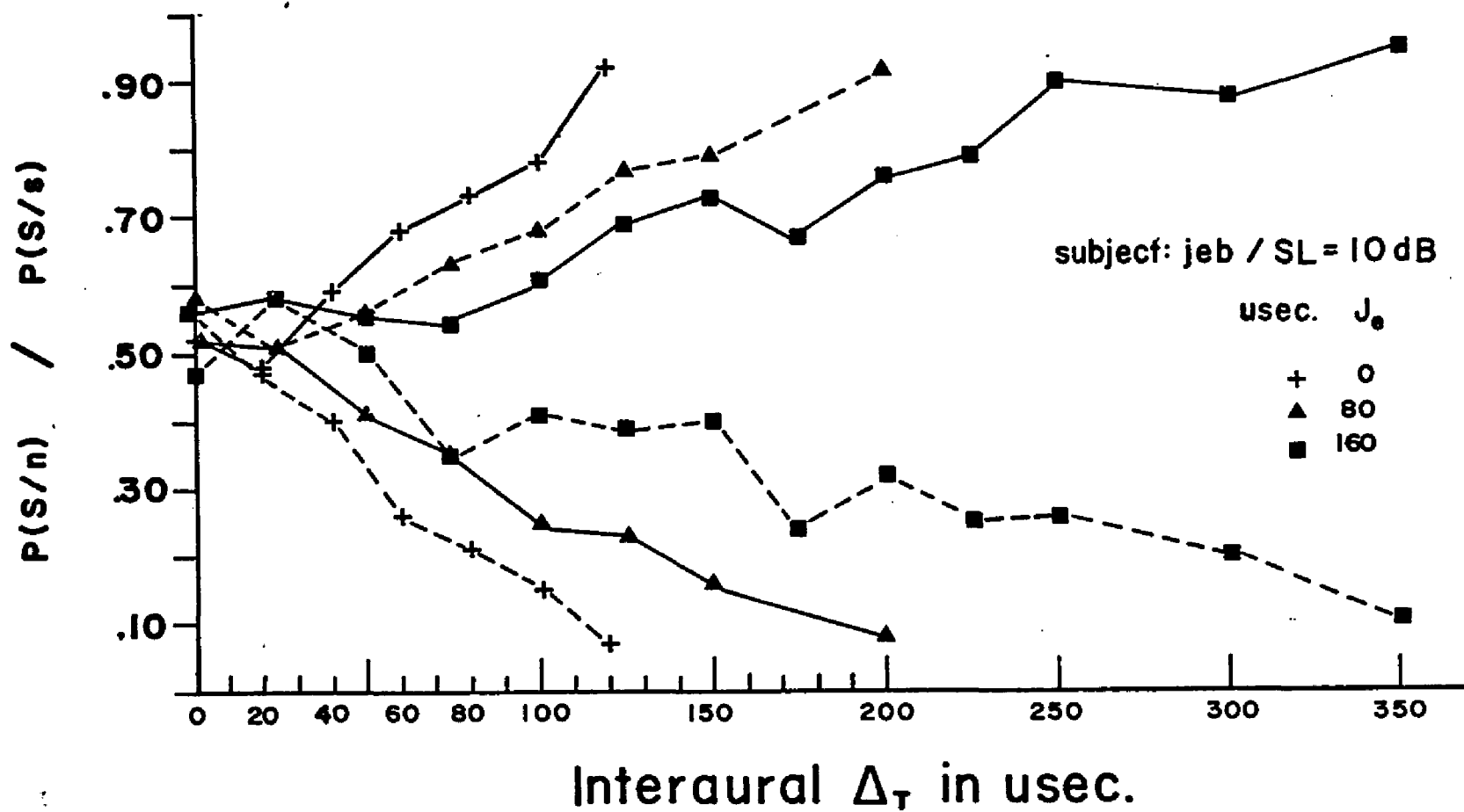


Table 8.5

$\beta_{obt}$  for Subject SLS by Sensation Level and  $J_e$ ; from Experiment II Data

Sensation Level		$J_e = 20 \mu\text{sec.}$	$J_e = 40 \mu\text{sec.}$	$J_e = 80 \mu\text{sec.}$	$J_e = 160 \mu\text{sec.}$
HIGH (60 dB)	$\bar{\beta}$	1.08	1.30	1.01	1.20
	$\beta$ Range	.99	1.03-2.20	.41-1.26	.72-2.00
	$\beta$ @ 0 $\mu\text{sec.}$	.99	1.03	1.00	1.04
	$\beta$ @ Max. $\mu\text{sec.}$	1.00	2.20	.41	1.35
	N Points	9	9	8	11
MEDIUM (40 dB)	$\bar{\beta}$		1.17	1.17	1.13
	$\beta$ Range		.83-1.93	.85-1.57	.66-2.04
	$\beta$ @ 0 $\mu\text{sec.}$		1.05	1.08	1.00
	$\beta$ @ Max. $\mu\text{sec.}$		1.93	.85	2.04
	N Points		6	8	11
LOW (10 dB)	$\bar{\beta}$			1.17	1.24
	$\beta$ Range			.97-1.56	.81-1.88
	$\beta$ @ 0 $\mu\text{sec.}$			.97	.93
	$\beta$ @ Max. $\mu\text{sec.}$			1.22	1.88
	N Points			7	12

Table 8.6

 $\beta_{\text{obt}}$  for Subject RFS by Sensation Level and  $J_e$ ; from Experiment II Data

Sensation Level		$J_e = 20 \mu\text{sec.}$	$J_e = 40 \mu\text{sec.}$	$J_e = 80 \mu\text{sec.}$	$J_e = 160 \mu\text{sec.}$
HIGH (40 dB)	$\bar{\beta}$	.91	1.01	.73	.95
	$\beta$ Range	.65-1.12	.62-1.31	.30-1.03	.55-1.49
	$\beta$ @ 0 $\mu\text{sec.}$	.99	1.08	1.03	1.01
	$\beta$ @ Max. $\mu\text{sec.}$	.65	1.29	.30	1.49
	N Points	5	7	7	9
MEDIUM (20 dB)	$\bar{\beta}$		.95	.98	.75
	$\beta$ Range		.77-1.06	.82-1.24	.34-1.00
	$\beta$ @ 0 $\mu\text{sec.}$		1.05	1.00	1.00
	$\beta$ @ Max. $\mu\text{sec.}$		.77	.82	.53
	N Points		5	7	11
LOW (10 dB)	$\bar{\beta}$			1.00	1.05
	$\beta$ Range			.67-1.40	.91-1.63
	$\beta$ @ 0 $\mu\text{sec.}$			1.00	.97
	$\beta$ @ Max. $\mu\text{sec.}$			1.40	1.63
	N Points			9	11

Table 8.7

 $\beta_{\text{obt}}$  for Subject JEB by Sensation Level and  $J_e$ ; from Experiment II Data

Sensation Level		$J_e = 20 \mu\text{sec.}$	$J_e = 40 \mu\text{sec.}$	$J_e = 80 \mu\text{sec.}$	$J_e = 160 \mu\text{sec.}$
HIGH (60 dB)	$\bar{\beta}$		1.06	1.01	.91
	$\beta$ Range		.83-1.63	.51-1.73	.53-1.11
	$\beta$ @ 0 $\mu\text{sec.}$		1.04	1.00	.99
	$\beta$ @ Max. $\mu\text{sec.}$		.83	1.73	1.05
	N Points		7	10	11
MEDIUM (40 dB)	$\bar{\beta}$		.98	.92	.98
	$\beta$ Range		.63-1.63	.82-1.13	.80-1.11
	$\beta$ @ 0 $\mu\text{sec.}$		.99	1.01	.99
	$\beta$ @ Max. $\mu\text{sec.}$		1.00	.92	1.06
	N Points		8	10	11
LOW (10 dB)	$\bar{\beta}$			1.04	.89
	$\beta$ Range			.98-1.18	.54-1.17
	$\beta$ @ 0 $\mu\text{sec.}$			.98	.99
	$\beta$ @ Max. $\mu\text{sec.}$			1.06	.59
	N Points			11	13



## CHAPTER IX

### GENERAL APPLICATIONS OF THE MODEL

It has been demonstrated in the preceding chapter that, within the given experimental constraints on pulse repetition frequency ( $\text{prf} = 20$ ) and critical stimulus duration ( $X_t = 1.00$  sec.), predictions of  $\Delta T$  performance in jitter, generated through the model, are accurate. It becomes evident that the validity of certain empirically derived constructs of the model may be examined critically by application to existing  $\Delta T$  data from the reported investigations of others.

It may be feasible to extrapolate the statistically based time discrimination features of this model to monaural and diotic frequency JND's, or more appropriately,  $\Delta 1/f$  or period JND's, noting the respective effects of jitter. Nordmark (1963) has discussed some analogies between pitch and lateralization phenomena. However, a number of factors presently preclude this test of the model's generality. These include the wide range of reported  $\Delta 1/f$  estimates (Harris, 1952), the absence of experimental detail and critical differences in stimulus or jitter control in potentially relevant studies (Pollack, 1968c, 1968d; Cardozo, et al., 1968; Nordmark, 1970).

By construing the  $\Delta T$  model as applicable with other binaural stimuli than pulse trains, viz. pure tones and noise; certain of its constructs and hypotheses may be evaluated. To be examined in this chapter are the statistical role of  $N$ ; generality of the efficiency factor,  $E$ ; and validity of the empirically derived values of  $SL$ -

dependent internal noise,  $J_{iy}$ .

#### CONSTRUCTS OF THE MODEL; N:

The model predicts  $\Delta T$  by dividing the square root of the average number of events or pulses per trial, used by a subject in arriving at his  $\Delta t$  detection decision, into the value of  $J_{iy}$  appropriate to the SL of stimulation:

$$\Delta T = J_{iy} / N_e^{1/2} \quad (5.28)$$

The efficiency factor,  $E$ , represents the degree of improvement in  $\Delta T$ , obtained as a result of using multiple stimulus observations of average sample size  $N_e$ , relative to the Ideal Observer, who always uses  $N$  sample observations:

$$E = (N_e / N)^{1/2} \quad (5.24)$$

In the general case, we have:

$$\Delta T = J_{iy} / E(N^{1/2}) \quad (5.48)$$

where  $E$  may be considered an observer characteristic interacting with the degree of definition of transient interaural time cues in the dichotic stimulus. For example, a burst of  $N$  pulses may be used more efficiently than a burst consisting of  $N$  cycles of a pure tone. A broad band of noise, with its sporadic amplitude peaks, may be more comparable to a pulse train than a pure tone stimulus.

The model predicts that  $\Delta T$  is proportional to  $N^{-1/2}$ . It is obvious that  $\Delta T$  is also proportional to  $X_t^{-1/2}$ , critical stimulus duration,

when frequency remains constant. Thus, the model should apply to  $\Delta T$  data regardless of whether  $N$  is altered by varying stimulus duration with frequency constant, or by varying frequency with duration constant. A stimulus duration of 1.00 second and a 1 kHz repetition frequency have been arbitrarily determined as the integration limits for  $N$  in the model.

#### $N$ ; DURATION VARIED, FREQUENCY CONSTANT:

9.3 In his doctoral thesis, Zerlin (1959) reported the effects of noise burst duration on the  $\Delta t$  JND for ongoing temporal disparity as an isolated lateralization cue. The delay line used in Zerlin's study preceded the binaural stimulus gate. This ruled out the other potential  $\Delta T$  cues of onset and offset disparity. In the present study, temporal onset disparity is the sole cue. The joint effects of onset, ongoing, and offset disparities have been reported for dichotic noise burst stimuli (Tobias, et al., 1959).

Major assumptions in predicting Zerlin's (1959) data are as follows:

1. That the 65 dB spl of his stimulus, a 5 kHz low-pass filtered noise band, is comparable to the Medium Sensation Level in the present study. The attendant internal noise level,  $J_{iy}$ , is empirically estimated, from the present study, at 45  $\mu$ sec..
2. That Zerlin's observers functioned as efficiently with noise stimuli as did those in the present study

with clicks. The average  $E$  is, therefore, taken as .37.

3. That, given Zerlin's 5 kHz low-pass noise stimulus, the maximum  $N$  events possible per second is 5 kHz. However, the maximum  $N$  events temporally processable is assumed to be 1 kHz. This estimate, nominally within the range of periodicity pitch, is derived from the upper limits of  $\Delta\phi$  perception for pure tones (Zwislocki, et al., 1956; Klumpp, et al., 1956). So, when Zerlin's  $T$  (in the model,  $X_t$ ) is equal to 1.00 second,  $N = 1000$ . When  $T = 300$ ,  $N = 300$ ; etc.. Among these assumptions, only this third may be considered a "free" parameter.

Zerlin's 1959 data were graphically reconstructed, with  $\Delta T$  recorded as a function of burst duration, in Fig. 9.1 and Table 9.1. Formula 5.48, above, was applied to each value of  $T$ , or  $X_t$  with  $N$  limited to 1000 Hz. The predicted and obtained data agree, within one  $\mu\text{sec.}$ , down to the asymptote of his obtained psychophysical function, at a duration of 700 msec.. Allowing for the frequency limit set at 1 kHz, the model appears fully supported by these data.

#### $N$ ; FREQUENCY VARIED, DURATION CONSTANT:

No study has, to date, reported the role of pulse repetition frequency on  $\Delta T$ , holding burst duration constant. The closest approximations, to which this model may apply, are the pure tone  $\Delta\phi$  JND studies of Zwislocki, et al. (1956) and Klumpp, et al. (1956).

Figure 9.1

Ongoing  $\Delta t$  JND's for 5 kHz low-pass filtered noise obtained by Zerlin (1959). Dashed lines represent  $\Delta T$  values predicted by the model. Constants are empirically estimated from the present study; N is assumed limited to 1 kHz.

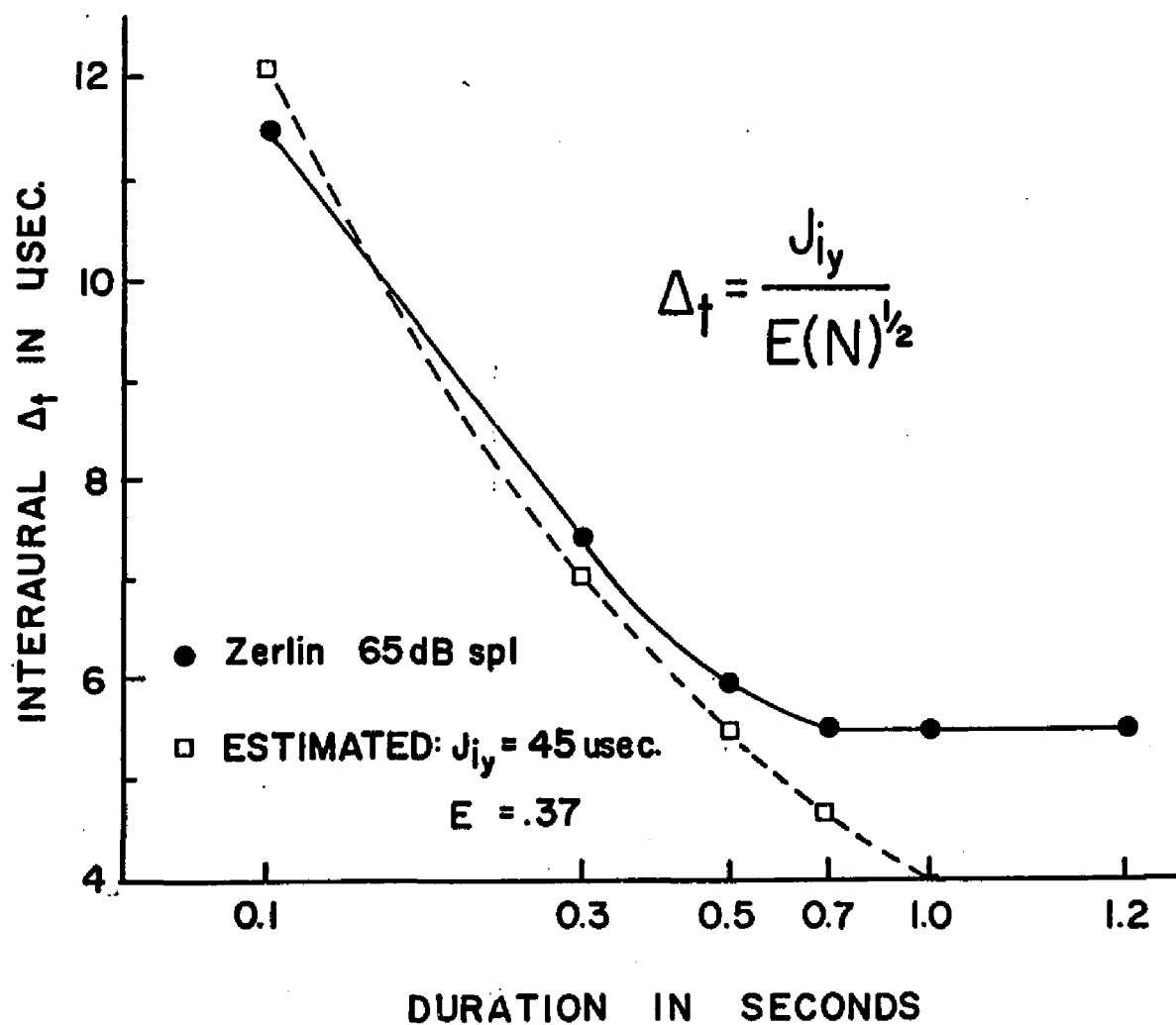


Table 9.1

Predicted  $\Delta T$  Values For Noise Burst Ongoing Disparity

As  $f(X_t)$ ; Data of Zerlin (1959)

5.0 kHz LP White Noise @ ~ 65 dB spl

$$\Delta T = J_{iy} / [E(N)^{\frac{1}{2}}]$$

Estimated Parameters:  $J_{iy} = 45 \mu\text{sec.}$  (Exp. II)

$E = .37$  (Exp. II)

$N/\text{sec.} = 1 \text{ kHz}$

<u>DURATION <math>X_t</math></u>	<u><math>\Delta T_{\text{obt.}}</math></u>	<u><math>\Delta T_{\text{pred.}}</math></u>
100 msec.	11.5 $\mu\text{sec.}$	12.2 $\mu\text{sec.}$
300	7.5	7.0
500	6.0	5.4
700	5.5	4.6
1000	5.5	3.9

The following assumptions were made prior to an a posteriori application of the model to their data:

1. That pure tone frequency in  $H_0$  is commensurate with pulse repetition frequency as a substitute for  $N$  in the model. The limitations for statistical processing in the model remain, as postulated, 1 kHz and a duration,  $X_t$ , of one second.
2. That the effective stimulus duration is 1000 msec. in both studies. That is, this figure is assumed as the limit for the temporal integration of  $N$ . Tone burst duration was actually 1000 msec. for Zwislowski, et al., but 1400 msec. for Klumpp et al.
3. That the  $J_{iy}$  for the two studies corresponds to the Medium SL average, of 45  $\mu$ sec. from the present study. Pure tones were presented at 65 dB spl in both experiments. This level is higher than the Medium SL for frequencies around 1 kHz, but less than Medium SL for 250 Hz and 125 Hz.
4. That the efficiency estimate,  $E$ , for processing sine waves as  $\Delta t$  stimuli, is less than that for pulses or broad band noise of the same repetition frequency.  $E$  was estimated at .10. This is the only "free" parameter in the post hoc fitting of the Zwislowski, et al. and Klumpp, et al. data.



Equation 5.48 was applied to the  $\Delta T$  and pure tone frequency data for each study, with  $X_t$  set to 1000 msec. and  $E$  estimated at .10. The obtained and predicted  $\Delta\phi$  data were converted to equivalent  $\Delta T$  values in  $\mu$ sec. (Table 9.2) for both studies. The model's predicted  $\Delta T$ 's are presented graphically with Zwislöcki, et al. and Klumpp, et al.'s data, in Figure 9.2.

Close agreement with the predictions of the model is found from 250 Hz through 1 kHz. The discrepancy with Klumpp, et al.'s data at 125 Hz may be due to 65 dB spl corresponding more to a Low Sensation Level at that frequency, with its concomitantly higher  $J_{iy}$  value, than the Medium SL. Predictions of the model, on the functional form following  $N^{-1/2}$ , are supported up to 1 kHz. The notion of  $E$  holding constant with frequency appears borne out as well.

#### $N$ ; OTHER STUDIES SUPPORTING $\Delta T$ PROPORTIONAL TO $N^{-1/2}$ :

In addition to the accurately predicted  $\Delta T$ 's above, a number of other investigations may be cited to generally support the concept of  $\Delta T$  proportionality to  $N^{-1/2}$  held in the model. While not a  $\Delta T$  study, an excerpt from Pollack (1968b) on jitter detection, per se, is reiterated:

"At low pulse frequencies, jitter thresholds are nearly inversely proportional to the square root of the number of interpulse intervals (IPI's) as might be expected from a statistical detection."

Figure 9.3 reproduces the  $\Delta T$ -related data from three studies (Guttman, et al., 1960; Houtgast et al., 1968; Yost, et al., 1971). The study of Guttman, et al. (1960) (Fig. 9.3a) is not strictly an

Figure 9.2

Pure tone  $\Delta\phi$  data of Klumpp and Eady (1956) with  $\Delta T$  values  
by the model.  $\Delta\phi$  has been converted to  $\Delta T$  (Table 9.2)

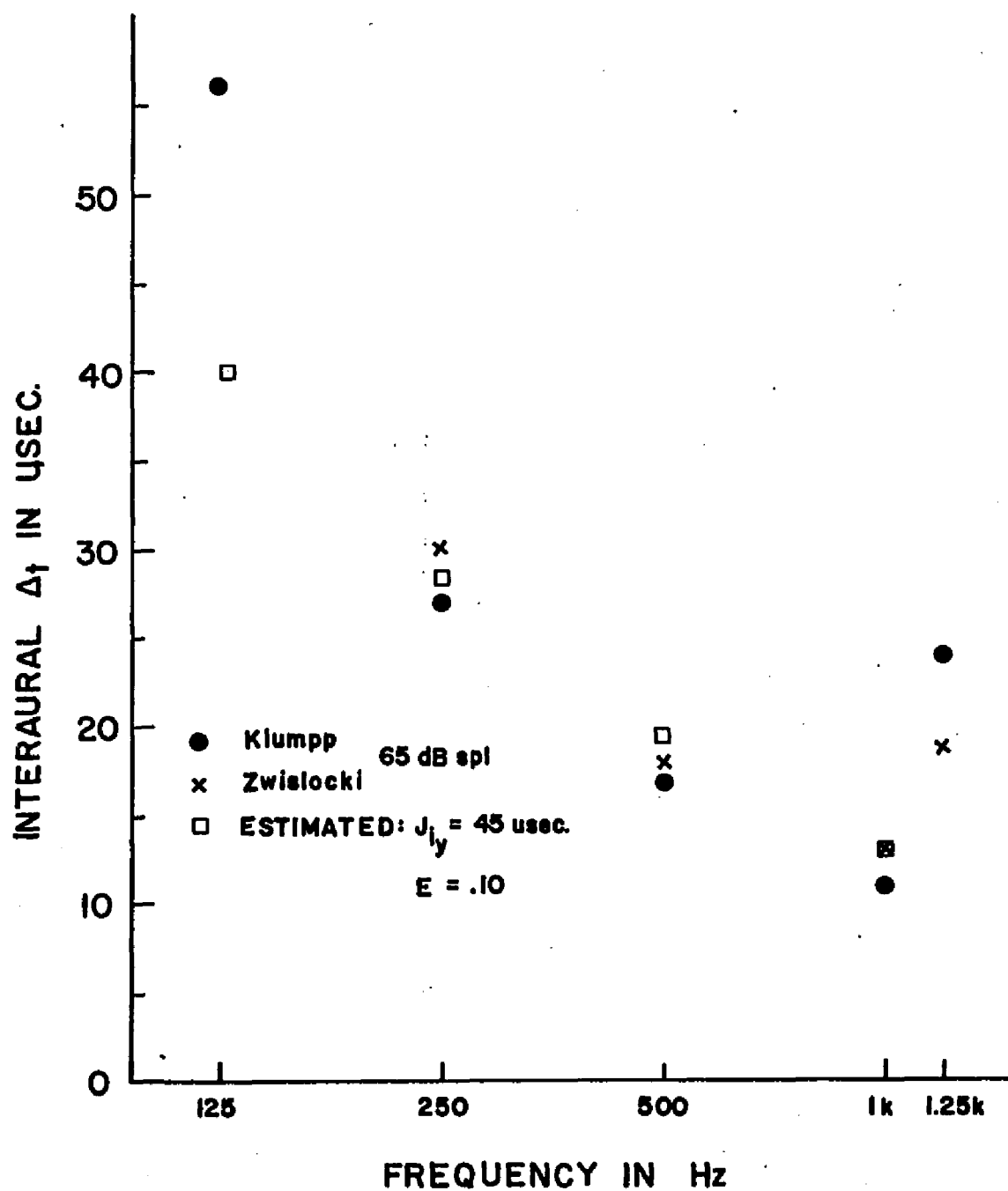


Table 9.2

Predicted  $\Delta T$  Values for  $\Delta\phi$  as  $f(\text{Hz})$ ; Data of Zwislocki and Feldman (1956); Klumpp and Eady (1956).

$X_t = 1.0 \text{ sec.}$ ; 65 dB spl;  $J_{iy}$  estimated @ 45  $\mu\text{sec.}$  (Exp.II);  $E$  estimated @ .10

$$\Delta T = J_{iy}/[E(N)^{\frac{1}{2}}]$$

<u>FREQUENCY</u>	<u>(<math>\Delta T</math>) K&amp;E</u>	<u>(<math>\Delta T</math>) Z&amp;F</u>	<u>(<math>\Delta T</math>) Pred.</u>
1000Hz	11 $\mu\text{sec.}$	14 $\mu\text{sec.}$	14 $\mu\text{sec.}$
500	17	19	20
250	27	30	28
125	56	—	40

Figure 9.3a

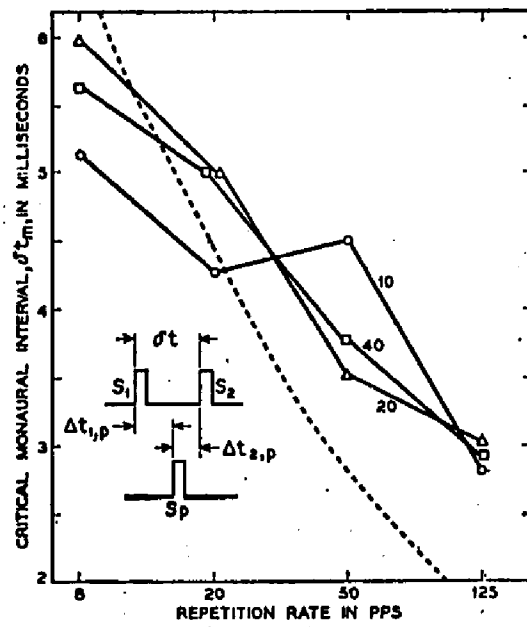
$\Delta T$  data of Guttman et. al., (1960 p. 1330) with slopes predicted by the model. Dependence of minimum resolvable monaural interval on cluster repetition rate and SL; average of four subjects. Levels of 10, 20, and 40 dB are curve parameters. All three pulses have equal intensity. Click doublet is delivered to one ear; single probe click to the other.  $\delta t_m$  is the shortest interval in which veridical fusion between  $S_p$  and  $S_2$  occurred. The dotted line is the function contour proportional to  $N^{-\frac{1}{2}}$ .

Figure 9.3b

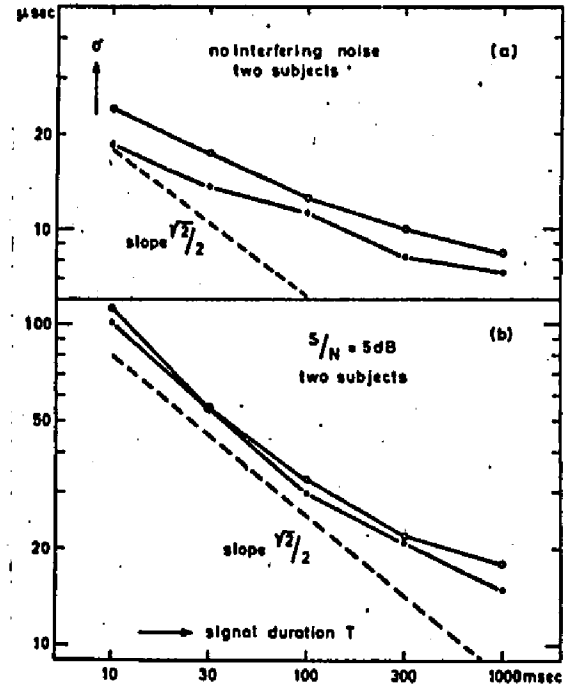
$\Delta T$  data of Yost, et. al., (1960 p. 1330) with slopes predicted by the model.  $\Delta T$  in  $\mu\text{sec.}$ , plotted as a function of number of pulse repetitions, with a basic prf of 50/sec.; 1 msec. duration clicks. Circles represent a high-pass click (2-10 kHz); the triangles, a low-pass click (4-500 Hz). Data are an average of 3 subjects. Dotted line slope is proportional to  $N^{-\frac{1}{2}}$ .

Figure 9.3c

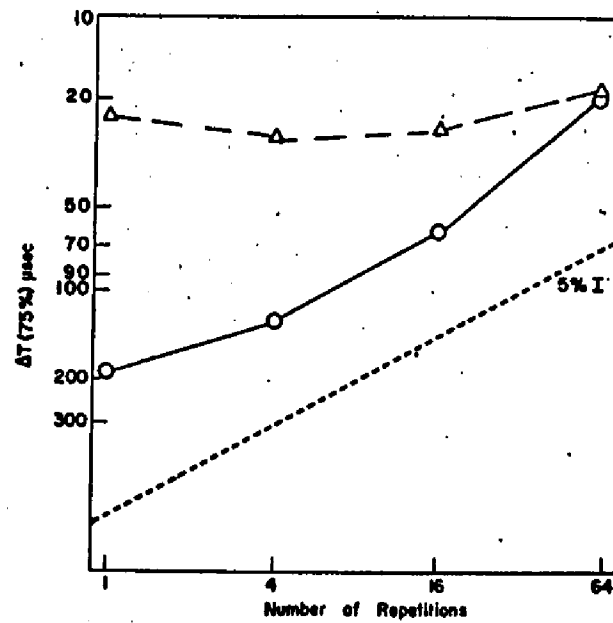
$\Delta T$  data of Houtgast, et. al., (1968 p. 810) with slopes predicted by the model.  $\Delta T$  in  $\mu\text{sec.}$  for 500 Hz octave band noise burst as a function of duration,  $\Delta T$ ; two subjects. Dotted line represents the slope for  $\sigma(T^{\frac{1}{2}}) = \text{Constant}$ .



A



B



C

investigation of the  $\Delta t$  JND. As mentioned in Chapter I, it dealt with the minimum resolvable monaural interval for a 3-click paradigm, and the dependence of this parameter on repetition rate and SL. It should be noted that the ordinate is labelled in milliseconds. The thin dashed line represents a general slope proportional to  $N^{-1/2}$  as predicted by the model.

Houtgast, et al. (1968) investigated  $\Delta T$  for an octave band of gated white noise, centered about 500 Hz, both in quiet and in a background of uncorrelated but similarly filtered noise. The background noise was spatially offset by a constant 400  $\mu$ sec. delay. Concerning their own predicted outcome, they state (1968, p. 810):

9.7 "The lateral position perceived is considered to be built up by averaging many distinct information units, each subject to statistical fluctuations introduced by both the masking noise and the internal noise. This would imply that the accuracy of the lateral position increases with signal duration,  $T$ , as long as  $T$  is below the time constant involved in the averaging process..If the information units contribute equally to the average, with no discrimination between the onset and ongoing part of the signal, one would expect the inaccuracy of the lateral position, expressed by  $\sigma$ , to be proportional to  $1/\sqrt{T}$ ."

These predictions seem supported by their data (Fig. 9.3b) for the noise signal-in-noise condition, but not as well in quiet. The apparent reason for the less-than- $X_t^{-1/2}$  improvement in  $\Delta T$  with stimulus duration may be the fact that Houtgast, et al., in contrast with Zerlin (1959), gated their stimulus prior to the delay line. This procedure would incorporate not only ongoing temporal disparity in the stimulus but onset and offset cues as well. The last two

cues may be masked in poorer signal-to-noise ratios. The authors conclude (1968, p. 812):

"For low S/N ratios, the influence of signal duration on the accuracy can be understood on a statistical basis; i.e. the accuracy is proportional to the square root of signal duration (up to at least 700 msec.). For high S/N ratios, the influence of signal duration on the accuracy is less than would be expected on the statistical basis. This can be understood by assuming that the onset of the signal contributes much more to the lateral position perceived than the ongoing does (onset effect)."

9.8  
The maximum integration time estimated from Fig. 9.3b is actually closer to 1 second. This is consistent with Zerlin's (1959) asymptote of 700 msec. (Fig. 9.1). Bekesy (1929; see also 1960, p.222) reported no improvement in pure tone pitch discrimination for durations longer than 1 second. The duration limit for integration of N is arbitrarily set to 1 second in the model. The internal noise estimate, empirically derived by Houtgast, et al., from their 1968 data, is presented below.

Yost, et al. (1971), in their  $\Delta T$  study, presented one msec. clicks, at a 50 pps rate, low-pass-filtered between 4 and 500 Hz or high-pass-filtered between 2 and 10 kHz. Stimuli were presented in a wide band noise background of 20 dB spectrum level. For the latter filtered condition (Fig. 9.3c) as N clicks vary from 1 to 64,  $\Delta T$  improves from 180  $\mu$ sec. to 20  $\mu$ sec.. The resultant functional form is accurately predicted by  $N^{-1/2}$ . For the low-pass condition,  $\Delta T$  hovers around 20  $\mu$ sec., decreasing from 25  $\mu$ sec. for  $N = 1$  to 18  $\mu$ sec.



for  $N = 64$ , nonmonotonically. While the clicks, both high- and low-pass, were equated in energy with a 70 dB spl sinusoid, discrepancies in SL between the two conditions may be partially responsible for the difference in slopes of these two psychophysical functions.

Finally Klumpp and Eady, (1956) , report a  $\Delta T$  of 28  $\mu\text{sec}$ . using a single unfiltered 1 msec. click. (Fig. 1.1b) When the stimulus was changed to a 2 second burst of 15 clicks per second,  $\Delta T$  falls to 11  $\mu\text{sec}$ .. Assuming a one second duration as the limit for statistical processing of  $\Delta t$  stimuli, the model predicts a  $\Delta T$  of 7.3  $\mu\text{sec}$ .. This is equivalent to  $N^{-1/2}$  clicks when  $N = 15$ .

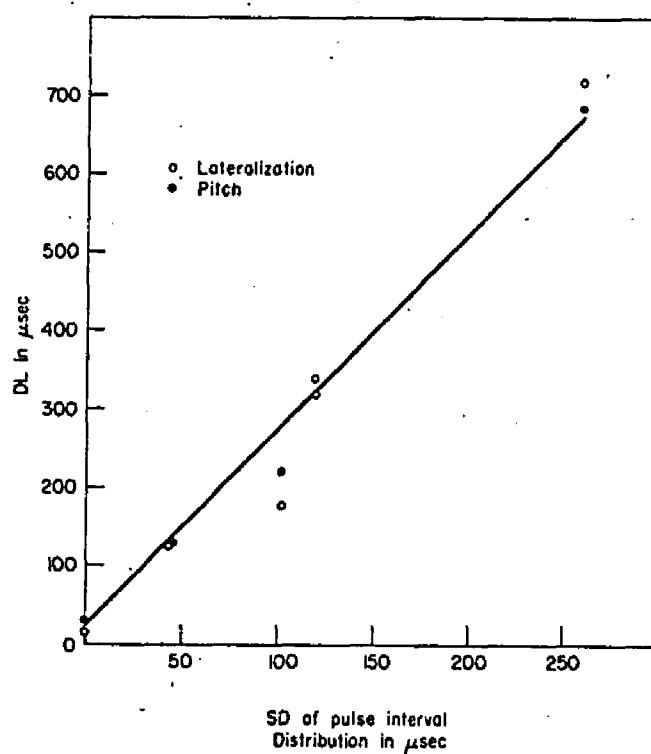
$N_e^{-1/2}$ ; A "NEURAL" WEBER FRACTION:

9.9 The concept of the "neural" Weber fraction is discussed in Chapter V. Data are presented in Chapter VIII to support the model's predictions of the  $\Delta T_J/J_e$  psychophysical functions. The potentially relevant results of a pilot experiment performed by Nordmark in the early 1960's (Nordmark, 1971), were reported (Nordmark, 1970) after completion of this present study (Fig. 9.4). Details of the experiment are lacking in publication. In the present study, the maximum limiting slope of the  $\Delta T_J/J_e$  psychophysical function,  $N_e^{-1/2}$ , is .79 for subject JEB. The slope of Nordmark's comparable function, obtained on two subjects, is on the order of 2.50. Dr. Nordmark has noted (1971) that his stimulus and jitter generation conditions may not have been entirely free of artifacts.

Additionally, the apparent coincidence of the jitter effects on both  $1/f$  and  $\Delta t$  JND's could result, according to the present model,

Figure 9.4

Data of Nordmark (1970, p. 75) on the effects of degree of randomness (SD) on the Just Noticeable Differences in time for pulse train pitch and lateralization.



if differing pulse periods were used for the pitch and lateralization experiments. The model predicts that an increase in pulse repetition frequency, with  $X_t$  remaining constant, results in shallower slopes of the  $\Delta T/J_e$  psychophysical function. In the absence of experimental detail, Nordmark's data cannot be analyzed in light of the model.

#### $J_{iy}$ ; ESTIMATES IN THE LITERATURE:

Table 9.3 presents internal time noise estimates derived, through various means, by other investigators. It should be noted that Pollack (1968b), quoted in Chapter VI, indicated that he could not empirically estimate internal noise on the basis of his jitter detection studies.

The empirically derived  $J_{iy}$  values of both Cardozo (1970), and Smoorenburg (1970), are basically inconsistent with the present research findings and the model. The model assumes that  $J_{iy}$  is independent of stimulus frequency and increases with decreasing Sensation Level. Both Cardozo and Smoorenburg ascribe no SL-dependence to  $J_{iy}$ , demonstrating that it increases with decreasing pulse frequency.

Based on their 1968 data, Houtgast and Plomp derive an empirical estimate of the statistical inaccuracy in a centrally projected lateralization "stimulation pattern". The statistical inaccuracy is analogous to  $J_{iy}$ . With no mention of the possible influence of Sensation Level, they estimate internal noise at 110  $\mu$ sec.. This figure is comparable to that obtained for the Low SL of the present study.

Finally, as an arbitrary fitting constant to his Equalization-Cancellation model, Durlach (1963) chooses a single value of 105

Table 9.3

Estimates Of Internal Temporal Noise In The Literature.

<u>INVESTIGATOR</u>	<u>DATE</u>	<u>J<sub>i</sub></u>	<u>METHOD</u>	<u>EXPERIMENT</u>	<u>FEATURES</u>
1) Durlach	1963	150 $\mu$ sec. (Bin.)	Estimated fitting constant	A Posteriori	Independent of SL and frequency; used in EC model together with an internal amplitude-noise constant.
2) Houtgast, et. al.	1968	110 $\mu$ sec. (Bin.)	Empirical, calculated	$\Delta T$ for filtered noise	Independent of SL and frequency; computed for a statistical model.
3) Cardozo	1970	*800 $\mu$ sec./50 Hz 80 $\mu$ sec./100 Hz 25 $\mu$ sec./200 Hz 15 $\mu$ sec./400 Hz	Empirical, calculated	$\Delta J_e$ for clicks in amplitude noise	Dependent on prf; independent of SL, computation assumes orthogonality of amplitude and time noise in the same system.
4) Smoorenburg	1970	* 70 $\mu$ sec./200 Hz 35 $\mu$ sec./400 Hz	Empirical, (calculated?)	$\Delta f$ for filtered clicks	Dependent on prf; Independent of SL, details not published.

\*(Monaural),

$\mu\text{sec.}$ , independent of stimulus parameters to represent the rms time error in a single channel. This leads to a value of  $150 \mu\text{sec.}$  for the combined binaural error. Concerning the validity of this estimate, Durlach (1963 , p. 1218), himself says:

"In the writers opinion, however, the overwhelming evidence is that the relevant comparison figure is on the order of 5 to  $40 \mu\text{sec.}$ ...The value [ $150 \mu\text{sec.}$ ] appears to be about an order of magnitude larger than the corresponding jnd."

The empirically derived  $J_{iy}$  estimates of the present study not only meet Durlach's standards, above, but may be intuitively perceived as correct by noting the points of inflection in the psychophysical  $\Delta T_j/J_e$  functions presented in Chapter VIII, (Figs. 8.10 - 8.12).

#### $J_{iy}$ : RELATION TO SENSATION LEVEL:

Empirical estimates of  $J_{iy}$ , derived through the model and based on data of the present study, indicate a growth in internal noise with decreasing Sensation Level. Lower limits of  $J_{iy}$  are reached at those SL's where a minimum  $\Delta T$  is achieved. This basic trend is supported by the data of Pollack (1969b) concerning the effect of pulse amplitude level upon jitter detection. (Fig. 9.5a).

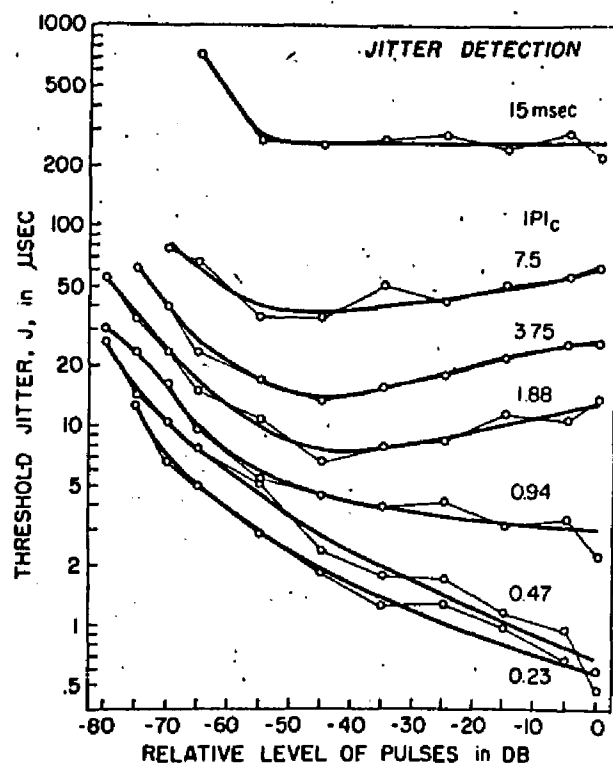
In order to assess the relative magnitude of  $J_{iy}$  growth with decreasing SL, the model was applied, a posteriori, to another section of the previously cited study by Zwislocki et al. (1956). Their findings (Fig. 9.5b) illustrate the effect of SL on the  $\Delta\phi$  JND for a 500 Hz sine wave. Their data were graphically extrapolated at

Figure 9.5a

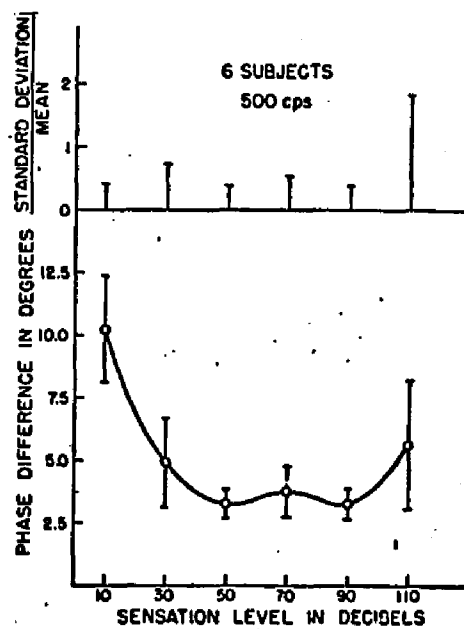
Data of Pollack (1971, p. 1023) on the effect of pulse amplitude upon diotic jitter thresholds. The parameter of each curve is IPI upon which jitter was introduced. Thresholds based on 14 listeners.

Figure 9.5b

Data of Zwislocki, et. al. (1956, p. 861)  $\Delta\phi$  as a function of SL at 500 Hz. Closed circles in the lower part of the figure indicate the means of 6 subjects. Vertical bars in lower part of the figure give the absolute standard deviation; those in upper part give the standard deviation relative to the mean.



A



B



three Sensation Levels, 10, 30, and 50 dB. Prior to determination of their internal noise levels, the following assumptions were made:

1. That the selected levels were equivalent to the Low, Medium, and High SL's of the present study.
2. That E remains .10, as postulated for the predicted of Zwislöcki, et al's. and Klumpp, et al's. pure tone  $\Delta T$  values.
3. That  $N = 500$  for a one second duration, 500 Hz tone.

The  $\Delta\phi$  JND's, averaged over 6 subjects, were converted to  $\Delta T$ 's in  $\mu\text{sec.}$  and inserted into formula 5.49:

$$J_{iy} = \Delta T [E(N^2)] \quad (5.49)$$

Results are given in Table 9.4. Internal noise estimates, empirically derived from their JND's are: 124  $\mu\text{sec.}$  for the Low SL; 62  $\mu\text{sec.}$  for the Medium; and 37  $\mu\text{sec.}$  for the High. These internal noise levels are slightly larger than the mean values of  $J_{iy}$  obtained for comparable SL's in the present study. However, Table 9.4 presents for comparison the largest individual  $J_{iy}$  estimates, from Table 8.4. Agreement is easily within the same order of magnitude for each of the three SL's.

Table 9.4

Predicted  $J_{iy}$  Values For 500Hz  $\Delta\phi$  Data Of Zwislocki And Feldman (1956).

$f = 500 \text{ Hz}$ ;  $X_t = 1.0 \text{ sec.}$ ;  $n = 6 \text{ subjects}$ ;  $E$  estimated @ .10

$$J_{iy} = \Delta T [E(N)^{\frac{1}{2}}]$$

<u>SL</u>	<u><math>\Delta\phi</math></u>	<u><math>\Delta T</math></u>	<u><math>(J_{iy})</math> obtained</u>	<u><math>(J_{iy})</math> predicted from:</u>	<u>Exp. II subject &amp; SL</u>
50 dB	3°	17 $\mu\text{sec.}$	37 $\mu\text{sec.}$	30 $\mu\text{sec.}$	SLS, 60 dB
30	5	28	62	49	RFS, 20
10	10	56	124	127	RFS, 10

## CHAPTER X

## SUMMARY

The study is reported in two parts. In Experiment I, detailed psychometric functions of  $\Delta t$  detectability for a 20 pps train of pulses were obtained from each of three subjects at three representative SL's. A YES/NO psychophysical procedure was used in an AXA paradigm. Obtained functions of  $d'$  as  $f(\Delta t)$  are least-squares best-fitted by lines intersecting the origin, suggesting an underlying normal distribution of errors. Slopes decrease systematically with intensity. Estimates of the  $\Delta t$  JND for periodicity-stable stimuli ( $\Delta T$ ) range from 11, 17 and 18  $\mu$ sec. at the High SL to 46, 47, and 69  $\mu$ sec. at the Low (10 dB) SL, respectively.

HIT and FALSE ALARM data were used to generate a posteriori estimates of the critical values of likelihood ratio ( $\beta_{\text{obt}}$ ) held by the subjects in arriving at  $\Delta t$  detection decisions. Results confirm their ability to approximate closely and maintain the constant optimum decision criterion ( $\beta_{\text{opt}} = 1.00$ ) characteristic of a Maximum Percent Correct Observer.

A model is proposed for  $\Delta t$  detection. With criterial inadequacy effectively ruled out, for the present study, as a significant limiting factor in  $\Delta T$  performance, two other constructs are implicated. The first is internal noise ( $J_{iy}$ ), an inherent temporal instability which increases with decreasing intensity of stimulation. The internal temporal variance ( $J_{iy}^2$ ) is additive

with any external temporal variance ( $J_e^2$ ) in the stimulus. The second factor is an inability of the human observer to integrate  $\Delta t$  information fully across  $N$  pulses given in a train of duration  $X_t$ . Rather, he functions in a statistical manner, basing decisions on some average number of multiple observations of the stimulus less than  $N$ , viz.  $N_e$ . It is further postulated that  $N_e$  is a constant proportion ( $E^2$ ) of  $N$ , independent of intensity.

Considering the pulse train  $\Delta t$  observation as if taken from a sampling distribution of sample size  $N_e$ , the  $\Delta t$  JND where  $J_e \neq 0$  ( $\Delta T_J$ ) is given in the model by:

$$\Delta T_J = [(J_e^2 + J_{iy}^2)/N_e]^{\frac{1}{2}}$$

In Experiment II, controlled rms external temporal instability ( $J_e$ ) is introduced into the stimulus periodicity in values of 20, 40, 80 and 160  $\mu\text{sec. rms.}$   $\Delta T_J$  psychometric functions are obtained from three subjects at three SL's. Results show an increase in  $\Delta T_J$  with increasing  $J_e$  similar to that noted as a function of decreasing SL when  $J_e = 0$ .

Constructs of the model are empirically assigned values as follows:

$$N_e = J_e^2 / (\Delta T_J^2 - \Delta T^2),$$

where both  $\Delta T$  and  $\Delta T_J$  are obtained at  $SL_y$ , the latter in  $J_e$ . Then,

$$J_{iy} = (\Delta T) N_e^{\frac{1}{2}}.$$

SL-dependent values of  $J_{iy}$  ranged from an average of 24  $\mu\text{sec.}$

at the High SL to 89  $\mu$ sec. at the 10 dB SL. Performance may be predicted for combinations of  $\Delta t$  and  $J_e$  at SL :

$$d'_{\text{pred}} = \Delta t (N_e^{\frac{1}{2}}) / (J_e^2 + J_{iy}^2)^{\frac{1}{2}}$$

The efficiency of the Human Observer, relative to the Ideal Observer, is given as:

$$E = (N_e/N)^{\frac{1}{2}}$$

In general,  $\Delta T$  may be predicted for binaural stimuli, nominally of repetition rates below 1 kHz and durations less than 1 sec.

$$\Delta T = J_{iy} / E(N^{\frac{1}{2}})$$

With parameters empirically estimated from the experiment, the model is applied, post hoc, to the  $\Delta T$  data of Zwislocki and Feldman (1956) and Klumpp and Eady (1956) for pure tones and of Zerlin (1959) for noise; et. al.

Validity of the empirically determined values of  $J_{iy}$  and  $E$ , as well as the proportionality  $\Delta T$  to  $N^{-\frac{1}{2}}$ , appear supported in the model. It is shown further that the asymptotic slope of the psychophysical function  $\Delta T_J / J_e$  is independent of stimulus intensity and may be approximated closely by  $N_e^{-\frac{1}{2}}$ .

## REFERENCES

- von Békésy, G. (1929) "Zur Theorie des Hörens; Über die eben merkbare Amplituden - und Frequenzänderung eines Tones; Die Theorie der Schwebungen," Physik. Zeits., 30, pp. 721-745 Translation appearing in G. von Békésy (1960) Experiments in Hearing, pp. 207-238 .
- (1930) "Zur Theorie des Hörens; Über das Richtungshören bei einer Zeitdifferenz oder Lautstärkenungleichheit der beiderseitigen Schalleinwirkungen," Physik. Zeits., 31, pp. 824-835, 857-868 [Translation in G. von Békésy (1960) Experiments in Hearing, pp. 272-301].
- (1933) "Über die Hörsamkeit der Ein - und Ausschwingvorgänge mit Berücksichtigung der Raumakustik," Ann. Physik., 16, pp. 844-860 [Translation in G. von Békésy (1960) Experiments in Hearing, pp. 321-332].
- (1960) Experiments in Hearing, New York: McGraw-Hill Book Company.
- Boring, E. (1942) Sensation and Perception in the History of Experimental Psychology, New York: Appleton-Century Company.
- Calvin, W. and Stevens, C. (1967) "Synaptic Noise as a Source of Variability in the Interval Between Action Potentials," Science, 155, pp. 842-844.
- Cardozo, B., Ritsma, R., Domburg, G., and Neelen, J. (1966) "Unipolar Pulse Trains with Perturbed Intervals; Perception of Jitter," Ann. Prog. Rep. 1, Inst. for Perceptual Research, Eindhoven, The Netherlands, p. 22 [unseen, cited in Pollack, I., 1968b].
- Cardozo, B., and Ritsma, R. (1968) "On the Perception of Imperfect Periodicity," IEEE Trans. on Audio and Electro-Acoustics, Au-16, pp. 159-164.
- Cardozo, B., and Neelen, J. (1968) "Audibility of Jitter in Pulse Trains as Affected by Filtering," Ann. Prog. Rep. 3, Inst. for Perceptual Research, Eindhoven, The Netherlands, pp. 13-15 [unseen, cited in Pollack, I., 1971a].
- Cardozo, B., (1970) "The Perception of Jittered Pulse Trains" in Frequency Analysis and Periodicity Detection in Hearing, edited by R. Plomp, and G. Smoorenburg, Leiden: A.W. Sijthoff, pp. 339-349.

- Christman, R., and Victor, G. (1955) "The Perception of Direction as a Function of Binaural Temporal and Amplitude Disparity," Technical Report RADC-TN-55-302, Rome Air Development Center.
- David, E., Guttman, N., and van Bergeijk, W. (1958) "On the Mechanism of Binaural Fusion," J. Acoust. Soc. Amer., 30, (L), pp. 801-802.
- (1959) "Binaural Interaction of High Frequency Complex Stimuli," J. Acoust. Soc. Amer., 31, pp. 774-782.
- Deatherage, B. (1961) "Binaural Interaction of Clicks of Different Frequency Content," J. Acoust. Soc. Amer. 33, pp. 139-145.
- Deatherage, B., and Hirsh, I., "Auditory Localization of Clicks," J. Acoust. Soc. Amer., 31, pp. 486-492.
- Durlach, N. (1963) "Equalization and Cancellation Theory of Binaural Masking-Level Differences," J. Acoust. Soc. Amer., 35, pp. 1206-1218.
- (1966) "On the Application of the EC Model to Interaural JND's," J. Acoust. Soc. Amer., 40, pp. 1392-1397.
- Egan, J., and Clarke, F. (1962) "Psychophysics and Signal Detection" Technical Report ESD-TDR-305, Hearing and Communications Laboratory, Indiana University.
- Elliot, P. (1959) "Tables of d'," Technical Report No. 97, Electronics Defense Group, Department of Electrical Engineering, University of Michigan Research Institute.
- Flanagan, J. (1962) "Models for Approximating Basilar Membrane Displacement-Part II. Effects of Middle-Ear Transmission and Some Relations Between Subjective and Physiological Behavior," Bell System Tech. J., 41, pp. 959-1009.
- Grason-Stadler Company (1965) Personal correspondence with S.A. Porter, West Concord, Mass.
- Gray, P. (1966) "Statistical Analysis of Electrophysiological Data for Auditory Nerve Fibers in Cat," Quart. Prog. Rpt. #82, Research Laboratory of Electronics, M.I.T., pp. 239-242.
- Green, D. (1960) "Psychoacoustics and Detection Theory," J. Acoust. Soc. Amer., 32, pp. 1189-1203.

"Consistency of Auditory Detection Judgements,"  
Psych. Rev., 71, pp. 392-407.

Green, D., and Swets, J. (1966) Signal Detection Theory and Psychophysics, New York: John Wiley and Sons, Inc.

Guttman, N., van Bergeijk, W., and David, E. (1960) "Monaural Temporal Masking Investigated by Binaural Interaction," J. Acoust. Soc. Amer., 32, pp. 1329-1336.

Hall, II, J. (1964) "Minimum Detectable Change in Interaural Time or Intensity Difference for Brief Impulsive Stimuli," J. Acoust. Soc. Amer., 36 (L), pp. 2411-2413.

Harmon, L., and Lewis, E. (1966) "Neural Modeling" Physiol. Rev., 46, pp. 513-591.

Harmon, L., Levinson, J., and van Bergeijk, W. (1963) "Studies with Artificial Neurons, IV: Binaural Temporal Resolution of Clicks," J. Acoust. Soc. Amer., 35, pp. 1924-1931.

Harris, J. (1952) "Pitch Discrimination" J. Acoust. Soc. Amer., 24, pp. 750-755.

(1963) "Loudness Discrimination," J. Sp. H. Dis. Monograph Suppl. #11.

von Hornbostel, E., and Wertheimer, M. (1920) "Über die Wahrnehmung der Schallrichtung," Sitz.-Ber. Akad. Wiss., Berlin, 15, pp. 388-396 [Translation in J.D. Harris, (1969) Forty Germinal Papers in Human Hearing, Journal of Auditory Research, pp. 369-375].

Houtgast, T., and Plomp, R. (1968) "Lateralization Threshold of a Signal in Noise," J. Acoust. Soc. Amer., 44, pp. 807-812.

ISO (1964) "ISO Recommendation R389-Standard Reference Zero for the Calibration of Pure Tone Audiometers," American National Standards Institute, New York.

Kiang, N. (1965) Discharge Patterns of Single Fibers in the Cat's Auditory Nerve, M.I.T. Research Monograph #15, Cambridge, Mass: M.I.T. Press.

Klumpp, R., and Eady, H. (1956) "Some Measurements of Interaural Time Difference Thresholds," J. Acoust. Soc. Amer., 28, pp. 859-860.



Mickunas, J. (1963) "Interaural Time Delay and Apparent Direction of Clicks," Unpublished Master's Thesis, Department of Psychology, Tufts University.

Nordmark, J. (1963) "Some Analogies Between Pitch and Lateralization Phenomena," J. Acoust. Soc. Amer., 35, pp. 1544-1547.

(1970) "Time and Frequency Analysis", Chapter in Foundations of Modern Auditory Theory, edited by J. Tobias, (1970) New York: Academic Press, pp. 57-83.

(1971) Personal Correspondence.

Pollack, I. (1968a) "Asynchrony II: Perception of Temporal Gaps within Periodic and Jittered Pulse Trains," J. Acoust. Soc. Amer., 43, pp. 74-76.

(1968b) "Detection and Relative Discrimination of Auditory Jitter," J. Acoust. Soc. Amer., 43, pp. 308-315.

(1968c) "Discrimination of Mean Temporal Interval within Jittered Auditory Pulse Trains," J. Acoust. Soc. Amer., 43, pp. 1107-1112.

(1968d) "Periodicity Discrimination for Pulse Trains," J. Acoust. Soc. Amer., 43, pp. 1113-1119.

(1968e) "Effects Upon Auditory Interval Discrimination by Perturbations in the Nanosecond Region," Psychon. Sci., 11, pp. 189-190.

(1968f) "Can the Binaural System Preserve Temporal Information for Jitter?," J. Acoust. Soc. Amer., 44, pp. 968-972.

(1969a) "Submicrosecond Auditory Jitter Discrimination Thresholds," J. Acoust. Soc. Amer., 45, pp. 1058-1059.

(1969b) "Effect of Masking Noise and Pulse Level Upon Jitter Detection," J. Acoust. Soc. Amer., 45, pp. 1022-1024.

(1969c) "From Gap to Jitter Discrimination," J. Acoust. Soc. Amer., 45, (L), pp. 1279-1281.

(1969d) "Auditory Random Walk Discrimination," J. Acoust. Soc. Amer., 46, pp. 422-425.

(1971a) "Spectral Basis of Auditory 'Jitter' Detection," J. Acoust. Soc. Amer., 50, pp. 555-558.

- (1971b) "Amplitude and Time Jitter Thresholds for Rectangular-Wave Trains," J. Acoust. Soc. Amer., 50, pp. 1133-1142.
- Poussart, D. (1969) "Current Noise in Nerve Membranes; Some Comments on Measurement Techniques," Quart. Prog. Rpt. #95, Research Laboratory of Electronics, M.I.T., pp. 110-115.
- Rand Corp. (1955) A Million Random Digits with 100,000 Normal Deviates, New York: The Free Press.
- Rosenberg, A. (1966) "Pitch Discrimination of Jittered Pulse Trains," J. Acoust. Soc. Amer., 39, pp. 920-928.
- Schenkel, K. (1967) "Accumulation Theory of Binaural-Masked Thresholds," J. Acoust. Soc. Amer., 41, pp. 20-31.
- Smooenburg, G. (1970) Comment, in Discussion on B. Cardozo "The Perception of Jittered Pulse Trains" appearing in Frequency Analysis and Periodicity Detection in Hearing, edited by Plomp, R., and Smooenburg, G. (1970) p. 348.
- Stewart, J. (1963) "Limits to Animal Discrimination and Recognition in a Noise-Free External Environment," IEEE Trans. on Mil. Electronics, MIL-7, pp. 116-131.
- Swets, J., Shipley, E. McKey, M., and Green, D. (1959) "Multiple Observations of Signals in Noise," J. Acoust. Soc. Amer., 31, pp. 514-521.
- Tobias, J., and Schubert, E. (1959) "Effective Onset Duration of Auditory Stimuli," J. Acoust. Soc. Amer., 31, pp. 1595-1605.
- Wallach, H., Newman, E., and Rosenzweig, M. (1949) "The Precedence Effect in Sound Localization," Am. J. Psychol., 62, pp. 315-336.
- Woodworth, R. Experimental Psychology, New York: Henry Holt and Co.
- Yost, W., Wightman, F., and Green, D. (1971) "Lateralization of Filtered Clicks," J. Acoust. Soc. Amer., 50, pp. 1526-1531.
- Zerlin, S. (1959) "An Operational Model of an Auditory Time Difference Detector," Unpublished Ph.D. dissertation, Western Reserve University.
- Zwislocki, J., and Feldman, A. (1956) "Just Noticeable Differences in Dichotic Phase," J. Acoust. Soc. Amer., 28, pp. 860-864.